University of Alberta

Modulation of Disabled-1 Activity by Alternative Splicing

by

Zhihua Gao

A thesis submitted to the Faculty of Graduate Studies and Research in partial fulfillment of the requirements for the degree of

Doctor of Philosophy

in

Experimental Oncology

Department of Oncology

Spring 2011

Edmonton, Alberta

Examining Committee

Dr. Roseline Godbout, Department of Oncology

Dr. Hanne Ostergaard, Department of Medical Microbiology & Immunology

Dr. Andrew Shaw, Department of Oncology

Dr. James Stone, Department of Biochemistry

Dr. Ruth Slack, University of Ottawa, Canada

Dedication

This thesis is dedicated to my parents, Gangsheng Gao (1940-1995) and Maiqiu Zhou for their unconditional love and lifetime support.

Abstract

The Reelin-Disabled-1 (Dab1) signaling pathway plays a key role in regulating neuronal positioning and synaptic plasticity. Binding of Reelin to its receptors induces tyrosine phosphorylation of the intracellular adaptor protein Dab1. Tyrosine-phosphorylated Dab1 not only rapidly transmits the Reelin signal to downstream effectors but also terminates Reelin-mediated signaling by targeting itself for degradation. Multiple alternatively-spliced Dab1 isoforms have been reported; however, the functions of Dab1 isoforms, other than the commonly studied Dab1 form, remain unknown.

Here, we show that an alternatively-spliced chicken Dab1 isoform, chDab1-E, is missing two critical tyrosine sites implicated in Reelin signaling, and is not tyrosine phosphorylated upon Reelin stimulation. Knockdown of Dab1-E in chick retina results in a significant reduction in the number of proliferating cells and promotes ganglion cell differentiation, suggesting that chDab1-E is involved in the maintenance of the retinal progenitor pool and retinogenesis. Furthermore, we show that chDab1-E is serine/threonine phosphorylated by cyclin-dependent kinase 2 (Cdk2) independent of Reelin. ChDab1-E phosphorylation destabilizes the protein through proteasome degradation, indicating that Dab1 turnover can be regulated by both Reelin-independent serine/threonine phosphorylation and Reelin-dependent tyrosine phosphorylation. Finally, we demonstrate that Dab1 alternative splicing is highly complex in mouse, with the potential of generating 16 isoforms that differ primarily in the tyrosine-rich region of Dab1. We have identified 11 murine Dab1 isoforms that are differentially phosphorylated on tyrosine residues, suggesting that different Dab1 isoforms may differentially

respond to Reelin stimulation.

We propose that Dab1 alternative splicing provides an exquisitely-regulated mechanism to fine-tune the activity of Reelin signaling in a temporal and spatial manner, allowing cells that express different Dab1 isoforms to differentially respond to the Reelin signal during development. Our studies support diverse roles for alternatively-spliced Dab1 isoforms during central nervous system development. We propose a model whereby Dab1 alternative splicing tightly regulates neurogenesis, neuronal migration and synaptic plasticity through both Reelin-independent and Reelin-dependent signaling events. Our findings provide new insight into the roles of developmentally-regulated alternative splicing in controlling gene function and coordinating complex processes at different developmental stages.

Acknowledgements

First and most, I owe my deepest gratitude to my supervisor, Dr. Roseline Godbout. Her enthusiasm, insight, guidance and support have made my study lots of fun. Her extraordinary care for students helped me to go through the difficulties in life. Without her constant encouragement, sound advice and patient correction during my thesis-writing period, it would have been impossible for me to finish this thesis. Her dedication to research and excellence in mentorship made her a role model for my career.

I am deeply indebted to the whole Godbout lab: Liz, who undertook the most demanding task of generating animals that are instrumental to my study; Darryl, who provided me remarkable help with tissue staining; Sachin, who initiated the stimulating Dab1 project; Mary, who introduced me to funny stories in making solutions; Stanley, who cloned numerous constructs for Dab1; Rongzong, Lucy and Lei, who patiently taught me a variety of techniques and are my continuous consultants with experiments and personal life; Raja, Miranda, Devon, Mat, Michael and Indrani, my great fellow students with whom I had inspiring discussions. It is the help and support from all of you that has made my study enjoyable and this thesis complete.

I am grateful to people in CCI for providing a friendly and supportive learning environment for me. In particular, I am grateful to Drs. Turner, Chan, Shaw, Hitt and Hendzel for their generosity and help with reagents and techniques. I would like to earnestly thank Dr. Sun, Gerry and Christy at the Cell Imaging Facility for their invaluable assistances with confocal imaging.

I have been very fortunate to have two new members, Daniel and Aliyah, joining the family during the course of my graduate study. My dearest cuties, thank you for bringing me the greatest joy in life. My mom and my mother-in-law came a long way solely to help me look after my children. I am grateful to my husband for his love and encouragements. My study and this thesis would not be possible without the love, help and care from my entire family.

Table of Contents

List of Tables

Table: Title Page

List of Figures

Figure Name Page

List of Abbreviations

Abbreviation	Full name
Aβ	amyloid β peptide
AD	Alzheimer's disease
ANOVA	analysis of variance
APLP1	amyloid precursor-like protein 1
APLP2	amyloid precursor-like protein 2
ApoER2	apolipoprotein E receptor 2
APP	amyloid precursor protein
AS	alternative splicing
ath	atonal
ATP	adenosine triphosphate
BBP	branch binding protein
bHLH	basic helix-loop-helix
bp	base pair
BrdU	bromodeoxyuridine
Cdk	cyclin dependent kinase
ch	chicken
CHX	cycloheximide
Chx10	Ceh-10 homeobox-containing homologue
CNS	central nervous system
CNTF	ciliary neurotrophic factor
CP	cortical plate
CsA	cyclosporine A
Cul5	cullin 5
Dab	Disabled
Dab1	Disabled-1
DDX1	dead-box protein 1
DSCAM	Down syndrome cell adhesion molecule
E	embryonic
ED	embryonic day
EGF	epidermal growth factor
ESE	exonic splicing enhancer
ESS	exonic splicing silencer
FGF	fibroblast growth factor
Fox	Feminizing gene on X
GCL	ganglion cell layer
GFP	green fluorescent protein
GnRH	gonadodotropin-releasing hormone
GS	glutamine synthetase
GSK	glycogen synthase kinase

GST	glutathione S-transferase
Hes1	hairy and enhancer of split 1
HH	Hamburger Hamilton
hnRNP	heterogeneous nuclear ribonucleoprotein
IAP	intracisternal A particle
INL	inner nuclear layer
ILM	inner limiting membrane
INM	interkinetic nuclear movement
IPL	inner plexiform layer
ISE	intronic splicing enhancer
ISS	intronic splicing silencer
IZ	intermediate zone
Jak	Janus kinase
LIMK1	LIM kinase 1
LTR	long terminal repeat
μM	micromolar
mTOR	mammalian target of rapamycin
MZ	marginal zone
n-cofilin	non-muscle cofilin
NICD	Notch intracellular domain
NMD	nonsense mediated mRNA decay
NMDAR	NMDA receptor
Nova1	neuron-oncological ventral antigen
nPTB	neuronal polypyrimidine tract-binding protein
NR	neural retina
Nrl	neural retinal leucine zipper protein
nt	nucleotide
OA	okadaic acid
OLM	outer limiting membrane
ONL	outer nuclear layer
OPL	outer plexiform layer
PBD	polo-box domain
PBS	phosphate-buffered saline
PCNA	proliferating cell nuclear antigen
PCR	polymerase chain reaction
PEI	polyethylenimine
PEST	proline, gluatamate, aspartate, serine and threonine
PI/PTB	protein interaction/phosphotyrosine binding
PI3K	phosphatidylinositide-3-kinase
PKA	protein kinase A
PKC	protein kinase C
PLK	polo-like kinase

POMA	paraneoplastic opsoclonus-myoclonus ataxia
PP	preplate
PP1	protein phosphatase 1
PP2A	protein phosphatase 2A
pre-mRNA	precursor mRNA
PTB	phosphotyrosine binding
PTC	premature termination codon
ptf1a	pancreas transcription factor 1a
RA	retinoic acid
RAP	receptor-associated protein
RG	arginine glycine
RGC	retinal ganglion cell
RIPA	radioimmunoprecipitation assay
Rorβ	retinoid-related orphan nuclear receptor β
RPC	retinal progenitor cell
RPE	retinal pigmented epithelium
RRM	RNA recognition motif
RS	arginine-serine
RT	reverse transcription
S	serine
S6K1	S6 kinase 1
SD	standard deviation
SEM	standard error of the mean
SFK	src family kinases
Shh	sonic hedgehog
shRNA	short hairpin RNA
siRNA	small interfering RNA
SOCS	suppressor of cytokine signaling
SP	subplate
SPP	superplate
SR	serine arginine
SRPK	serine arginine protein kinase
STAT	signal transducer and activator of transcription
T	threonine
TBS	Tris-buffered saline
U2AF	U2 auxiliary factor
VLDLR	very low density lipoprotein receptor
VZ	ventricular zone
Y	tyrosine

CHAPTER 1: INTRODUCTION

1.1 THE REELIN-DISABLED-1 (DAB1) SIGNALING PATHWAY

1.1.1 Brain development, neuronal cell migration and the reeler phenotype

Central nervous system (CNS) development requires the orchestration of multiple complex processes, including neuronal cell production, migration, differentiation and modulation of synaptic circuitry. Migration of postmitotic neurons from the proliferative ventricular zone (VZ) to their final destination, resulting in the ordered assembly of different classes of neurons into distinct layers, is critical for the formation of laminated structures in the brain such as the cortex, cerebellum, hippocampus and retina.

Neuronal migration has been well-characterized during cortical development. In the cerebral cortex, neuronal migration begins when the first wave of postmitotic neurons leaves the VZ in a radial direction along the radial glial fibers to establish a neuronal layer known as the preplate. The preplate is then split by the arrival of a second wave of postmitotic neurons into the superficial marginal zone (MZ) and the deeper subplate. Late-born neurons subsequently migrate radially to traverse the subplate and pass early-born neurons, leading to an “inside-out” distribution of the cortical neurons in the cortical plate, with early-born neurons located in deeper layers, and late-born neurons forming the more superficial layers (Figure 1.1) (Gupta et al. 2002; Nadarajah et al. 2003).

In 1951, Falconer first described the *reeler* phenotype in mice that harbour a naturally occurring mutation (Falconer 1951). These mice exhibit ataxia, tremors and the typical reeling gait associated with severe cerebellar hypoplasia.

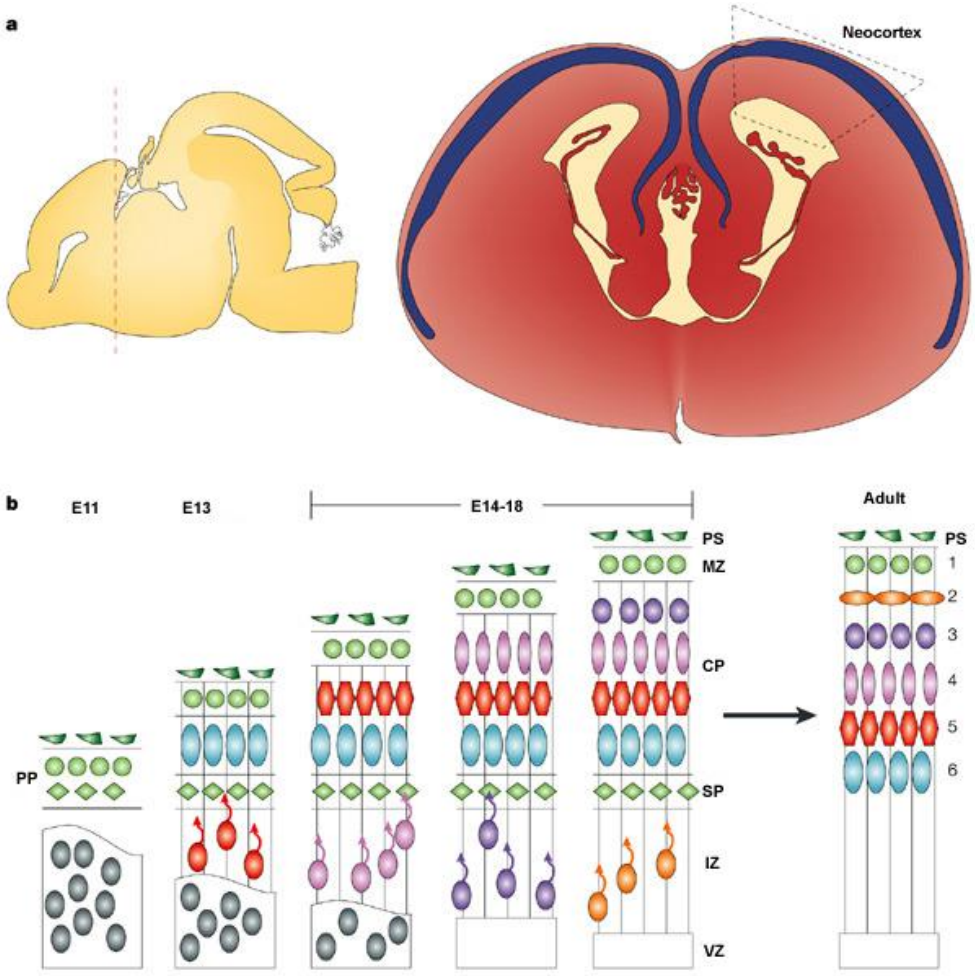

Figure 1.1 Neocortical layer formation. a. Location of the neocortex in the central nervous system. A lateral view of an embryonic day (E)16 mouse brain (left). The red dashed line indicates the plane of section from which a coronal section (right) has been taken. **b.** Organization of the adult neocortex into distinct neuronal layers. Key developmental stages of the radial component of neocortical-layer formation are shown, which occurs mainly by migration along radial glia (shown as vertical bars). At E11, the preplate (PP) is established by a postmitotic wave of neurons that has migrated from the ventricular zone (VZ) to the pial surface (PS). By E13, a second postmitotic neuronal wave has migrated through the intermediate zone (IZ) and split the PP into the marginal zone (MZ) and subplate (SP), creating the cortical plate (CP). From E14–E18, subsequent waves of neurons expand the CP in an inside-out fashion, as each wave of neurons passes its predecessors to settle underneath the MZ. In adulthood, the SP degenerates, leaving behind a six-layered neocortex.

Reproduced and adapted with permission from MacMillan Publishers Ltd: [Nat Rev Genet] (Gupta A, Tsai LH, Wynshaw-Boris A (2002) 3: 342-55) copyright (2002).

Importantly, neurons in *reeler* mice are ectopically positioned in laminated brain structures; in particular, cortical neurons are inversely positioned, with late-born neurons residing in deep layers underneath the early-born neurons (Figure 1.2) (Caviness 1973; Caviness and Sidman 1973; Caviness 1982). For decades, *reeler* mice have been used as a model to investigate the molecular and cellular mechanisms governing neuronal migration in laminated brain structures. In 1995, *Reelin*, the gene mutated in *reeler* mice, was cloned (D'Arcangelo et al. 1995). Interestingly, spontaneous mutations or targeted mutations in several other genes in mice, including Disabled-1 (Dab1), very low density lipoprotein receptor (VLDLR) and apolipoprotein E receptor 2 (ApoER2), generate a phenotype indistinguishable from that of *reeler* mice, with wide-ranging migration defects in the brain (D'Arcangelo et al. 1995; Howell et al. 1997b; Sheldon et al. 1997; Trommsdorff et al. 1999). Biochemical studies reveal that the products of these genes are components of a linear signaling pathway involved in the regulation of neuronal migration: Reelin binding to VLDLR and ApoER2 receptors activates the adaptor protein Dab1 by tyrosine phosphorylation, leading to precise neuronal cell positioning (D'Arcangelo et al. 1999; Howell et al. 1999a).

1.1.2 Key components in Reelin signaling

1.1.2.1 Reelin is a key regulator in neuronal cell positioning

The *Reelin* gene encodes a secreted glycoprotein of 3461 amino acids (aa). The N-terminus of Reelin protein contains a signal peptide and a region similar to F-spondin, whereas the C-terminus harbors an arginine-rich stretch that is

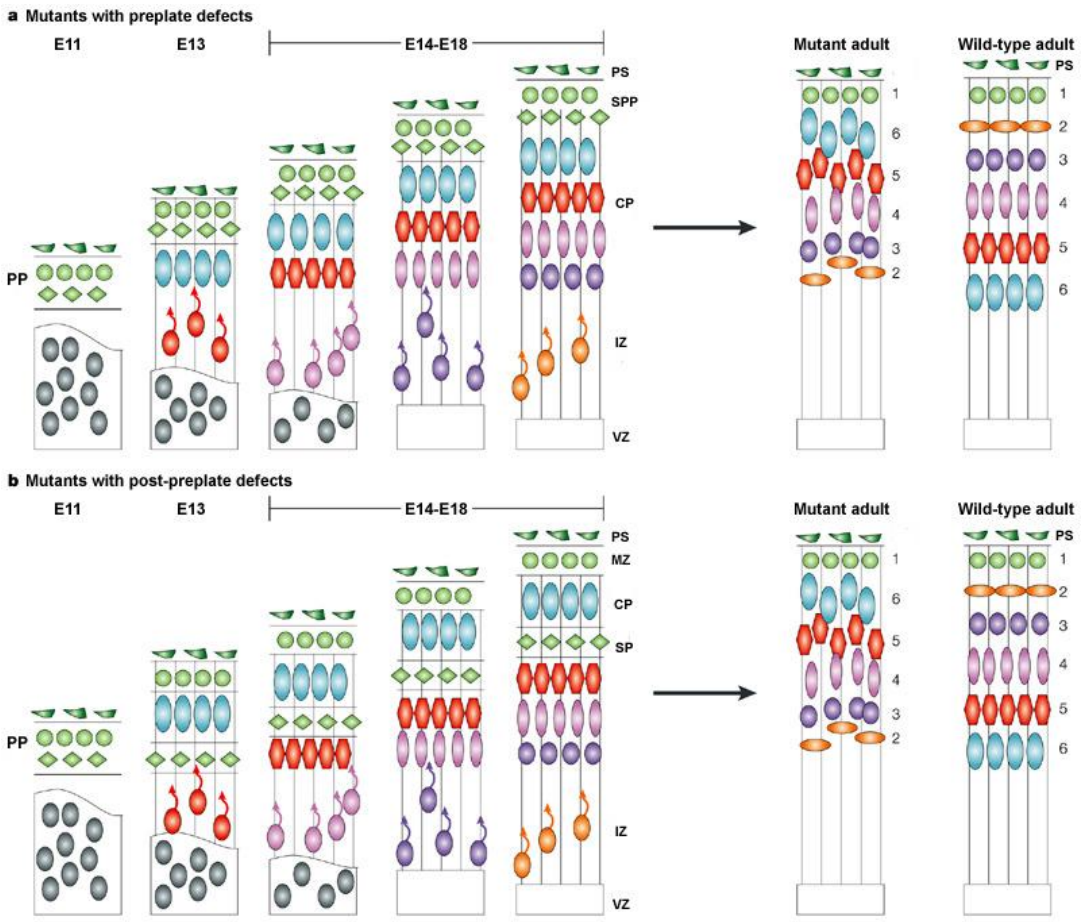

Figure 1.2 Mouse mutants with preplate and post-preplate defects. a. In mice with mutations in *Reelin*, *Dab1*, and both *Vldlr* and *Apoer2*, the preplate (PP) does not split and forms a structure called the superplate (SPP). The cortical plate (CP) forms under the SPP and is inverted, which indicates that late-migrating neurons are unable to migrate past their predecessors. Early-migrating and late-migrating neurons are positioned in the superficial and deep layers of the CP, respectively, and layering is disorganized. **b.** In post-preplate mouse mutants such as *p35*$^{-/-}$ and *Cdk5*$^{-/-}$ mutants, PP-splitting is fairly normal. The CP is organized in an inverted fashion, and individual layers are disorganized, albeit less than in the preplate mouse mutants. Notably, most of the CP initially settles beneath the SP in the upper intermediate zone (IZ). E, embryonic day; MZ, marginal zone; PS, pial surface; VZ, ventricular zone.

required for full signaling activity (Figure 1.3) (Nakano et al. 2007). The major part of Reelin consists of a unique region and 8 Reelin repeats (~350 aa each), with each repeat containing an epidermal growth factor (EGF)-like motif (~30 aa) flanked by two related subrepeats, A and B. During cortical development, Reelin is primarily expressed in Cajal-Retzius cells in the marginal zone of the cortex before the first wave of cortical plate neurons reaches the preplate (D'Arcangelo et al. 1995). In adult brain, Reelin is primarily found in GABAergic interneurons. In the cerebellum, Reelin is expressed in the granule cells (Schiffmann et al. 1997; Goffinet et al. 1999; Bernier et al. 2000).

Reelin can be cleaved *in vivo* at two main locations (one between repeats 2 and 3, and the other between repeats 6 and 7), generating three fragments (D'Arcangelo et al. 1999; Lambert de Rouvroit et al. 1999). A region within the N-terminus, recognized by the Reelin neutralizing CR-50 antibody, mediates the formation of Reelin homodimeric/multimeric complexes (Utsunomiya-Tate et al. 2000). Truncation of the N-terminal region or blocking with CR-50 antibody does not induce Dab1 tyrosine phosphorylation, suggesting that dimerization/multimerization is required for Reelin activity (Utsunomiya-Tate et al. 2000; Kubo et al. 2002). The central fragment of Reelin can directly bind to Reelin receptors, induce Dab1 tyrosine phosphorylation, and rescue the *reeler* phenotype in cortical slice cultures, indicating that the central fragment is necessary for Reelin function (Jossin et al. 2004).

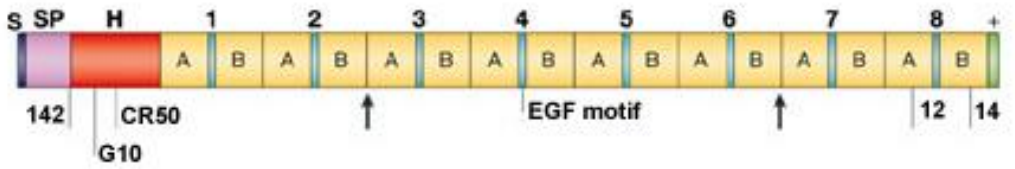

Figure 1.3 Schematic representation of the Reelin protein. Reelin sequence begins with a signal peptide of 27 residues, followed by a region with similarity to F-spondin (segment 'SP', amino acids 28–190). A unique region (segment 'H') between amino acids 191 and 500 is followed by eight repeats of about 350 aa. Each repeat contains an epidermal growth factor (EGF) motif at the centre, flanked by two subrepeats, A and B, which show weak similarity to each other. The protein terminates with a stretch of 33 amino acids that is rich in basic residues (3429–3461, indicated by +). The epitopes recognized by antibodies 142, G10, CR50, 12 and 14 are shown, and the two arrows point approximately to the sites of processing. s, signal peptide.

Reproduced and adapted with permission from MacMillan Publishers Ltd: [Nat Rev Neurosci.] (Tissir F. Goffinet AM (2003) 4: 496-505), copyright (2003).

1.1.2.2 Very low density lipoprotein receptor (VLDLR) and apolipoprotein E receptor 2 (ApoER2) are Reelin receptors

The first evidence that lipoprotein receptors can function as signaling receptors comes from the genetic inactivation of both V*ldlr* and *Apoer2*. *Vldlr*$^{-/-}$ *Apoer2*$^{-/-}$ mice display a phenotype identical to that of *reeler* mice, featured by a reeling gait and extensive lamination defects in the brain (Trommsdorff et al. 1999). Both VLDLR and ApoER2 are expressed in migrating neurons located in the developing cortical plate and intermediate zone during cortical development. Biochemical studies show that the extracellular domain of these lipoprotein receptors bind to Reelin, whereas the Reelin neutralizing antibody, CR-50 and the lipoprotein chaperone, receptor-associated protein (RAP) can inhibit the binding of Reelin to VLDLR and ApoER2 (D'Arcangelo et al. 1999; Hiesberger et al. 1999; Jossin et al. 2004). Therefore, both biochemical and genetic evidence demonstrate that VLDLR and ApoER2 are the signaling receptors for Reelin. The cytoplasmic region of VLDLR and ApoER2 contains the FxNPxY motif, a docking site for protein interaction (PI)/phosphotyrosine binding (PTB) domain-containing proteins, such as the adaptor protein Dab1 (Trommsdorff et al. 1998; Howell et al. 1999b).

1.1.2.3 Tyrosine phosphorylation of the adaptor protein Dab1 is critical for Reelin signaling

The *Disabled (Dab)* gene was first discovered as a genetic modifier for the Abl tyrosine kinase in *Drosophila* (Gertler et al. 1989). The haploinsufficiency of

Dab in an Abl-deficient background leads to defects in axonogenesis (Gertler et al. 1993). *Dab* is also involved in sevenless (sev) receptor kinase signaling. Loss of *Dab* function disrupts ommatidial development and results in the loss of R7 photoreceptor cells in *Drosophila* (Le and Simon 1998).

Mammalian *Disabled-1* (Dab1) was identified as a src-interacting protein in a yeast-two hybrid screen (Howell et al. 1997a). Several Dab1 isoforms have been described, with the predominant mammalian Dab1 form containing an open reading frame of 1668 bp that encodes a protein of 555 aa (Howell et al. 1997a; Bar et al. 2003). Like VLDLR and ApoER2, Dab1 is expressed in migrating neurons in the brain (Howell et al. 1997b). Targeted disruption (*Dab1*$^{-/-}$) or spontaneous mutations (*yotari* or *scrambler*) of the *Dab1* gene in mice, generates a phenotype similar to that of *reeler* and *Vldlr*$^{-/-}$*Apoer2*$^{-/-}$ mice, indicating that these proteins act in a linear signaling pathway (Howell et al. 1997b; Sheldon et al. 1997).

The Dab1 protein contains an N-terminal protein interaction/phosphotyrosine binding (PI/PTB) domain that binds to the FxNPxY motif within Reelin receptors (Trommsdorff et al. 1999), an internal tyrosine-rich region responsive to Reelin stimulation (Keshvara et al. 2001) and a C-terminal serine/threonine-rich region (Figure 1.4). The tyrosine-rich region consists of five highly conserved tyrosine residues (Y185, Y198, Y200, Y220, Y232) that correspond to four consensus tyrosine kinase recognition sites: Y185 and Y198/Y200 are located within two consensus SFK recognition sites (YQXI), whereas Y220 and Y232 are found within two consensus Abl recognition sites

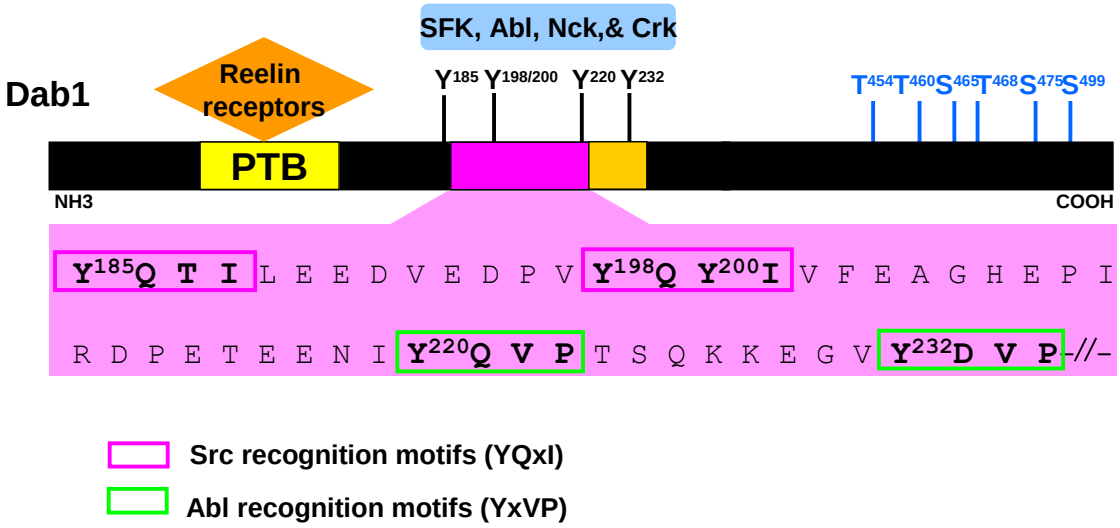

Figure 1.4 Schematic diagram of Dab1 domains. The phosphotyrosine binding (PTB) domain that associates with the Reelin receptors is shown in yellow. Tyrosine and serine residues at the central and C-terminal regions of Dab1 are indicated. YQXI is a consensus Src family kinase phosphorylation site, whereas YXVP is a consensus Abl family kinase recognition site.

(YXVP) (Figure 1.4) (Songyang et al. 1993). At least three of the tyrosine residues, Y198, Y220 and Y232, have been shown to be phosphorylated upon Reelin stimulation in cultured cortical neurons (Keshvara et al. 2001; Ballif et al. 2004). Tyrosine-phosphorylated Dab1 leads to activation of an intracellular signaling cascade by recruiting Src homology 2 (SH2) domain-containing proteins, including non-receptor tyrosine kinase SFK, cellular adaptors such as the Crk family and Nckβ, and p85 (phosphatidylinositide-3-kinase regulatory subunit 1) (Howell et al. 1997a; Ballif et al. 2004; Chen et al. 2004; Huang et al. 2004).

The importance of Dab1 tyrosine phosphorylation in Reelin signaling has been elegantly demonstrated using a knock-in strategy. Mice expressing a mutant Dab1 form with substitutions at all five tyrosine residues exhibit a phenotype similar to that observed in *reeler* and *Dab1*$^{-/-}$ mice (Howell et al. 2000), demonstrating an essential role for Dab1 tyrosine phosphorylation in Reelin signaling. Different tyrosine residues in Dab1 appear to play distinct roles in Reelin signaling. Keshavara et al. showed that Y198 is the primary site that is phosphorylated in response to Reelin (Keshvara et al. 2001), whereas Sanada et al. demonstrated that Y220 or Y232, but not Y198, is required for Reelin-regulated neuronal detachment from radial glia (Sanada et al. 2004). Recent studies using mice expressing mutant forms of Dab1 carrying substitutions at different tyrosine residues suggest that Y185 and Y198 function as primary kinase switches to activate the phosphatidylinositide-3-kinase (PI3K) and Akt pathway and regulate Dab1 protein turnover. In contrast, Y220 and Y232 serve

as scaffold domains to recruit downstream signaling molecules including Crk and Nck adaptor proteins (see below for details) (Feng et al. 2007; Feng and Cooper 2009).

1.1.2.4 Src family kinase (SFK) phosphorylates Dab1 upon Reelin stimulation

Reelin stimulates Dab1 tyrosine phosphorylation by binding to its cell surface receptors, VLDLR and ApoER2 (Bock and Herz 2003). Unlike receptor tyrosine kinases, VLDLR and ApoER2 do not contain kinase domains, thus are not directly involved in Dab1 tyrosine phosphorylation. Biochemical studies have revealed that the non-receptor tyrosine kinase SFK, including Fyn and Src, mediates Reelin-induced Dab1 tyrosine phosphorylation. Inhibition of SFK decreases Dab1 tyrosine phosphorylation in primary cortical neurons and induces a *reeler*-like malformation of the cortical plate in cortical slice cultures (Arnaud et al. 2003; Bock and Herz 2003; Jossin et al. 2003). Furthermore, combined absence of Src and Fyn abolishes Dab1 tyrosine phosphorylation and causes migration defects similar to those of *Reeler* mice, in support of a key role for SFK in the Reelin signaling pathway (Kuo et al. 2005).

SFK activation usually involves an interaction between its kinase SH2 domain and the substrate, which displaces the intramolecular pY527-SH2 domain associations and induces an allosteric rearrangement. Studies have shown that Reelin-induced SFK activation depends on Dab1, as SFK activation is reduced in *Dab1*$^{-/-}$ neurons (Arnaud et al. 2003; Bock and Herz 2003). Dab1 is

therefore both a substrate and an activator of SFK in Reelin signaling. Intriguingly, in order for Dab1 to associate with the SFK SH2 domain, Dab1 has to be tyrosine phosphorylated prior to Reelin-induced SFK activation. However, molecular mechanisms governing the basal phosphorylation of Dab1 are unclear and likely occur in a Reelin-independent manner, as Dab1 basal tyrosine phosphorylation is observed in *reeler* mice (Howell et al. 1999a).

Recently, it has been shown that the clustering of ApoER2 and VLDLR at the plasma membrane upon binding to oligomeric Reelin is required for SFK recruitment to Dab1 and Dab1 tyrosine phosphorylation (Strasser et al. 2004). Treatment of neuronal cells with bivalent agents that specifically bind to ApoER2 and VLDLR and promote receptor clustering also induces Dab1 tyrosine phosphorylation. Moreover, artificial dimerization of Dab1 in HEK293 cells leads to its phosphorylation in the absence of Reelin receptors, indicating that dimerization is critical for the activation of Dab1 (Strasser et al. 2004). It is likely that dimerized Dab1 allows the transphosphorylation of adjacent Dab1 molecules by SFK, which, in turn, leads to further recruitment and activation of SFK. Investigating how the clustering of receptors or Dab1 dimerization activates SFK and induces Dab1 phosphorylation is critical to our understanding of the mechanisms underlying Dab1 activation.

1.1.2.5 Crk-C3G and PI3K-Akt pathways are important downstream targets in the Reelin signaling

As described above, tyrosine-phosphorylated Dab1 transmits the Reelin

signaling to a host of downstream effectors to regulate neuronal cell positioning. The Crk and PI3K mediated pathways have been shown to be important downstream targets in Reelin signaling.

1.1.2.5.1 Essential roles for Crk adaptor proteins in Reelin signaling

The SH2-SH3-SH3 domain proteins Crk (CrkI, CrkII and CrkL) are important intracellular adaptors involved in cell migration, cell adhesion and immune cell response. Crk can bind and activate C3G, a guanine nucleotide exchange factor for the Ras superfamily member Rap1, involved in actin rearrangement (Feller 2001). Reelin promotes Dab1-Crk interaction through Y220 and Y232 (YXVP sites) phosphorylation in Dab1 and activates the C3G-Rap1 pathway (Ballif et al. 2004; Chen et al. 2004); (Huang et al. 2004; Feng and Cooper 2009). *CrkII*$^{-/-}$*CrkL*$^{-/-}$ mice exhibit a phenotype similar to that of *reeler* mice, indicating that Crk proteins are essential components in Reelin signaling. Importantly, Reelin-induced Dab1 tyrosine phosphorylation appears to be normal in the *CrkII*$^{-/-}$*CrkL*$^{-/-}$ mice; however, two Dab1 phosphorylation-dependent downstream signaling events, C3G and Akt activation, are abolished, suggesting that Crk proteins function downstream of Dab1 in the Reelin signaling pathway (Park and Curran 2008). Mice that lack C3G fail to split the preplate and form the cortical plate, a phenotype reminiscent of that observed in *reeler* mice (Voss et al. 2008), suggesting a role for C3G in the regulation of neuronal migration. However, phenotypic differences/divergences are observed between the *CrkII*$^{-/-}$ *CrkL*$^{-/-}$ mice and *C3G*$^{-/-}$ mice, indicating that additional molecules downstream of

Crk, other than C3G, are important in Reelin signaling-mediated neuronal migration.

1.1.2.5.2 PI3K-Akt pathway and n-cofilin

PI3K is a family of related kinases capable of phosphorylating the 3 position hydroxyl group of the inositol ring of phosphatidylinositol (PtdIns). A direct interaction between the Reelin-induced tyrosine-phosphorylated Dab1 (likely Y185 and Y198 sites) and the SH2 domain in the p85 regulatory subunit activates PI3K, which subsequently activates the serine/threonine kinase Akt (Beffert et al. 2002; Ballif et al. 2003; Bock et al. 2003). Akt activation inhibits the glycogen synthase kinase (GSK) 3β, a major kinase for the microtubule-stabilizing protein tau, thus reducing the phosphorylation of tau. Inhibition of the PI3K disrupts normal cortical plate formation in slice cultures, suggesting that PI3K is required for Reelin signaling to mediate the normal cortical development (Bock et al. 2003; Jossin and Goffinet 2007).

Importantly, a recent study has revealed that cofilin, an actin-depolymerizing protein is a downstream target in the Reelin signaling pathway (Chai et al. 2009). Cofilin binds and depolymerizes the actin filaments (Jovceva et al. 2007). Its phosphorylation by the serine/threonine kinase LIM kinase 1 (LIMK1) on serine residue 3 abolishes its ability to depolymerize actin (Arber et al. 1998; Yang et al. 1998a). Chai et al. have shown that Reelin activates LIMK1 and induces cofilin phosphorylation on serine 3 (Chai et al. 2009). Inhibition of PI3K reduced the Reelin-induced phosphorylation of n-cofilin (non-muscle

cofilin), suggesting that these events are located downstream of PI3K (Chai et al. 2009). In the cerebral cortex, phosphorylation of n-cofilin mainly occurs in the leading processes of migrating neurons when they move toward the Reelin-expressing marginal zone (Chai et al. 2009), indicating that Reelin-induced n-cofilin phosphorylation may stabilize and attach these neuronal processes to the marginal zone. However, whether phosphorylation of n-cofilin is required for Reelin-mediated neuronal migration needs further investigation.

1.1.3 Reelin signaling is terminated by Dab1 tyrosine phosphorylation-triggered proteasome degradation

Most signaling pathways use a desensitization mechanism to regain sensitivity to repeated stimulation. A striking feature in mice deficient with key components of Reelin signaling, including Reelin (*reeler mice*), VLDLR and ApoER2 (*Vldlr*$^{-/-}$*Apoer2*$^{-/-}$ mice), Dab1 (Dab1Y5F mice) and Fyn/Src (*Src*$^{-/-}$*Fyn*$^{-/-}$ mice), is the accumulation of Dab1 protein (Sheldon et al. 1997; Rice et al. 1998; Howell et al. 1999a; Trommsdorff et al. 1999; Howell et al. 2000; Kuo et al. 2005). All these genetic deficiencies result in either reduced levels or absence of Dab1 tyrosine phosphorylation, suggesting that Dab1 tyrosine phosphorylation is an important mechanism for the regulation of Dab1 levels and may provide a negative feedback to desensitize the Reelin signaling pathway.

Several studies have shown that Reelin-induced Dab1 tyrosine phosphorylation targets Dab1 for proteasome degradation through the ubiquitination pathway (Arnaud et al. 2003; Bock et al. 2004). In particular,

Reelin-induced Dab1 tyrosine phosphorylation on Y185 and Y198 (YQXI sites) recruits the SH2 domain-containing SOCS proteins (adaptors for cullin-based E3 ubiquitin ligase), resulting in the polyubquitination and degradation of Dab1 protein via the cullin-5 (Cul5) E3 ligase. Knockdown of C*ul5* in the cortex leads to increased levels of Dab1 and an “overmigration” phenotype, with *Cul5* knockdown neurons positioned at the surface of the cortical plate, not allowing late-born neurons to bypass them. This phenotype can be partially rescued by introducing Dab1 shRNA into the Cul5-knockdown cortex (Feng et al. 2007). Electroporation of a Dab1 mutant with lysine to arginine substitutions, which is resistant to the Cul5-mediated proteasome degradation, into the wild-type cortex leads to a phenotype similar to that seen in Cul5-knockdown cortex, suggesting that the “overmigration” phenotype is a consequence of accumulation of active tyrosine-phosphorylated Dab1 protein (Simo et al. 2010). These studies demonstrate that Dab1 tyrosine phosphorylation-triggered Cul5-mediated proteasome degradation is an important mechanism to down-regulate Reelin signaling and prevent the “overmigraton” of cortical neurons. Thus, a tight regulation of Dab1 levels is required to control precise neuronal positioning (Figure 1.5).

1.1.4 Crosstalk between Reelin and other signaling pathways

1.1.4.1 Reelin and amyloid precursor proteins (APP) signaling

The Dab1 PTB domain associates with the YxNPxY motif located within the cytoplasmic tails of APP family members including APP, amyloid precursor-

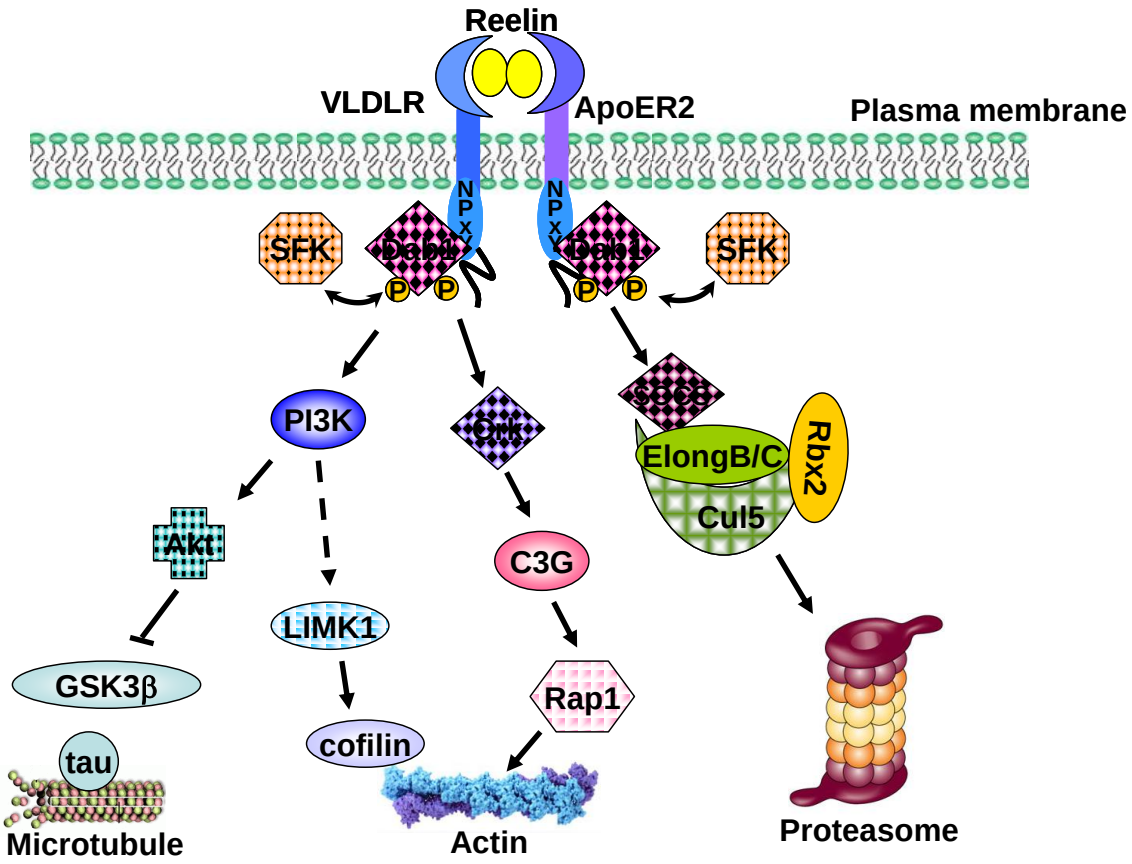

Figure 1.5 Reelin-Dab1 signaling pathway.

like protein 1 (APLP1) and amyloid precursor-like protein 2 (APLP2) (Trommsdorff et al. 1998; Homayouni et al. 1999; Howell et al. 1999b). Proteolysis of APP by the β-secretase, presenilin-1, generates the amyloid β peptide (Aβ), whose homeostasis is critical in the pathogenesis of Alzheimer's disease (AD). Aβ accumulates in amyloid plaques in AD patients, and mutations in APP are associated with familial AD (Bertram et al. 2010).

Dab1 increases cell surface expression of APP but decreases the levels of Aβ-C-terminal fragment and secreted Aβ in primary neurons (Hoe et al. 2006), suggesting that association between Dab1 and APP alters trafficking and processing of APP. Interestingly, this effect appears to be dependent on the Dab1 PTB domain but not on tyrosine phosphorylation (Hoe et al. 2006). Moreover, reduced Reelin expression is associated with premature production of Aβ and increased number and size of Aβ plaques, further supporting a role for Reelin signaling in preventing the formation of Aβ plaques (Kocherhans et al. 2010). A recent study shows that Reelin signaling helps to restore normal synaptic plasticity caused by Aβ accumulation in the brains of AD patients, suggesting that Reelin can antagonize Aβ-induced synaptic failure (Durakoglugil et al. 2009). In addition, studies have shown that APP and Dab1 cooperatively function in the normal cortical plate entry, with Dab1 acting downstream of APP to regulate neuronal cell migration during the formation of the cortical plate (Young-Pearse et al. 2007). Together, these studies suggest that Dab1 and APP interactions may be involved in the regulation of multiple neurodevelopmental processes as well as pathogenesis of AD.

1.1.4.2 Reelin and Notch signaling

Cell-cell interaction-mediated Notch signaling is a crucial signaling pathway governing metazoan development (Louvi and Artavanis-Tsakonas 2006). Delta/Serrate (known as Jagged in mammals) ligand binding to Notch receptors leads to proteolytic release of the Notch intracellular domain (NICD). Translocation of NICD to the nucleus and association with the Rbpj (also known as CBF-1) transcription factors activate target genes such as Hes1 and Hes5 (Louvi and Artavanis-Tsakonas 2006). Notch signaling has a well-characterized role in neuronal differentiation, glial fate determination and neurite elaboration. Interestingly, recent studies also reveal that interactions between Notch and Reelin signaling regulate neuronal migration in the cerebral cortex and hippocampus (Hashimoto-Torii et al. 2008; Sibbe et al. 2009).

Earlier studies have shown that the *Drosophila Dab* PTB domain binds Notch *in vitro* (Giniger 1998; Le Gall et al. 2008). Recently, Dab1 has been found to co-immunoprecipitate with Notch1 in a neural stem cell line and in the embryonic cerebral cortex (Hashimoto-Torii et al. 2008; Keilani and Sugaya 2008). Moreover, reduced levels of the activated NICD and the Notch transcriptional target Hes5, have been reported in *Reeler* mice (Hashimoto-Torii et al. 2008; Sibbe et al. 2009). Electroporation of NICD into *reeler* cortical neurons alleviate the migration defects, whereas inhibition of Notch signaling blocks the Reelin-dependent rescue of the *reeler* phenotype in a hippocampal slice assay (Hashimoto-Torii et al. 2008; Sibbe et al. 2009), suggesting that

Notch and Reelin signaling cooperatively regulate neuronal migration. Biochemical studies show that Reelin-stimulated Dab1 phosphorylation blocks NICD degradation (Hashimoto-Torii et al. 2008), suggesting an important role for Dab1 in regulating Notch signaling. The mechanisms underlying the inhibition of NICD degradation by Dab1 remain unknown. It is possible that Dab1 may regulate NICD trafficking by altering its subcellular localization, resulting in the protection of NICD from ubiquitin-triggered proteasome degradation.

1.1.4.3 Reelin and cyclin dependent kinase 5 (Cdk5)

Cdk5 is a member of the Cdk family that regulates neuronal cell migration. Unlike other Cdks, Cdk5 is mainly active in postmitotic neurons, due to the specific expression of its regulatory subunit p35 in neurons (Tsai et al. 1993). *Cdk5*$^{-/-}$ or *p35*$^{-/-}$ mice exhibit migration defects similar but not identical to those seen in *reeler* mice (Figure 1.2). In contrast to a failure of the subplate split observed in *reeler* mice, the first wave of migrating neurons in *Cdk5*$^{-/-}$ or *p35*$^{-/-}$ mice can successfully split the subplate; however, subsequent migration failures lead to the inversion of layers underneath the preplate (Ohshima et al. 1996; Chae et al. 1997; Gilmore et al. 1998; Kwon and Tsai 1998). *Dab1*$^{-/-}$*p35*$^{-/-}$ mice or *Reelin*$^{-/-}$*p35*$^{-/-}$ mice display additional migration defects in the cerebellum and hippocampus, suggesting that Cdk5 and Reelin synergistically contribute to normal neuronal migration in the developing brain (Ohshima and Mikoshiba 2002; Beffert et al. 2004). The similar migration defects observed in *reeler* and *Cdk5*$^{-/-}$ mice, combined with the well-documented synergy between the Reelin and Cdk5

pathways, suggest that these two pathways may function independently or in parallel to regulate neuronal positioning.

Interestingly, Dab1 has been shown to be phosphorylated by Cdk5 independent of Reelin (Keshvara et al. 2002; Ohshima et al. 2007). In particular, S491 located in the C-terminus of Dab1 has been shown to be an important Cdk5 phosphorylation target both *in vitro* and *in vivo* (Keshvara et al. 2002). *Cdk5*$^{-/-}$ mice have elevated Dab1 levels, suggesting that Cdk5 may be involved in regulating Dab1 levels (Keshvara et al. 2002). In addition, Cdk5-mediated Dab1 phosphorylation appears to inhibit Fyn-mediated Dab1 tyrosine phosphorylation *in vitro*. *Cdk5*$^{-/-}$ neurons show enhanced Dab1 tyrosine phosphorylation in response to Reelin stimulation, suggesting a potential role for Cdk5 in modulating Reelin signaling (Ohshima et al. 2007). Additional studies addressing the functional and physiological significance of Cdk5-mediated Dab1 phosphorylation *in vivo* would be important to reveal the interplay between Cdk5 and Reelin signaling and determine whether Dab1 serves as a convergence point for Reelin and Cdk5 to fine tune neuronal cell migration.

1.1.5 The Reelin pathway regulates dendritic development and synaptic plasticity

The role of Reelin signaling in neuronal positioning is well-established in embryonic brain development. In addition to the laminar defects described in Section 1.1.1, abnormalities in dendrite development and synaptic plasticity have been observed in *reeler* mice, as well as mice deficient in key components of

Reelin signaling (Sheldon et al. 1997; Niu et al. 2004; Olson et al. 2006; Park and Curran 2008). Moreover, components of Reelin signaling are consistently expressed in the adult brain. Recent studies have shown that the Reelin signaling pathway also plays an important role in regulating dendritic development and synaptic plasticity in postnatal brain.

1.1.5.1 Reelin promotes dendritic development

Dendritic arborization of hippocampal neurons has been reported to be severely disrupted in *reeler* mice (Niu et al. 2004). Addition of exogenous Reelin to hippocampal neuron cultures derived from *reeler* mice rescues dendritic developmental defects, suggesting a direct role for Reelin in promoting dendritic development. Similar to neuronal cell migration, Reelin-induced dendritogenesis requires lipoprotein receptors, SFK activation, Dab1 and Crk adaptor protein (Niu et al. 2004; Olson et al. 2006; Katyal et al. 2007; Matsuki et al. 2008; Park and Curran 2008). Moreover, the mTOR (mammalian target of rapamycin)-S6K1 (S6 kinase 1) pathway downstream of PI3K-Akt has also been implicated in Reelin-mediated dendritic development of hippocampal neurons (Jossin and Goffinet 2007). Recent studies show that Reelin regulates the morphology and subcellular distribution of the Golgi apparatus in hippocampal and cortical neurons *in vivo* (Matsuki et al. 2010). As the position of the Golgi apparatus is important in dendritic growth and cell migration (Horton et al. 2005; Fidalgo et al. 2010), these studies provide mechanistic insight into the role of Reelin in regulating dendritic development.

1.1.5.2 Reelin regulates synaptic plasticity

Reelin has been shown to induce long term potentiation (LTP) in wild-type but not *Vldlr*$^{-/-}$*Apoer2*$^{-/-}$ hippocampal slices, suggesting that Reelin regulates synaptic transmission, memory and learning through VLDLR and ApoER2 (Weeber et al. 2002). Further studies have demonstrated that the inclusion of an alternatively spliced exon (exon 19) in *Apoer2* is required for Reelin-mediated synaptic transmission. Exon 19 encodes a domain that mediates interaction between ApoER2 and postsynaptic density protein 95 (PSD-95). This interaction is essential for recruiting ApoER2 and the activated Dab1-SFK complex to the NMDA receptor (NMDAR), which is subsequently phosphorylated by SFK in the postsynaptic density (Beffert et al. 2005). The Dab1 binding sites (FxNPxY motif) in ApoER2 are also necessary for Reelin-enhanced synaptic plasticity, since mice expressing a mutant ApoE2 form with substitutions at these sites display severe abnormalities in LTP and abnormal neurobiological behaviour (Beffert et al. 2006).

Reelin also regulates the subunit composition of synaptic NMDARs and controls the surface mobility of NR2B subunits during synaptic maturation (Groc et al. 2007). A decreased participation of NR1/NR2B receptor in NMDAR-mediated synaptic currents concomitant with an accumulation of Reelin was observed at active synapses. Reelin treatment dramatically reduced NR2B-mediated synaptic currents, whereas blocking Reelin prevented the maturation-dependent reduction of NR1/NR2B-mediated synaptic currents (Isosaka et al.

2006; Groc et al. 2007), suggesting that Reelin regulates synaptic NMDAR assembly at postnatal hippocampal synapses.

1.1.6 Early or late, pro-migratory or anti-migratory - models for Reelin signaling in cortical development

Despite significant advances in our understanding of the importance of Reelin signaling in cortical development, the exact role of Reelin signaling in regulating neuronal migration remains elusive. As Reelin is expressed primarily in Cajal-Retzius cells in the marginal zone of the cortex, it has been proposed that Reelin functions to stop the migration of neurons at the final stages (Rice and Curran 2001). Importantly, in order for late-born neurons to bypass their predecessors, the early-born neurons have to detach from their radial glial guides. Sanada et al. (2004) have shown that neurons from *scrambler* mice (harbouring a spontaneous mutation of Dab1) fail to detach from the radial glial fiber, suggesting that Reelin-Dab1 signaling can promote detachment from radial glia (Sanada et al. 2004). In support of this hypothesis, Reelin has been reported to serve as a detachment signal for chain-migrating interneuron precursors in the olfactory bulb of postnatal mouse brain (Hack et al. 2002).

Earlier studies have shown that association of Reelin with $\alpha 3\beta 1$ integrin inhibits neuronal cell migration, suggesting a mechanism whereby Reelin could promote the detachment of neurons and stop migration (the “detach and stop” model) (Dulabon et al. 2000; Tabata and Nakajima 2002). However, recent studies support a “detach and go” model for Reelin-mediated promotion of

neuronal migration (Cooper 2008). First, ectopic expression of Reelin in the ventricular zone can rescue the subplate split phenotype in the *reeler* cortex and cortical slice cultures (Magdaleno et al. 2002; Jossin et al. 2004) Ectopic Reelin also induces neuronal aggregation, with an “inside-out” assembly of cortical neurons in the developing cerebral cortex (Kubo et al. 2010). Second, functional Reelin fragments have been found to diffuse throughout the cortex, suggesting that neurons can be exposed to Reelin before they reach the layer adjacent to the Reelin-expressing marginal zone (Jossin et al. 2004). In support of this idea, Uchida et al. have detected Reelin-induced downregulation of functional Reelin receptors in the intermediate zone, away from the marginal zone (Uchida et al. 2009). Third, knockdown of *Dab1* in the wild-type cortex delays neuronal migration (Olson et al. 2006), whereas introducing wild-type Dab1 into *Dab1*$^{-/-}$ cortex promotes the migration of neurons out of the ventricular zone or the deep layers of the cortical plate (Simo et al. 2010).

It should be noted that neither the “detach and stop” nor “detach and go” models can completely explain the *reeler* phenotype resulting from Reelin signaling deficiency. Time-lapse studies tracking the migratory behaviour of neurons may help to understand the underlying mechanisms for Reelin-regulated neuronal positioning during development. Further studies may reveal additional regulatory mechanisms (e.g. developmentally-regulated alternative splicing of Dab1 and effect of Reelin on radial glial cells) involved in modulating neuronal migration at different developmental stages (Kim et al. 2002; Keilani and Sugaya 2008; Yano et al. 2010).

1.1.7 Alternative splicing of Dab1 during development

The *Dab1* gene has a highly complex organization. The mammalian *Dab1* gene spans over 1 Mb with an open reading frame of 1668 bp (Bar et al. 2003). Different alternative splicing events, including alternative promoter usage, alternative cassette exons and mutually exclusive alternative exons, have been documented for Dab1 in multiple species including zebrafish, lizard, chick, mouse and human (Howell et al. 1997a; Bar et al. 2003; Katyal and Godbout 2004; Costagli et al. 2006; Yano et al. 2010).

Other than the commonly-studied Dab1 form, Dab1 ($Dab1^{555}$), three Dab1 isoforms $Dab1^{217}$, $Dab1^{271}$ and $Dab1^{555*}$(Dab1.7bc), generated from alternative splicing events occurring in the coding region, have been described in mice (Howell et al. 1997a; Bar et al. 2003; Yano et al. 2010). All these Dab1 isoforms retain the intact PI/PTB domain at the N-terminus, but differ in the middle tyrosine-enriched region or in the C-terminus. $Dab1^{217}$ contains an alternative exon (57 bp) inserted after exon 7, whereas $Dab1^{271}$ contains an alternative exon (93 bp) inserted after exon 9 (Howell et al. 1997a). It is noteworthy that alternative exons included in both $Dab1^{217}$ and $Dab1^{271}$ introduce in-frame premature termination codons (PTC), which may promote RNA degradation through nonsense mediated mRNA decay (NMD). In contrast, $Dab1^{555*}$ contains two alternative exons [exons 9b (51 bp) and 9c (48 bp), 99 bp in total] inserted in-frame between exons 9 and 10 (Howell et al. 1997a; Bar et al. 2003; Yano et al. 2010). Homologues of exons 9b and 9c have been also detected in chicken and

lizard (Katyal and Godbout 2004). Interestingly, Dab1^{555*} appears to be specifically expressed in non-neuronal cells, suggesting that the exclusion of exons 9b and 9c parallels neuronal differentiation (Bar et al. 2003; Yano et al. 2010).

In chicken, two Dab1 isoforms arising from mutually exclusive splicing events have been identified at different stages of retinal and brain development (Katyal and Godbout 2004). Dab1-Late (Dab1-L), expressed in neurons at late developmental stages, represents the extensively-studied Dab1 isoform which contains the four conserved tyrosine phosphorylation sites described above. In contrast, Dab1-Early (Dab1-E), expressed in undifferentiated cells in the retina and brain, is missing exons 7 and 8 (105 bp) but includes an additional exon 9b (57 bp). Exon 9b is homologous to the duplicated murine exons 9b and 9c in Dab1^{555*} (Bar et al. 2003; Katyal and Godbout 2004; Yano et al. 2010). The exclusion of exons 7 and 8 in Dab1-E leads to deletion of a 35 aa region containing the Y198 and Y220 phosphorylation sites, whereas the inclusion of exon 9b results in insertion of a 19 aa region with unknown function. Interestingly, the Y185 phosphorylation site (YQXI, SFK recognition site) in Dab1-E is converted to an Abl recognition site (Y^{185}QVP). Thus, Dab1-E lacks two SFK phosphorylation sites but retains two Abl phosphorylation sites (converted Y185 and Y232). To date, Dab1 isoforms that skip both exons 7 and 8 have not been reported in other species; however, a Dab1 isoform that skips exons 8 and 9 has been reported in zebrafish (Costagli et al. 2006).

Although multiple Dab1 isoforms have been documented, the only Dab1

form that has been studied in detail to date is the Dab1^{555} (Dab1-L in chicken). We have shown that transfection of a Dab1-L expression construct into primary chick retinal cultures induces the formation of neurite-like processes, accompanied by induction of tyrosine phosphorylation, phosphorylation of Dab1-L and activation of SFK (Katyal and Godbout 2004). In contrast, primary retinal cultures transfected with a Dab1-E expression construct retain an epithelial-like appearance with no induction of either tyrosine phosphorylation or SFK activation. These results indicate that Dab1-E and Dab1-L isoforms may have distinct functions during development (Katyal and Godbout 2004).

Transfection of the Dab1 isoform, Dab1^{555*} into wild-type mouse cortex specifically affects the migration of late-born neurons, with late-born neurons jammed in the deeper layers of the cortex, whereas the preplate formation remains normal (Yano et al. 2010). The neuronal-specific splicing factors neuron-oncological ventral antigen (Nova1 and Nova2) have been recently shown to inhibit the inclusion of exons 9b and 9c in Dab1 (Ule et al. 2005; Ule et al. 2006; Yano et al. 2010). Ablation of Nova2 in mice leads to increased expression of Dab1^{555*} and migration defects similar to those observed in *reeler* mice (Yano et al. 2010). Introduction of a wild-type Dab1 expression construct into *Nova2*$^{-/-}$ mice rescues the migration defects, suggesting that Dab1 and Dab1^{555*} may function antagonistically to regulate neuronal migration. Intriguingly, biochemical studies show that Dab1^{555*} is tyrosine-phosphorylated and recruits Crk adaptor proteins, suggesting that it is capable of transmitting the Reelin signal. How Dab1^{555*} antagonizes Dab1 function needs to be further investigated. The fact

that increased expression of Dab1^{555*} only affects migration of late-born neurons suggests a specific role for Dab1^{555*} in the migration of early-born neurons.

1.1.8 Reelin signaling and neurological disorders

Deficiency in Reelin signaling leads to widespread defects in neuronal positioning, synaptic plasticity and dendritogenesis in mice. In humans, Reelin signaling has been implicated in a wide range of neurological disorders, including lissencephaly, schizophrenia, epilepsy and Alzheimer's disease (AD).

Mutations in *Reelin* are directly associated with autosomal recessive lissencaphaly, a disorder characterized by severe neuronal migration defects in the cerebral cortex and cerebellum, along with ataxia, severe cognitive delay, hypotonia and seizures (Hong et al. 2000; Zaki et al. 2007). Recently, mutations in *Vldlr* have been identified as a cause for autosomal recessive cerebellar ataxia with mental retardation (dysequilibrium syndrome) and VLDLR-associated cerebellar hypoplasia has become a clinically, and molecularly well-defined genetic syndrome (Boycott et al. 2005; Ozcelik et al. 2008; Boycott et al. 2009; Kolb et al. 2010). Mutations in *Dab1* or *ApoER2* in human diseases have not been reported to date.

Reduced levels of Reelin expression are associated with schizophrenia, autism, epilepsy and AD (Impagnatiello et al. 1998; Fatemi et al. 1999; Fatemi et al. 2000; Guidotti et al. 2000; Dong et al. 2005; Fatemi et al. 2005; Grayson et al. 2005; Noh et al. 2005). In particular, multiple aspects of Reelin signaling have been implicated in AD. First, Dab1 directly regulates the trafficking of APP and

inhibits the proteolytic cleavage of APP, thus reducing the levels of Aβ (Hoe et al. 2006), whose accumulation and resulting plaque formation disrupts synaptic function and ultimately leads to neuronal death in AD patients. Second, Reelin signaling antagonizes Aβ-induced synaptic dysfunction by preventing LTP suppression (Durakoglugil et al. 2009). Third, fibrillar aggregates of hyperphosphorylated tau, the axonal microtubule stabilizing protein, are toxic to neurons and are associated with the pathogenesis of AD. As described earlier (Section 1.1.2.5.2), Reelin signaling inhibits the phosphorylation of tau, and accumulation of hyperphosphorylated tau has been observed in *Reelin*$^{-/-}$, *Vldlr*$^{-/-}$ *Apoer2*$^{-/-}$ and *Dab1*$^{-/-}$ mice (Hiesberger et al. 1999; Brich et al. 2003). Fourth, reduced Reelin expression and deficiency in Reelin receptors accelerate Aβ plaque formation and tau pathology in transgenic AD mice (Kocherhans et al. 2010). Together, these studies suggest that Reelin signaling likely plays a protective role in neurons by reducing Aβ generation and inhibiting tau phosphorylation.

1.2 DEVELOPMENT OF THE EYE IN VERTEBRATES

The vertebrate eye develops primarily from three types of embryonic tissue: the neuroectoderm which gives rise to the retina and retinal pigmented epithelium (RPE); the mesoderm which differentiates into the sclera, iris and choroid; and the surface ectoderm which generates the lens and cornea.

The earliest events in eye development involve the formation of the optic vesicle which evaginates from the walls of the part of the neural tube destined to

become the forebrain (Figure 1.6). The optic vesicle expands laterally into the surrounding mesoderm and remains connected to the developing forebrain by the optic stalk, which eventually becomes the optic nerve. When the optic vesicle contacts the surface ectoderm, inductive signals trigger the thickening of the surface ectoderm to form the lens placode (Eglen et al. 2006). The lens placode then internalizes, pinches off, and forms the lens vesicle. Meanwhile, invagination of the optic vesicle results in the formation of the bilayered optic cup. The outer layer of the optic cup gives rise to the RPE, whereas the inner layer differentiates into the neural retina. During optic cup formation, surrounding mesenchymal cells migrate in to form the sclera, iris, choroid, ciliary body, and blood vessels of the eye. The cornea is derived from the surface ectoderm (Eglen et al. 2006).

1.2.1 Retinal development

The retina consists of six major classes of neurons (cone, rod, bipolar, amacrine, horizontal and ganglion) and one class of glia cell (Müller) (Figure 1.7). The cell bodies and processes of retinal cells are organized into six distinct layers in the mature retina, with cell bodies located in the outer nuclear, inner nuclear and ganglion cell layers, whereas the processes and synaptic contacts are mainly found in the inner plexiform, outer plexiform and optic nerve fiber layers. Cone and rod photoreceptors in the outer nuclear layer (ONL) capture light photons and transmit electrical signals across the outer plexiform layer (OPL) to the inner nuclear layer (INL). Horizontal, bipolar and amacrine cells,

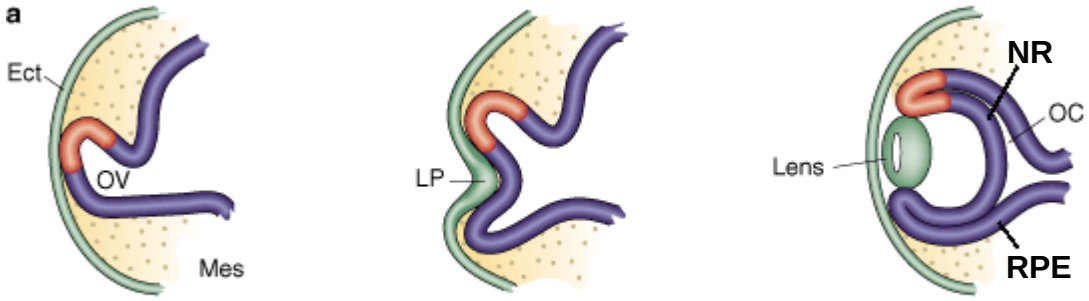

Figure 1.6 Vertebrate eye development. OV, optic vesicle; Ect, ectoderm; Mes: mesenchyme; LP, lens placode; NR, neural retina; RPE: retina pigmented epithelium

Reproduced and adapted with permission from MacMillan Publishers Ltd: [Nat Cell Biol.] (Weaver M, Hogan B (2001) 3: E165-7) copyright (2001).

A

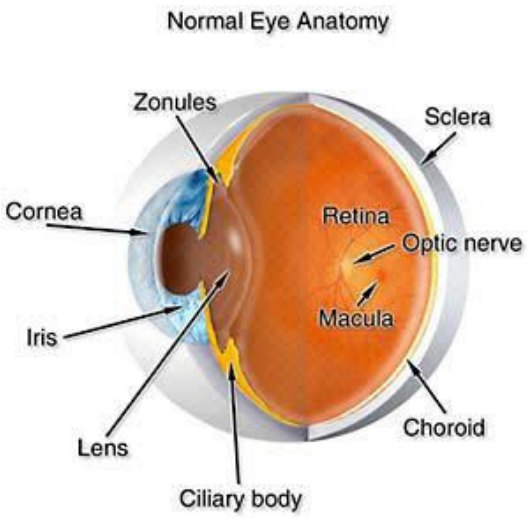

B

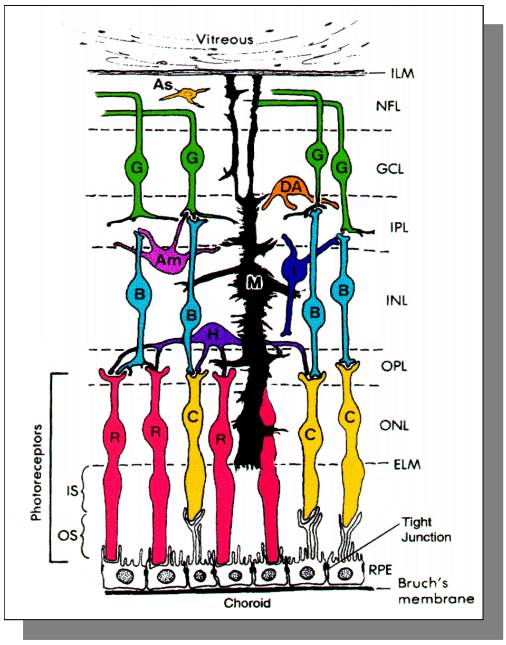

G= Ganglion cells
DA= Displaced amacrine cells
Am= Amacrine cells
I= Interplexiform cells
M= Müller glial cells
B= Bipolar cells
H= Horizontal cells
R= Rod photoreceptors
C= Cone photoreceptors

Figure 1.7 Schematic of the vertebrate eye and retinal organization.

A is reproduced from http://www.eye-exercises-for-good-vision.com/eye-exercises.html. B is reproduced from Retina. Basic Science and Inherited Retinal Diseases. The C.V. Mosby Company, St. Louis (1989).

located in the INL, process and convey the signal through the inner plexiform layer (IPL) to the ganglion cell layer (GCL). Ganglion cell axons pass on the visual signal through the optic nerve to the visual cortex (Eglen et al. 2006).

Retinal development involves cell proliferation, cell birth, cell migration, cell differentiation and cell maturation which occur in a sequential and overlapping manner (Adler 2000). At early developmental stages, the retinal neuroepithelium consists of multipotent retinal progenitor cells (RPCs) that have the potential to differentiate into all seven retinal cell types described above (Turner and Cepko 1987; Holt et al. 1988). As development proceeds, RPCs go through a series of competence states that gradually restrict their multipotency (Cepko et al. 1996; Livesey and Cepko 2001; Cayouette et al. 2006; Wong and Rapaport 2009). This ensures that retinal cells are generated in a specific order: ganglion first; followed by horizontal, amacrine, cone and rod; finally bipolar and Müller glial cells (Figure 1.8). A combination of extrinsic and intrinsic factors tightly regulates RPC competence and proliferation, ensuring that the right number of the right cell type is produced at the right time in the retina.

1.2.2 Regulation of RPC proliferation

1.2.2.1 Extrinsic signals regulating RPC competence

Extrinsic factors shown to regulate retinogenesis include the Notch, fibroblast growth factor (FGF), sonic hedgehog (Shh) and ciliary neurotrophic factor

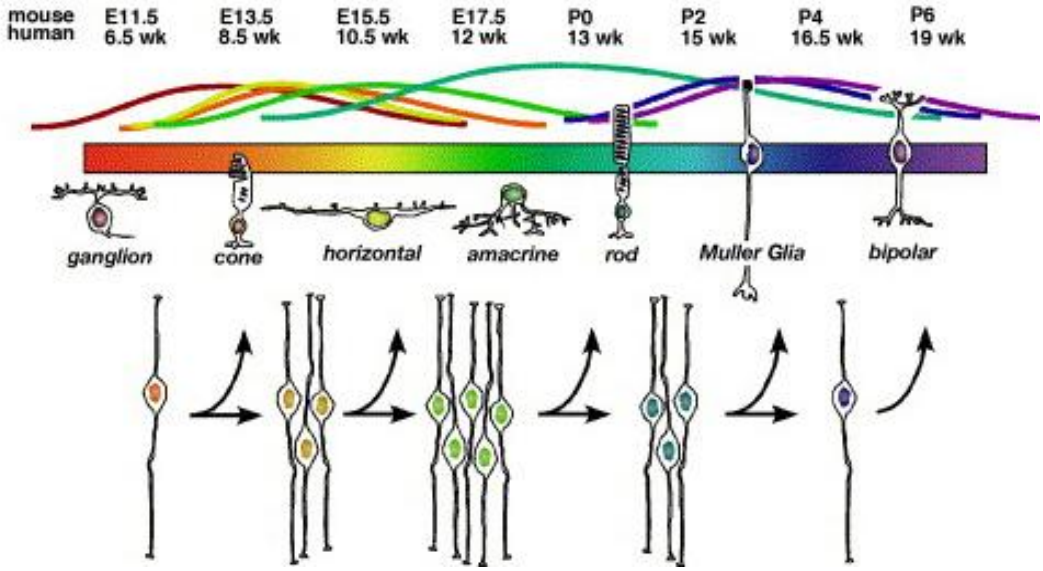

Figure 1.8 Retinal progenitor cells give rise to the seven major classes of cells in a conserved birth order. Multipotent retinal progenitor cells undergo unidirectional changes in competence. For example, early progenitors produce early-born cell types (ganglion cells) and late progenitors produce later-born cell types (bipolar cells). The change in the colour of the nuclei in the bottom panel reflects the changes in competence. The curves above each cell type indicate the birth order. Abbreviations; ONL, outer nuclear layer; OPL, outer plexiform layer; INL, inner nuclear layer; IPL, inner plexiform layer; GCL, ganglion cell layer.

Reproduced and adapted with permission from Donovan SL, Dyer MA (2005) Semin Cell Dev Biol. 16: 407-21.

(CNTF) signaling pathways (Ezzeddine et al. 1997; Wang et al. 2005; Bhattacharya et al. 2008). These extrinsic signals regulate RPC proliferation by influencing the activities of intrinsic regulators.

The Notch signaling has been shown to maintain progenitor cell competence by preventing premature cell cycle exit and differentiation of progenitor cells (Gaiano et al. 2000; Jadhav et al. 2006). Binding of Notch ligand, Delta-1 or Serrate, induces a proteolytic cleavage and releases the Notch intracellular domain (NICD). NICD translocates to the nucleus and associates with the DNA-binding CSL transcription factor (also known as Rbpj), resulting in the activation of basic helix-loop-helix (bHLH) transcription repressor Hes1 (hairy and enhancer of split 1) and Hes5 (Artavanis-Tsakonas et al. 1995; Artavanis-Tsakonas et al. 1999; Nelson et al. 2006). Hes1 and Hes5 repress the expression of proneuronal bHLH genes including *atonal (ath)* in the developing retina, thus maintaining the progenitor pool and inhibiting neuronal differentiation (Jadhav et al. 2006; Yaron et al. 2006). Depending on the developmental stages, Notch inhibition can promote either ganglion cell differentiation or photoreceptor fate (Austin et al. 1995; Yaron et al. 2006). Misexpression of Notch at late stages of development promotes gliogenesis at the expense of retinal neurons (Furukawa et al. 2000; Jadhav et al. 2006). Recent studies have shown that other signaling pathways can regulate RPC proliferation either in conjunction with Notch or by directly targeting the downstream effectors of Notch signaling. For example, CNTF activates the Janus kinase-signal transducer and activator of transcription (Jak-STAT) pathway in concert with Notch signaling to prevent RPC differentiation

along the photoreceptor lineage (Bhattacharya et al. 2008), whereas Shh signaling directly activates Hes1 to maintain RPC competence, independently of Notch signaling (Wall et al. 2009).

1.2.2.2 Intrinsic factors regulating RPC proliferation

Accumulating evidence demonstrates that a multitude of transcription factors, including Rx1, Pax6, Lhx2, Six3, Six6/Optx2, Prox1 and Chx10 are involved in the regulation of RPC proliferation at early stages of development. Forced expression of Pax6, Six3, Rx1 and Six6 leads to ectopic eye formation (Mathers et al. 1997; Chow et al. 1999; Loosli et al. 1999; Zuber et al. 1999; Zuber et al. 2003). In contrast, genetic inactivation of *Rx*, *Pax6*, *Six3* and *Lhx3* leads to early arrest, or failure to form the optic vesicle, resulting in a complete loss of eye structures, making it difficult to evaluate the specific roles of these factors in regulating RPC proliferation (Mathers et al. 1997; Chow et al. 1999; Loosli et al. 1999; Zuber et al. 1999; Zuber et al. 2003).

Interestingly, conditional inactivation of *Pax6* in the distal optic cup before the onset of cell differentiation results in exclusive amacrine cell differentiation, indicating that Pax6 is essential for the multipotency of RPCs and the generation of neuronal diversity in the retina (Marquardt et al. 2001). Recent studies show that RPCs from *Pax6*$^{-/-}$ mice exhibit reduced proliferation with defects in cell cycle, whereas over-expression of *Pax6* promotes RPC proliferation, supporting a role for Pax6 in the regulation of RPC proliferation (Marquardt et al. 2001; Philips et al. 2005; Oron-Karni et al. 2008). Null mutation of *Chx10* (ceh-10 homeobox-

containing homologue) results in a much smaller retina with absence of bipolar cells, demonstrating that Chx10 is required for normal RPC proliferation as well as bipolar cell differentiation (Burmeister et al. 1996). The homeobox protein Prox1 also plays a key role in the regulation of RPC proliferation (Dyer 2003). Inactivation of Prox1 leads to continuous proliferation of progenitor cells and a shift of retinal cells from early-born to late-born cell types. Ectopic expression of Prox1 in rat RPCs leads to premature cell cycle exit, suggesting that Prox1 regulates the timely cell cycle exit of RPCs (Dyer et al. 2003).

1.2.3 Cell fate determination in the retina

The vertebrate retina is a well-established system for studying neuronal cell specification. The interplay between PRC proliferation and cell fate specification is important for retinal development. RPC proliferation ensures that the required number of retinal cells is produced, whereas cell fate specification ensures that the required types of retinal cells are produced (Dyer 2003). Combinatorial action of extrinsic signals (e.g. environmental cues) and intrinsic factors (e.g. transcription factors) controls cell fate specification (Ohsawa and Kageyama 2008).

1.2.3.1 Ganglion cells

Retinal ganglion cells (RGCs) are the earliest-born cells in the retina. A regulatory hierarchy including Notch signaling and a number of transcription factors such as Pax6, Ath5 and Brn3 are involved in the specification of RGCs

(Liu et al. 2001; Matter-Sadzinski et al. 2005). Notch signaling negatively regulates RGC specification. RPCs with slightly higher Delta-Notch activity prevent their immediate neighboring cells from becoming neurons, including ganglion cells (Schneider et al. 2001). Notch and the homeobox transcription factor Pax6 oppose each other in regulating downstream genes required for RGC specification: Pax6 activates *Ath5*, a gene essential for RGC specification, whereas Notch inhibits *Ath5* expression (Marquardt et al. 2001; Schneider et al. 2001; Mu and Klein 2004). The opposing effect of Pax6 and Notch signaling ensures that *Ath5* is expressed in the subset of RPCs that is competent for RGC specification.

Targeted disruption of *Ath5* in mice leads to loss of 80% RGCs along with overproduction of amacrine cells, whereas overexpression of Ath5 promotes RGC differentiation at the expense of amacrine cells (Brown et al. 1998; Brown et al. 2001; Wang et al. 2001). In *Ath5*$^{-/-}$ mouse retina, the expression of genes involved in amacrine cell lineage specification such as Ath3 and NeuroD is up-regulated, indicating that Ath5 not only promotes RGC formation but also suppresses the production of amacrine cells (Mu et al. 2005).

An important downstream target of Ath5 in RGC specification is the POU domain transcription factors Brn3 family (Liu et al. 2000; Liu et al. 2001; Wang et al. 2001). Although Brn3a, 3b and 3c were initially shown to be primarily involved in RGC differentiation, recent studies suggest that Brn3b is critical for specifying RGC fate rather than differentiation (Qiu et al. 2008). In addition, different

members of the Brn3 family have recently been shown to play distinct roles in determining RGC diversity (Badea et al. 2009).

1.2.3.2 Amacrine cells

Specification of amacrine cell fate requires combinatorial control of different classes of transcription factors. The forkhead transcription factor FoxN4 has been shown to be critical in determining amacrine cell fate (Li et al. 2004). Targeted disruption of *FoxN4* leads to a severe reduction in the number of amacrine cells and complete loss of horizontal cells (Li et al. 2004). Downstream of *FoxN4* lies three bHLH transcription factors involved in amacrine cell genesis, including Ptf1a (pancreas transcription factor 1a), NeuroD and Ath3. In *FoxN4*$^{-/-}$ mouse retina, the expression of Ptf1a is completely lost, whereas the expression of Ath3 and NeuroD is retained in a small population of amacrine cells, indicating that *FoxN4* only regulates *NeuroD* and *Ath3* expression in a subset of cells (Li et al. 2004; Fujitani et al. 2006). The presence of *Ath3* and *NeuroD* in a subset of cells may account for the residual amacrine cells observed in *FoxN4*$^{-/-}$ mice.

Inactivation of *Ptf1a* in mice leads to absence of horizontal cells, a significant decrease of amacrine cells, suggesting that Ptf1a is required for both amacrine and horizontal cell generation (Fujitani et al. 2006). Levels of Ath3 and NeuroD remain unaffected in *Ptf1a* null mutants, suggesting that these bHLH transcription factors are likely to function downstream of FoxN4. Inactivation of *NeuroD* or *Ath3* alone in mice either leads to delayed amacrine cell differentiation or has no effect on amacrine cell differentiation, whereas inactivation of both *NeuroD* and

Ath3 results in a severe reduction in amacrine cells (Hatakeyama et al. 2001; Inoue et al. 2002). Misexpression of either NeuroD or Ath3 does not lead to increased production of amacrine cells, although misexpression of NeuroD or Ath3 along with Pax6 or Six3 promotes amacrine cell fate. These combined data indicate that amacrine cell fate determination is dependent on both bHLH and homeobox transcriptional factors (Inoue et al. 2002).

Amacrine cells include many subtypes of cells characterized by the expression of different neurotransmitters. Recent analyses have shown that the specification of different amacrine cell subtypes depends on different transcription factors: the homeobox transcription factor Barhl2 which specifies glycinergic amacrine cells (Mo et al. 2004), bHLH factor Bhlhb5 which is required for GABAergic amacrine cell specification (Feng et al. 2006), and Isl1 which is essential for cholinergic amacrine cell specification (Elshatory et al. 2007).

1.2.3.3 Horizontal cells

As described above, both FoxN4 and Ptf1a are critical for horizontal cell fate specification based on mouse knockout experiments. However, misexpression of FoxN4 promotes amacrine, but not horizontal cell fate, suggesting that additional factors are required for horizontal cell fate specification (Li et al. 2004). In contrast, inactivation of Prox1 leads to absence of horizontal cells, whereas ectopic expression of Prox1 promotes horizontal cell differentiation, indicating that Prox1 is essential for horizontal cell production (Dyer et al. 2003) (Figure 1.9).

1.2.3.4 Photoreceptor cells

Two homeobox proteins Otx2 and Crx have been implicated in photoreceptor cell determination. The paired-type homeobox transcription factor Otx2 is expressed in RPCs as well as early photoreceptor precursors. Conditional inactivation of O*tx2* in RPCs leads to complete loss of rods and cones, whereas overexpression of Otx2 promotes rod cell fate (Nishida et al. 2003). Otx2 transactivates the cone-rod homeobox protein Crx, which is required for the terminal differentiation and maintenance of photoreceptors (Furukawa et al. 1997). The ligand-activated transcription factor retinoid-related orphan nuclear receptor beta (Rorβ) acts downstream of Crx and promotes the differentiation of rod photoreceptors (Jia et al. 2009). *Ror$\beta^{-/-}$* mice are completely devoid of rods, a phenotype that is accompanied by an overproduction of primitive S cones lacking outer segments. Like Rorβ, the neural retinal leucine zipper protein (Nrl), a basic motif-leucine zipper transcription factor that is preferentially expressed in rod photoreceptors, is also involved in the determination of rod cell fate (Cheng et al. 2004). Genetic inactivation of *Nrl* in mouse retina leads to the absence of Nr2e3, a photoreceptor-specific orphan nuclear receptor that activates rod-specific genes but represses cone-specific genes. Thus, Nrl promotes rod cell fate by

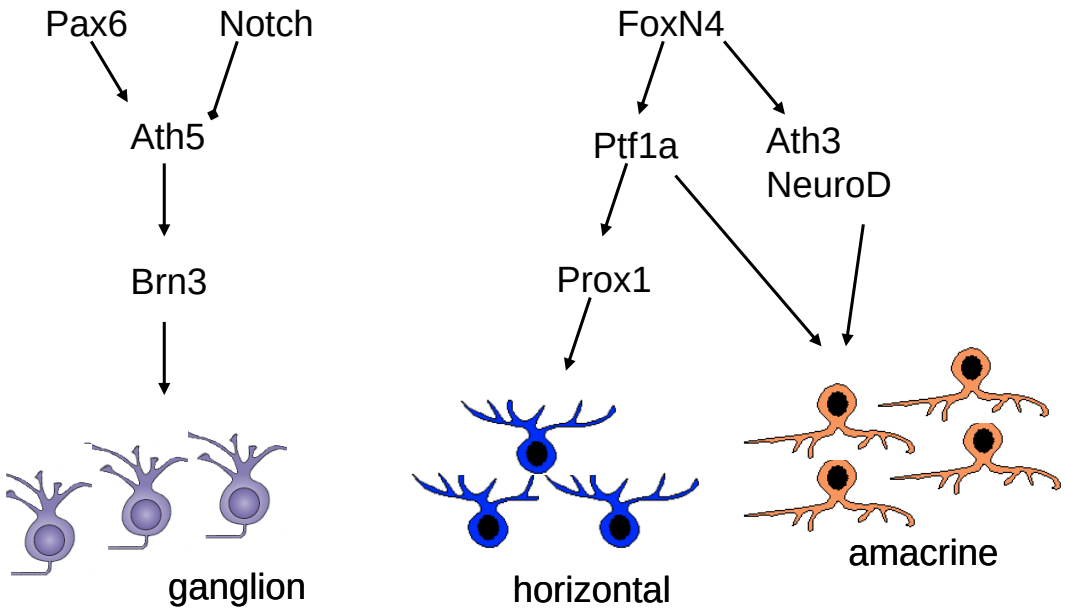

Figure 1.9 Cell fate specifications of ganglion, amacrine and horizontal cells

regulating the expression N2e3 which suppresses cone differentiation (Cheng et al. 2004; Cheng et al. 2006). Interestingly, Nrl expression is lost in *Rorβ-/-* mice and reexpression of Nrl converts cones to rod-like cells, suggesting that Rorβ promotes rod cell differentiation, likely by inducing the Nrl-mediated rod pathway (Jia et al. 2009).

1.2.3.5 Bipolar cells

Bipolar cell specification involves the bHLH factors Math3 and Mash1 as well as the paired-like homeobox protein Chx10. Misexpression of Mash1 or Math3 alone does not promote bipolar cell fate. *Mash1*$^{-/-}$ mice show a reduced number of bipolar cells, whereas *Math3*$^{-/-}$ mice show no obvious alterations in bipolar cell fate (Hatakeyama et al. 2001). However, in *Mash1*$^{-/-}$*Math3*$^{-/-}$ double mutant mouse retina, there is an absence of bipolar cells accompanied by increased Müller gliogenesis, suggesting that Mash1 and Math3 promote bipolar cell specification and inhibit gliogenesis (Tomita et al. 2000; Hatakeyama et al. 2001).

Another important factor in bipolar cell determination is Chx10. As described above, Chx10 is expressed in both RPCs and differentiated bipolar cells. *Chx10* null mice display a complete loss of bipolar cells, indicating that Chx10 is required for bipolar cell specification (Burmeister et al. 1996). Ectopic expression of Chx10 alone does not promote mature bipolar cell production; however, expression of Chx10 along with Mash1 or Math3 leads to bipolar cell generation (Hatakeyama et al. 2001). Together, these studies suggest that full specification of bipolar cells requires the activities of both Chx10 and Mash1 or Math3. Recent

studies have revealed additional factors specifying subtypes of bipolar cells, with the homeobox gene Vsx1 required for the generation of OFF-cone bipolar cells (Chow et al. 2004; Ohtoshi et al. 2004), and Bhlh4 required for rod bipolar cell differentiation (Bramblett et al. 2004).

1.2.3.6 Müller cells

Müller cells are the last cell type produced during retinogenesis. Down-regulation of Notch signaling, either by inhibition of Notch receptor cleavage, or by targeted disruption of downstream effectors, Hes1 or Hes5, leads to decreased Müller glia cell generation. Activation of the Notch signaling pathway at late developmental stages promotes Müller glial cell fate (Furukawa et al. 2000; Yaron et al. 2006). In addition, Sox9, a HMG-box transcription factor, specifically expressed in RPCs and Müller glia cells promotes Müller glia cell fate, as demonstrated by the reduced number of Müller glia cells in *Sox9*$^{-/-}$ mice (Figure 1.10) (Poche et al. 2008).

1.2.4 Cell migration

RPCs undergo a cell cycle-dependent nuclear movement, known as interkinetic nuclear movement (INM), within the neuroepithelium (Frade 2002; Murciano et al. 2002), with mitosis occurring at the apical surface (next to the RPE) and DNA synthesis occurring on the opposite side (next to the vitreous body) (Baye and Link 2007). As a result, retinal cells are always generated at the

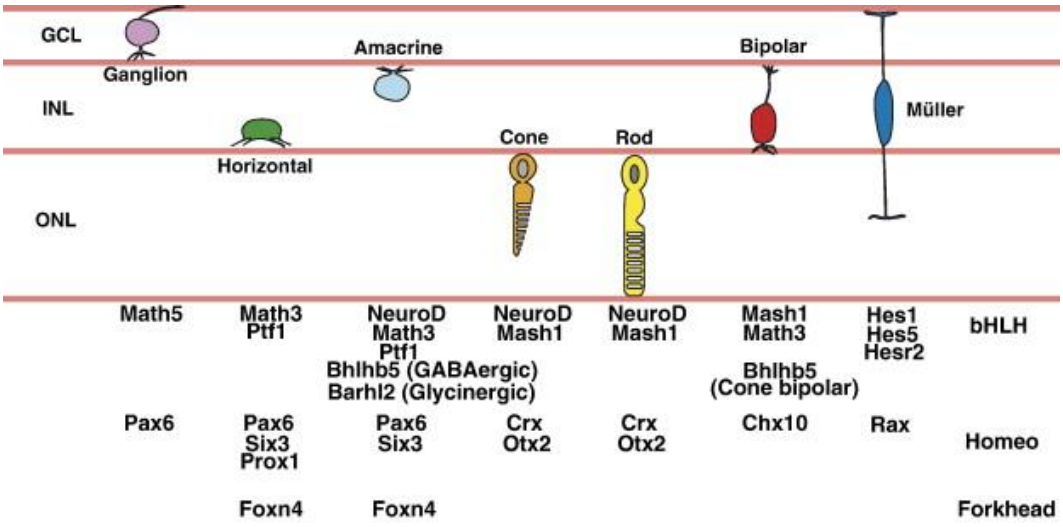

Figure 1.10 Regulation of retinal cell fate specification by transcription factors. Combinations of transcription factors, such as bHLH-type and homeobox-type factors, are required for proper specification of retinal cell types.

Reproduced with permission from Ohsawa R, Kageyama R (2008) Brain Res. 1192: 90-8.

apical surface, and newly generated cells have to migrate to their final position in order to form appropriate layers and synaptic connections, similar to that observed in most parts of the brain (Prada et al. 1981; Prada et al. 1991; Lillien 1994; Livesey and Cepko 2001). Given its small size, laminated structure and temporal appearance of different cell types, the retina may not use the same migratory mechanisms adopted by other parts of the brain (Hatten 1999).

Studies on retinal cell migration are in its infancy. Early studies on the migratory property of postmitotic retinal precursors were mainly based on Golgi impregnations and electron microscopy studies at different developmental stages (Prada et al. 1981; Prada et al. 1991). These studies, combined with more recent time-lapse microscopic analysis, have revealed two main migratory modes for retinal cells to reach their final laminations: somal translocation and unconstrained migration, (McLoon and Barnes 1989; Poggi et al. 2005b).

RGCs, the earliest born retinal cells, migrate to the prospective ganglion cell layer (GCL) using somal translocation. Upon exiting the cell cycle, RGCs at the apical surface extend a leading process towards the basal side, while remaining attached to the outer limiting membrane (OLM) through a trailing process. The ganglion cell body then translocates within the leading process until it reaches the appropriate layer in the retina (McLoon and Barnes 1989; Poggi et al. 2005a). Somal translocation is also used by other retinal cell types, with cone and rod photoreceptors as well as bipolar cells shown to adopt somal translocation to reach their final position (Poggi et al. 2005a; Morgan et al. 2006).

In contrast, amacrine cells use a distinct migratory mode, namely,

unconstrained migration, to reach their final position. These cells migrate without obvious leading or trailing processes. Time-lapse studies have shown that most amacrine cells extend numerous undirected neurites during migration, likely to sense local migration cues, with no attachments to the OLM or INM (inner limiting membrane) (Godinho et al. 2005). Horizontal cells also migrate without forming attachments but retain a bipolar morphology. A unique feature of horizontal cell migration is its bi-directionality, whereby newborn horizontal cells first move to the vitreal side of the retina (adjacent to the ILM), bypassing the final layer, and then migrate back towards the RPE to arrive at the outer part of the INL (Edqvist and Hallbook 2004).

It has also been proposed that Müller glial cells, like radial glial cells in the cortex, may provide guidance for retinal cell migration (Wolburg et al. 1991). However, radial glial cells are present at the earliest stages of cortical development, whereas Müller glial cells are the last cell type to be generated during retinogenesis. As Müller glial cells appear after ganglion and amacrine cells have reached their final destination, it is unlikely that Müller glial cells can provide guidance for retinal cell migration, at least at the earlier stages of development.

Molecular mechanisms governing neuronal cell migration in the cortex may also apply to retinal cell migration. In particular, signaling molecules regulating somal translocation, including Cdk5 and focal adhesion kinases involved in microtubule-coupled nucleokinesis, may be important for retinal cell migration (Tsai and Gleeson 2005). Notably, the Reelin signaling pathway, a key regulator

of radial glial-guided migration during cortical development (D'Arcangelo et al. 1995), appears to be dispensable for retinal lamination, as retinal layers are intact in *Reelin*$^{-/-}$ mice (Rice and Curran 2001). Further analysis using time-lapse microscopy combined with genetic analysis may help to elucidate the mechanisms regulating retinal cell migration.

1.2.5 Retinal synaptic circuitry

Upon reaching their final destination, retinal cells start synthesizing neurotransmitters, extending processes and forming synaptic connections. Formation of the retinal synaptic circuitry occurs from the IPL to the OPL, with lateral connections within the plexiform layers forming first, followed by the vertical connections through the bipolar cells. In the IPL, the connections between ganglion dendrites and amacrine processes are the first noticeable conventional synapses. Connections between the different types of amacrine cells appear later, followed by the formation of ribbon synapses involving bipolar cells (Nishimura and Rakic 1987). In the OPL, the synapses between photoreceptors and horizontal cells occur first, with the bipolar and photoreceptor connections emerging later (Nishimura and Rakic 1987).

One of the fundamental features of the visual system is the segregation of visual information into parallel ON and OFF pathways. This segregation relies on the synaptic connections between bipolar, amacrine and RGCs in distinct sublaminae of the IPL (Figure 1.11). ON RGCs extend processes only in sublamina *b* and connect with ON cone bipolar cells, whereas OFF RGCs ramify

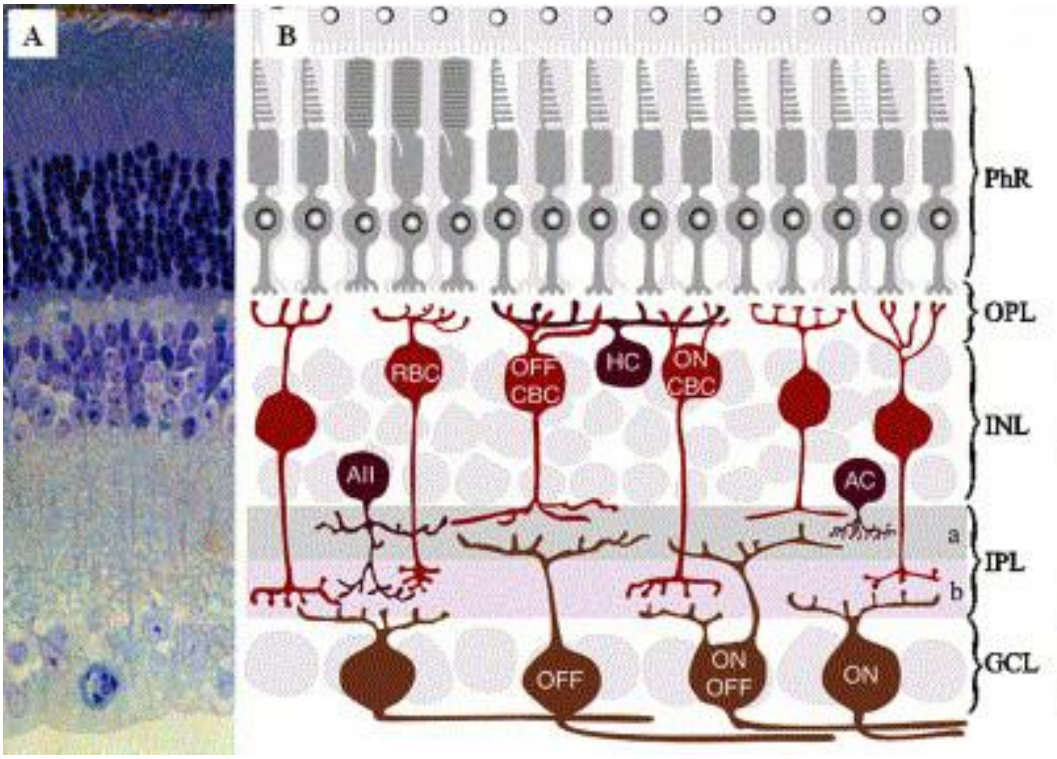

Figure 1.11 Cellular structure of retina. (A) Cross section of an adult mouse retina. Note that the IPL represents 30% of the total thickness of the retina. (B) Schematic drawing of the principal anatomical components and synaptic connections of the retina. Photoreceptors (rods and cones) synapse with bipolar and horizontal cells in the OPL. RGCs synapse with bipolar and amacrine cells in the IPL. All ON RGCs synapse with bipolar cells in sublamina *b*. All OFF RGCs synapse with bipolar cells in the sublamina *a* of the IPL. Subpopulations of RGCs receive synaptic inputs from both ON and OFF bipolar cells. Rod-driven bipolar cells synapse with AII amacrine cells, which in turn make electrical synapses with cone-driven OFF bipolar cells and glycinergic synapses with cone-driven ON bipolar cells. PhR, photoreceptor; AC, amacrince cell; AII, AII amacrine cell; HC, horizontal cell; GC, ganglion cell; OFF CBC, cone-driven OFF bipolar cell; ON CBC, cone-driven ON bipolar cell; RBC, rod-driven bipolar cell.

Reproduced with permission from Tian N (2004) Vision Res. 44: 3307-16.

only in sublamina *a* and synapse with OFF cone bipolar cells. In contrast, rod bipolar cells do not make direct contacts with RGCs. Instead, they synapse with AII amacrine cells, whose processes terminate into both sublaminae *a* and *b* in the IPL. Upon light stimulation, AII amacrine cells depolarize first, followed by depolarization of ON-cone bipolar cells (sublamina *b*) and hyperpolarization of OFF-cone bipolar cells and OFF RGCs (sublamina *a*), thus leading to the segregation of the rod-driven ON-OFF pathway (Strettoi et al. 1990; Tian 2008).

The molecular cues guiding the formation of the laminar-specific synaptic circuits remain poorly understood. Recent studies have shown that immunoglobulin superfamily (IgSF) adhesion molecules, including the Down syndrome cell adhesion molecule (DSCAM) and sidekicks, may direct laminar-specific synaptic connections between RGCs and bipolar cells in the retina (Fuerst et al. 2008; Yamagata and Sanes 2008). Interestingly, Dab1 is specifically expressed in AII amacrine cells in postnatal mouse retina and disruption of Reelin-Dab1 signaling pathway in the mouse retina leads to an attenuated rod-driven response (Rice and Curran 2000; Rice et al. 2001). It would be interesting to determine whether Dab1 is involved in the laminar-specific synaptic connections in the IPL of the retina.

1.2.6 Reelin-Dab1 signaling in the retina

Similar to the brain, the retina is an elegantly arranged laminated structure and many pathways that control neural development in the brain are also involved in retinal development. Reelin is expressed in RGCs and cone bipolar

cells in the vertebrate retina (Schiffmann et al. 1997; Goffinet et al. 1999; Bernier et al. 2000; Rice and Curran 2001). VLDLR is expressed in the ganglion cell layer (GCL) and retinal pigmented epithelium (RPE) in adult mouse retina (Hu et al. 2008). Vldlr knockout mice have been reported to induce subretinal neovascularization (Heckenlively et al. 2003). The adaptor protein Dab1 is expressed in different populations of retinal cells at different stages of development (Rice and Curran 2000; Katyal and Godbout 2004; Lee et al. 2004). In postnatal mouse retina, Dab1 is mainly detected in the AII amacrine cells. In the chick, Dab1 (Dab1-L) has been shown to be expressed in the amacrine and ganglion cells, whereas Dab1-E is expressed in undifferentiated retinal progenitor cells at early developmental stages (Katyal and Godbout 2004). Moreover, Dab1 is also prominently detected in the IPL, a region rich in synaptic connections between interneurons and ganglion cells in the retina.

Inactivation of *Disabled,* the orthologue of Dab1 in *Drosophila*, disrupts ommatidial development and leads to a frequent loss of R7 photoreceptors (Le and Simon 1998). Interestingly, the retinal architecture appears to be normal in *Reelin*$^{-/-}$ and *Dab1*$^{-/-}$ mice, suggesting that Reelin signaling is dispensible for retinal lamination. Further analysis revealed a number of defects associated with retinal synapse formation in *Reelin*$^{-/-}$ and *Dab1*$^{-/-}$ mouse retina, including a reduced number of rod bipolar cells, a decreased density of amacrine cell dendrites and abnormal distribution of amacrine cell processes in the IPL (Rice et al. 2001). Moreover, electroretinograph analyses reveal an attenuated rod-driven retinal response to visual stimulation. Together, these studies suggest that

Reelin-Dab1 signaling regulates retinal synaptic circuitry rather than retinal lamination. Moreover, a reduced bipolar cell density in *Reelin*$^{-/-}$ and *Dab1*$^{-/-}$ mice and a loss of R7 photoreceptors in *Drosophila* suggest that Reelin-Dab1 pathway may be involved in retinogenesis.

1.3 SPLICING, ALTERNATIVE SPLICING AND NEURONAL MIGRATION

1.3.1 Pre-mRNA splicing

Eukaryotic genes consist of relatively short exons that are interrupted by much longer introns. All the exonic and intronic sequences are transcribed into precursor-mRNA (pre-mRNA). In order to generate the correct and mature mRNAs, exons must be accurately identified and precisely joined together. Splicing is a process by which introns are removed and exons are joined together to form the mature mRNA.

1.3.2 Splicing mechanism

Splicing is directed by core sequence elements in the intron to define the intron-exon boundaries. These elements include the 5' splice site (GU dinucleotide at the 5' end of the intron), the 3' splice site (AG dinucleotide at the 3' end of the intron), the adenosine-containing branch point sequence upstream of the 3' splice site, and a polypyrimidine tract between the branch point and the 3' splice site (Black 2003). These sequences are recognized by components of the splicing machinery that assemble to form a large macromolecular complex, called the spliceosome, which carries out the splicing reactions (Black 2003).

The spliceosome consists of five small ribonucleoproteins (snRNPs, U1, U2, U4, U5 and U6) and ~120 accessory proteins (Black 2003). The earliest complex in spliceosome assembly, the E (early) complex, involves the binding of: i) the U1 snRNP to the 5' splice site; ii) the SF1/BBP (branch binding protein) to the branch point, and iii) the U2 auxiliary factor (U2AF) to the polypyrimidine tract and the 3' splice site. The replacement of SF1 with U2 snRNP at the branch point, accompanied by ATP hydrolysis and a structural rearrangement, results in the formation the A complex. The B complex assembles upon the joining of U4/U5/U6 tri-snRNP. The displacement of U1 snRNP by U6 snRNP at the 5' splice site and the release of U1 and U4 snRNPs form the C complex. This C complex catalyzes the two critical transesterification reactions of pre-mRNA splicing. In the first step, the 2'-OH group of the adenosine at the branch point attacks the phosphate of the guanosine at the 5' splice site, leading to cleavage of the 5' exon and a branched lariat at the 5' end of the intron. The second step involves the attack of the 3'-OH group of the cleaved exon to the phosphate of the first nucleotide in the downstream exon, which ligates the two exons and releases introns in the lariat form (Black 2003) (Figure 1.12).

1.3.3 Regulation of splicing

The core sequence elements in the introns are necessary but not sufficient for defining intron-exon junctions. Precise intron excision and exon joining require

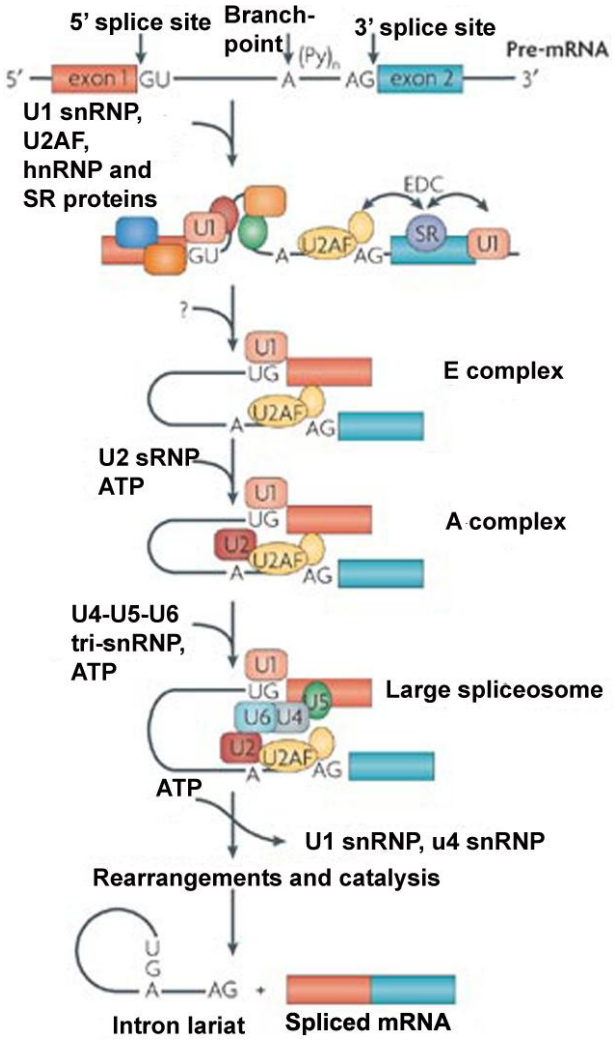

Figure 1.12 The pathway of spliceosome assembly *in vitro*. The 5' splice site of an intron is recognized by the U1 small nuclear ribonucleoprotein (snRNP), through complementary pairing of the RNA bases; the 3′ splice site, with its upstream polypyrimidine tract ((Py)n), is bound by the protein U2 auxiliary factor (U2AF)10. These factors bind with additional proteins to form a complex called the E (for early) or commitment complex, which bridges the intron and brings the splice sites that are to be cleaved and joined into juxtaposition. U2AF recruits the U2 snRNP, and an ATP-dependent step allows the RNA portion of the U2 snRNP to base pair with a sequence called the branchpoint, which lies upstream of the 3′ splice site. The pairing of the U2 snRNA at the branchpoint completes the pre-spliceosomal A complex. Subsequently, ATP-dependent steps lead to the binding of the U4–U5–U6 tri-snRNP and the formation of the large spliceosome; rearrangements that detach the U1 and U4 snRNPs then follow. This forms the catalytic spliceosome, which performs two transesterification reactions on the splice sites. These reactions result in the ligation of the exons and the excision of the intron, in the form of a lariat RNA that has its 5′ phosphate joined to the 2′ hydroxyl at the branch point.

Reproduced and adapted with permission from MacMillan Publishers Ltd: [Nat Rev Neurosci.] (Li Q, Black D (2007) 8: 819-31), copyright (2007).

auxiliary sequence elements in both the introns and exons that recruit trans-regulatory splicing factors to regulate splice site selection/recognition and spliceosome assembly (Sun and Chasin 2000). Depending on their position and function, these elements are classified into four categories: exonic splicing enhancers (ESEs), intronic splicing enhancers (ISEs), exonic splicing silencers (ESSs), intronic splicing silencers (ISSs). ESEs are usually bound by the serine-arginine-rich (SR) proteins to increase exon inclusion, whereas ESSs and ISSs are bound by heterogeneous nuclear ribonucleoproteins (hnRNPs) to decrease exon inclusion (Lopez 1998; Graveley 2000). The ISEs have been recently shown to be bound by the neuron-oncological ventral antigen (Nova) and Feminizing gene on X (FOX) proteins to promote splicing (Ule et al. 2006; Yeo et al. 2009).

SR proteins are required for constitutive pre-mRNA splicing and regulate alternative splicing site selection in a concentration-dependent manner (Zuo and Maniatis 1996). SR proteins contain 1-2 RNA recognition motifs (RRM) followed by a C-terminal domain highly enriched in arginine/serine dipeptides (the RS domain). Like SR proteins, hnRNP proteins contain RRMs; however, rather than a RS domain, they contain an arginine-glycine rich domain (the RG domain). The RRMs of SR proteins preferentially bind to specific ESEs on the substrate pre-mRNAs, whereas the RS domain mediates protein-protein interactions that facilitate spliceosome assembly at an adjacent splice site, thus promoting exon inclusion (Graveley 2000; Hertel and Graveley 2005). The activity of SR proteins can be regulated by the phosphorylation of the serine residues in the RS domain

by the SR protein kinases (SRPK1 and SRPK2) (Xiao and Manley 1997; Ngo et al. 2005). In contrast, RRMs in hnRNP proteins bind to specific exonic splicing silencers (ESSs) and the RG domain antagonizes the “pro-splicing” activity of SR proteins, resulting in exon skipping (Smith and Valcarcel 2000; Singh et al. 2004). The combinatorial action of splicing factors bound to both core and auxiliary *cis*-acting elements determine the final levels of exon inclusion in the mRNA (Smith and Valcarcel 2000) (Figure 1.13).

1.3.4 Alternative splicing and regulation

Alternative splicing (AS) is the process by which the exons of pre-mRNAs are spliced in different combinations, allowing a single gene to produce multiple mRNA and protein variants. AS can result in either subtle or dramatic changes at both the RNA and protein levels, and represents an important mechanism to expand the diversity of the transcriptome. An extreme case of alternative splicing is the *Drosophila DSCAM* (Down’s syndrome cell adhesion molecule) gene, which encodes a cell surface protein involved in axon guidance. *DSCAM* is alternatively spliced and, if all the alternative exon combinations were used, the single DSCAM gene would produce 38,016 different isoforms, more than twice the number of genes (14,000 genes) in the whole Drosophila genome (Schmucker et al. 2000; Park and Graveley 2007). It is estimated that ~94% of human genes are alternatively spliced (Wang et al. 2008), which likely explains the large proteomic complexity achieved with the limited number of genes (31,000-39,000 genes) in the human genome.

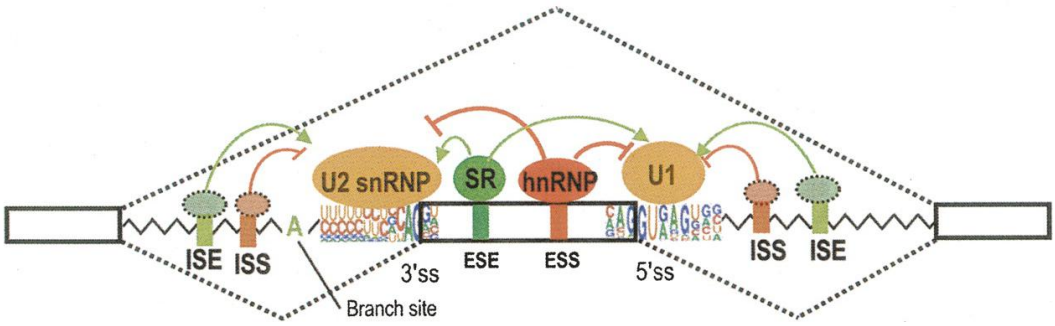

Figure 1.13 Schematic of splicing regulation. Exons, open boxes; introns, jagged lines; splice sites (ss), brackets. The consensus motifs of ss and the branch point adenosine are indicated in the pictogram. Two alternative splicing pathways are represented by dashed lines. Splicing is regulated by *cis*-elements (ESE, ESS, ISS, and ISE) and *trans*-acting splicing factors (SR proteins, hnRNP, and unknown factors).

Reproduced with permission from Wang Z, Burge CB (2008) RNA 5: 802-13. © RNA Society.

1.3.4.1 AS patterns

There are seven AS patterns (Figure 1.14): i) cassette alternative exons, the most prominent AS pattern; ii) mutually exclusive alternative exons; iii) alternative 5' splice sites; iv) alternative 3' splice sites; v) intron retention; vi) alternative promoter; and vii) alternative polyadenylation sites. Approximately 80% of human AS events occur within the coding regions of mRNAs, which affect the encoded protein sequences and contribute to proteomic diversity. The remaining 20% events occur within the nontranslated regions and affect mRNA localization, stability and translation efficiency (Modrek and Lee 2002; Hughes 2006). In addition, one-third of alternative splicing events introduce premature termination codons (PTCs), leading to mRNA degradation by nonsense-mediated mRNA decay (NMD) (Lewis et al. 2003; Lejeune and Maquat 2005). By adding or removing sequences in the open-reading frames, alternative splicing induces changes in the protein primary structure, which can affect the binding capacity of proteins, modify their enzymatic activity, and alter their subcellular localization and post-modifications, such as phosphorylation by protein kinases (Stamm et al. 2005).

1.3.4.2 Regulation of AS

AS contributes to proteome diversity and tissue specificity, and is tightly regulated at multiple levels: i) the abundance of core splice factors in the spliceosome which directly regulates exon usage/selection; ii) the tissue-specific or developmental stage-specific ratio of SR/hnRNP proteins bound to auxiliary

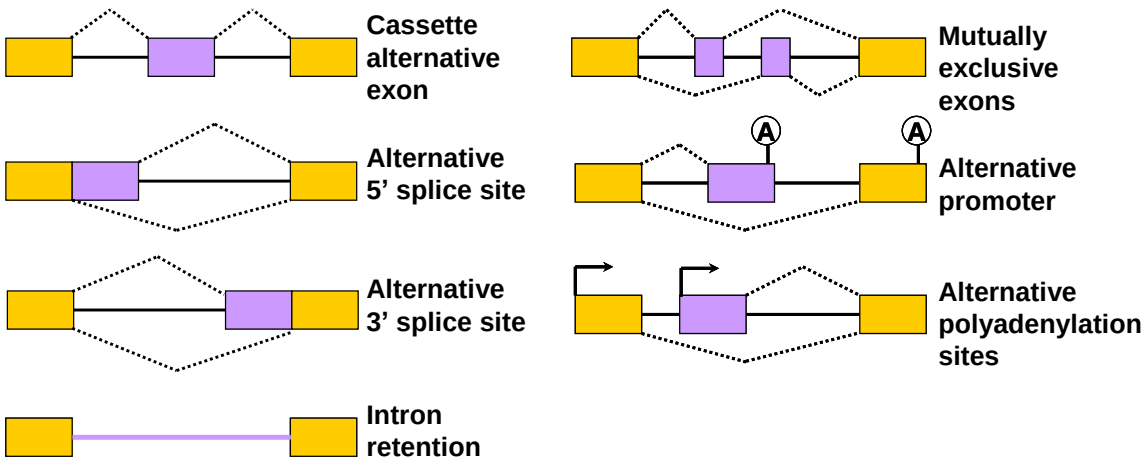

Figure 1.14 Patterns of alternative splicing

elements which modulates AS in a tissue-specific or developmentally-regulated manner (Ge and Manley 1990; Caceres et al. 1994); iii) the expression of tissue-specific splicing factors such as Nova and FOX which directly regulate tissue-specific AS patterns (Li et al. 2007); and iv) cellular signaling induced post-translational modifications, including phosphorylation and subcellular sequestration of splicing regulators, which regulate the activities of both ubiquitously-expressed and tissue-specific splicing factors (Ding et al. 2006; Hagopian et al. 2008). These elaborate regulatory mechanisms ensure that functionally diverse mRNA and protein variants are expressed in the right cell type at the right time or in response to environmental stimuli, and when disrupted, can lead to disease.

1.3.5 Regulation of neuronal migration by Nova-mediated Disabled-1 alternative splicing

The most prominent alternative splicing events occur in the mammalian nervous system. A diverse array of neuronal-specific splicing factors, such as the neuronal polypyrimidine tract-binding protein (nPTB), FOX and Nova are involved in neuronal-specific alternative splicing. Alternative splicing modulates the inclusion and exclusion of exons in the transcripts that encode proteins involved in the multiple processes of neurodevelopment, including neurotransmitter receptors, ion channels, post-synaptic density components, neuronal signaling molecules and scaffold proteins. Here, we focus on the role of Nova in the regulation of neuronal cell migration through alternative splicing of *Dab1*.

Nova was first identified as an autoantigen in a human neurological syndrome, called paraneoplastic opsoclonus-myoclonus ataxia (POMA). This neurologic disorder is characterized by ataxia and tremors, a phenotype similar to that observed in mice deficient in Reelin signaling (*reeler, Vldlr*$^{-/-}$*Apoer2*$^{-/-}$ *and Dab1*$^{-/-}$) (Buckanovich et al. 1993; Yang et al. 1998b). Two closely-related Nova proteins, Nova1 and Nova2, have been identified, with Nova1 expressed in the hindbrain and ventral spinal cord, whereas Nova2 is found in the cerebral cortex, hippocampus and cerebellum (Yang et al. 1998b; Yano et al. 2010).

Nova proteins bind to clusters of YCAY (Y indicates pyrimidine) usually adjacent to the regulated exons (within ~200 bp) in pre-mRNAs (Ule et al. 2003; Jelen et al. 2007). Depending on the positions of the binding sites relative to the alternatively regulated exons, Nova can either enhance or inhibit exon inclusion in the transcripts (Ule et al. 2006). Interestingly, the majority of genes (34/40 identified genes) regulated by Nova encode proteins involved in synaptic plasticity and transmission (Ule et al. 2005), suggesting an important role for Nova in regulating genes involved in shaping synapse function.

A recent study shows that Nova2 directly regulates neuronal cell migration by modulating the alternative splicing of Dab1 (Yano et al. 2010). Nova2 binds to intronic YCAY clusters located upstream of the alternatively spliced exons 9b and 9c in *Dab1* and inhibits the inclusion of these two exons. In the absence of Nova2, levels of the Dab1 isoform containing exons 9b and 9c (Dab1^{555*} or Dab1.7bc) are significantly increased, a feature that is accompanied by aberrant positioning of late-born neurons in the cerebral cortex. Introducing wild-type Dab1 into

Nova2$^{-/-}$ mice rescues the migration defects, whereas ectopic expression of Dab1^{555*} in wild-type mice mimics the migration defects observed in *Nova2*$^{-/-}$ mice. These combined data suggest that an appropriate balance between Dab1 and Dab1^{555*} is critical for precise neuronal positioning (Yano et al. 2010).

In contrast to the migratory disruption of both early- and late-born neurons observed in *reeler, Dab1*$^{-/-}$ *and Vldlr*$^{-/-}$*Apoer2*$^{-/-}$ mice, only late-born neuron migration is affected in *Nova2*$^{-/-}$ mice. It would be interesting to determine whether the increased levels of Dab1^{555*} in *Nova2*$^{-/-}$ mice specifically interfere with ApoER2 function in the developing cortex, as this phenotype is similar to that observed in *Apoer2*$^{-/-}$ mice (Hack et al. 2007). Divergent roles for VLDLR and ApoER2 in regulating cortical neuron migration have been described, leading to the possibility that different Dab1 isoforms may differentially associate with VLDLR and ApoER2, thus affecting different aspects of neuronal migration (Hack et al. 2007). Developmentally-regulated Dab1 alternative splicing may provide a fine-tuning mechanism to modulate the activity of Reelin signaling in a temporal-spatial manner, leading to precise neuronal positioning during brain development.

1.4 CHAPTER SUMMARIES

1.4.1 Chapter 2

The Reelin-Disabled-1 (Dab1) signaling pathway plays a key role in the positioning of neurons during brain development. Two alternatively spliced Dab1 isoforms have been identified in chick retina and brain: Dab1-E, expressed at early stages of development, and Dab1-L (commonly referred to as Dab1),

expressed at later developmental stages. The well-studied Dab1-L serves as an adaptor protein linking Reelin signal to its downstream effectors; however, nothing is known regarding the role of Dab1-E. Here we show that Dab1-E is primarily expressed in proliferating retinal progenitor cells, whereas Dab1-L is exclusively found in differentiated neuronal cells. In contrast to Dab1-L which is tyrosine-phosphorylated upon Reelin stimulation, Dab1-E is not tyrosine-phosphorylated and may function independently of Reelin. Knockdown of Dab1-E in chick retina results in a significant reduction in the number of proliferating cells and promotes ganglion cell differentiation. Our results demonstrate a role for Dab1-E in the maintenance of the retinal progenitor pool and determination of cell fate.

1.4.2 Chapter 3

The Reelin-Disabled 1 (Dab1) signaling pathway plays an important role in neuronal cell migration during brain development. Dab1, an intracellular adapter protein which is tyrosine phosphorylated upon Reelin stimulation, has been directly implicated in the transmission and termination of Reelin-mediated signaling. Two main forms of Dab1 have been identified in the developing chick retina, an early isoform (Dab1-E) expressed in progenitor cells and a late isoform (Dab1-L, a.k.a. Dab1) expressed in differentiated cells. Dab1-E is missing two Src family kinase (SFK) phosphorylation sites that are critical for Reelin-Dab1 signaling and is not tyrosine phosphorylated. We have recently demonstrated a role for Dab1-E in the maintenance of retinal progenitor cells. Here, we report

that Dab1-E is phosphorylated at serine/threonine residues independent of Reelin. Cdk2, highly expressed in retinal progenitor cells, mediates Dab1-E phosphorylation at serine 475 which in turn promotes ubiquitination-triggered proteasome degradation of Dab1-E. Inhibition of protein phosphatase 1 and/or protein phosphatase 2A leads to increased Dab1-E instability. We propose that Dab1 turnover is regulated by both Reelin-independent serine/threonine phosphorylation and Reelin-dependent tyrosine phosphorylation.

1.4.3 Chapter 4

Disabled-1 (Dab1) is a key adaptor that regulates neuronal cell positioning and synaptic plasticity in the Reelin signaling pathway during brain development. Binding of Reelin to its receptors induces tyrosine phosphorylation of Dab1 through activation of Src family kinases (SFK). Tyrosine-phosphorylated Dab1 not only transmits but also down-regulates the Reelin signal to ensure precise neuronal positioning. We have previously reported that alternative splicing modulates Dab1 function during chick retinal development. Recently, Nova2-mediated Dab1 isoform switch has been shown to regulate neuronal migration in mouse brain. Here, we demonstrate that Dab1 alternative splicing is highly complex in mouse, with the potential of generating 16 isoforms that differ primarily in the tyrosine-rich region of Dab1. We have identified 11 Dab1 variants that are expressed at different developmental stages in the mouse brain and retina. *In vitro* studies show that these Dab1 isoforms are differentially phosphorylated on tyrosine residues. Our results suggest that different Dab1

isoforms may differentially respond to Reelin stimulation and may regulate different aspects of Reelin signaling. We propose that Dab1 alternative splicing provides an exquisitely-regulated mechanism to fine-tune the activity of Reelin signaling in a temporal and spatial manner, thus tightly controlling Reelin-Dab1 signaling-modulated neuronal migration and synaptic circuitry.

1.5 REFERENCES

Adler R. 2000. A model of retinal cell differentiation in the chick embryo. *Prog Retin Eye Res* **19**: 529-557.

Arber S, Barbayannis FA, Hanser H, Schneider C, Stanyon CA, Bernard O, Caroni P. 1998. Regulation of actin dynamics through phosphorylation of cofilin by LIM-kinase. *Nature* **393**: 805-809.

Arnaud L, Ballif BA, Cooper JA. 2003. Regulation of protein tyrosine kinase signaling by substrate degradation during brain development. *Mol Cell Biol* **23**: 9293-9302.

Artavanis-Tsakonas S, Matsuno K, Fortini ME. 1995. Notch signaling. *Science* **268**: 225-232.

Artavanis-Tsakonas S, Rand MD, Lake RJ. 1999. Notch signaling: cell fate control and signal integration in development. *Science* **284**: 770-776.

Austin CP, Feldman DE, Ida JA, Jr., Cepko CL. 1995. Vertebrate retinal ganglion cells are selected from competent progenitors by the action of Notch. *Development* **121**: 3637-3650.

Badea TC, Cahill H, Ecker J, Hattar S, Nathans J. 2009. Distinct roles of transcription factors brn3a and brn3b in controlling the development, morphology, and function of retinal ganglion cells. *Neuron* **61**: 852-864.

Ballif BA, Arnaud L, Arthur WT, Guris D, Imamoto A, Cooper JA. 2004. Activation of a Dab1/CrkL/C3G/Rap1 pathway in Reelin-stimulated neurons. *Curr Biol* **14**: 606-610.

Ballif BA, Arnaud L, Cooper JA. 2003. Tyrosine phosphorylation of Disabled-1 is essential for Reelin-stimulated activation of Akt and Src family kinases. *Brain Res Mol Brain Res* **117**: 152-159.

Bar I, Tissir F, Lambert de Rouvroit C, De Backer O, Goffinet AM. 2003. The gene encoding disabled-1 (DAB1), the intracellular adaptor of the Reelin pathway, reveals unusual complexity in human and mouse. *J Biol Chem* **278**: 5802-5812.

Baye LM, Link BA. 2007. Interkinetic nuclear migration and the selection of neurogenic cell divisions during vertebrate retinogenesis. *J Neurosci* **27**: 10143-10152.

Beffert U, Durudas A, Weeber EJ, Stolt PC, Giehl KM, Sweatt JD, Hammer RE, Herz J. 2006. Functional dissection of Reelin signaling by site-directed disruption of Disabled-1 adaptor binding to apolipoprotein E receptor 2: distinct roles in development and synaptic plasticity. *J Neurosci* **26**: 2041-

2052.

Beffert U, Morfini G, Bock HH, Reyna H, Brady ST, Herz J. 2002. Reelin-mediated signaling locally regulates protein kinase B/Akt and glycogen synthase kinase 3beta. *J Biol Chem* **277**: 49958-49964.

Beffert U, Weeber EJ, Durudas A, Qiu S, Masiulis I, Sweatt JD, Li WP, Adelmann G, Frotscher M, Hammer RE et al. 2005. Modulation of synaptic plasticity and memory by Reelin involves differential splicing of the lipoprotein receptor Apoer2. *Neuron* **47**: 567-579.

Beffert U, Weeber EJ, Morfini G, Ko J, Brady ST, Tsai LH, Sweatt JD, Herz J. 2004. Reelin and cyclin-dependent kinase 5-dependent signals cooperate in regulating neuronal migration and synaptic transmission. *J Neurosci* **24**: 1897-1906.

Bernier B, Bar I, D'Arcangelo G, Curran T, Goffinet AM. 2000. Reelin mRNA expression during embryonic brain development in the chick. *J Comp Neurol* **422**: 448-463.

Bertram L, Lill CM, Tanzi RE. 2010. The genetics of Alzheimer disease: back to the future. *Neuron* **68**: 270-281.

Bhattacharya S, Das AV, Mallya KB, Ahmad I. 2008. Ciliary neurotrophic factor-mediated signaling regulates neuronal versus glial differentiation of retinal stem cells/progenitors by concentration-dependent recruitment of mitogen-activated protein kinase and Janus kinase-signal transducer and activator of transcription pathways in conjunction with Notch signaling. *Stem Cells* **26**: 2611-2624.

Black DL. 2003. Mechanisms of alternative pre-messenger RNA splicing. *Annu Rev Biochem* **72**: 291-336.

Bock HH, Herz J. 2003. Reelin activates SRC family tyrosine kinases in neurons. *Curr Biol* **13**: 18-26.

Bock HH, Jossin Y, Liu P, Forster E, May P, Goffinet AM, Herz J. 2003. Phosphatidylinositol 3-kinase interacts with the adaptor protein Dab1 in response to Reelin signaling and is required for normal cortical lamination. *J Biol Chem* **278**: 38772-38779.

Bock HH, Jossin Y, May P, Bergner O, Herz J. 2004. Apolipoprotein E receptors are required for reelin-induced proteasomal degradation of the neuronal adaptor protein Disabled-1. *J Biol Chem* **279**: 33471-33479.

Boycott KM, Bonnemann C, Herz J, Neuert S, Beaulieu C, Scott JN, Venkatasubramanian A, Parboosingh JS. 2009. Mutations in VLDLR as a cause for autosomal recessive cerebellar ataxia with mental retardation

(dysequilibrium syndrome). *J Child Neurol* **24**: 1310-1315.

Boycott KM, Flavelle S, Bureau A, Glass HC, Fujiwara TM, Wirrell E, Davey K, Chudley AE, Scott JN, McLeod DR et al. 2005. Homozygous deletion of the very low density lipoprotein receptor gene causes autosomal recessive cerebellar hypoplasia with cerebral gyral simplification. *Am J Hum Genet* **77**: 477-483.

Bramblett DE, Pennesi ME, Wu SM, Tsai MJ. 2004. The transcription factor Bhlhb4 is required for rod bipolar cell maturation. *Neuron* **43**: 779-793.

Brich J, Shie FS, Howell BW, Li R, Tus K, Wakeland EK, Jin LW, Mumby M, Churchill G, Herz J et al. 2003. Genetic modulation of tau phosphorylation in the mouse. *J Neurosci* **23**: 187-192.

Brown NL, Kanekar S, Vetter ML, Tucker PK, Gemza DL, Glaser T. 1998. Math5 encodes a murine basic helix-loop-helix transcription factor expressed during early stages of retinal neurogenesis. *Development* **125**: 4821-4833.

Brown NL, Patel S, Brzezinski J, Glaser T. 2001. Math5 is required for retinal ganglion cell and optic nerve formation. *Development* **128**: 2497-2508.

Buckanovich RJ, Posner JB, Darnell RB. 1993. Nova, the paraneoplastic Ri antigen, is homologous to an RNA-binding protein and is specifically expressed in the developing motor system. *Neuron* **11**: 657-672.

Burmeister M, Novak J, Liang MY, Basu S, Ploder L, Hawes NL, Vidgen D, Hoover F, Goldman D, Kalnins VI et al. 1996. Ocular retardation mouse caused by Chx10 homeobox null allele: impaired retinal progenitor proliferation and bipolar cell differentiation. *Nat Genet* **12**: 376-384.

Caceres JF, Stamm S, Helfman DM, Krainer AR. 1994. Regulation of alternative splicing in vivo by overexpression of antagonistic splicing factors. *Science* **265**: 1706-1709.

Caviness VS, Jr. 1973. Time of neuron origin in the hippocampus and dentate gyrus of normal and reeler mutant mice: an autoradiographic analysis. *J Comp Neurol* **151**: 113-120.

Caviness VS, Jr. 1982. Neocortical histogenesis in normal and reeler mice: a developmental study based upon [3H]thymidine autoradiography. *Brain Res* **256**: 293-302.

Caviness VS, Jr., Sidman RL. 1973. Time of origin or corresponding cell classes in the cerebral cortex of normal and reeler mutant mice: an autoradiographic analysis. *J Comp Neurol* **148**: 141-151.

Cayouette M, Poggi L, Harris WA. 2006. Lineage in the vertebrate retina. *Trends*

Neurosci **29**: 563-570.

Cepko CL, Austin CP, Yang X, Alexiades M, Ezzeddine D. 1996. Cell fate determination in the vertebrate retina. *Proc Natl Acad Sci U S A* **93**: 589-595.

Chae T, Kwon YT, Bronson R, Dikkes P, Li E, Tsai LH. 1997. Mice lacking p35, a neuronal specific activator of Cdk5, display cortical lamination defects, seizures, and adult lethality. *Neuron* **18**: 29-42.

Chai X, Forster E, Zhao S, Bock HH, Frotscher M. 2009. Reelin stabilizes the actin cytoskeleton of neuronal processes by inducing n-cofilin phosphorylation at serine3. *J Neurosci* **29**: 288-299.

Chen K, Ochalski PG, Tran TS, Sahir N, Schubert M, Pramatarova A, Howell BW. 2004. Interaction between Dab1 and CrkII is promoted by Reelin signaling. *J Cell Sci* **117**: 4527-4536.

Cheng H, Aleman TS, Cideciyan AV, Khanna R, Jacobson SG, Swaroop A. 2006. In vivo function of the orphan nuclear receptor NR2E3 in establishing photoreceptor identity during mammalian retinal development. *Hum Mol Genet* **15**: 2588-2602.

Cheng H, Khanna H, Oh EC, Hicks D, Mitton KP, Swaroop A. 2004. Photoreceptor-specific nuclear receptor NR2E3 functions as a transcriptional activator in rod photoreceptors. *Hum Mol Genet* **13**: 1563-1575.

Chow RL, Altmann CR, Lang RA, Hemmati-Brivanlou A. 1999. Pax6 induces ectopic eyes in a vertebrate. *Development* **126**: 4213-4222.

Chow RL, Volgyi B, Szilard RK, Ng D, McKerlie C, Bloomfield SA, Birch DG, McInnes RR. 2004. Control of late off-center cone bipolar cell differentiation and visual signaling by the homeobox gene Vsx1. *Proc Natl Acad Sci U S A* **101**: 1754-1759.

Cooper JA. 2008. A mechanism for inside-out lamination in the neocortex. *Trends Neurosci* **31**: 113-119.

Costagli A, Felice B, Guffanti A, Wilson SW, Mione M. 2006. Identification of alternatively spliced dab1 isoforms in zebrafish. *Dev Genes Evol* **216**: 291-299.

D'Arcangelo G, Homayouni R, Keshvara L, Rice DS, Sheldon M, Curran T. 1999. Reelin is a ligand for lipoprotein receptors. *Neuron* **24**: 471-479.

D'Arcangelo G, Miao GG, Chen SC, Soares HD, Morgan JI, Curran T. 1995. A protein related to extracellular matrix proteins deleted in the mouse mutant

reeler. *Nature* **374**: 719-723.

Ding JH, Zhong XY, Hagopian JC, Cruz MM, Ghosh G, Feramisco J, Adams JA, Fu XD. 2006. Regulated cellular partitioning of SR protein-specific kinases in mammalian cells. *Mol Biol Cell* **17**: 876-885.

Dong E, Agis-Balboa RC, Simonini MV, Grayson DR, Costa E, Guidotti A. 2005. Reelin and glutamic acid decarboxylase67 promoter remodeling in an epigenetic methionine-induced mouse model of schizophrenia. *Proc Natl Acad Sci U S A* **102**: 12578-12583.

Dulabon L, Olson EC, Taglienti MG, Eisenhuth S, McGrath B, Walsh CA, Kreidberg JA, Anton ES. 2000. Reelin binds alpha3beta1 integrin and inhibits neuronal migration. *Neuron* **27**: 33-44.

Durakoglugil MS, Chen Y, White CL, Kavalali ET, Herz J. 2009. Reelin signaling antagonizes beta-amyloid at the synapse. *Proc Natl Acad Sci U S A* **106**: 15938-15943.

Dyer MA. 2003. Regulation of proliferation, cell fate specification and differentiation by the homeodomain proteins Prox1, Six3, and Chx10 in the developing retina. *Cell Cycle* **2**: 350-357.

Dyer MA, Livesey FJ, Cepko CL, Oliver G. 2003. Prox1 function controls progenitor cell proliferation and horizontal cell genesis in the mammalian retina. *Nat Genet* **34**: 53-58.

Edqvist PH, Hallbook F. 2004. Newborn horizontal cells migrate bi-directionally across the neuroepithelium during retinal development. *Development* **131**: 1343-1351.

Eglen S, Harris B, Wong R. 2006. *Retinal development*. Cambridge University Press.

Elshatory Y, Everhart D, Deng M, Xie X, Barlow RB, Gan L. 2007. Islet-1 controls the differentiation of retinal bipolar and cholinergic amacrine cells. *J Neurosci* **27**: 12707-12720.

Ezzeddine ZD, Yang X, DeChiara T, Yancopoulos G, Cepko CL. 1997. Postmitotic cells fated to become rod photoreceptors can be respecified by CNTF treatment of the retina. *Development* **124**: 1055-1067.

Falconer D. 1951. Two mutant mutants, Tremler and Reeler, with neurological actions in the house mouse. *J Genet* **50**: 192-201.

Fatemi SH, Earle JA, McMenomy T. 2000. Reduction in Reelin immunoreactivity in hippocampus of subjects with schizophrenia, bipolar disorder and major depression. *Mol Psychiatry* **5**: 654-663, 571.

Fatemi SH, Emamian ES, Kist D, Sidwell RW, Nakajima K, Akhter P, Shier A, Sheikh S, Bailey K. 1999. Defective corticogenesis and reduction in Reelin immunoreactivity in cortex and hippocampus of prenatally infected neonatal mice. *Mol Psychiatry* **4**: 145-154.

Fatemi SH, Snow AV, Stary JM, Araghi-Niknam M, Reutiman TJ, Lee S, Brooks AI, Pearce DA. 2005. Reelin signaling is impaired in autism. *Biol Psychiatry* **57**: 777-787.

Feller SM. 2001. Crk family adaptors-signalling complex formation and biological roles. *Oncogene* **20**: 6348-6371.

Feng L, Allen NS, Simo S, Cooper JA. 2007. Cullin 5 regulates Dab1 protein levels and neuron positioning during cortical development. *Genes Dev* **21**: 2717-2730.

Feng L, Cooper JA. 2009. Dual functions of Dab1 during brain development. *Mol Cell Biol* **29**: 324-332.

Feng L, Xie X, Joshi PS, Yang Z, Shibasaki K, Chow RL, Gan L. 2006. Requirement for Bhlhb5 in the specification of amacrine and cone bipolar subtypes in mouse retina. *Development* **133**: 4815-4825.

Fidalgo M, Fraile M, Pires A, Force T, Pombo C, Zalvide J. 2010. CCM3/PDCD10 stabilizes GCKIII proteins to promote Golgi assembly and cell orientation. *J Cell Sci* **123**: 1274-1284.

Frade JM. 2002. Interkinetic nuclear movement in the vertebrate neuroepithelium: encounters with an old acquaintance. *Prog Brain Res* **136**: 67-71.

Fuerst PG, Koizumi A, Masland RH, Burgess RW. 2008. Neurite arborization and mosaic spacing in the mouse retina require DSCAM. *Nature* **451**: 470-474.

Fujitani Y, Fujitani S, Luo H, Qiu F, Burlison J, Long Q, Kawaguchi Y, Edlund H, MacDonald RJ, Furukawa T et al. 2006. Ptf1a determines horizontal and amacrine cell fates during mouse retinal development. *Development* **133**: 4439-4450.

Furukawa T, Morrow EM, Cepko CL. 1997. Crx, a novel otx-like homeobox gene, shows photoreceptor-specific expression and regulates photoreceptor differentiation. *Cell* **91**: 531-541.

Furukawa T, Mukherjee S, Bao ZZ, Morrow EM, Cepko CL. 2000. rax, Hes1, and notch1 promote the formation of Muller glia by postnatal retinal progenitor cells. *Neuron* **26**: 383-394.

Gaiano N, Nye JS, Fishell G. 2000. Radial glial identity is promoted by Notch1 signaling in the murine forebrain. *Neuron* **26**: 395-404.

Ge H, Manley JL. 1990. A protein factor, ASF, controls cell-specific alternative splicing of SV40 early pre-mRNA in vitro. *Cell* **62**: 25-34.

Gertler FB, Bennett RL, Clark MJ, Hoffmann FM. 1989. Drosophila abl tyrosine kinase in embryonic CNS axons: a role in axonogenesis is revealed through dosage-sensitive interactions with disabled. *Cell* **58**: 103-113.

Gertler FB, Hill KK, Clark MJ, Hoffmann FM. 1993. Dosage-sensitive modifiers of Drosophila abl tyrosine kinase function: prospero, a regulator of axonal outgrowth, and disabled, a novel tyrosine kinase substrate. *Genes Dev* **7**: 441-453.

Gilmore EC, Ohshima T, Goffinet AM, Kulkarni AB, Herrup K. 1998. Cyclin-dependent kinase 5-deficient mice demonstrate novel developmental arrest in cerebral cortex. *J Neurosci* **18**: 6370-6377.

Giniger E. 1998. A role for Abl in Notch signaling. *Neuron* **20**: 667-681.

Godinho L, Mumm JS, Williams PR, Schroeter EH, Koerber A, Park SW, Leach SD, Wong RO. 2005. Targeting of amacrine cell neurites to appropriate synaptic laminae in the developing zebrafish retina. *Development* **132**: 5069-5079.

Goffinet AM, Bar I, Bernier B, Trujillo C, Raynaud A, Meyer G. 1999. Reelin expression during embryonic brain development in lacertilian lizards. *J Comp Neurol* **414**: 533-550.

Graveley BR. 2000. Sorting out the complexity of SR protein functions. *RNA* **6**: 1197-1211.

Grayson DR, Jia X, Chen Y, Sharma RP, Mitchell CP, Guidotti A, Costa E. 2005. Reelin promoter hypermethylation in schizophrenia. *Proc Natl Acad Sci U S A* **102**: 9341-9346.

Groc L, Choquet D, Stephenson FA, Verrier D, Manzoni OJ, Chavis P. 2007. NMDA receptor surface trafficking and synaptic subunit composition are developmentally regulated by the extracellular matrix protein Reelin. *J Neurosci* **27**: 10165-10175.

Guidotti A, Auta J, Davis JM, Di-Giorgi-Gerevini V, Dwivedi Y, Grayson DR, Impagnatiello F, Pandey G, Pesold C, Sharma R et al. 2000. Decrease in reelin and glutamic acid decarboxylase67 (GAD67) expression in schizophrenia and bipolar disorder: a postmortem brain study. *Arch Gen Psychiatry* **57**: 1061-1069.

Gupta A, Tsai LH, Wynshaw-Boris A. 2002. Life is a journey: a genetic look at neocortical development. *Nat Rev Genet* **3**: 342-355.

Hack I, Bancila M, Loulier K, Carroll P, Cremer H. 2002. Reelin is a detachment signal in tangential chain-migration during postnatal neurogenesis. *Nat Neurosci* **5**: 939-945.

Hack I, Hellwig S, Junghans D, Brunne B, Bock HH, Zhao S, Frotscher M. 2007. Divergent roles of ApoER2 and Vldlr in the migration of cortical neurons. *Development* **134**: 3883-3891.

Hagopian JC, Ma CT, Meade BR, Albuquerque CP, Ngo JC, Ghosh G, Jennings PA, Fu XD, Adams JA. 2008. Adaptable molecular interactions guide phosphorylation of the SR protein ASF/SF2 by SRPK1. *J Mol Biol* **382**: 894-909.

Hashimoto-Torii K, Torii M, Sarkisian MR, Bartley CM, Shen J, Radtke F, Gridley T, Sestan N, Rakic P. 2008. Interaction between Reelin and Notch signaling regulates neuronal migration in the cerebral cortex. *Neuron* **60**: 273-284.

Hatakeyama J, Tomita K, Inoue T, Kageyama R. 2001. Roles of homeobox and bHLH genes in specification of a retinal cell type. *Development* **128**: 1313-1322.

Hatten ME. 1999. Central nervous system neuronal migration. *Annu Rev Neurosci* **22**: 511-539.

Heckenlively JR, Hawes NL, Friedlander M, Nusinowitz S, Hurd R, Davisson M, Chang B. 2003. Mouse model of subretinal neovascularization with choroidal anastomosis. *Retina* **23**: 518-522.

Hertel KJ, Graveley BR. 2005. RS domains contact the pre-mRNA throughout spliceosome assembly. *Trends Biochem Sci* **30**: 115-118.

Hiesberger T, Trommsdorff M, Howell BW, Goffinet A, Mumby MC, Cooper JA, Herz J. 1999. Direct binding of Reelin to VLDL receptor and ApoE receptor 2 induces tyrosine phosphorylation of disabled-1 and modulates tau phosphorylation. *Neuron* **24**: 481-489.

Hoe HS, Tran TS, Matsuoka Y, Howell BW, Rebeck GW. 2006. DAB1 and Reelin effects on amyloid precursor protein and ApoE receptor 2 trafficking and processing. *J Biol Chem* **281**: 35176-35185.

Holt CE, Bertsch TW, Ellis HM, Harris WA. 1988. Cellular determination in the Xenopus retina is independent of lineage and birth date. *Neuron* **1**: 15-26.

Homayouni R, Rice DS, Sheldon M, Curran T. 1999. Disabled-1 binds to the cytoplasmic domain of amyloid precursor-like protein 1. *J Neurosci* **19**: 7507-7515.

Hong SE, Shugart YY, Huang DT, Shahwan SA, Grant PE, Hourihane JO, Martin ND, Walsh CA. 2000. Autosomal recessive lissencephaly with cerebellar hypoplasia is associated with human RELN mutations. *Nat Genet* **26**: 93-96.

Horton AC, Racz B, Monson EE, Lin AL, Weinberg RJ, Ehlers MD. 2005. Polarized secretory trafficking directs cargo for asymmetric dendrite growth and morphogenesis. *Neuron* **48**: 757-771.

Howell BW, Gertler FB, Cooper JA. 1997a. Mouse disabled (mDab1): a Src binding protein implicated in neuronal development. *Embo J* **16**: 121-132.

Howell BW, Hawkes R, Soriano P, Cooper JA. 1997b. Neuronal position in the developing brain is regulated by mouse disabled-1. *Nature* **389**: 733-737.

Howell BW, Herrick TM, Cooper JA. 1999a. Reelin-induced tryosine phosphorylation of disabled 1 during neuronal positioning. *Genes Dev* **13**: 643-648.

Howell BW, Herrick TM, Hildebrand JD, Zhang Y, Cooper JA. 2000. Dab1 tyrosine phosphorylation sites relay positional signals during mouse brain development. *Curr Biol* **10**: 877-885.

Howell BW, Lanier LM, Frank R, Gertler FB, Cooper JA. 1999b. The disabled 1 phosphotyrosine-binding domain binds to the internalization signals of transmembrane glycoproteins and to phospholipids. *Mol Cell Biol* **19**: 5179-5188.

Hu W, Jiang A, Liang J, Meng H, Chang B, Gao H, Qiao X. 2008. Expression of VLDLR in the retina and evolution of subretinal neovascularization in the knockout mouse model's retinal angiomatous proliferation. *Invest Ophthalmol Vis Sci* **49**: 407-415.

Huang Y, Magdaleno S, Hopkins R, Slaughter C, Curran T, Keshvara L. 2004. Tyrosine phosphorylated Disabled 1 recruits Crk family adapter proteins. *Biochem Biophys Res Commun* **318**: 204-212.

Hughes TA. 2006. Regulation of gene expression by alternative untranslated regions. *Trends Genet* **22**: 119-122.

Impagnatiello F, Guidotti AR, Pesold C, Dwivedi Y, Caruncho H, Pisu MG, Uzunov DP, Smalheiser NR, Davis JM, Pandey GN et al. 1998. A decrease of reelin expression as a putative vulnerability factor in schizophrenia. *Proc Natl Acad Sci U S A* **95**: 15718-15723.

Inoue T, Hojo M, Bessho Y, Tano Y, Lee JE, Kageyama R. 2002. Math3 and NeuroD regulate amacrine cell fate specification in the retina. *Development* **129**: 831-842.

Isosaka T, Hattori K, Yagi T. 2006. NMDA-receptor proteins are upregulated in the hippocampus of postnatal heterozygous reeler mice. *Brain Res* **1073-1074**: 11-19.

Jadhav AP, Cho SH, Cepko CL. 2006. Notch activity permits retinal cells to progress through multiple progenitor states and acquire a stem cell property. *Proc Natl Acad Sci U S A* **103**: 18998-19003.

Jelen N, Ule J, Zivin M, Darnell RB. 2007. Evolution of Nova-dependent splicing regulation in the brain. *PLoS Genet* **3**: 1838-1847.

Jia L, Oh EC, Ng L, Srinivas M, Brooks M, Swaroop A, Forrest D. 2009. Retinoid-related orphan nuclear receptor RORbeta is an early-acting factor in rod photoreceptor development. *Proc Natl Acad Sci U S A* **106**: 17534-17539.

Jossin Y, Goffinet AM. 2007. Reelin signals through phosphatidylinositol 3-kinase and Akt to control cortical development and through mTor to regulate dendritic growth. *Mol Cell Biol* **27**: 7113-7124.

Jossin Y, Ignatova N, Hiesberger T, Herz J, Lambert de Rouvroit C, Goffinet AM. 2004. The central fragment of Reelin, generated by proteolytic processing in vivo, is critical to its function during cortical plate development. *J Neurosci* **24**: 514-521.

Jossin Y, Ogawa M, Metin C, Tissir F, Goffinet AM. 2003. Inhibition of SRC family kinases and non-classical protein kinases C induce a reeler-like malformation of cortical plate development. *J Neurosci* **23**: 9953-9959.

Jovceva E, Larsen MR, Waterfield MD, Baum B, Timms JF. 2007. Dynamic cofilin phosphorylation in the control of lamellipodial actin homeostasis. *J Cell Sci* **120**: 1888-1897.

Katyal S, Gao Z, Monckton E, Glubrecht D, Godbout R. 2007. Hierarchical disabled-1 tyrosine phosphorylation in Src family kinase activation and neurite formation. *J Mol Biol* **368**: 349-364.

Katyal S, Godbout R. 2004. Alternative splicing modulates Disabled-1 (Dab1) function in the developing chick retina. *Embo J* **23**: 1878-1888.

Keilani S, Sugaya K. 2008. Reelin induces a radial glial phenotype in human neural progenitor cells by activation of Notch-1. *BMC Dev Biol* **8**: 69.

Keshvara L, Benhayon D, Magdaleno S, Curran T. 2001. Identification of reelin-induced sites of tyrosyl phosphorylation on disabled 1. *J Biol Chem* **276**: 16008-16014.

Keshvara L, Magdaleno S, Benhayon D, Curran T. 2002. Cyclin-dependent kinase 5 phosphorylates disabled 1 independently of Reelin signaling. *J*

Neurosci **22**: 4869-4877.

Kim HM, Qu T, Kriho V, Lacor P, Smalheiser N, Pappas GD, Guidotti A, Costa E, Sugaya K. 2002. Reelin function in neural stem cell biology. *Proc Natl Acad Sci U S A* **99**: 4020-4025.

Kocherhans S, Madhusudan A, Doehner J, Breu KS, Nitsch RM, Fritschy JM, Knuesel I. 2010. Reduced Reelin expression accelerates amyloid-beta plaque formation and tau pathology in transgenic Alzheimer's disease mice. *J Neurosci* **30**: 9228-9240.

Kolb LE, Arlier Z, Yalcinkaya C, Ozturk AK, Moliterno JA, Erturk O, Bayrakli F, Korkmaz B, DiLuna ML, Yasuno K et al. 2010. Novel VLDLR microdeletion identified in two Turkish siblings with pachygyria and pontocerebellar atrophy. *Neurogenetics* **11**: 319-325.

Kubo K, Honda T, Tomita K, Sekine K, Ishii K, Uto A, Kobayashi K, Tabata H, Nakajima K. 2010. Ectopic Reelin induces neuronal aggregation with a normal birthdate-dependent "inside-out" alignment in the developing neocortex. *J Neurosci* **30**: 10953-10966.

Kubo K, Mikoshiba K, Nakajima K. 2002. Secreted Reelin molecules form homodimers. *Neurosci Res* **43**: 381-388.

Kuo G, Arnaud L, Kronstad-O'Brien P, Cooper JA. 2005. Absence of Fyn and Src causes a reeler-like phenotype. *J Neurosci* **25**: 8578-8586.

Kwon YT, Tsai LH. 1998. A novel disruption of cortical development in p35(-/-) mice distinct from reeler. *J Comp Neurol* **395**: 510-522.

Lambert de Rouvroit C, de Bergeyck V, Cortvrindt C, Bar I, Eeckhout Y, Goffinet AM. 1999. Reelin, the extracellular matrix protein deficient in reeler mutant mice, is processed by a metalloproteinase. *Exp Neurol* **156**: 214-217.

Le Gall M, De Mattei C, Giniger E. 2008. Molecular separation of two signaling pathways for the receptor, Notch. *Dev Biol* **313**: 556-567.

Le N, Simon MA. 1998. Disabled is a putative adaptor protein that functions during signaling by the sevenless receptor tyrosine kinase. *Mol Cell Biol* **18**: 4844-4854.

Lee EJ, Kim HJ, Lim EJ, Kim IB, Kang WS, Oh SJ, Rickman DW, Chung JW, Chun MH. 2004. AII amacrine cells in the mammalian retina show disabled-1 immunoreactivity. *J Comp Neurol* **470**: 372-381.

Lejeune F, Maquat LE. 2005. Mechanistic links between nonsense-mediated mRNA decay and pre-mRNA splicing in mammalian cells. *Curr Opin Cell Biol* **17**: 309-315.

Lewis BP, Green RE, Brenner SE. 2003. Evidence for the widespread coupling of alternative splicing and nonsense-mediated mRNA decay in humans. *Proc Natl Acad Sci U S A* **100**: 189-192.

Li Q, Lee JA, Black DL. 2007. Neuronal regulation of alternative pre-mRNA splicing. *Nat Rev Neurosci* **8**: 819-831.

Li S, Mo Z, Yang X, Price SM, Shen MM, Xiang M. 2004. Foxn4 controls the genesis of amacrine and horizontal cells by retinal progenitors. *Neuron* **43**: 795-807.

Lillien L. 1994. Neurogenesis in the vertebrate retina. *Perspect Dev Neurobiol* **2**: 175-182.

Liu W, Khare SL, Liang X, Peters MA, Liu X, Cepko CL, Xiang M. 2000. All Brn3 genes can promote retinal ganglion cell differentiation in the chick. *Development* **127**: 3237-3247.

Liu W, Mo Z, Xiang M. 2001. The Ath5 proneural genes function upstream of Brn3 POU domain transcription factor genes to promote retinal ganglion cell development. *Proc Natl Acad Sci U S A* **98**: 1649-1654.

Livesey FJ, Cepko CL. 2001. Vertebrate neural cell-fate determination: lessons from the retina. *Nat Rev Neurosci* **2**: 109-118.

Loosli F, Winkler S, Wittbrodt J. 1999. Six3 overexpression initiates the formation of ectopic retina. *Genes Dev* **13**: 649-654.

Lopez AJ. 1998. Alternative splicing of pre-mRNA: developmental consequences and mechanisms of regulation. *Annu Rev Genet* **32**: 279-305.

Louvi A, Artavanis-Tsakonas S. 2006. Notch signalling in vertebrate neural development. *Nat Rev Neurosci* **7**: 93-102.

Magdaleno S, Keshvara L, Curran T. 2002. Rescue of ataxia and preplate splitting by ectopic expression of Reelin in reeler mice. *Neuron* **33**: 573-586.

Marquardt T, Ashery-Padan R, Andrejewski N, Scardigli R, Guillemot F, Gruss P. 2001. Pax6 is required for the multipotent state of retinal progenitor cells. *Cell* **105**: 43-55.

Mathers PH, Grinberg A, Mahon KA, Jamrich M. 1997. The Rx homeobox gene is essential for vertebrate eye development. *Nature* **387**: 603-607.

Matsuki T, Matthews RT, Cooper JA, van der Brug MP, Cookson MR, Hardy JA, Olson EC, Howell BW. 2010. Reelin and stk25 have opposing roles in neuronal polarization and dendritic Golgi deployment. *Cell* **143**: 826-836.

Matsuki T, Pramatarova A, Howell BW. 2008. Reduction of Crk and CrkL expression blocks reelin-induced dendritogenesis. *J Cell Sci* **121**: 1869-1875.

Matter-Sadzinski L, Puzianowska-Kuznicka M, Hernandez J, Ballivet M, Matter JM. 2005. A bHLH transcriptional network regulating the specification of retinal ganglion cells. *Development* **132**: 3907-3921.

McLoon SC, Barnes RB. 1989. Early differentiation of retinal ganglion cells: an axonal protein expressed by premigratory and migrating retinal ganglion cells. *J Neurosci* **9**: 1424-1432.

Mo Z, Li S, Yang X, Xiang M. 2004. Role of the Barhl2 homeobox gene in the specification of glycinergic amacrine cells. *Development* **131**: 1607-1618.

Modrek B, Lee C. 2002. A genomic view of alternative splicing. *Nat Genet* **30**: 13-19.

Morgan JL, Dhingra A, Vardi N, Wong RO. 2006. Axons and dendrites originate from neuroepithelial-like processes of retinal bipolar cells. *Nat Neurosci* **9**: 85-92.

Mu X, Fu X, Sun H, Beremand PD, Thomas TL, Klein WH. 2005. A gene network downstream of transcription factor Math5 regulates retinal progenitor cell competence and ganglion cell fate. *Dev Biol* **280**: 467-481.

Mu X, Klein WH. 2004. A gene regulatory hierarchy for retinal ganglion cell specification and differentiation. *Semin Cell Dev Biol* **15**: 115-123.

Murciano A, Zamora J, Lopez-Sanchez J, Frade JM. 2002. Interkinetic nuclear movement may provide spatial clues to the regulation of neurogenesis. *Mol Cell Neurosci* **21**: 285-300.

Nadarajah B, Alifragis P, Wong RO, Parnavelas JG. 2003. Neuronal migration in the developing cerebral cortex: observations based on real-time imaging. *Cereb Cortex* **13**: 607-611.

Nakano Y, Kohno T, Hibi T, Kohno S, Baba A, Mikoshiba K, Nakajima K, Hattori M. 2007. The extremely conserved C-terminal region of Reelin is not necessary for secretion but is required for efficient activation of downstream signaling. *J Biol Chem* **282**: 20544-20552.

Nelson BR, Gumuscu B, Hartman BH, Reh TA. 2006. Notch activity is downregulated just prior to retinal ganglion cell differentiation. *Dev Neurosci* **28**: 128-141.

Ngo JC, Chakrabarti S, Ding JH, Velazquez-Dones A, Nolen B, Aubol BE, Adams JA, Fu XD, Ghosh G. 2005. Interplay between SRPK and Clk/Sty kinases

in phosphorylation of the splicing factor ASF/SF2 is regulated by a docking motif in ASF/SF2. *Mol Cell* **20**: 77-89.

Nishida A, Furukawa A, Koike C, Tano Y, Aizawa S, Matsuo I, Furukawa T. 2003. Otx2 homeobox gene controls retinal photoreceptor cell fate and pineal gland development. *Nat Neurosci* **6**: 1255-1263.

Nishimura Y, Rakic P. 1987. Synaptogenesis in the primate retina proceeds from the ganglion cells towards the photoreceptors. *Neurosci Res Suppl* **6**: S253-268.

Niu S, Renfro A, Quattrocchi CC, Sheldon M, D'Arcangelo G. 2004. Reelin promotes hippocampal dendrite development through the VLDLR/ApoER2-Dab1 pathway. *Neuron* **41**: 71-84.

Noh JS, Sharma RP, Veldic M, Salvacion AA, Jia X, Chen Y, Costa E, Guidotti A, Grayson DR. 2005. DNA methyltransferase 1 regulates reelin mRNA expression in mouse primary cortical cultures. *Proc Natl Acad Sci U S A* **102**: 1749-1754.

Ohsawa R, Kageyama R. 2008. Regulation of retinal cell fate specification by multiple transcription factors. *Brain Res* **1192**: 90-98.

Ohshima T, Mikoshiba K. 2002. Reelin signaling and Cdk5 in the control of neuronal positioning. *Mol Neurobiol* **26**: 153-166.

Ohshima T, Suzuki H, Morimura T, Ogawa M, Mikoshiba K. 2007. Modulation of Reelin signaling by Cyclin-dependent kinase 5. *Brain Res* **1140**: 84-95.

Ohshima T, Ward JM, Huh CG, Longenecker G, Veeranna, Pant HC, Brady RO, Martin LJ, Kulkarni AB. 1996. Targeted disruption of the cyclin-dependent kinase 5 gene results in abnormal corticogenesis, neuronal pathology and perinatal death. *Proc Natl Acad Sci U S A* **93**: 11173-11178.

Ohtoshi A, Wang SW, Maeda H, Saszik SM, Frishman LJ, Klein WH, Behringer RR. 2004. Regulation of retinal cone bipolar cell differentiation and photopic vision by the CVC homeobox gene Vsx1. *Curr Biol* **14**: 530-536.

Olson EC, Kim S, Walsh CA. 2006. Impaired neuronal positioning and dendritogenesis in the neocortex after cell-autonomous Dab1 suppression. *J Neurosci* **26**: 1767-1775.

Oron-Karni V, Farhy C, Elgart M, Marquardt T, Remizova L, Yaron O, Xie Q, Cvekl A, Ashery-Padan R. 2008. Dual requirement for Pax6 in retinal progenitor cells. *Development* **135**: 4037-4047.

Ozcelik T, Akarsu N, Uz E, Caglayan S, Gulsuner S, Onat OE, Tan M, Tan U. 2008. Mutations in the very low-density lipoprotein receptor VLDLR cause

cerebellar hypoplasia and quadrupedal locomotion in humans. *Proc Natl Acad Sci U S A* **105**: 4232-4236.

Park JW, Graveley BR. 2007. Complex alternative splicing. *Adv Exp Med Biol* **623**: 50-63.

Park TJ, Curran T. 2008. Crk and Crk-like play essential overlapping roles downstream of disabled-1 in the Reelin pathway. *J Neurosci* **28**: 13551-13562.

Philips GT, Stair CN, Young Lee H, Wroblewski E, Berberoglu MA, Brown NL, Mastick GS. 2005. Precocious retinal neurons: Pax6 controls timing of differentiation and determination of cell type. *Dev Biol* **279**: 308-321.

Poche RA, Furuta Y, Chaboissier MC, Schedl A, Behringer RR. 2008. Sox9 is expressed in mouse multipotent retinal progenitor cells and functions in Muller glial cell development. *J Comp Neurol* **510**: 237-250.

Poggi L, Vitorino M, Masai I, Harris WA. 2005a. Influences on neural lineage and mode of division in the zebrafish retina in vivo. *J Cell Biol* **171**: 991-999.

Poggi L, Zolessi FR, Harris WA. 2005b. Time-lapse analysis of retinal differentiation. *Curr Opin Cell Biol* **17**: 676-681.

Prada C, Puelles L, Genis-Galvez JM. 1981. A golgi study on the early sequence of differentiation of ganglion cells in the chick embryo retina. *Anat Embryol (Berl)* **161**: 305-317.

Prada C, Puga J, Perez-Mendez L, Lopez, Ramirez G. 1991. Spatial and Temporal Patterns of Neurogenesis in the Chick Retina. *Eur J Neurosci* **3**: 1187.

Qiu F, Jiang H, Xiang M. 2008. A comprehensive negative regulatory program controlled by Brn3b to ensure ganglion cell specification from multipotential retinal precursors. *J Neurosci* **28**: 3392-3403.

Rice DS, Curran T. 2000. Disabled-1 is expressed in type AII amacrine cells in the mouse retina. *J Comp Neurol* **424**: 327-338.

-. 2001. Role of the reelin signaling pathway in central nervous system development. *Annu Rev Neurosci* **24**: 1005-1039.

Rice DS, Nusinowitz S, Azimi AM, Martinez A, Soriano E, Curran T. 2001. The reelin pathway modulates the structure and function of retinal synaptic circuitry. *Neuron* **31**: 929-941.

Rice DS, Sheldon M, D'Arcangelo G, Nakajima K, Goldowitz D, Curran T. 1998. Disabled-1 acts downstream of Reelin in a signaling pathway that controls

laminar organization in the mammalian brain. *Development* **125**: 3719-3729.

Sanada K, Gupta A, Tsai LH. 2004. Disabled-1-regulated adhesion of migrating neurons to radial glial fiber contributes to neuronal positioning during early corticogenesis. *Neuron* **42**: 197-211.

Schiffmann SN, Bernier B, Goffinet AM. 1997. Reelin mRNA expression during mouse brain development. *Eur J Neurosci* **9**: 1055-1071.

Schmucker D, Clemens JC, Shu H, Worby CA, Xiao J, Muda M, Dixon JE, Zipursky SL. 2000. Drosophila Dscam is an axon guidance receptor exhibiting extraordinary molecular diversity. *Cell* **101**: 671-684.

Schneider ML, Turner DL, Vetter ML. 2001. Notch signaling can inhibit Xath5 function in the neural plate and developing retina. *Mol Cell Neurosci* **18**: 458-472.

Sheldon M, Rice DS, D'Arcangelo G, Yoneshima H, Nakajima K, Mikoshiba K, Howell BW, Cooper JA, Goldowitz D, Curran T. 1997. Scrambler and yotari disrupt the disabled gene and produce a reeler-like phenotype in mice. *Nature* **389**: 730-733.

Sibbe M, Forster E, Basak O, Taylor V, Frotscher M. 2009. Reelin and Notch1 cooperate in the development of the dentate gyrus. *J Neurosci* **29**: 8578-8585.

Simo S, Jossin Y, Cooper JA. 2010. Cullin 5 regulates cortical layering by modulating the speed and duration of Dab1-dependent neuronal migration. *J Neurosci* **30**: 5668-5676.

Singh NN, Androphy EJ, Singh RN. 2004. The regulation and regulatory activities of alternative splicing of the SMN gene. *Crit Rev Eukaryot Gene Expr* **14**: 271-285.

Smith CW, Valcarcel J. 2000. Alternative pre-mRNA splicing: the logic of combinatorial control. *Trends Biochem Sci* **25**: 381-388.

Songyang Z, Shoelson SE, Chaudhuri M, Gish G, Pawson T, Haser WG, King F, Roberts T, Ratnofsky S, Lechleider RJ et al. 1993. SH2 domains recognize specific phosphopeptide sequences. *Cell* **72**: 767-778.

Stamm S, Ben-Ari S, Rafalska I, Tang Y, Zhang Z, Toiber D, Thanaraj TA, Soreq H. 2005. Function of alternative splicing. *Gene* **344**: 1-20.

Strasser V, Fasching D, Hauser C, Mayer H, Bock HH, Hiesberger T, Herz J, Weeber EJ, Sweatt JD, Pramatarova A et al. 2004. Receptor clustering is involved in Reelin signaling. *Mol Cell Biol* **24**: 1378-1386.

Strettoi E, Dacheux RF, Raviola E. 1990. Synaptic connections of rod bipolar cells in the inner plexiform layer of the rabbit retina. *J Comp Neurol* **295**: 449-466.

Sun H, Chasin LA. 2000. Multiple splicing defects in an intronic false exon. *Mol Cell Biol* **20**: 6414-6425.

Tabata H, Nakajima K. 2002. Neurons tend to stop migration and differentiate along the cortical internal plexiform zones in the Reelin signal-deficient mice. *J Neurosci Res* **69**: 723-730.

Tian N. 2008. Synaptic activity, visual experience and the maturation of retinal synaptic circuitry. *J Physiol* **586**: 4347-4355.

Tomita K, Moriyoshi K, Nakanishi S, Guillemot F, Kageyama R. 2000. Mammalian achaete-scute and atonal homologs regulate neuronal versus glial fate determination in the central nervous system. *Embo J* **19**: 5460-5472.

Trommsdorff M, Borg JP, Margolis B, Herz J. 1998. Interaction of cytosolic adaptor proteins with neuronal apolipoprotein E receptors and the amyloid precursor protein. *J Biol Chem* **273**: 33556-33560.

Trommsdorff M, Gotthardt M, Hiesberger T, Shelton J, Stockinger W, Nimpf J, Hammer RE, Richardson JA, Herz J. 1999. Reeler/Disabled-like disruption of neuronal migration in knockout mice lacking the VLDL receptor and ApoE receptor 2. *Cell* **97**: 689-701.

Tsai LH, Gleeson JG. 2005. Nucleokinesis in neuronal migration. *Neuron* **46**: 383-388.

Tsai LH, Takahashi T, Caviness VS, Jr., Harlow E. 1993. Activity and expression pattern of cyclin-dependent kinase 5 in the embryonic mouse nervous system. *Development* **119**: 1029-1040.

Turner DL, Cepko CL. 1987. A common progenitor for neurons and glia persists in rat retina late in development. *Nature* **328**: 131-136.

Uchida T, Baba A, Perez-Martinez FJ, Hibi T, Miyata T, Luque JM, Nakajima K, Hattori M. 2009. Downregulation of functional Reelin receptors in projection neurons implies that primary Reelin action occurs at early/premigratory stages. *J Neurosci* **29**: 10653-10662.

Ule J, Jensen KB, Ruggiu M, Mele A, Ule A, Darnell RB. 2003. CLIP identifies Nova-regulated RNA networks in the brain. *Science* **302**: 1212-1215.

Ule J, Stefani G, Mele A, Ruggiu M, Wang X, Taneri B, Gaasterland T, Blencowe BJ, Darnell RB. 2006. An RNA map predicting Nova-dependent splicing regulation. *Nature* **444**: 580-586.

Ule J, Ule A, Spencer J, Williams A, Hu JS, Cline M, Wang H, Clark T, Fraser C, Ruggiu M et al. 2005. Nova regulates brain-specific splicing to shape the synapse. *Nat Genet* **37**: 844-852.

Utsunomiya-Tate N, Kubo K, Tate S, Kainosho M, Katayama E, Nakajima K, Mikoshiba K. 2000. Reelin molecules assemble together to form a large protein complex, which is inhibited by the function-blocking CR-50 antibody. *Proc Natl Acad Sci U S A* **97**: 9729-9734.

Voss AK, Britto JM, Dixon MP, Sheikh BN, Collin C, Tan SS, Thomas T. 2008. C3G regulates cortical neuron migration, preplate splitting and radial glial cell attachment. *Development* **135**: 2139-2149.

Wall DS, Mears AJ, McNeill B, Mazerolle C, Thurig S, Wang Y, Kageyama R, Wallace VA. 2009. Progenitor cell proliferation in the retina is dependent on Notch-independent Sonic hedgehog/Hes1 activity. *J Cell Biol* **184**: 101-112.

Wang ET, Sandberg R, Luo S, Khrebtukova I, Zhang L, Mayr C, Kingsmore SF, Schroth GP, Burge CB. 2008. Alternative isoform regulation in human tissue transcriptomes. *Nature* **456**: 470-476.

Wang SW, Kim BS, Ding K, Wang H, Sun D, Johnson RL, Klein WH, Gan L. 2001. Requirement for math5 in the development of retinal ganglion cells. *Genes Dev* **15**: 24-29.

Wang Y, Dakubo GD, Thurig S, Mazerolle CJ, Wallace VA. 2005. Retinal ganglion cell-derived sonic hedgehog locally controls proliferation and the timing of RGC development in the embryonic mouse retina. *Development* **132**: 5103-5113.

Weeber EJ, Beffert U, Jones C, Christian JM, Forster E, Sweatt JD, Herz J. 2002. Reelin and ApoE receptors cooperate to enhance hippocampal synaptic plasticity and learning. *J Biol Chem* **277**: 39944-39952.

Wolburg H, Willbold E, Layer PG. 1991. Muller glia endfeet, a basal lamina and the polarity of retinal layers form properly in vitro only in the presence of marginal pigmented epithelium. *Cell Tissue Res* **264**: 437-451.

Wong LL, Rapaport DH. 2009. Defining retinal progenitor cell competence in Xenopus laevis by clonal analysis. *Development* **136**: 1707-1715.

Xiao SH, Manley JL. 1997. Phosphorylation of the ASF/SF2 RS domain affects both protein-protein and protein-RNA interactions and is necessary for splicing. *Genes Dev* **11**: 334-344.

Yamagata M, Sanes JR. 2008. Dscam and Sidekick proteins direct lamina-specific synaptic connections in vertebrate retina. *Nature* **451**: 465-469.

Yang N, Higuchi O, Ohashi K, Nagata K, Wada A, Kangawa K, Nishida E, Mizuno K. 1998a. Cofilin phosphorylation by LIM-kinase 1 and its role in Rac-mediated actin reorganization. *Nature* **393**: 809-812.

Yang YY, Yin GL, Darnell RB. 1998b. The neuronal RNA-binding protein Nova-2 is implicated as the autoantigen targeted in POMA patients with dementia. *Proc Natl Acad Sci U S A* **95**: 13254-13259.

Yano M, Hayakawa-Yano Y, Mele A, Darnell RB. 2010. Nova2 regulates neuronal migration through an RNA switch in disabled-1 signaling. *Neuron* **66**: 848-858.

Yaron O, Farhy C, Marquardt T, Applebury M, Ashery-Padan R. 2006. Notch1 functions to suppress cone-photoreceptor fate specification in the developing mouse retina. *Development* **133**: 1367-1378.

Yeo GW, Coufal NG, Liang TY, Peng GE, Fu XD, Gage FH. 2009. An RNA code for the FOX2 splicing regulator revealed by mapping RNA-protein interactions in stem cells. *Nat Struct Mol Biol* **16**: 130-137.

Young-Pearse TL, Bai J, Chang R, Zheng JB, LoTurco JJ, Selkoe DJ. 2007. A critical function for beta-amyloid precursor protein in neuronal migration revealed by in utero RNA interference. *J Neurosci* **27**: 14459-14469.

Zaki M, Shehab M, El-Aleem AA, Abdel-Salam G, Koeller HB, Ilkin Y, Ross ME, Dobyns WB, Gleeson JG. 2007. Identification of a novel recessive RELN mutation using a homozygous balanced reciprocal translocation. *Am J Med Genet A* **143A**: 939-944.

Zuber ME, Gestri G, Viczian AS, Barsacchi G, Harris WA. 2003. Specification of the vertebrate eye by a network of eye field transcription factors. *Development* **130**: 5155-5167.

Zuber ME, Perron M, Philpott A, Bang A, Harris WA. 1999. Giant eyes in Xenopus laevis by overexpression of XOptx2. *Cell* **98**: 341-352.

Zuo P, Maniatis T. 1996. The splicing factor U2AF35 mediates critical protein-protein interactions in constitutive and enhancer-dependent splicing. *Genes Dev* **10**: 1356-1368.

CHAPTER 2: EARLY ISOFORM OF DISABLED-1 FUNCTIONS INDEPENDENTLY OF REELIN-MEDIATED TYROSINE PHOSPHORYLATION IN CHICK RETINA

A version of this chapter has been published. Gao Z, Monckton EA, Glubrecht DD, Logan C, Godbout R. The early isoform of disabled-1 functions independently of Reelin-mediated tyrosine phosphorylation in chick retina. Mol Cell Biol. 2010 (17):4339-53. *In ovo* electroporation was done by Elizabeth Monckton. Immunohistochemical analysis and immunofluorescence analysis of Chx10 was done by Darryl Glubrecht.

2.1 INTRODUCTION

Retinal progenitor cells give rise to six major classes of neurons (cone, rod, bipolar, amacrine, horizontal and ganglion) and one class of glia (Müller) (Turner and Cepko 1987; Holt et al. 1988). The temporal birth of retinal cells follows a specific order, with ganglion cells differentiating first, followed by horizontal, amacrine, cone, rod, then bipolar and Müller glial cells (Cepko et al. 1996). Retinal cells in the mature retina are assembled into three nuclear layers (ganglion, inner and outer) separated by the inner and outer plexiform layers.

The Reelin-Disabled-1 (Dab1) signaling pathway is a key regulator of neuronal cell positioning. Binding of the extracellular glycoprotein Reelin to its lipoprotein receptors, the very low density lipoprotein receptor (VLDLR) and the apolipoprotein E receptor 2 (ApoER2), activates Src family kinases (SFK) and induces tyrosine phosphorylation of Dab1 (Hiesberger et al. 1999; Howell et al. 1999; Arnaud et al. 2003). The intracellular adaptor protein Dab1 contains three major domains: an N-terminal protein interaction/phosphotyrosine binding (PI/PTB) domain that binds to the NPxY motif within Reelin receptors (Trommsdorff et al. 1999), an internal tyrosine-rich region responsive to Reelin stimulation (Keshvara et al. 2001) and a C-terminal serine/threonine-rich region involved in Reelin-Dab1 signaling modulation (Herrick and Cooper 2002). The tyrosine-rich domain of Dab1 consists of five highly conserved tyrosine residues (Y185, Y198, Y200, Y220, Y232) that correspond to four tyrosine kinase recognition sites. Y185 and Y198/Y200 are located within two consensus SFK recognition sites (YQXI), whereas Y220 and Y232 are found within two

consensus Abl recognition sites (YXVP) (Songyang et al. 1993).

Upon phosphorylation, Dab1 triggers a host of signaling events, including activation of the SFK, phosphatidylionsitol 3 kinase (PI-3K)/Akt, mTOR, CrkL/C3G/Rap and LIMK1 (LIM kinase 1) pathways, and phosphorylation of n-cofilin (Arnaud et al. 2003; Bock and Herz 2003; Bock et al. 2003; Ballif et al. 2004; Jossin and Goffinet 2007; Chai et al. 2009). Together, these events result in the cytoskeleton remodeling and correct positioning of neurons during development. Dab1 tyrosine phosphorylation is essential for Reelin signaling, as mice expressing non-phosphorylated Dab1 protein have similar phenotypes to Reelin (*reeler*), Dab1 (*yotari/scrambler/Dab1*$^{-/-}$) or VLDLR and ApoER2 (*VLDLR*$^{-/-}$ *ApoER2*$^{-/-}$) deficient mice (Howell et al. 2000). These mice exhibit extensive defects in neuronal migration, including layer disruption in the cerebral cortex, cerebellum and hippocampus (D'Arcangelo et al. 1995; Howell et al. 1997b; Sheldon et al. 1997; Trommsdorff et al. 1999).

Defects associated with disruption of Reelin-Dab1 signaling are also observed in mouse retina, and include a reduction in the number of rod bipolar cells, abnormal synaptic layering of rod bipolar cells, reduction in the density of AII amacrine dendrites and alteration in the positioning of amacrine cell processes (Rice et al. 2001). In humans, *Reelin* mutations are associated with serious ocular and visual abnormalities, including retinal dysplasia and macular hypoplasia (Nabi et al. 2003). In *Drosophila,* inactivation of *Disabled* disrupts ommatidium development and leads to a frequent loss of R7 photoreceptors (Le and Simon 1998). Thus, Reelin-Dab1 signaling appears critical for proper

development of the retina as well as the brain.

Alternative splicing of the *Dab1* gene has been observed in a number of species including Drosophila (Gertler et al. 1993), mouse (Howell et al. 1997a; Bar et al. 2003) and zebrafish (Costagli et al. 2006). We have identified two alternatively-spliced Dab1 isoforms in the chick retina: Dab1-E and Dab1-L expressed at early and late stages of development, respectively (Katyal and Godbout 2004). Dab1-L, normally referred to as Dab1, has the five tyrosine residues described earlier. Dab1-E is missing a 35 aa region that includes Y198 and Y220, the major Reelin-induced Dab1 phosphorylation sites (Keshvara et al. 2001). Dab1-E also has a 19 aa insertion located downstream of the tyrosine-rich domain (Figure 2.1). To address the role of Dab1-E in retina, we have carried out a detailed analysis of Dab1-E expression during development. We demonstrate that Dab1-E is primarily found in retinal progenitor cells and that knock-down of Dab1-E affects the pool of progenitor cells in the retina. Our data suggest a tyrosine phosphorylation-independent and possibly Reelin-independent role for Dab1-E in the regulation of cell proliferation and commitment.

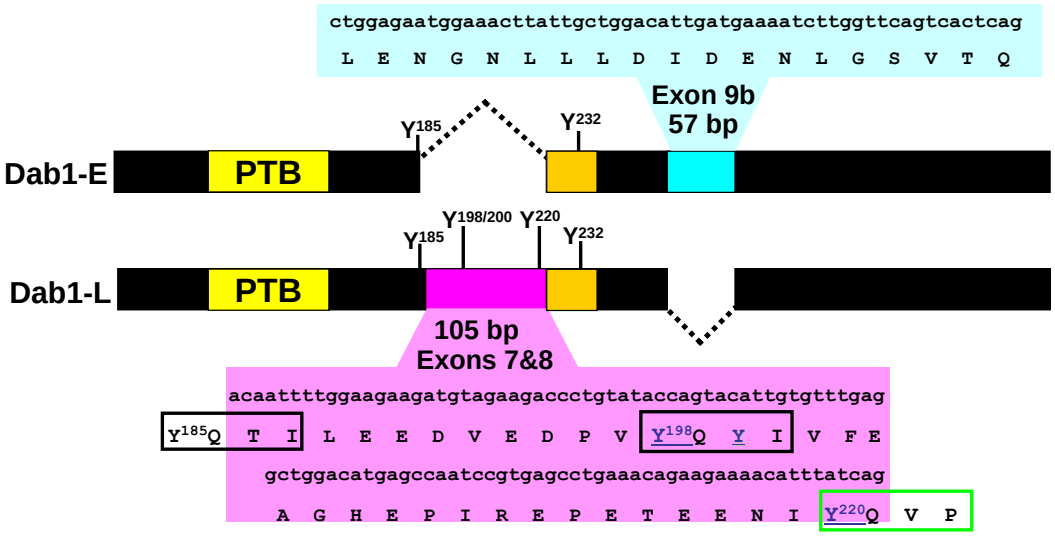

Figure 2.1 Schematic diagram of exon exclusion and inclusion in Dab1 isoforms. The two exons deleted in Dab1-E but included in Dab1-L are shown in magenta; the exon included in Dab1-E but excluded from Dab1-L is shown in blue. The phosphotyrosine binding (PTB) domain common to both Dab1 isoforms is shown in yellow. Two tyrosines at 185 and 232 are indicated in Dab1-E. Five tyrosines at 185, 198, 200, 220 and 232 are indicated in Dab1-L. Alternative splicing converts Y^{185}QTI (in Dab1-L) to Y^{185}QVP (in Dab1-E). YQXI is a consensus Src family kinase phosphorylation site, whereas YXVP is a consensus Abl family kinase recognition site.

2.2 MATERIALS AND METHODS

2.2.1 Generation of anti-Dab1-E antibody

Rabbit anti-Dab1-E antiserum was generated by injecting rabbits with the KLH-conjugated Dab1-E peptide (LENGNLLLDIDEN, residues 207-220, specific to chicken Dab1-E) (SACRI Antibody Service, Univ. Calgary). The antiserum was affinity-purified using a Dab1-E peptide-conjugated Affi-gel column (BioRad).

2.2.2 Generation of pSUPER RNAi constructs

pSUPER RNAi constructs were generated by ligating annealed oligonucleotides containing hairpin sequences targeting different regions of chicken *Dab1-E* mRNA into the pSUPER vector (Oligoengine) at the *Bgl*II and *Hin*dIII sites. Oligonucleotides were designated as Dab1 i# (with # specifying the first nt of the 19 nt targeted region based on Dab1-E cDNA sequence AY242122). Five constructs targeting different regions of Dab1-E were tested: Dab1 i227, Dab1 i334, Dab1 i576, Dab1 i632 and Dab1 i1314. The Dab1 i632 oligonucleotide specifically targets Dab1-E, whereas the other four oligonucleotides target both the Dab1-E and Dab1-L isoforms.

Full-length Dab1-E and Dab1-L constructs with GFP fused at the N-terminus have been previously described (Katyal and Godbout 2004). To test the efficacy of the pSUPER Dab1 RNAi constructs, HEK293T or HeLa cells were co-transfected with pEGFP-Dab1-E and pSUPER Dab1 RNAi constructs by calcium phosphate-mediated DNA precipitation. GFP-Dab1-E levels in transiently transfected cells were compared by western blot analysis using actin as a

loading control.

2.2.3 Retroviral RNAi constructs

The avian retroviral RCASBP (B) vector system (Federspiel and Hughes 1997) was used to deliver shRNAs into the eyes of developing chick embryos. Dab1 i576, identified as the most effective targeting oligonucleotide, and control scrambled oligonucleotide, under the control of the H1 promoter, were subcloned into the pSLAX12 Nco shuttle vector (Hughes et al. 1987) at the *Eco*RI and *Hin*dIII sites. Next, the GFP coding region from the pEGFP-C1 vector was inserted into the pSLAX12 shuttle vector at the *Nco*I and *Sma*I sites, upstream of the H1 promoter. After sequence verification, plasmids were digested with *Cla*I, releasing either the GFP-H1-Dab1 or scrambled oligonucleotide DNA fragment, which was then inserted into the *Cla*I site of RCASBP (B). This strategy results in GFP being placed under the control of the viral 5' long terminal repeat (LTR). All constructs were sequenced to ensure that no mutations were introduced during the cloning process.

2.2.4 *In ovo* electroporation of retroviral constructs

Fertilized eggs were obtained from a local supplier and incubated at 37°C for ~40 hrs prior to *in ovo* electroporation. At Hamburger Hamilton (HH) stages 10-12 (ED1.5-2) (Hamburger 1951), eggs were windowed and 1.5 ml of albumin removed. One to two μl of RCASBP(B) DNA (3 μg/ml) mixed with Fast Green was injected into the right optic vesicle of the embryo using a PV820 Pneumatic

Picopump (World Precision Instruments, Inc.). Electrodes spaced 2 mm apart were placed so that the current passed through the right eye. Five square pulses of 15 volts at 25 milliseconds were applied using a BTX Electro Square Porator (ECM830). At ED5 or ED7, embryos were sacrificed and eyes were dissected and screened for GFP expression by epifluorescence. GFP+ eyes were processed for further analysis.

2.2.5 Immunohistochemistry and immunofluorescence analysis

For immunohistochemistry, chick embryos or eyes were collected at specific developmental stages, fixed in formalin and embedded in paraffin, as previously described (Li et al. 2008). For immunofluorescence analysis, eyes were fixed in 4% paraformaldehyde, cryoprotected in a gradient of sucrose (12%, 16% and 18%) and embedded in OCT. Antigen retrieval was by microwaving in 0.01 M citrate (pH 6.0) for 20 min followed by blocking in 500 mM glycine. Antibodies used for immunohistochemistry: rabbit anti-Dab1-E (1:400); rabbit anti-Dab1 B3, a gift from Dr. Jonathan Cooper, Fred Hutchinson Cancer Research Center (1:500); rabbit anti-ApoER2 2562, a gift from Dr. Joachim Herz, University of Texas Southwestern Medical Center (1:2000); and mouse anti-Reelin (553730, Calbiochem) (1:1000). Antibodies used for immunofluorescence analysis: rabbit anti-Dab1-E (1:400); mouse anti-BrdU (#1170376, Roche) (1:100); mouse anti-Islet-1 (39.4D5, University of Iowa Hybridoma Bank (1:1500); mouse anti-AP2α (3B5, University of Iowa Hybridoma Bank) (1:250); goat anti-GFP (ab6673, Abcam) (1:2000); mouse anti-TUJ1 (MMS-435P, Covance)

(1:2000); mouse anti-proliferating cell nuclear antigen (PCNA) (N1529, Dako) (1:5000); mouse anti-glutamine synthetase (610517, BD Bioscience) (1:500); and rabbit anti-phospho-histone H3 serine 10 (ab5176. Abcam) (1:5000); and sheep anti-Chx10 antibody (a gift from Dr. Rod Bremner, University of Toronto, Canada (1:3000). The Dab1-E peptide competition assay was carried out by adding Dab1-E peptide to the diluted anti-Dab1-E antibody at a concentration of 0.1 μM.

2.2.6 Quantitative analyses of BrdU, Chx10 and phospho-histone H3

For BrdU labeling, one to two μl of a 1 mM BrdU solution was injected into the right eye of chick embryos 3 hrs prior to collection at ED5. To verify reduction in Dab1-E levels in GFP+ cells and measure the percentage of BrdU+ cells in regions of the retina with reduced levels of Dab1-E, we immunostained two consecutives tissue sections with either goat anti-GFP (1:2000) and rabbit anti-Dab1-E (1:400) antibodies, or goat anti-GFP and mouse anti-BrdU (1:100) antibodies. Micrographs were collected using a Zeiss Axio Imager Z1 with a 40X lens.

BrdU+ and GFP+ cells were counted using Metamorph software. The percentage of BrdU+ cells was obtained by dividing the number of BrdU+ cells by the total number of GFP+ cells or Hoechst 33342-stained cells in peripheral, intermediate and central areas of the retina. This analysis was carried out on 6 eyes obtained from control embryos, 6 eyes from embryos electroporated with the scrambled shRNA construct and 8 eyes electroporated with the Dab1 shRNA construct. Data were analyzed using Metamorph and exported to Excel.

Statistical analysis was performed with one-way Anova or Student *t*-test.

Chx10+ and GFP+ cells were counted using Metamorph software as described above. Analysis was carried out at ED5 on 4 eyes electroporated with the scrambled shRNA construct and 4 eyes electroporated with the Dab1 shRNA construct.

Quantification of phospho-histone H3+ and GFP+ cells in ED5 retinal sections was carried out on 6 eyes electroporated with the scrambled shRNA construct and 8 eyes electroporated with the Dab1 shRNA construct.

2.2.7 Western blot analysis and immunoprecipitations

Chick retina, stomach, liver, brain, heart, gut, as well as retinal cultures, were lysed in RIPA buffer [50 mM Tris-HCl pH 7.5, 150 mM NaCl, 1% Triton X-100, 0.5% sodium deoxycholate, 0.1% SDS, 50 mM NaF, 1 mM PMSF, 1 mM Na_3VO_4 and 1X Complete protease inhibitor cocktail (Roche)]. To maximize the separation between the different Dab1-E isoforms, cell lysates were electrophoresed through a 20 cm X 20 cm 8% polyacrylamide-SDS gel for 5 hrs. The following antibodies were used for western blot analysis: rabbit anti-Dab1-E (1:500); rabbit anti-Dab1 (100-4101-225, Rockland; 1:5000); goat anti-Dab1 (AB9012, Chemicon; 1:500); rabbit anti-Dab1 (B3; 1:1000); mouse anti-actin (A5441, Sigma; 1:100,000); goat anti-GFP (ab6673, Abcam; 1:2000); rabbit anti-ApoER2 2562 (1:2000); mouse anti-CrkL (05-414, Millipore; 1:2000) and mouse anti-Reelin (553730, Calbiochem; 1:500).

For immunoprecipitation, cell lysates were precleared with Protein A or

Protein G Sepharose beads (GE Healthcare) for 1 hr at 4˚C, followed by incubation with primary antibodies or IgG control overnight at 4˚C and collection of the immunoprecipitates with Protein A or Protein G Sepharose beads. Immunoprecipitates or cell lysates were separated by SDS-PAGE, blotted onto nitrocellulose membranes and immunostained with the indicated antibodies.

2.2.8 Dissociation of chick retinal cells and immunofluorescence analysis

Retinas from scrambled or Dab1 shRNA-electroporated embryos at ED7 were screened for GFP expression by epifluorescence. For comparison, only GFP+ retinal tissues from similar locations were used for analysis. GFP+ retinal tissues were dissociated with trypsin and collagenase as previously described (Altshuler and Cepko 1992). Cells were plated onto 100 μg/ml poly-D-lysine-coated glass coverslips and incubated at 37°C for 2 hrs before immunofluorescence analysis.

For immunofluorescence analysis, cells were fixed in 4% paraformaldehyde for 10 min, permeabilized in 0.1% Triton X-100 for 5 min and blocked in 1% normal donkey serum for 1 hr. Cells were then incubated with primary antibodies (1:4000 goat anti-GFP, 1:1500 mouse anti-Islet-1, 1:500 mouse anti-AP2α) overnight at 4°C, followed by Alexa dye-conjugated secondary antibodies for 2 hrs. For quantification of Islet1+ and AP2α+ cells in retinal tissue electroporated with RCAS constructs, we collected micrographs in the tile scan (mosaic scan) mode (3X3) using a confocal microscope (LSM 710) and a 20X lens. The number of immunoreactive cells was scored using the Metamorph

software. A minimum of three independently electroporated retinas were analyzed with three tile scan images from each retina.

2.2.9 Primary retinal cultures and Reelin treatment

Primary retinal cultures were prepared by trypsinizing ED5-5.5 or ED10 retinas, and plating the dissociated cells in Dulbecco's Modified Eagle Medium supplemented with 10% fetal calf serum and penicillin/streptomycin. For generation of Reelin-conditioned medium, HEK293T cells at 50% confluence were transfected with pCrl-Reelin (a gift from Dr. Tom Curran, Univ. Pennsylvania) or pcDNA3 constructs. The medium was replaced with OPTI-MEM I (Invitrogen) 24 hrs after transfection. Supernatants were collected 36 hr later and concentrated 30X using Amicon Ultra Centrifugal Filter Devices (100,000 MWCO, Millipore). ED10 primary retinal cells were treated for 15 min with concentrated supernatants diluted 1:15.

2.2.10 Drug treatment and RT-PCR analysis

ED5.5 primary retinal cultures were treated with DMSO, 20 µM cyclopamine (Calbiochem) and 10 µM DAPT (Calbiochem) for 24 hrs, followed by total RNA extraction using TRIzol reagent (Invitrogen). 5 µg total RNA from ED5.5 primary retinal cells treated with DMSO, cyclopamine and DAPT were reverse transcribed using an oligo (dT) primer and Superscript reverse transcriptase (Invitrogen). Single-strand cDNAs were PCR-amplified using primers P1, P2, P3 and P4 (Katyal and Godbout 2004). PCR products were run

on a 9% polyacrylamide gel.

2.3 RESULTS

2.3.1 Expression of Dab1-E and Dab1-L in the developing chick retina

We have identified two main isoforms of Dab1 in chick retina and brain: Dab1-E, previously shown by RT-PCR and *in situ* hybridization analysis to be expressed at early stages of retinal development, and Dab1-L, primarily found in ganglion and amacrine cells (Katyal and Godbout 2004). To carry out a more detailed analysis of the spatial and temporal Dab1-E distribution pattern, we generated anti-Dab1-E antiserum by immunizing rabbits with a Dab1-E specific peptide (encoded by exon 9b – shown in Figure 2.1). The specificity of the anti-Dab1-E antiserum was determined by western blot analysis of chick retinal cells transfected with GFP, GFP-Dab1-E or GFP-Dab1-L expression constructs. As shown in Figure 2.2A, a commercially available anti-Dab1 antibody raised against the C-terminus of Dab1 recognized both the GFP-Dab1-E and GFP-Dab1-L proteins, and at least five lower molecular weight bands. The anti-Dab1-E antiserum specifically recognized GFP-Dab1-E, as well as lower molecular weight bands which were also observed in untransfected cells.

Next, we examined endogenous Dab1-E and Dab1-L expression in chick retinal tissues at different stages of development. At ED5, when 85% of retinal cells are proliferating (Dutting et al. 1983), similar banding patterns (consisting of at least 4 bands) were observed using either the anti-Dab1 antibody or the anti-Dab1-E antiserum (Figure 2.2B). At ED7, when 60% of cells are proliferating, immunostaining with either anti-Dab1-E or anti-Dab1 antibody revealed the same four bands detected at ED5. However, a weakly-staining slower migrating band

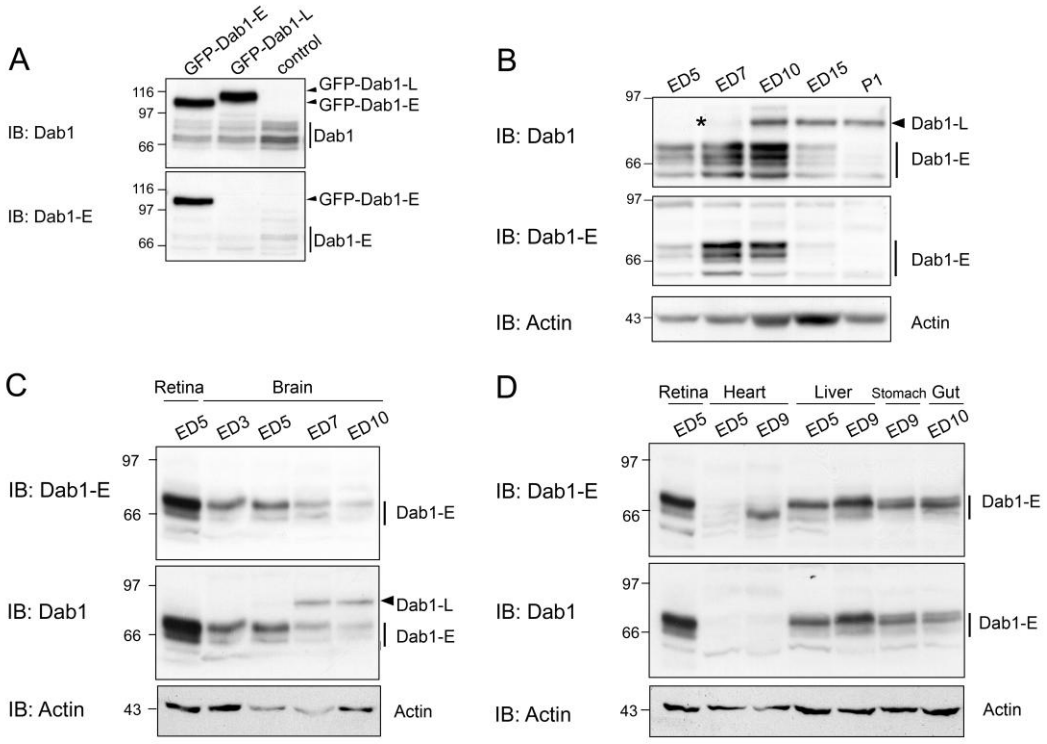

Figure 2.2 Dab1 expression in the chick embryo. (A) Determination of anti-Dab1-E antibody specificity. Fifty μg cell lysates prepared from embryonic day (ED) 5 retinal cultures transfected with GFP (control), GFP-chDab1-E or GFP-chDab1-L expression constructs were resolved by 8% SDS-PAGE and transferred to a PVDF membrane. The membrane was immunostained with anti-Dab1 (raised against the C-terminus of Dab1, top panel) and anti-Dab1-E (raised against the E-specific region, bottom panel) antibodies, respectively. Anti-Dab1 antibody recognizes both Dab1-E and -L, whereas the anti-Dab1-E antibody specifically recognizes Dab1-E. The endogenous Dab1 and Dab1-E proteins are indicated by vertical bars. **(B) Western blot analysis of Dab1 in the chick retina.** To maximize the separation between the Dab1 isoforms, 100 μg retinal cell lysates prepared from ED5, ED7, ED10, ED15 and P1 were resolved on a 20 cm X 20 cm 8% SDS acrylamide gel and transferred to a PVDF membrane. The membrane was immunostained with anti-Dab1 (top panel) and anti-Dab1-E (middle panel) antibodies, respectively. The arrowhead indicates Dab1-L, whereas the vertical bars show the early form(s) of Dab1 (Dab1-E). The asterisk indicates a weakly stained Dab1-L band in ED7 retina. **(C) Western blot analysis of Dab1 in the chick brain.** Cell lysates prepared from ED5 chick retina, ED3 chick head, ED5, ED7 and ED10 chick brain were analyzed by western blotting as indicated in (A). **(D) Western blot analysis of Dab1 in embryonic chick tissues.** Cell lysates prepared from chick retina, heart, stomach, liver and gut at different developmental stages (as indicated) were analyzed by western blotting. Actin was used as a loading control.

(indicated by the asterisk) was also detected with anti-Dab1 antibody. This slower migrating band was prominently displayed at later developmental stages (ED10, ED15 and post-hatching P1) using anti-Dab1, but not anti-Dab-E, antibodies. The four lower bands recognized by both the anti-Dab1 and anti-Dab1-E antibodies remained abundant at ED10, but were greatly reduced in intensity by ED15 and barely detectable in the fully-differentiated P1 retina (Figure 2.2B). Our data indicate that the slower migrating band represents Dab1-L, while the four faster migrating bands likely represent different forms of Dab1-E.

As bands extraneous to Dab1/Dab1-E were observed upon immunostaining with anti-Dab1-E serum, we affinity-purified this serum using a Dab1-E peptide-conjugated Affi-gel column. Immunoblot analysis of ED5 retina using the affinity-purified anti-Dab1-E antibody produced identical results to that obtained with anti-Dab1 antibody, demonstrating the specificity of the anti-Dab1-E antibody (Figure 2.2C). Using the anti-Dab1-E antibody, we carried out western blot analysis of brain lysates at different stages of development (ED3 to ED10). Dab1-E was expressed in brain at all developmental stages examined, albeit at lower levels than in the retina (Figure 2.2C). In contrast, Dab1-L was first detected in the brain at ED7. Other tissues such as liver, stomach and gut, also expressed Dab1-E. The slower migrating Dab1-L was not detected in these tissues (Figure 2.2D), suggesting tissue-specific alternative splicing of Dab1 pre-mRNA during development. Of note, Dab1-E was barely detectable in ED5 heart; however, we observed a strong band migrating at ~66 kDa in ED9 heart upon staining the blot with anti-Dab1-E but not anti-Dab1 antibody. Since the anti-Dab1

antibody was generated against the C-terminus of Dab1, this suggests that heart tissue expresses a third isoform of Dab1 that contains the Dab1-E-specific region but lacks the C-terminus of Dab1.

2.3.2 Distribution of Dab1-E and Dab1-L in the developing chick retina

To examine the cellular distribution of Dab1-E and Dab1-L in the developing retina, we carried out immunohistochemical analysis of serial retinal sections. For these analyses, we used anti-Dab1 B3 antibody raised against the central domain of mouse Dab1 (aa 107-243), including the tyrosine phosphorylation domain (Howell et al. 1997a). When this antibody was used for western blot analysis of ED10 chick retina lysates, it was found to specifically recognize the slower migrating band, Dab1-L (Figure 2.3). This suggests that the epitopes recognized by the anti-Dab1 B3 antibody are located within the tyrosine-rich region that is excluded in Dab1-E.

We used anti-Dab1 B3 and anti-Dab1-E antibodies to specifically examine the temporal and spatial distribution of Dab1-L and Dab1-E in the developing retina. At ED4, when the vast majority of retinal cells are proliferating (>90%), cytoplasmic Dab1-E was found throughout the retina with slightly stronger staining in the emerging ganglion cell layer (GCL). The B3 antibody produced a weak background signal with slightly stronger staining of the emerging ganglion cells (Figure 2.4A). At ED5, the B3 antibody generated a strong signal in the GCL whereas Dab1-E staining intensity was similar throughout the retina (Figure 2.4B). At ED7, Dab1-E was abundantly expressed throughout the retina with the

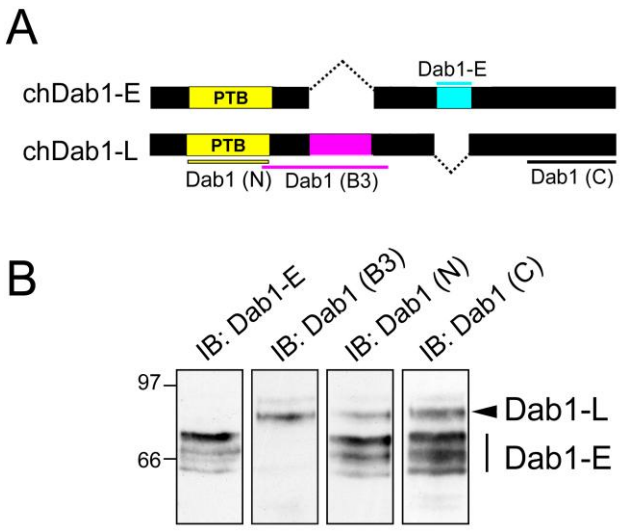

Figure 2.3 Western blot analysis of ED10 chick retinal lysates using different anti-Dab1 antibodies. (A) Schematic illustration of Dab1 domains. Colored lines indicate the location of the antigens used to generate the different Dab1 antibodies used for our experiments: yellow, anti-Dab1 (N-terminus, N) antibody raised against the PTB domain; magenta, anti-Dab1 (B3) antibody raised against the 107-243 aa of mouse Dab1 (-L); blue, anti-Dab1-E antibody raised against the 207-220 amino acid peptide specific to chicken Dab1-E; black, anti-Dab1 (C-terminus, C) antibody raised against the 440-555 aa of mouse Dab1. **(B) Western blot analysis of ED10 chick retinal lysates.** Twenty µg ED10 retinal lysates were analyzed by western blotting using anti-Dab1-E, anti-Dab1 (B3), anti-Dab1 (N) and anti-Dab1 (C) antibodies. Anti-Dab1 (N) and anti-Dab1 (C) antibodies recognize both the Dab1-E and Dab1-L isoforms. Dab1-E and anti-Dab1 (B3) antibodies specifically recognize Dab1-E and Dab1-L, respectively.

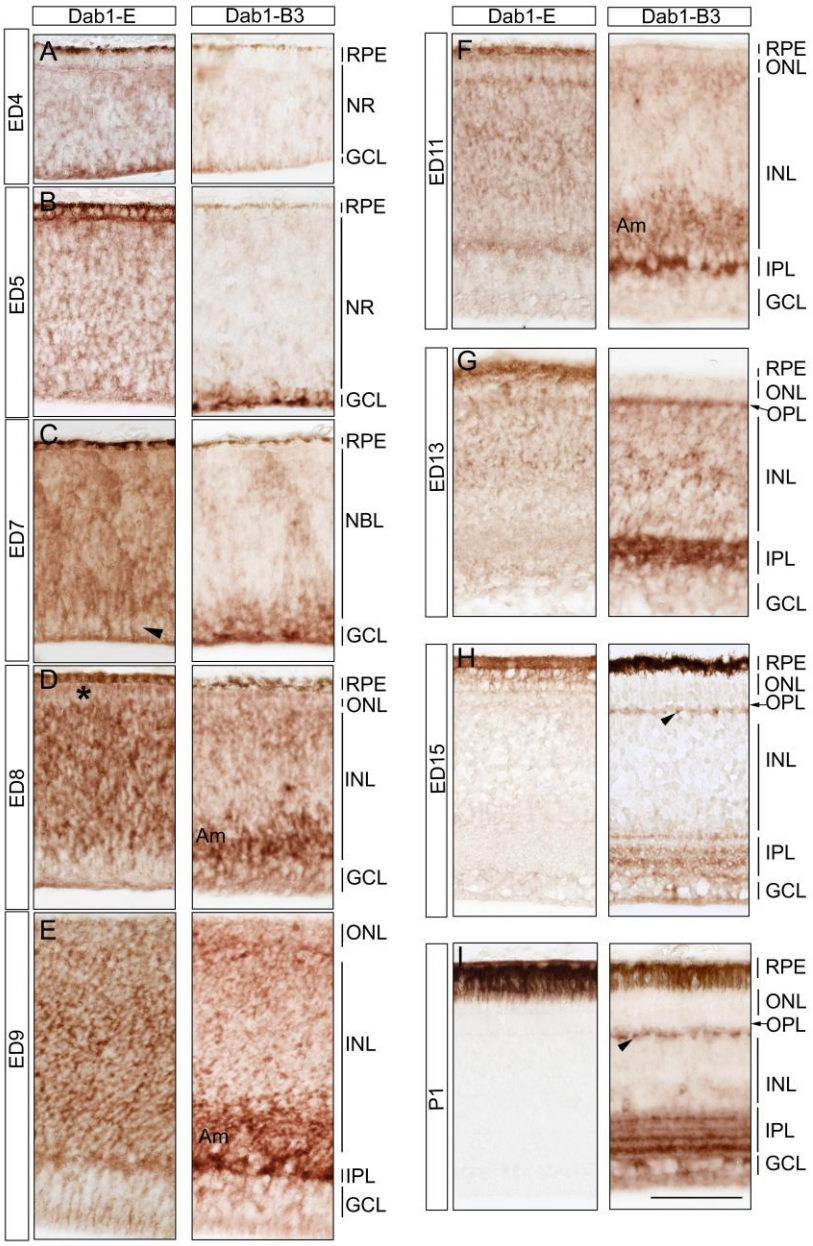

Figure 2.4 Immunohistochemical analysis of Dab1 isoforms in the developing chick retina. Consecutive sections from formalin-fixed paraffin-embedded chick retina at different developmental stages (as indicated) were immunostained with anti-Dab1-E or anti-Dab1 B3 antibody, respectively. Sections were not counterstained in order to better visulalize Dab1 staining. The arrowhead in panel C points to the reduced expression of Dab1-E in the GCL. In panel D, the asterisk indicates the reduced levels of Dab1-E in the emerging ONL. Abbreviations: RPE, retinal pigmented epithelium; NR, neural retina; NBL, neuroblastic layer; INL, inner nuclear layer; IPL, inner plexiform layer; GCL, ganglion cell layer; ONL, outer nuclear layer; OPL, outer plexiform layer; Am, amacrine. Scale bar, 50 μm.

exception of the GCL. Dab1-L remained prominent in ganglion cells. At ED8 and ED9, during the peak of amacrine and photoreceptor cell accumulation (Prada et al. 1991), we observed elevated levels of Dab1-E in the inner nuclear layer (INL), with reduced staining in the outer nuclear layer (ONL) where photoreceptors are located (Figure 2.4D and E). Dab1-L was prominently expressed in amacrine cells at ED8 and ED9.

By ED11 (towards the end of retinal neurogenesis), Dab1-E levels were significantly reduced in the retina, with residual staining in the middle of the INL (Figure 2.4F). Dab1-L was abundantly expressed in the IPL and in amacrine cells. At ED13, Dab1-L was strongly expressed in the IPL and to a lesser extent in the outer plexiform layer (OPL). Two days later, Dab1-E was barely detectable in the retina whereas Dab1-L was found in the IPL and OPL, with a distinct layering pattern in the IPL, in keeping with the reported expression of Dab1 (Dab1-L) in distinct subsets of amacrine and ganglion cells (Rice and Curran 2000). Shortly after hatching at P1, intense Dab1-L staining was observed in the IPL, ganglion fibers, as well as in a layer of cells located in the outer part of the INL (likely horizontal cells based on location, indicated by the arrowheads in Figure 2.4H and I).

Competition experiments with the Dab1-E peptide confirmed that the signal detected with the Dab1-E antibody was specific to Dab1-E (Figure 2.5). Immunostaining with an anti-Dab1 antibody (raised against the N-terminus of Dab1) that recognizes both Dab1-E and Dab1-L revealed a Dab1-E-specific expression pattern at ED5, a mixed Dab1-E/Dab1-L expression pattern at ED7

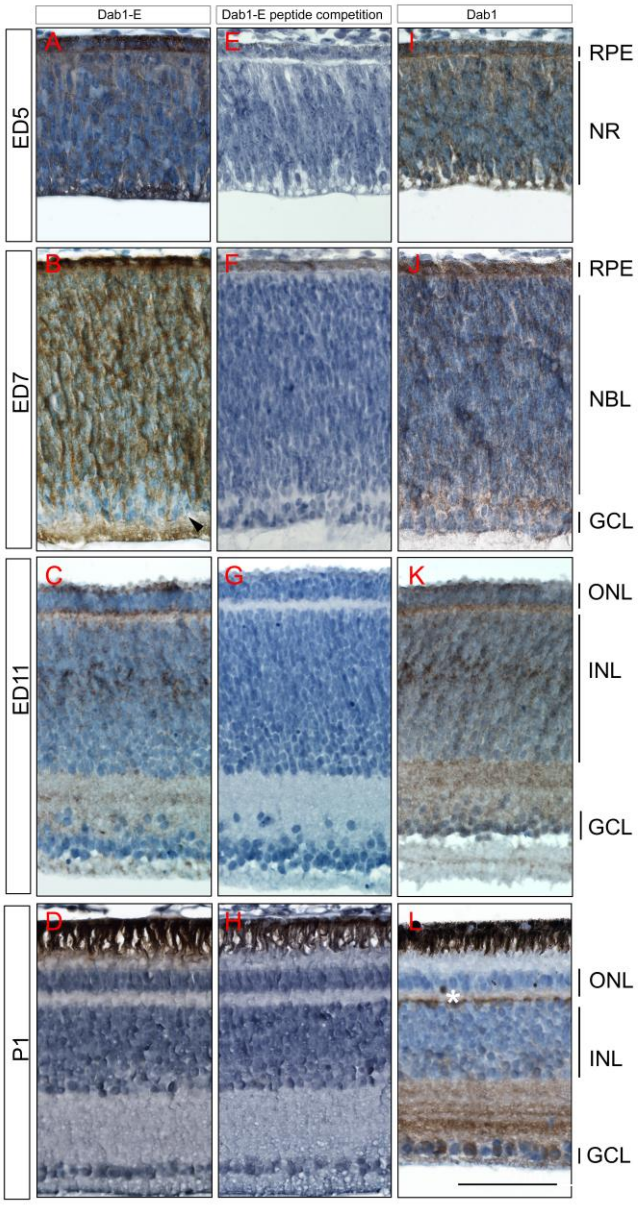

Figure 2.5 Immunohistochemical analysis of Dab1 isoforms in the developing chick retina. Consecutive sections from formalin-fixed paraffin-embedded chick retinas at ED5, ED7, ED11 and P1 were immunostained with: (i) anti-Dab1-E antibody, (ii) anti-Dab1-E antibody pre-incubated with 1 µM Dab1-E peptide, and (iii) anti-Dab1 antibody (raised against the N-terminus). The signals were detected using the DakoCytomationEnvision+ system and nuclei were labeled with hematoxylin. The arrowhead indicates that Dab1-E expression is significantly reduced in the ganglion cell layer (GCL) at ED7 (panel B), whereas the asterisk indicates Dab1 expression in horizontal cells at P1 (panel L). Micrographs were collected with a 40X lens using a Zeiss Axioskop 2 Plus microscope. Abbreviations: RPE, retinal pigment epithelium; NR, neural retina; NBL, neuroblastic layer; INL, inner nuclear layer; IPL, inner plaxiform layer; GCL, ganglion cell layer; ONL, outer nuclear layer. Scale bar, 50 µm.

and ED11, and a Dab1-L-specific expression pattern at P1 (Figure 2.5). Together, our data demonstrate that Dab1-E and Dab1-L have distinct temporal and spatial distribution patterns in the developing retina, with Dab1-E being primarily expressed in neuroblastic cells and newly-committed cells, and Dab1-L first expressed in ganglion, followed by amacrine and horizontal cells at later developmental stages. Particularly striking is the intensity of the Dab1-L signal in the IPL from ED9 to post-hatching.

2.3.3 Expression of Dab1-E in proliferating cells and in newly-committed postmitotic cells

The spatial and temporal distribution pattern of Dab1-E suggests a role specific to progenitor cells during retinal development. To directly address whether Dab1-E is expressed in actively proliferating cells, we co-immunostained ED5 retinal tissue with antibodies to Dab1-E and the proliferation marker PCNA. As shown in Figure 2.6A, Dab1-E and PCNA localize to the same cells throughout most of the retina. Ganglion cells are positive for Dab1-E but negative for PCNA. By injecting BrdU in the eyes of ED5 chick embryos, we show that Dab1-E co-localizes with BrdU+ cells (Figure 2.6A). Our combined data indicate that Dab1-E is predominantly found in proliferating retinal progenitor cells at early stages of development.

In addition to proliferating cells, Dab1-E is transiently expressed in postmitotic retinal cells. For example, Dab1-E is detected in ganglion cells at ED5

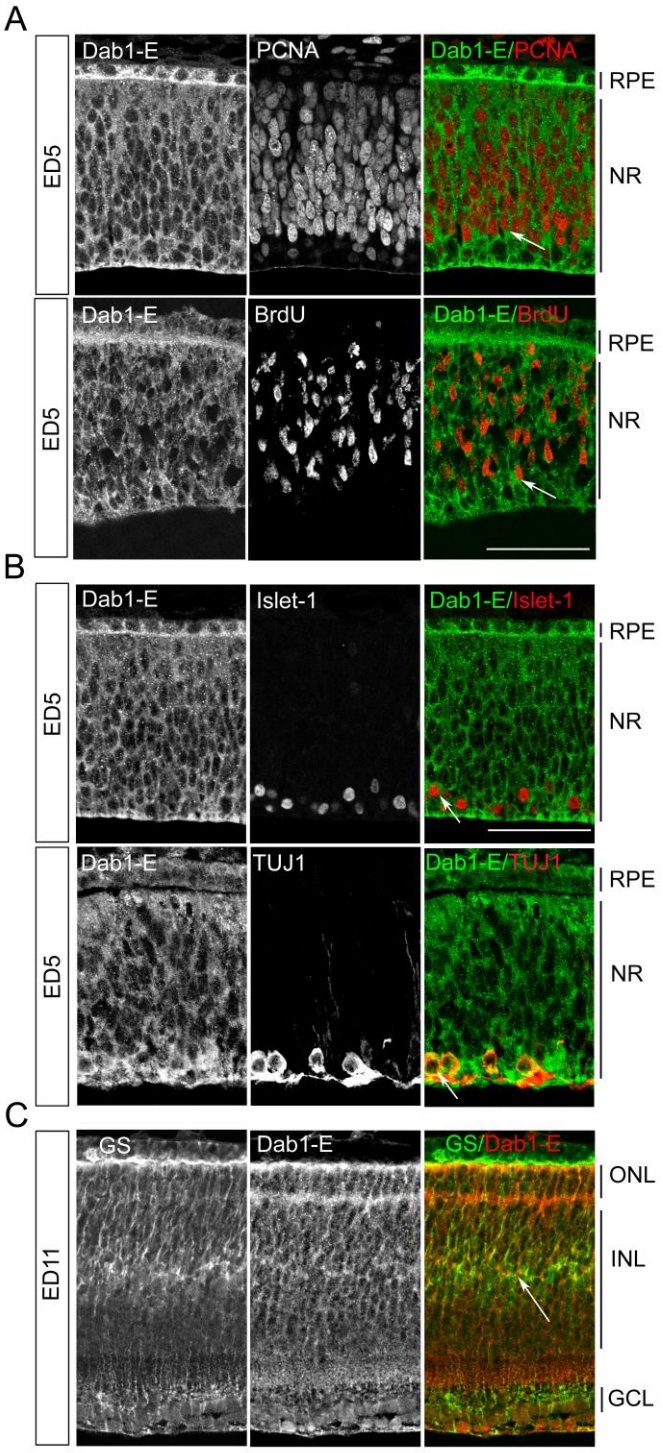
A
ED5
Dab1-E
PCNA
Dab1-E/PCNA
RPE
NR
ED5
Dab1-E
BrdU
Dab1-E/BrdU
RPE
NR
B
ED5
Dab1-E
Islet-1
Dab1-E/Islet-1
RPE
NR
ED5
Dab1-E
TUJ1
Dab1-E/TUJ1
RPE
NR
C
ED11
GS
Dab1-E
GS/Dab1-E
ONL
INL
GCL

Figure 2.6 Expression of Dab1-E in proliferating retinal progenitor cells and newly committed postmitotic cells. (A) Co-immunostaining of Dab1-E and PCNA or Dab1-E and BrdU in ED5 chick retina. Retinal sections were double-stained with rabbit anti-Dab1-E (1:400) and either mouse anti-PCNA (1:5000) or mouse anti-BrdU (1:50) antibodies, followed by donkey anti-rabbit and donkey anti-mouse secondary antibodies conjugated with fluorescent Alexa 488 and Alexa 555, respectively. Arrows indicate the co-labeling of Dab1-E (cytoplasmic) and PCNA (nuclear) or BrdU (nuclear) in retinal cells. **(B) Co-immunostaining of Dab1-E and Islet-1 or Dab1-E and TUJ1 in ED5 chick retina.** Retinal sections were double-stained with rabbit anti-Dab1-E and mouse anti-Islet-1 (1:1500) or mouse anti-TUJ1 (1:2000) antibodies as indicated in (A). Arrows indicate the co-labeling of Dab1-E and Islet-1 or TUJ1 in retinal cells. **(C) Co-immunostaining analysis of Dab1-E and glutamine synthetase (GS) in ED11 chick retina.** Retinal sections were double-stained with rabbit anti-Dab1-E and mouse anti-GS (1:500) antibodies, followed by donkey anti-rabbit or donkey anti-mouse secondary antibodies conjugated with Alexa 555 and Alexa 488, respectively. Arrows indicate the co-labeling of Dab1-E and GS in ED11 chick retina. Micrographs were collected with a Zeiss LSM 510 confocal microscope equipped with a 40X lens. Abbreviations: RPE, retinal pigmented epithelium; NR, neural retina; INL, inner nuclear layer; GCL, ganglion cell layer; ONL, outer nuclear layer. Scale bar, 50 μm.

but is excluded from ganglion cells by ED8 (Figure 2.4B and E). Similarly, Dab1-E is expressed in amacrine cells at ED8 but is excluded from these cells by ED13 (Figure 2.4D and G). Furthermore, the distribution pattern of Dab1-E at ED11 suggests that Dab1-E may also be found in Müller glial cells, last to differentiate in chick retina (Figure 2.4F and Figure 2.5C).

To verify that Dab1-E is indeed expressed in ganglion cells at ED5, we carried out co-immunofluorescence analysis of Dab1-E and either Islet-1, a marker of retinal ganglion cells (Austin et al. 1995), or class III β-tubulin TUJ1, a marker of postmitotic neurons. As shown in Fig. 4B, Dab1-E and Islet-1 are co-expressed in retinal ganglion cells at ED5. We also observed co-staining of TUJ1 and Dab1-E in ganglion cells (Figure 2.6B). To determine whether Dab1-E is transiently expressed in Müller glial cells, we carried out co-immunofluorescence analysis of Dab1-E with glutamine synthetase (GS), a marker of Müller glial cells. At ED11, the peak of Müller glia cell generation (Prada et al. 1991), we observed co-staining of Dab1-E and GS in the middle of the INL (Figure 2.6C), indicating that Dab1-E is expressed in Müller glia cells. At P1, Dab1-E could no longer be detected in Müller glial cells (Figure 2.4I), demonstrating the transitory nature of Dab1-E expression in these cells.

2.3.4 Expression of Reelin and its receptors in the developing chick retina

Previous studies have demonstrated that Dab1 (i.e. Dab1-L) functions through Reelin and its receptors VLDLR and ApoER2 (Trommsdorff et al. 1998; Howell et al. 1999). Although Dab1-E retains the PI/PTB domain required for

interaction with Reelin receptors, it is not clear whether Dab1-E activity in the developing retina requires Reelin and its receptors. To examine the temporal expression of Dab1-E in relation to Reelin and its receptors, we carried out western blot analysis with the same retinal cell lysates used to generate Figure 2.2B. Reelin was not detected at ED5; however, weak bands were visible at ED7 upon longer exposure (Figure 2.7A and data not shown). Three bands representing full-length Reelin (top band), N-terminally-truncated Reelin (middle band) and the active form of Reelin (bottom band) (Lambert de Rouvroit et al. 1999) were observed at ED10, with peak levels of active Reelin at ED15. Immunohistochemical analysis revealed prominent Reelin expression in ganglion cells at both ED5 and ED7 (Figure 2.7B). By ED11, high levels of Reelin were observed in bipolar cells (arrow), some of the cells in the GCL (arrowhead), OPL and IPL. At P1, Reelin was primarily found in bipolar cells and in the plexiform and fiber layers. These results are consistent with the Reelin mRNA and protein expression patterns previously reported for chick and mouse retina (Schiffmann et al. 1997; Bernier et al. 2000) .

Both ApoER2 and VLDLR were detected in the ED5 and ED7 retina by western blot analysis (Figure 2.7A); however, protein levels were lower than those observed at ED10 and ED15. Two forms of ApoER2 and VLDLR were observed in the retina, consistent with previous reports indicating that these two receptors have alternatively spliced isoforms (Iijima et al. 1998; Sun and Soutar 1999). Immunohistochemical analysis of ApoER2 revealed intense staining of ganglion cells at ED5 and ED7 (Figure 2.7B). ApoER2 expression was

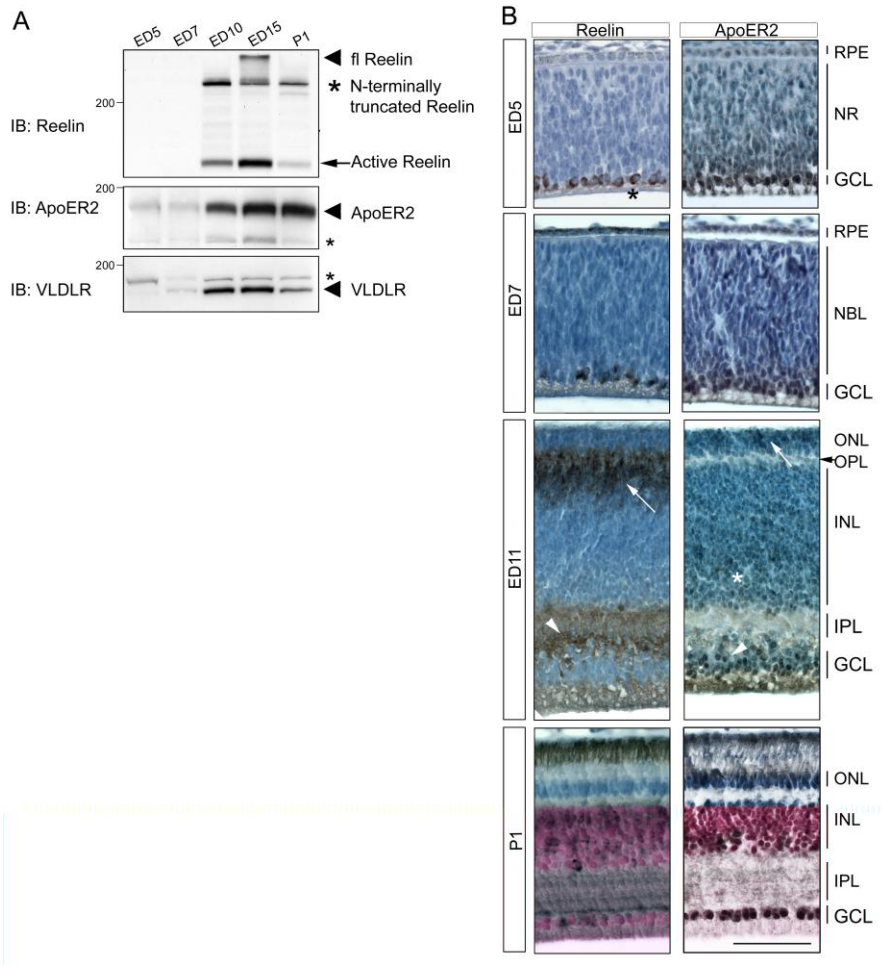

Figure 2.7 Expression of Reelin, ApoER2 and VLDLR in the developing chick retina. (A) Western blot analysis of Reelin, ApoER2 and VLDLR in the developing chick retina. Western blotting of Reelin, ApoER2 and VLDLR was carried out as described in Fig. 2B. The membrane was immunostained with anti-Reelin (1:500, top panel), ApoER2 (1:2000, middle panel) and VLDLR (1:200, bottom panel) antibodies, respectively. Actin was used as a loading control. The arrowhead in the top panel indicates the full-length Reelin, whereas the large asterisk and the arrow indicate N-terminally truncated Reelin and active Reelin, respectively. Arrowheads in the middle and bottom panels indicate the most abundant forms of ApoER2 and VLDLR, whereas small asterisks indicate alternatively spliced isoforms. **(B) Immunohistochemical analysis of Reelin and ApoER2 in the developing chick retina.** Chick retinal sections at different developmental stages (as indicated) were immunostained with mouse anti-Reelin (1:500) or rabbit anti-ApoER2 (1:2000) antibodies and nuclei were labeled with hematoxylin. At ED5, the asterisk (left panel) indicates Reelin expression in ganglion cells. At ED11, the arrow and arrowhead (left panel) point to the expression of Reelin in bipolar and ganglion cells, respectively. The arrow, asterisk and arrowhead (right panel) indicate ApoER2 expression in a subset of photoreceptors, amacrine and ganglion cells in ED11 chick retina. Abbreviations: RPE, retinal pigmented epithelium; NR, neural retina; NBL, neuroblastic layer; INL, inner nuclear layer; IPL, inner plexiform layer; GCL, ganglion cell layer; ONL, outer nuclear layer; OPL, outer plexiform layer. Scale bar, 50 μm.

widespread at ED11, whereas the ApoER2 signal was strongest in ganglion, amacrine and a subset of photoreceptor cells at P1. These data indicate that there is a good correlation between the expression patterns of Reelin, ApoER2, VLDLR and Dab1-L in the developing retina, in keeping with a role for Dab1-L in Reelin-mediated signaling. However, there is little correlation between the expression pattern of Dab1-E and that of Reelin and its receptors, suggesting that Dab1-E may function independently of Reelin signaling.

2.3.5 Dab1-E is not tyrosine phosphorylated and does not interact with CrkL in the developing retina

A major difference between Dab1-E and Dab1-L is the absence of two tyrosine phosphorylation sites (Y198 and Y220) implicated in the relay of the Reelin signal in Dab1-E. As the Y185 phosphorylation site is converted from a Src to a Abl recognition site (Y^{185}Q TI → Y^{185}QVP) in Dab1-E (Katyal and Godbout 2004), a consequence of Dab1 alternative splicing is the loss of two consensus SFK phosphorylation sites and the retention of two consensus Abl phosphorylation sites in Dab1-E (Figure 2.1). In previous reports, we have shown that exogenous GFP-Dab1-L, but not GFP-Dab1-E, is robustly tyrosine phosphorylated in transfected retinal cells (Katyal and Godbout 2004; Katyal et al. 2007).

As indicated earlier, 4 bands are detected in retinal lysates immunostained with anti-Dab1-E antibody (Figure 2.2B), suggesting Dab1-E post-translational modification. To investigate whether endogenous Dab1-E is tyrosine

phosphorylated, we immunoprecipitated Dab1 from ED10 retinal lysates using an anti-Dab1 antibody that recognizes both Dab1-E and Dab1-L. We selected ED10 for our analyses because of the relative abundance of both Dab1-E and Dab1-L at this developmental stage. Immunoprecipitates were immunoblotted with an anti-phosphotyrosine antibody (clone 4G10, Millipore). As shown in Figure 2.8A, the anti-phosphotyrosine antibody recognized Dab1-L, but none of the Dab1-E bands. Dab1-L identity was confirmed by reprobing the blot with anti-Dab1 antibody which also revealed the presence of the non-tyrosine phosphorylated Dab1-E bands. We used two additional phosphotyrosine antibodies (pY 1000 and pY PT-66) to verify that Dab1-E was not detectably tyrosine phosphorylated (data not shown).

Next, we addressed the possibility that Reelin stimulation might induce Dab1-E tyrosine phosphorylation. ED10 primary retinal cultures (which also express endogenous Reelin) were treated with Reelin-conditioned medium. As shown in Figure 2.8B, Reelin treatment induced Dab1-L tyrosine phosphorylation by ~2X in retinal cultures, but had no effect on Dab1-E. These data indicate that Dab1-E is not tyrosine phosphorylated in response to exogenous Reelin treatment, and are consistent with a Reelin-independent role for Dab1-E.

Reelin signaling promotes association of Dab1 with Crk adaptors, CrkII and CrkL (Chen et al. 2004). *CrkII*$^{-/-}$*CrkL*$^{-/-}$ double knock-out mice exhibit phenotypes similar to that of *reeler*, but retain normal Reelin-induced Dab1 tyrosine phosphorylation. However, two downstream Reelin-Dab1-dependent signaling events, phosphorylation of guanine nucleotide exchange factor C3G

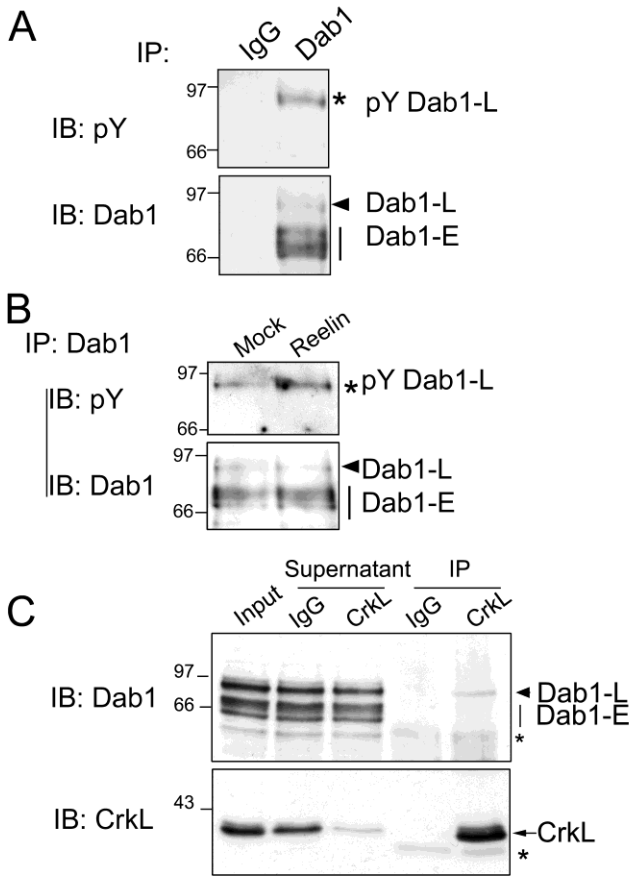

Figure 2.8 Examination of Dab1 tyrosine phosphorylation in the retina. (A) Tyrosine phosphorylation of Dab1-L in ED10 chick retina. Western blotting of anti-Dab1 antibody and IgG control immunoprecipitates from ED10 chick retinal extracts was carried out as in Fig. 2A. The membrane was immunostained with mouse anti-pY 4G10 and rabbit anti-Dab1 antibodies. (**B) Reelin stimulates Dab1-L tyrosine phosphorylation, but not Dab1-E, in ED10 retinal cells.** ED10 primary retinal cultures were treated with mock or Reelin-conditioned medium for 15 min followed by cell lysis in RIPA buffer. Dab1 proteins were immunoprecipitated from the cell lysates and analyzed by western blotting. Tyrosine phosphorylated Dab1 was detected with a mouse anti-pY 4G10 antibody and Dab1 identity was confirmed with an anti-Dab1 antibody. **(C) Dab1-L, but not Dab1-E, associates with CrkL.** Immunocomplexes were immunoprecipitated using mouse anti-CrkL or mouse IgG control from ED10 chick retinal lysates. The immunoprecipitates, supernatants and 10% input were analyzed by western blotting using anti-Dab1 and CrkL antibodies. Asterisks indicate non-specific bands.

and Akt phosphorylation, are abolished in the double knock-out mice, suggesting that Crk proteins play essential roles downstream of Dab1 (Park and Curran 2008). Two YXVP sites (Y220 and Y232) in Dab1 have been shown to be critical for the recruitment of Crk proteins (Ballif et al. 2004). Like Dab1-L, Dab1-E contains two YXVP sites (converted Y185 and Y232). To determine whether both Dab1-L and Dab1-E can interact with CrkL, we carried out co-immunoprecipitation experiments with proteins extracted from ED10 retina, when both Dab1-E and Dab1-L are relatively abundant. As shown in Figure 2.8C, only Dab1-L co-immunoprecipitates with CrkL proteins, suggesting that tyrosine phosphorylation is required for interaction with CrkL and that only Dab1-L can transmit the signal to CrkL and downstream molecules.

2.3.6 Knockdown of Dab1-E in the developing retina

Dab1-E expression in proliferating retinal progenitor cells and postmitotic cells suggest that Dab1-E may be important in retinal cell proliferation and/or commitment. To examine the role of Dab1-E in the retina, we used RNAi to knockdown Dab1-E at early stages of retinal development. Five RNAi constructs were tested (including one that specifically targets Dab1-E, Dab1 i632). Of these five RNAi constructs, Dab1 i576 was the most effective at reducing Dab1-E levels in HeLa and HEK293T cells co-transfected with the GFP-Dab1-E expression construct (Figure 2.9A and data not shown). A significant decrease in GFP-Dab1-E level was also observed in cells co-transfected with Dab1 i334.

To test whether these two shRNAs (Dab1 i576 and Dab1 i334) are also

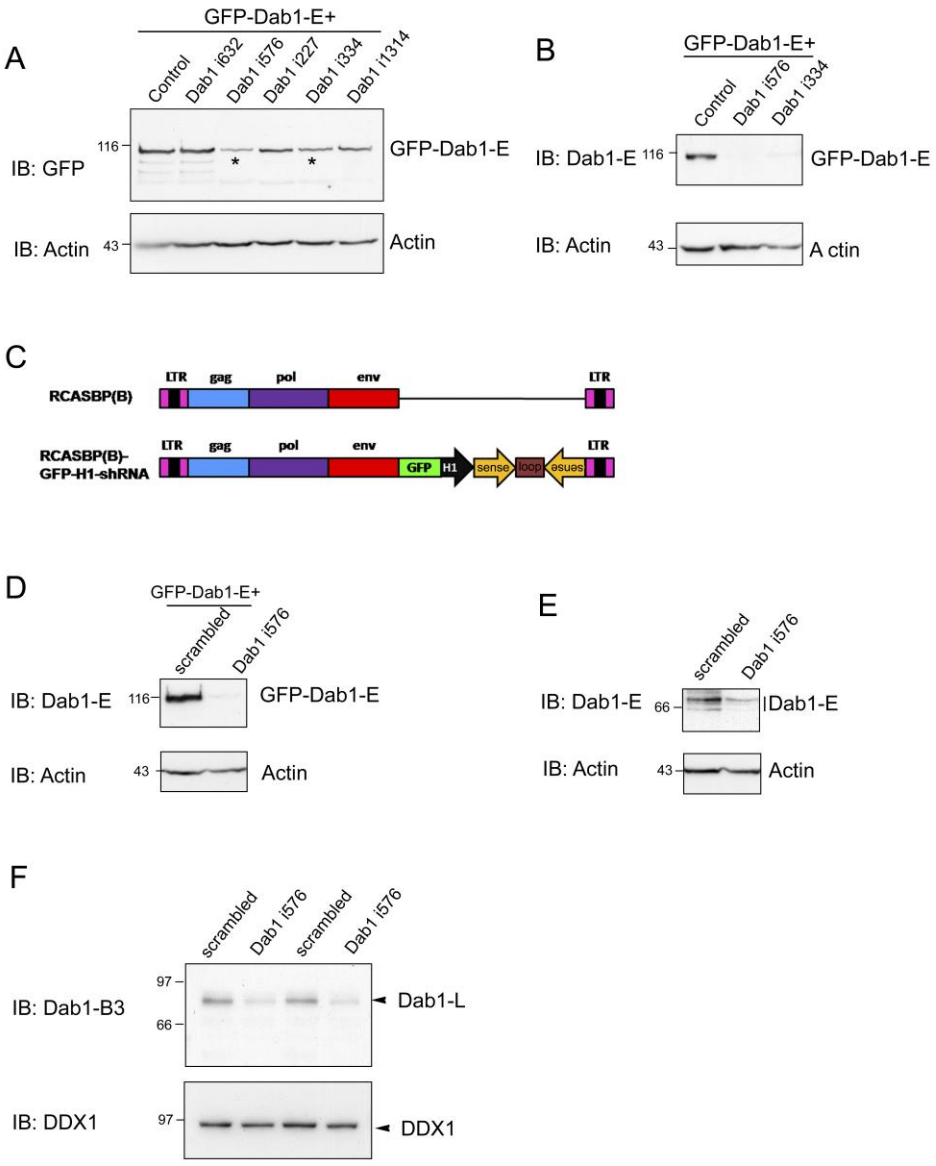
A
GFP-Dab1-E+
Control
Dab1 i632
Dab1 i576
Dab1 i227
Dab1 i334
Dab1 i1314
IB: GFP
116
GFP-Dab1-E
IB: Actin
43
Actin
B
GFP-Dab1-E+
Control
Dab1 i576
Dab1 i334
IB: Dab1-E
116
GFP-Dab1-E
IB: Actin
43
A ctin
C
RCASBP(B)
LTR
gag
pol
env
LTR
RCASBP(B)-
GFP-H1-shRNA
GFP
H1
sense
loop
esues
D
GFP-Dab1-E+
scrambled
Dab1 i576
IB: Dab1-E
116
GFP-Dab1-E
IB: Actin
43
Actin
E
scrambled
Dab1 i576
IB: Dab1-E
66
IDab1-E
IB: Actin
43
Actin
F
scrambled
Dab1 i576
scrambled
Dab1 i576
IB: Dab1-B3
97
66
Dab1-L
IB: DDX1
97
DDX1

Figure 2.9 Knockdown of Dab1-E in HeLa cells and primary retinal cultures. (A) Screening of Dab1 short hairpin RNAs (shRNAs) in Hela cells. Cell lysates from HeLa cells co-transfected with pEGFPC1-Dab1-E and pSUPER (control) or different pSUPER-Dab1 shRNA constructs were resolved on an 8% SDS-polyacrylamide gel and transferred to a nitrocellulose membrane, followed by immunostaining with a rabbit anti-GFP antibody. Asterisks indicate the most efficient shRNA constructs (Dab1 i576 and Dab1 i334). (**B) Analysis of Dab1-E shRNAs in primary retinal cultures.** Western blotting of cell lysates from ED5 retinal cultures co-transfected with pEGFPC1-Dab1-E and pSUPER (control) or pSUPER-Dab1 i576 and Dab1 i334 was carried out as in (A). The membrane was immunostained with rabbit anti-Dab1-E antibody. (**C) Schematic representation of the RCAS-GFP-Dab1 i constructs.** LTR, long terminal repeat. (**D) Analysis of RCAS-mediated shRNA in primary retinal cultures.** Cell lysates prepared from ED5 retinal cultures co-transfected with pEGFPC1-Dab1-E and either RCAS-scrambled (control) or RCAS-Dab1 i576 were analyzed as in (B). (**E) RCAS-mediated Dab1-E knockdown in primary retinal cultures.** Cell lysates from ED5 retinal cultures transfected with RCAS-scrambled or RCAS-Dab1 i576 were analyzed as in (B). Actin was used as a loading control. **(F) RCAS-mediated Dab1-L knockdown in primary retinal cultures.** Cell lysates from ED8 retinal cultures transfected with RCAS-scrambled or RCAS-Dab1 i576 were immunoblotted using anti-Dab1 B3 antibody. DDX1 was used as a loading control.

effective at reducing Dab1-E levels in chick retinal cells, we co-transfected ED5 primary retinal cultures with the GFP-Dab1-E expression construct along with the pSUPER Dab1 RNAi constructs. Both RNAi constructs suppressed exogenous GFP-Dab1-E expression in chick retinal cells (Figure 2.9B).

To maximize our transfection/infection efficiency, we subcloned GFP-H1-Dab1 i576 or GFP-H1-scrambled cassettes from pSUPER-RNAi constructs into the replication competent avian retroviral vector, RCAS. GFP, under the control of the 5' LTR, allows for identification of cells infected with the RCAS constructs (as illustrated in Figure 2.9C). This RCAS-GFP-Dab1 i576 construct effectively reduced the levels of exogenous GFP-Dab1-E (Figure 2.9D) and endogenous Dab1-E and Dab1-L (Figures 2.9E and 2.9F) in primary retinal cultures.

GFP-Dab1 i576 or GFP-scrambled constructs were introduced into chick embryos at stages 10-12 (ED1.5 - 2) by *in ovo* electroporation. As Dab1 i576 targets a region shared by both Dab1-E and Dab1-L, we terminated the experiments at either ED5 or ED7 (when Dab1-L levels are very low), to specifically address the role of Dab1-E in early retinal development. Immunostaining analysis revealed significantly reduced Dab1-E expression in the GFP+ regions of both ED5 (Figure 2.10A) and ED7 (Figure 2.10B) retinas electroporated with RCAS Dab1 i576. In general, the reduction in Dab1-E expression was most apparent in the vitreal (inner) part of the retina. Scrambled shRNAs had no effect on Dab1-E staining.

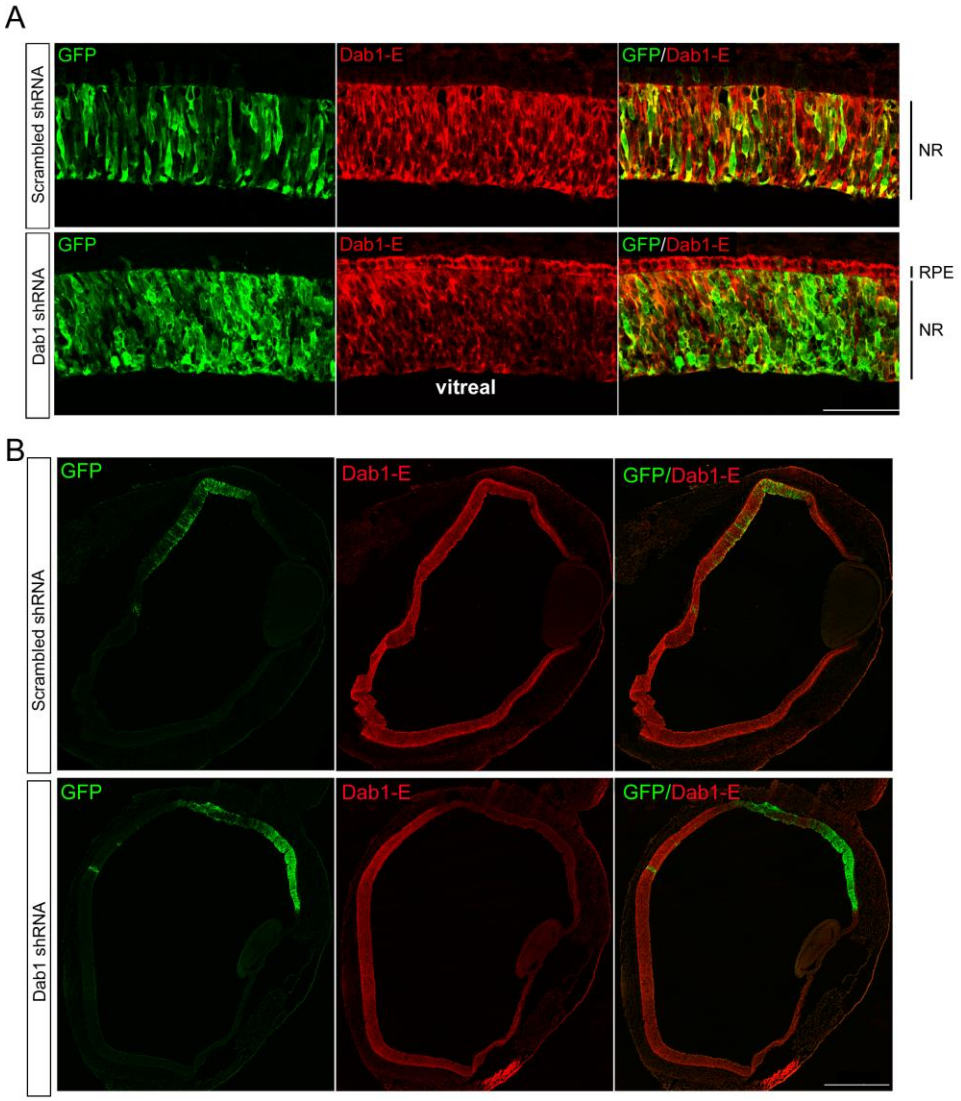

Figure 2.10 Knockdown of Dab1-E in the developing chick retina. (**A) Knockdown of Dab-E in ED5 chick retina.** Cryosections from ED5 chick retinas electroporated with RCAS-GFP-Scrambled or RCAS-GFP-Dab1 shRNA were co-immunostained with goat anti-GFP and rabbit anti-Dab1-E antibodies. (**B) Knockdown of Dab1-E in ED7 chick retina.** Cryosections from ED7 chick retinas electroporated with RCAS-GFP-scrambled or RCAS-GFP-Dab1 shRNA were double-immunostained with goat anti-GFP and rabbit anti-Dab1-E antibodies. Micrographs were collected with a Zeiss LSM 510 confocal microscope equipped with a 40X (A) or 10X lens (B). A 3 X 3 tile scan was applied to cover the entire retina in (B). Abbreviations: RPE, retinal pigmented epithelium; NR, neural retina. Scale bars, 50 μm in (A) or 500 μm in (B).

2.3.7 Knock-down of Dab1-E in the developing retina reduces cell proliferation and the number of progenitor cells

As disruption of the Reelin-Dab1 signaling pathway causes extensive migration and lamination defects in the developing brain (D'Arcangelo et al. 1995; Howell et al. 1997b), we first examined the gross architecture of the retina with reduced Dab1-E levels. The overall structure of the retina appeared normal at both ED5 and ED7, with no apparent laminar defects associated with Dab1-E knockdown (data not shown).

The expression pattern of Dab1-E in proliferating cells and newly-committed cells is compatible with a role in neurogenesis. We therefore examined the effect of Dab1-E knockdown on retinal cell proliferation. BrdU was injected into the eyes of ED5 chick embryos (approximately 68 hrs after *in ovo* electroporation) in order to label S phase cells. Eyes were harvested 3 hrs after BrdU injection and processed for immunostaining. As there is a strong central to peripheral differentiation gradient in the developing retina, we first measured BrdU incorporation in the peripheral, intermediate and central zones of six non-manipulated normal ED5 retinas (Figure 2.11). Two micrographs from each of the three zones were collected and cells positive for BrdU and Hoechst 33342 were scored using Metamorph software. The percentage of BrdU+ cells in the total cell population was 45-50% regardless of zone examined, consistent with previous reports demonstrating that the central to peripheral differentiation gradient (as measured by cell proliferation) is not apparent until ED6 in the chick retina (Prada et al. 1991).

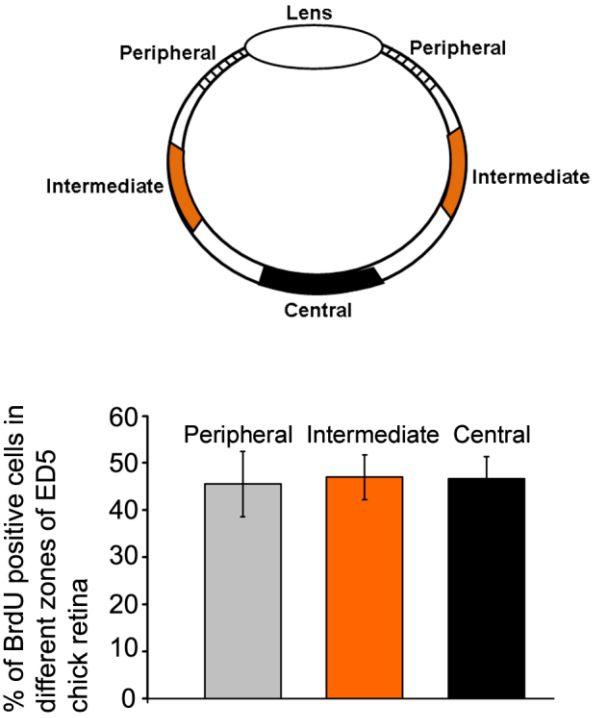

Figure 2.11 BrdU incorporation in ED5 chick retina. The top panel is a schematic representation of the three differentiation zones of the retina (peripheral, intermediate and central). The bottom panel shows a histogram of the percentage of BrdU+ cells after 3 hr BrdU labeling of the ED5 chick retina. Values were derived from 6 retinas. A total of 3370 cells labeled with Hoechst 33342 (724 cells from the peripheral region, 969 cells from the intermediate region and 1677 cells from the central region) were counted using Metamorph software. No significant differences were found between the different zones ($P>0.05$, one-way Anova).

We then carried out BrdU labeling experiments in electroporated embryos at ED5. To exclude the possibility that *in ovo* electroporation might affect cell proliferation, we first compared the BrdU labeling index (percentage of BrdU+ cells in GFP+ cells) in scrambled shRNA electroporated retinas versus control retinas. Although the BrdU labeling index was slightly decreased in the scrambled shRNA electroporated retinas compared to control, the difference was not statistically different (Figure 2.12). Next, we compared the BrdU labeling index in retinas electroporated with scrambled versus Dab1 shRNA. The BrdU labeling index was significantly reduced in the Dab1-E knockdown group [25% (n=8) versus 42% (n=6); $p<0.01$] (Figure 2.12), suggesting a role for Dab1-E in cell proliferation.

Chx10 is expressed in retinal progenitor cells at early stages of retinal development (Belecky-Adams et al. 1997). To determine whether the number of progenitor cells was decreased upon Dab1-E knock-down, we compared the number of GFP+/Chx10+ cells in retinas electroporated with scrambled versus Dab1 shRNA. A highly significant decrease in GFP+/Chx10+ cells was observed upon Dab1-E knockdown (from 78% to 55%) (Figure 2.13). The BrdU/Chx10 combined data indicate that both proliferation and the number of progenitor cells are decreased in retinas with reduced Dab1-E expression. Of note, we observed a general decrease in BrdU+ and Chx10+ cells in the vitreal half of the retina (Figures 2.12 and 2.13).

We used the TUNEL (terminal deoxynucleotidyl transferase dUTP nick

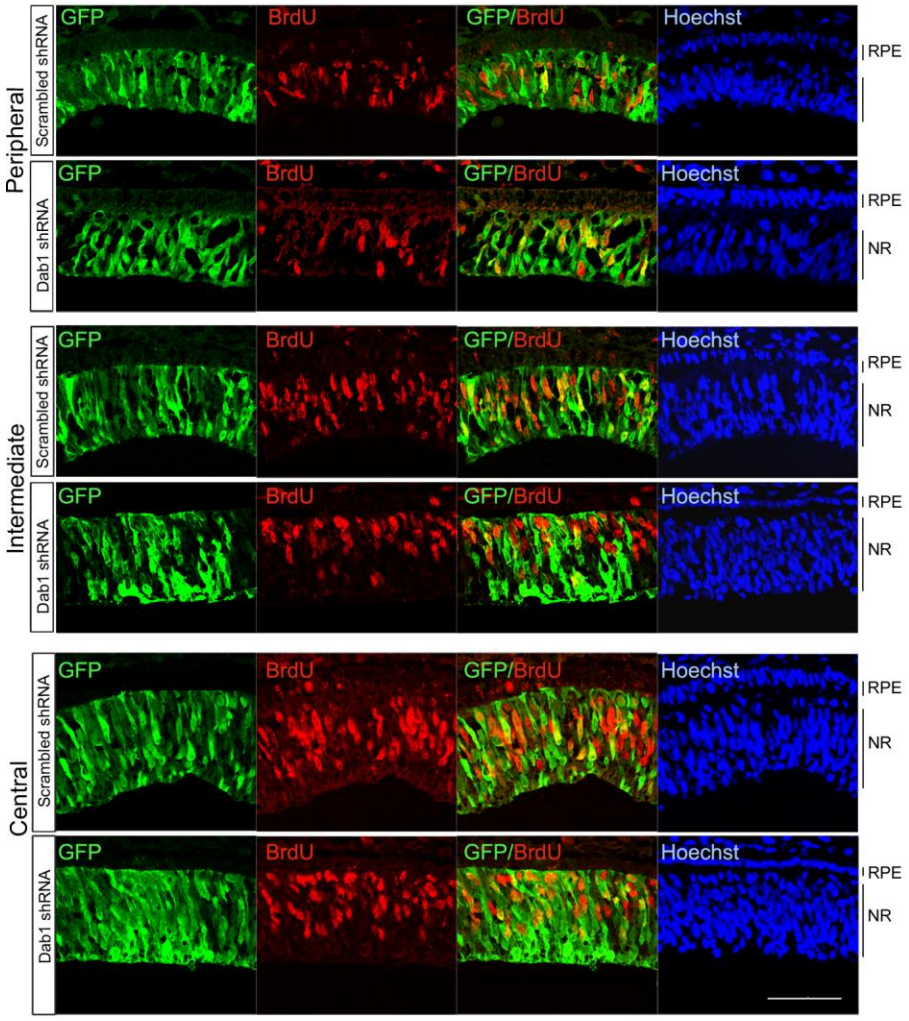
Peripheral
Intermediate
Central
Scrambled shRNA
Dab1 shRNA
GFP
BrdU
GFP/BrdU
Hoechst
RPE
NR

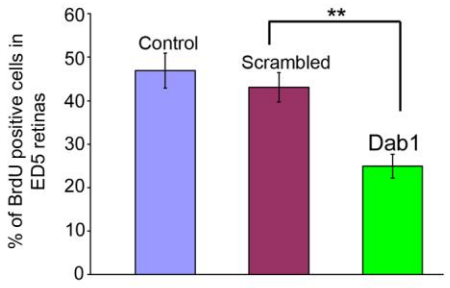
% of BrdU positive cells in ED5 retinas
60
50
40
30
20
10
0
Control
Scrambled
Dab1
**

Figure 2.12 BrdU incorporation in ED5 chick retinas electroporated with scrambled or Dab1 shRNA. BrdU and GFP were visualized by immunostaining with anti-mouse BrdU (1:100) and anti-goat GFP (1:2000) antibodies. Sections were counterstained with Hoechst 33342 to label the nuclei. Representative images from peripheral, intermediate and central zones from *in ovo* electroporated ED5 chick retinas are shown. Micrographs were collected with a Zeiss LSM 510 confocal microscope equipped with a 40X lens. Scale bar, 50 μm. The histogram shows the percentage of GFP+ cells that are positive for BrdU. Values were derived from 6 controls, 6 scrambled and 8 Dab1 knockdown embryos. No significant difference was found between the control and scrambled groups. There was a significant difference between the scrambled and Dab1-E knockdown groups. ** indicates that $P<0.01$ (*t* test). Abbreviations: RPE, retinal pigmented epithelium; NR, neural retina.

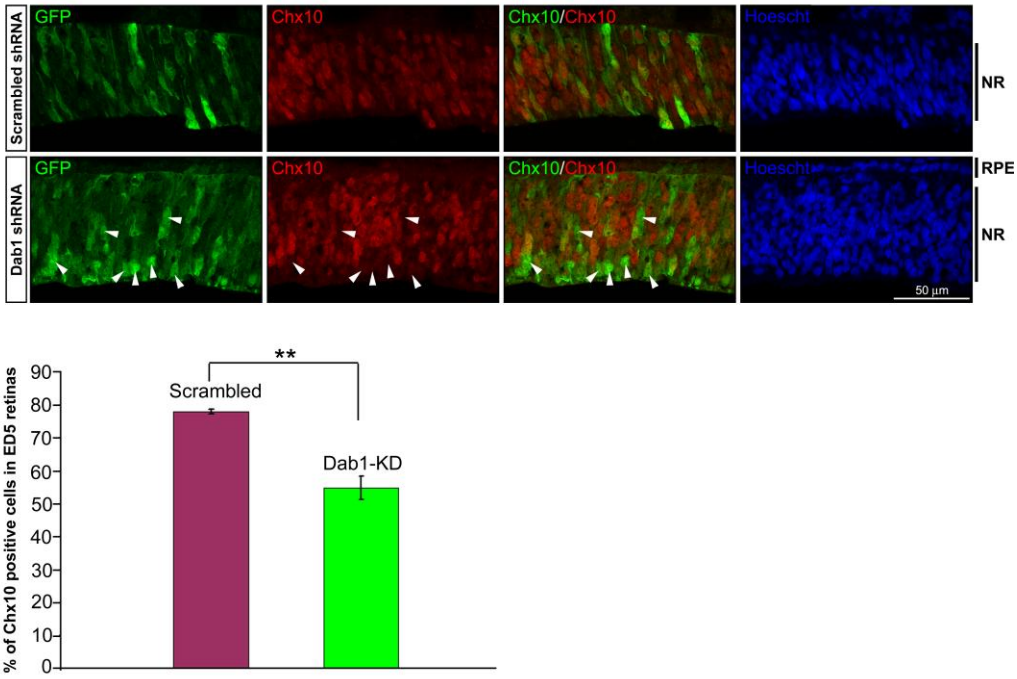

Figure 2.13 Chx10 expression in ED5 chick retinas electroporated with scrambled or Dab1 shRNA. Chx10 and GFP were visualized by immunostaining with anti-sheep Chx10 (1:3000) and anti-rabbit GFP (1:4000) antibodies. Sections were counterstained with Hoechst 33342 to label the nuclei. Micrographs were collected from 4 eyes electroporated with scrambled shRNA and 4 eyes electroporated with Dab1 shRNA as described in Fig. 8. The arrows point to some of the GFP+/Chx10- cells observed upon electroporation with Dab1 shRNA. Scale bar, 50 μm. The histogram shows the percentage of GFP+ retinal cells that are positive for Chx10. There was a significant difference between the scrambled and Dab1-E knockdown groups. ** indicates that $P<0.01$ (*t* test). Abbreviations: RPE, retinal pigmented epithelium; NBL, neuroblastic layer; GCL, ganglion cell layer.

end labeling) assay and anti-pH3 antibody labeling to demonstrate that neither apoptosis nor mitosis was affected by Dab1-E knockdown in the developing retina (Figure 2.14 and data not shown).

2.3.8 Knockdown of Dab1-E in the developing retina promotes ganglion cell differentiation

If Dab1-E knockdown affects cell proliferation, might it also affect retinal cell fate? To address this question, we first examined the number of early-born retinal neurons, ganglion and amacrine cells, in the GFP+ regions of ED7 chick retinas electroporated with either Dab1 shRNA or scrambled shRNA control. Similar numbers of ganglion cells (Islet-1+) were observed in scrambled versus Dab1-E knockdown retinas (Figure 2.15A). However, there appeared to be comparatively more GFP+ cells in the GCL of Dab1-E knockdown retinas compared to scrambled retinas. To specifically measure the percentage of GFP+ cells expressing Islet-1 in scrambled versus Dab1-E knockdown cells, we first screened for retinas that had GFP expression in the same differentiation zone (intermediate zone in the ventral retina was selected for our analyses). These matched retinas were then dissociated and co-immunostained with anti-GFP antibody and either anti-Islet-1 (ganglion marker) or AP-2α (3B5; amacrine marker) antibody. A significant increase in the percentage of Islet-1+/GFP+ cells was observed in Dab1-E knockdown retinas (~3%) compared to scrambled controls (~1.7%) (Figure 2.15B). Although we also observed more AP-2α+/GFP+ cells in Dab1-E knockdown retinas compared to control, this difference was not

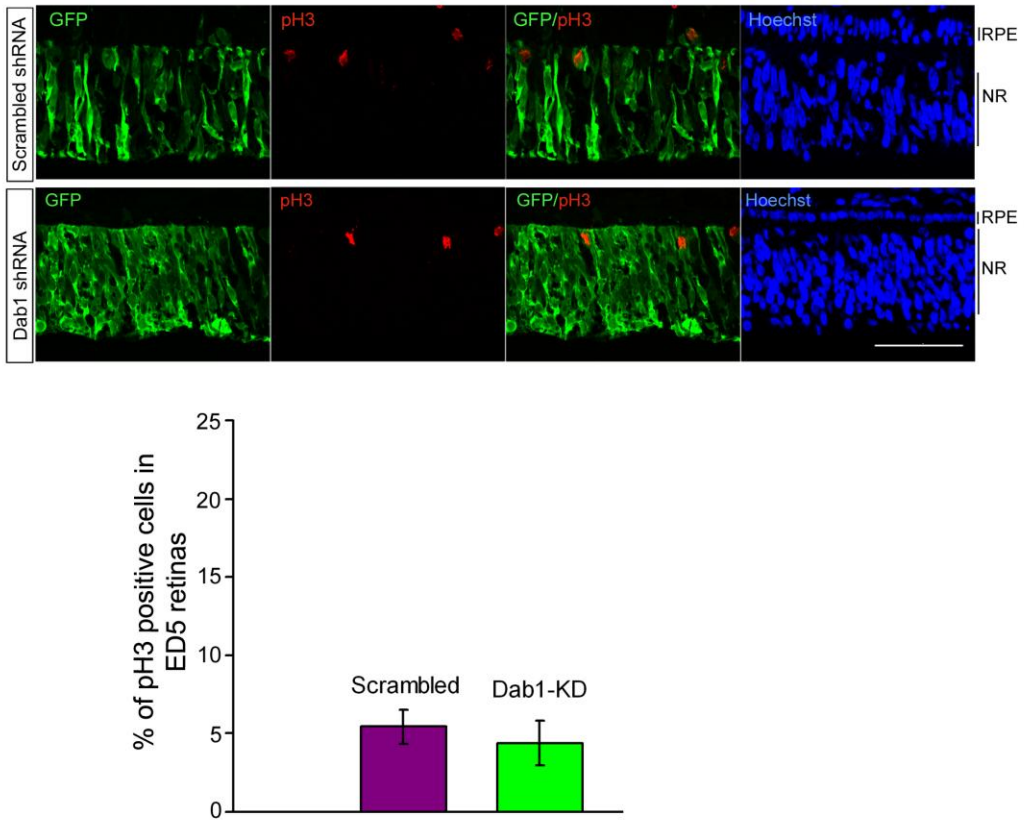

Figure 2.14 Analysis of phospho-histone H3 (pH3) in ED5 chick retina electroporated with scrambled or Dab1 shRNA. pH3 and GFP were visualized by immunostainning ED5 chick retina tissue sections with anti-rabbit pH3 (1:5,000) and anti-goat GFP antibodies. Sections were counterstained with Hoechst 33342 to label the nuclei. Micrographs were collected with a Zeiss LSM 510 confocal microscope equipped with a 40X lens. Scale bar, 50 µm. The bottom panel shows the percentage of electroporated/infected retinal cells positive for GFP and pH3. Values were derived from 6 scrambled and 8 Dab1 knockdown embryos. No significant difference was found between the scrambled and Dab1-E knockdown groups ($P>0.05$, *t* test). Abbreviations: RPE, retinal pigmented epithelium; NR, neural retina.

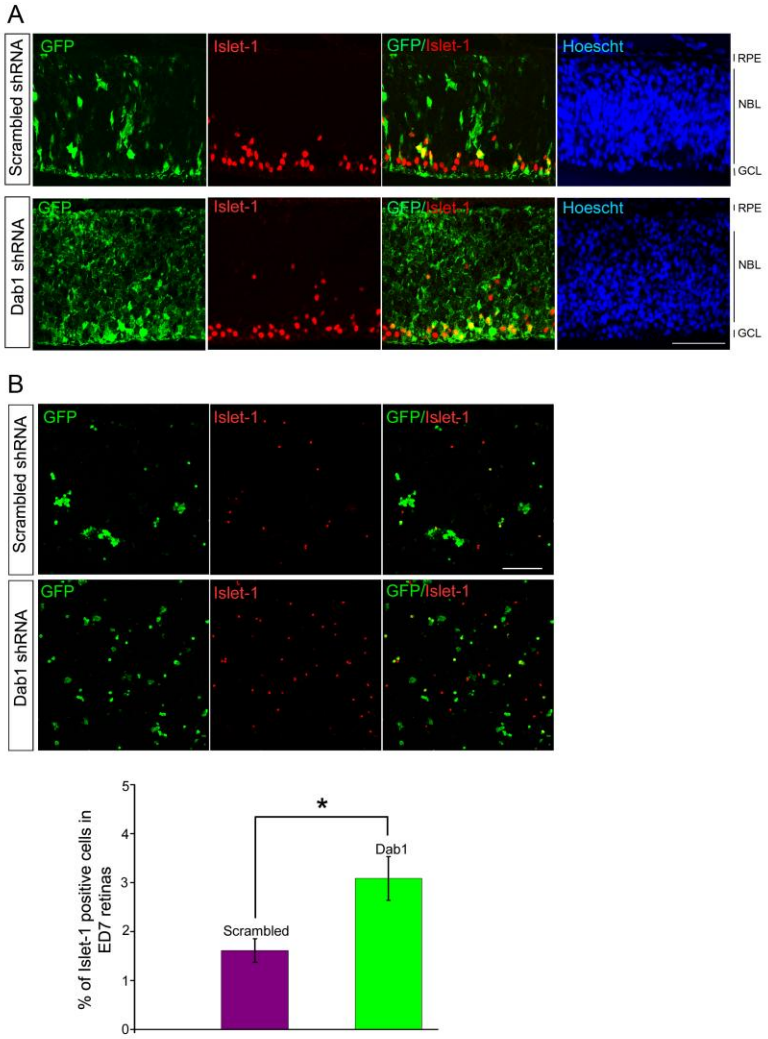

Figure 2.15 Knock-down of Dab1 in chick retina promotes ganglion cell differentiation. (A) Co-immunostaining of Islet-1 and GFP in ED7 chick retinas electroporated with scrambled or Dab1 shRNA. Islet-1 and GFP were visualized by immunostaining with anti-mouse Islet-1 (1:1500) and anti-goat GFP antibodies. Sections were counterstained with Hoechst 33342 to label the nuclei. Representative images from *in ovo* electroporated ED7 chick retinas are shown. Micrographs were collected with a Zeiss LSM 510 confocal microscope equipped with a 40X lens. Scale bar, 50 μm. **(B) Analysis of Islet-1 positive cells in dissociated cells from ED7 chick retinas electroporated with scrambled or Dab1 shRNA.** Dissociated retinal cells were co-immunostained with anti-mouse Islet-1 and anti-goat GFP, followed by donkey anti-mouse or donkey anti-goat secondary antibodies conjugated with Alexa 555 and Alexa 488, respectively. Micrographs were collected with a Zeiss LSM 510 confocal microscope equipped with a 20X lens in a tile scan mode (3X3). Scale bar, 100 μm. The bottom panel shows the quantitative analysis of electroporated/infected retinal cells positive for both GFP and Islet-1. Values were derived from 3 scrambled and 3 Dab1 knockdown embryos. There was a significant difference between the scrambled and Dab1-E knockdown group. * indicates that $P<0.05$ (*t* test). Abbreviations: RPE, retinal pigmented epithelium; NBL, neuroblastic layer; GCL, ganglion cell layer.

statistically significant (Figure. 2.16).

2.3.9 γ-secretase inhibition promotes conversion of Dab1-E to Dab1-L

Both Sonic Hedgehog (SHH) and Notch signaling have been shown to regulate retinal progenitor proliferation and neuronal cell fate in embryonic vertebrate retina (Henrique et al. 1997; Wang et al. 2005). To examine whether SHH and Notch can function through Dab1-E, we treated primary retinal cultures with either SHH inhibitor cyclopamine or γ-secretase inhibitor DAPT. The latter also inhibits Notch signaling. A significant decrease in Dab1-E transcripts, accompanied by a concomitant increase in Dab1-L transcripts, was observed upon DAPT, but not cyclopamine, treatment (Figure 2.17). These data suggest that Dab1 alternative splicing may be regulated by γ-secretase-controlled protein cleavages and that inhibition of γ-secretase, possibly through the inhibition of Notch signaling, promotes isoform switch from Dab1-E to Dab1-L.

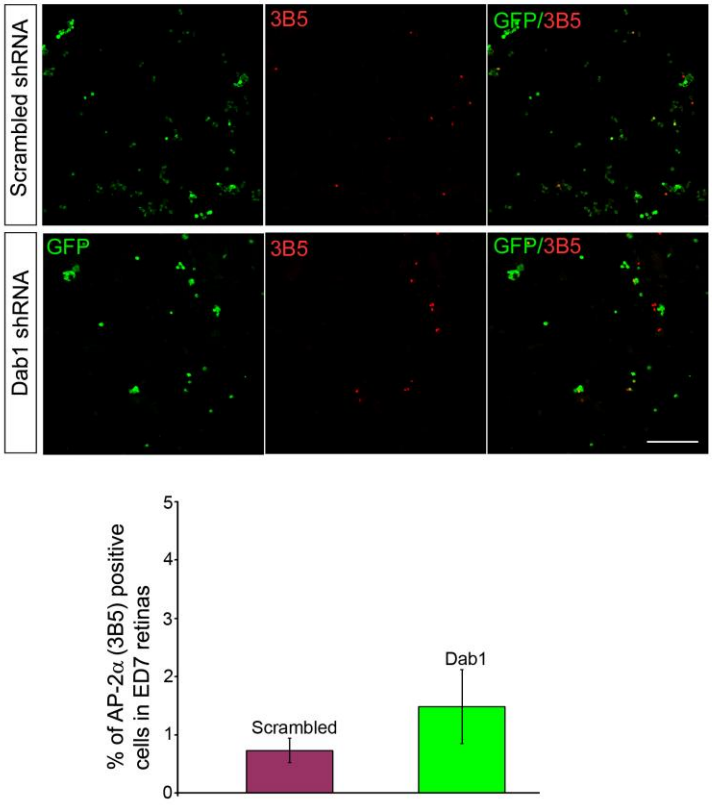

Figure 2.16 Analysis of amacrine cells in dissociated ED7 chick retinas electroporated with scrambled or Dab1 shRNA. Dissociated retinal cells were co-immunostained with anti-mouse AP-2α (3B5) and anti-goat GFP antibodies, followed by donkey anti-mouse or donkey anti-goat secondary antibodies conjugated with Alexa 555 and Alexa 488, respectively. Micrographs were collected with a Zeiss LSM 510 confocal microscope equipped with a 20X lens in a tile scan mode (3X3). Scale bar, 100 µm. The bottom panel shows the percentage of AP-2α+ cells in electroporated GFP+ ED7 retinal cells. Values were derived from 3 scrambled and 3 Dab1 knockdown embryos. No significant difference was found between the scrambled and Dab1-E knockdown group ($P>0.05$, *t* test).

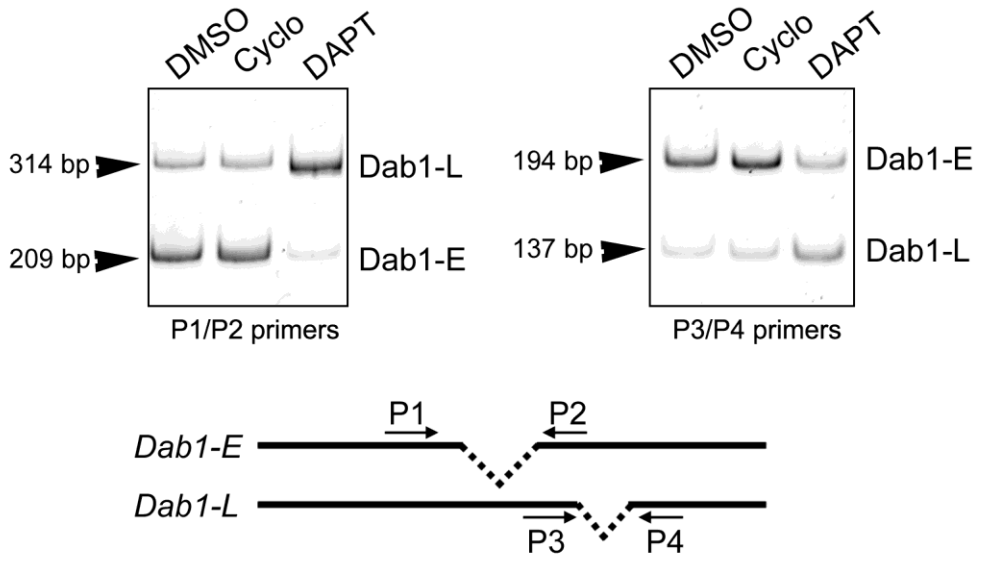

Figure 2.17 RT-PCR analysis of Dab1-E and Dab1-L in ED5.5 retinal cells treated with DMSO, cyclopamine and DAPT. cDNAs from ED5.5 retinal cells with indicated treatments were amplified using primer sets P1/P2 or P3/P4 (top panel). Sizes of amplified bands are indicated. Relative locations of primers in Dab1 transcripts are shown (bottom panel). Cyclo:cyclopamine.

2.4 DISCUSSION

Alternative splicing is key to functional diversification of proteins in higher eukaryotes. Alternatively spliced Dab1 products have been documented in mouse, zebrafish, lizard, fruit fly and chicken (Gertler et al. 1993; Howell et al. 1997a; Bar et al. 2003; Katyal and Godbout 2004; Costagli et al. 2006). However, other than a well-characterized role for Dab1 (Dab1-L) in Reelin-mediated neuronal cell migration, the function of the other Dab1 isoforms remains poorly understood. Here, we show that a form of Dab1 expressed at early stages of retinal development (Dab1-E) plays an important role in retinal neurogenesis. Of note, Dab1-E appears to function independently of Reelin-mediated tyrosine phosphorylation, revealing a novel aspect to Dab1 signaling.

2.4.1 Dab1-L function in the retina

In keeping with the observation that Dab1 is expressed in the IPL and AII amacrine cells of P7 and adult mouse retina (Rice and Curran 2000), we found highest levels of Dab1-L in the IPL of the chick retina with a similar layering pattern to that reported in mouse. However, two important differences were noted: (i) in contrast to mouse Dab1, chicken Dab1-L is not restricted to the amacrine lineage, and (ii) peaks of Dab1-L expression in chick retina correspond to peaks of neuronal differentiation, with elevated levels of Dab1-L sequentially observed in ganglion (ED5 - ED7), amacrine (ED8 - ED11) and horizontal (ED15 - P1) cells. These discrepancies can be partly explained by the fact that mouse retinas were only examined postnatally.

Although horizontal cells become postmitotic before amacrine cells (Kahn 1974; Reh and Kljavin 1989), they retain the ability to divide until relatively late stages of development (Boije et al. 2009). Furthermore, in contrast to other retinal cells which directly reach their correct destination by somal translocation (Baye and Link 2008), horizontal cells show an unusual bi-directional migratory behavior, bypassing their correct layer before changing directions and migrating to their final destination (Edqvist and Hallbook 2004). Thus, expression of Dab1-L in horizontal cells may be required for cell migration as well as for the formation of processes and/or synapses.

2.4.2 Dab1-E function in the retina

Dab1-E is widely expressed in proliferating retinal cells as well as in newly committed cells. Knock-down of Dab1-E at early stages of retinal development results in a significant decrease in proliferating cells, accompanied by a concomitant increase in ganglion cells. Dab1-E lacks two SFK tyrosine phosphorylation sites (Y198 and Y220) implicated in Reelin signaling, but retains two Abl tyrosine phosphorylation sites (converted Y185 and Y232) and an intact PI/PTB domain, giving rise to the possibility that Dab1-E can bind Reelin receptors and function through Reelin. Importantly, our data indicate that Dab1-E plays a role that is independent of Reelin-mediated tyrosine phosphorylation in the retina. First, endogenous Dab1-L, but not Dab1-E, is tyrosine phosphorylated in the retina. Second, exogenous Reelin induces Dab1-L, but not Dab1-E, tyrosine phosphorylation in primary retinal cultures. Third, we observed an

excellent correlation between the temporal expression patterns of Reelin, Reelin receptor ApoER2 and Dab1-L, but not Dab1-E, in the developing retina. Although VLDLR is generally more abundant at later stages of retinal development, it should be noted that our attempts at immunostaining retina tissue sections with anti-VLDLR antibody were not successful, leaving open the possibility that VLDLR may co-localize and interact with Dab1-E in the early retina. One possibility is that Dab1-E can compete with Dab1-L for binding to Reelin receptors and plays a dominant-negative role in Reelin signaling. Importantly, Dab1-E does not associate with CrkL (and likely CrkII based on the similarity of their SH2 domains). Thus, Dab1-E appears unable to transmit Reelin-initiated signaling to well-established downstream effectors of this pathway.

A number of proteins other than Reelin receptors bind the Dab1 PI/PTB domain, including amyloid precursor proteins and Notch (Giniger 1998; Homayouni et al. 1999; Le Gall et al. 2008). Notch is of particular interest as it is preferentially expressed in retinal progenitor cells, and regulates progenitor cell competence by preventing premature cell cycle exit and differentiation of progenitor cells (Henrique et al. 1997; Del Bene et al. 2008). Importantly, inhibition of Notch signaling in the chick retina mimics the Dab1-E knock-down phenotype, particularly as related to elevated ganglion cell differentiation (Austin et al. 1995). Furthermore, recent studies have shown that Dab1 enhances Notch signaling, likely by regulating the trafficking of the Notch intracellular domain (NICD) to prevent its degradation (Hashimoto-Torii et al. 2008). This raises the possibility that Dab1-E may maintain the retinal progenitor pool by controlling

NICD trafficking.

2.4.3 Is Dab1-E specific to the chicken?

Our data suggest a role for Dab1-E in the maintenance of the chick retina progenitor pool that is independent of Reelin-mediated tyrosine phosphorylation. Although Dab1-E-like isoforms have been detected in mice and other species by RT-PCR and *in situ* hybridization (Bar et al. 2003; Costagli et al. 2006), it is not clear what role, if any, these isoforms play in these species. Dab1 555*, which contains the Dab1-E-specific insertion region, is expressed in the ventricular zone of the mouse cerebral cortex at E14, at the peak of neurogenesis (Bar et al. 2003). In addition, knock-in of a Dab1 allele missing the two consensus SFK phosphorylation sites (Y185 and Y198) in mice, effectively mimicking Dab1-E, results in a milder phenotype in the cortex, hippocampus and cerebellum compared to Dab1 knock-out mice (Feng and Cooper 2009). The Y185/Y198 mutant Dab1 protein shows little or no response to Reelin and does not recruit SFKs, in support of a Reelin-independent Dab1 function.

A number of factors may explain why Reelin-independent Dab1-E has not been detected in other species to date. First, the Dab1 B3 antibody, documented here to specifically recognize Dab1-L, has been commonly used to detect Dab1 expression in mice. Directly relevant to our study, Dab1 B3 antibody was used to examine Dab1 expression in mouse retina (Rice and Curran 2000; Rice et al. 2001). Murine Dab1-E-like isoforms may have been missed using this antibody. Second, Bar *et al*. (Bar et al. 2003) only used primers/probes specific to the

insertion region of Dab1-E in their search for Dab1 isoforms in mice, humans and other species. Primers/probes spanning both the deletion and insertion regions may reveal the presence of Dab1-E in these species. Third, whereas the insertion in chicken Dab1-E spans 19 aa, the insertion in the putative mammalian Dab1-E (based on RT-PCR analysis) is 33 aa due to exon duplication. Thus, the difference in size between mammalian Dab1-L and the predicted mammalian Dab1-E is only 2 amino acids, making it difficult to distinguish these two forms based on northern and western blots. Fourth, as shown here, Dab1-E is primarily expressed at early stages of development, and consequently, may have been missed in studies concentrating on later stages. Finally, a compelling reason not to invoke the need for a Reelin-independent isoform has been the similarity in the phenotypes reported for Reelin and Dab1 mutant mice, suggesting that all Dab1 functions are mediated through Reelin (Howell et al. 1997b; Sheldon et al. 1997). However, some differences have been noted between *Dab1*-deficient and *reeler* mice. For example, the number of Purkinje cells is higher in the cerebellum of *scrambler* mice compared to *reeler*, and chain formation defects in the rostral migratory stream have been observed in *Dab1-/-* but not in *reeler* mice (Goldowitz et al. 1997; Andrade et al. 2007). A detailed analysis of the phenotypes resulting from Reelin and Dab1 knock-out may reveal additional differences.

In summary, we present evidence that developmentally-regulated alternative splicing of the *Dab1* gene gives rise to two key functional isoforms in the chick retina: Dab1-E, which is expressed in retinal progenitor cells and plays

a role in maintaining the retinal progenitor pool at early developmental stages, and Dab1-L, which is expressed in differentiated retinal cells and is likely involved in the formation of dendrites/axons and synaptic connections. We propose that phenotypes traditionally associated with Dab1 depletion or knock-out may actually represent an amalgamation of Dab1-E and Dab1-L loss-of-function. Future studies characterizing the molecular mechanisms underlying Dab1 alternative splicing will be instrumental to understanding this precisely-timed developmentally-regulated process.

2.5 ACKNOWLEDGMENTS

We are grateful to Dr. Jonathan A. Cooper for the anti-Dab1 (B3) antibody, Dr. Tom Curran for the pCrl-Reelin construct, Dr. Joachim Herz for the ApoER2 antibody, Dr. Rod Bremner for the anti-Chx10 antiboy and Jianxun Han for the γ-secretase inhibitor DAPT. We thank Dr. Xuejun Sun and Ms. Gerry Barron for their help with cell scoring using Metamorph software. This work was supported by the Canadian Institutes of Health Research. ZG is supported by an Alberta Heritage Foundation for Medical Research studentship and a Dissertation Fellowship from the University of Alberta.

2.6 REFERENCES

Altshuler D, Cepko C. 1992. A temporally regulated, diffusible activity is required for rod photoreceptor development in vitro. *Development* **114**: 947-957.

Andrade N, Komnenovic V, Blake SM, Jossin Y, Howell B, Goffinet A, Schneider WJ, Nimpf J. 2007. ApoER2/VLDL receptor and Dab1 in the rostral migratory stream function in postnatal neuronal migration independently of Reelin. *Proc Natl Acad Sci U S A* **104**: 8508-8513.

Arnaud L, Ballif BA, Forster E, Cooper JA. 2003. Fyn tyrosine kinase is a critical regulator of disabled-1 during brain development. *Curr Biol* **13**: 9-17.

Austin CP, Feldman DE, Ida JA, Jr., Cepko CL. 1995. Vertebrate retinal ganglion cells are selected from competent progenitors by the action of Notch. *Development* **121**: 3637-3650.

Ballif BA, Arnaud L, Arthur WT, Guris D, Imamoto A, Cooper JA. 2004. Activation of a Dab1/CrkL/C3G/Rap1 pathway in Reelin-stimulated neurons. *Curr Biol* **14**: 606-610.

Bar I, Tissir F, Lambert de Rouvroit C, De Backer O, Goffinet AM. 2003. The gene encoding disabled-1 (DAB1), the intracellular adaptor of the Reelin pathway, reveals unusual complexity in human and mouse. *J Biol Chem* **278**: 5802-5812.

Baye LM, Link BA. 2008. Nuclear migration during retinal development. *Brain Res* **1192**: 29-36.

Belecky-Adams T, Tomarev S, Li HS, Ploder L, McInnes RR, Sundin O, Adler R. 1997. Pax-6, Prox 1, and Chx10 homeobox gene expression correlates with phenotypic fate of retinal precursor cells. *Invest Ophthalmol Vis Sci* **38**: 1293-1303.

Bernier B, Bar I, D'Arcangelo G, Curran T, Goffinet AM. 2000. Reelin mRNA expression during embryonic brain development in the chick. *J Comp Neurol* **422**: 448-463.

Bock HH, Herz J. 2003. Reelin activates SRC family tyrosine kinases in neurons. *Curr Biol* **13**: 18-26.

Bock HH, Jossin Y, Liu P, Forster E, May P, Goffinet AM, Herz J. 2003. Phosphatidylinositol 3-kinase interacts with the adaptor protein Dab1 in response to Reelin signaling and is required for normal cortical lamination. *J Biol Chem* **278**: 38772-38779.

Boije H, Edqvist PH, Hallbook F. 2009. Horizontal cell progenitors arrest in G2-phase and undergo terminal mitosis on the vitreal side of the chick retina.

Dev Biol **330**: 105-113.

Cepko CL, Austin CP, Yang X, Alexiades M, Ezzeddine D. 1996. Cell fate determination in the vertebrate retina. *Proc Natl Acad Sci U S A* **93**: 589-595.

Chai X, Forster E, Zhao S, Bock HH, Frotscher M. 2009. Reelin stabilizes the actin cytoskeleton of neuronal processes by inducing n-cofilin phosphorylation at serine3. *J Neurosci* **29**: 288-299.

Chen K, Ochalski PG, Tran TS, Sahir N, Schubert M, Pramatarova A, Howell BW. 2004. Interaction between Dab1 and CrkII is promoted by Reelin signaling. *J Cell Sci* **117**: 4527-4536.

Costagli A, Felice B, Guffanti A, Wilson SW, Mione M. 2006. Identification of alternatively spliced dab1 isoforms in zebrafish. *Dev Genes Evol* **216**: 291-299.

D'Arcangelo G, Miao GG, Chen SC, Soares HD, Morgan JI, Curran T. 1995. A protein related to extracellular matrix proteins deleted in the mouse mutant reeler. *Nature* **374**: 719-723.

Del Bene F, Wehman AM, Link BA, Baier H. 2008. Regulation of neurogenesis by interkinetic nuclear migration through an apical-basal notch gradient. *Cell* **134**: 1055-1065.

Dutting D, Gierer A, Hansmann G. 1983. Self-renewal of stem cells and differentiation of nerve cells in the developing chick retina. *Brain Res* **312**: 21-32.

Edqvist PH, Hallbook F. 2004. Newborn horizontal cells migrate bi-directionally across the neuroepithelium during retinal development. *Development* **131**: 1343-1351.

Federspiel MJ, Hughes SH. 1997. Retroviral gene delivery. *Methods Cell Biol* **52**: 179-214.

Feng L, Cooper JA. 2009. Dual functions of Dab1 during brain development. *Mol Cell Biol* **29**: 324-332.

Gertler FB, Hill KK, Clark MJ, Hoffmann FM. 1993. Dosage-sensitive modifiers of Drosophila abl tyrosine kinase function: prospero, a regulator of axonal outgrowth, and disabled, a novel tyrosine kinase substrate. *Genes Dev* **7**: 441-453.

Giniger E. 1998. A role for Abl in Notch signaling. *Neuron* **20**: 667-681.

Goldowitz D, Cushing RC, Laywell E, D'Arcangelo G, Sheldon M, Sweet HO,

Davisson M, Steindler D, Curran T. 1997. Cerebellar disorganization characteristic of reeler in scrambler mutant mice despite presence of reelin. *J Neurosci* **17**: 8767-8777.

Hamburger VH, HL. 1951. A series of normal stages in the development of the chick embryo. *J Morphol* **88**: 49-92.

Hashimoto-Torii K, Torii M, Sarkisian MR, Bartley CM, Shen J, Radtke F, Gridley T, Sestan N, Rakic P. 2008. Interaction between Reelin and Notch signaling regulates neuronal migration in the cerebral cortex. *Neuron* **60**: 273-284.

Henrique D, Hirsinger E, Adam J, Le Roux I, Pourquie O, Ish-Horowicz D, Lewis J. 1997. Maintenance of neuroepithelial progenitor cells by Delta-Notch signalling in the embryonic chick retina. *Curr Biol* **7**: 661-670.

Herrick TM, Cooper JA. 2002. A hypomorphic allele of dab1 reveals regional differences in reelin-Dab1 signaling during brain development. *Development* **129**: 787-796.

Hiesberger T, Trommsdorff M, Howell BW, Goffinet A, Mumby MC, Cooper JA, Herz J. 1999. Direct binding of Reelin to VLDL receptor and ApoE receptor 2 induces tyrosine phosphorylation of disabled-1 and modulates tau phosphorylation. *Neuron* **24**: 481-489.

Holt CE, Bertsch TW, Ellis HM, Harris WA. 1988. Cellular determination in the Xenopus retina is independent of lineage and birth date. *Neuron* **1**: 15-26.

Homayouni R, Rice DS, Sheldon M, Curran T. 1999. Disabled-1 binds to the cytoplasmic domain of amyloid precursor-like protein 1. *J Neurosci* **19**: 7507-7515.

Howell BW, Gertler FB, Cooper JA. 1997a. Mouse disabled (mDab1): a Src binding protein implicated in neuronal development. *Embo J* **16**: 121-132.

Howell BW, Hawkes R, Soriano P, Cooper JA. 1997b. Neuronal position in the developing brain is regulated by mouse disabled-1. *Nature* **389**: 733-737.

Howell BW, Herrick TM, Cooper JA. 1999. Reelin-induced tryosine phosphorylation of disabled 1 during neuronal positioning. *Genes Dev* **13**: 643-648.

Howell BW, Herrick TM, Hildebrand JD, Zhang Y, Cooper JA. 2000. Dab1 tyrosine phosphorylation sites relay positional signals during mouse brain development. *Curr Biol* **10**: 877-885.

Hughes SH, Greenhouse JJ, Petropoulos CJ, Sutrave P. 1987. Adaptor plasmids simplify the insertion of foreign DNA into helper-independent retroviral

vectors. *J Virol* **61**: 3004-3012.

Iijima H, Miyazawa M, Sakai J, Magoori K, Ito MR, Suzuki H, Nose M, Kawarabayasi Y, Yamamoto TT. 1998. Expression and characterization of a very low density lipoprotein receptor variant lacking the O-linked sugar region generated by alternative splicing. *J Biochem* **124**: 747-755.

Jossin Y, Goffinet AM. 2007. Reelin signals through phosphatidylinositol 3-kinase and Akt to control cortical development and through mTor to regulate dendritic growth. *Mol Cell Biol* **27**: 7113-7124.

Kahn AJ. 1974. An autoradiographic analysis of the time of appearance of neurons in the developing chick neural retina. *Dev Biol* **38**: 30-40.

Katyal S, Gao Z, Monckton E, Glubrecht D, Godbout R. 2007. Hierarchical disabled-1 tyrosine phosphorylation in Src family kinase activation and neurite formation. *J Mol Biol* **368**: 349-364.

Katyal S, Godbout R. 2004. Alternative splicing modulates Disabled-1 (Dab1) function in the developing chick retina. *Embo J* **23**: 1878-1888.

Keshvara L, Benhayon D, Magdaleno S, Curran T. 2001. Identification of reelin-induced sites of tyrosyl phosphorylation on disabled 1. *J Biol Chem* **276**: 16008-16014.

Lambert de Rouvroit C, de Bergeyck V, Cortvrindt C, Bar I, Eeckhout Y, Goffinet AM. 1999. Reelin, the extracellular matrix protein deficient in reeler mutant mice, is processed by a metalloproteinase. *Exp Neurol* **156**: 214-217.

Le Gall M, De Mattei C, Giniger E. 2008. Molecular separation of two signaling pathways for the receptor, Notch. *Dev Biol* **313**: 556-567.

Le N, Simon MA. 1998. Disabled is a putative adaptor protein that functions during signaling by the sevenless receptor tyrosine kinase. *Mol Cell Biol* **18**: 4844-4854.

Li X, Glubrecht DD, Mita R, Godbout R. 2008. Expression of AP-2delta in the developing chick retina. *Dev Dyn* **237**: 3210-3221.

Nabi NU, Mezer E, Blaser SI, Levin AA, Buncic JR. 2003. Ocular findings in lissencephaly. *J Aapos* **7**: 178-184.

Park TJ, Curran T. 2008. Crk and Crk-like play essential overlapping roles downstream of disabled-1 in the Reelin pathway. *J Neurosci* **28**: 13551-13562.

Prada C, Puga J, Perez-Mendez L, Lopez R, Ramirez G. 1991. Spatial and Temporal Patterns of Neurogenesis in the Chick Retina. *Eur J Neurosci* **3**:

559-569.

Reh TA, Kljavin IJ. 1989. Age of differentiation determines rat retinal germinal cell phenotype: induction of differentiation by dissociation. *J Neurosci* **9**: 4179-4189.

Rice DS, Curran T. 2000. Disabled-1 is expressed in type AII amacrine cells in the mouse retina. *J Comp Neurol* **424**: 327-338.

Rice DS, Nusinowitz S, Azimi AM, Martinez A, Soriano E, Curran T. 2001. The reelin pathway modulates the structure and function of retinal synaptic circuitry. *Neuron* **31**: 929-941.

Schiffmann SN, Bernier B, Goffinet AM. 1997. Reelin mRNA expression during mouse brain development. *Eur J Neurosci* **9**: 1055-1071.

Sheldon M, Rice DS, D'Arcangelo G, Yoneshima H, Nakajima K, Mikoshiba K, Howell BW, Cooper JA, Goldowitz D, Curran T. 1997. Scrambler and yotari disrupt the disabled gene and produce a reeler-like phenotype in mice. *Nature* **389**: 730-733.

Songyang Z, Shoelson SE, Chaudhuri M, Gish G, Pawson T, Haser WG, King F, Roberts T, Ratnofsky S, Lechleider RJ et al. 1993. SH2 domains recognize specific phosphopeptide sequences. *Cell* **72**: 767-778.

Sun XM, Soutar AK. 1999. Expression in vitro of alternatively spliced variants of the messenger RNA for human apolipoprotein E receptor-2 identified in human tissues by ribonuclease protection assays. *Eur J Biochem* **262**: 230-239.

Trommsdorff M, Borg JP, Margolis B, Herz J. 1998. Interaction of cytosolic adaptor proteins with neuronal apolipoprotein E receptors and the amyloid precursor protein. *J Biol Chem* **273**: 33556-33560.

Trommsdorff M, Gotthardt M, Hiesberger T, Shelton J, Stockinger W, Nimpf J, Hammer RE, Richardson JA, Herz J. 1999. Reeler/Disabled-like disruption of neuronal migration in knockout mice lacking the VLDL receptor and ApoE receptor 2. *Cell* **97**: 689-701.

Turner DL, Cepko CL. 1987. A common progenitor for neurons and glia persists in rat retina late in development. *Nature* **328**: 131-136.

Wang Y, Dakubo GD, Thurig S, Mazerolle CJ, Wallace VA. 2005. Retinal ganglion cell-derived sonic hedgehog locally controls proliferation and the timing of RGC development in the embryonic mouse retina. *Development* **132**: 5103-5113.

CHAPTER 3: SERINE PHOSPHORYLATION REGULATES DISABLED-1 EARLY ISOFORM TURNOVER INDEPENDENTLY OF REELIN

A version of this chapter has been published. Gao Z, Godbout R. Serine phosphorylation regulates disabled-1 early isoform turnover independently of Reelin. Cell Signal. (2010), doi:10.1016/j.cellsig.2010.11.007. The immunohistochemical analysis was done by Darryl Glubrecht.

3.1 INTRODUCTION

The cytoplasmic adaptor protein, Disabled-1 (Dab1), regulates the proper positioning of migrating neurons in response to Reelin signaling (Howell et al. 1997; Howell et al. 1999a). Dab1 contains an N-terminal protein interaction/phosphotyrosine binding (PI/PTB) domain, which associates with the NPxY motifs of the two Reelin receptors, very low density lipoprotein receptor (VLDLR) and apolipoprotein E receptor 2 (ApoER2) (Trommsdorff et al. 1998; Howell et al. 1999b). The N-terminal domain is followed by a tyrosine-rich region, which consists of five highly-conserved tyrosine (Y) residues (Y185, Y198, Y200, Y220 and Y232) corresponding to two consensus Src family kinase (SFK) recognition sites (Y185 and Y198/Y200) and two consensus Abl recognition sites (Y220 and Y232) (Songyang et al. 1993). At least three of the four tyrosine phosphorylation sites (Y198, Y220 and Y232) are phosphorylated by SFKs and/or involved in the activation of SFKs in cultured neurons upon Reelin stimulation (Keshvara et al. 2001; Ballif et al. 2004; Katyal et al. 2007). Tyrosine phosphorylation of Dab1 is essential for Reelin signaling, as mice expressing Dab1 with substitutions at these five tyrosine residues have neuronal cell positioning defects similar to those observed in Reelin-deficient (*reeler*) and *Dab1-/-* mice (Howell et al. 2000).

Tyrosine-phosphorylated Dab1 transmits the Reelin signal by activating a host of downstream effectors, including SFK, phosphatidylinositol 3 kinase (PI-3K)/Akt, mTOR, CrkL/C3G/Rap and LIMK1 (LIM kinase 1) (Arnaud et al. 2003b; Bock and Herz 2003; Bock et al. 2003; Ballif et al. 2004; Jossin and Goffinet

2007; Chai et al. 2009). These events ultimately lead to cytoskeleton remodeling and correct neuronal positioning during development. Importantly, tyrosine-phosphorylated Dab1 also down-regulates Reelin signaling by recruiting SOCS (suppressors of cytokine signaling) proteins, adaptors for cullin-based E3 ligase complexes, thus targeting itself for ubiquitination and degradation(Arnaud et al. 2003a; Bock et al. 2004; Feng et al. 2007). This negative feedback mechanism prevents “overmigration” of neurons and ensures precise positioning of migrating neurons during development (Feng et al. 2007; Kerjan and Gleeson 2007).

In addition to tyrosine phosphorylation, Dab1 is phosphorylated by the serine/threonine (S/T) kinase cyclin dependent kinase 5 (Cdk5)(Keshvara et al. 2002; Ohshima et al. 2007). In particular, S491 in the C-terminus of Dab1 has been shown to be an important Cdk5 phosphorylation target both *in vitro* and *in vivo* (Keshvara et al. 2002). Like Reelin and Dab1, Cdk5 plays an important role in neuronal cell positioning by phosphorylating substrates involved in cytoskeleton reorganization and cell migration. However, whether Dab1 serves as a convergence point for Reelin and Cdk5 signaling to fine tune neuronal cell migration is not clear at the present time. There is evidence implicating S/T phosphorylation in the modulation of Dab1 tyrosine phosphorylation (Arnaud et al. 2003a; Ohshima et al. 2007). Moreover, Dab1 levels have been shown to be either elevated or unaltered in *Cdk5-/-* mice depending on the study, further confounding the importance of Dab1 S/T phosphorylation in Dab1 function (Ohshima et al. 2001; Keshvara et al. 2002; Beffert et al. 2004; Ohshima et al. 2007).

We have identified two alternatively-spliced Dab1 isoforms in the developing chick retina: Dab1-E expressed in undifferentiated retinal progenitor cells, and Dab1-L expressed in differentiated ganglion, horizontal and amacrine cells (Katyal and Godbout 2004; Gao et al. 2010). Dab1-L, commonly referred to as Dab1, contains the five tyrosine residues described above, whereas Dab1-E is missing two SFK tyrosine phosphorylation sites, but retains two Abl tyrosine phosphorylation sites. In addition, Dab1-E has a 19 aa region encoded by alternatively-spliced exon 9b. Dab1-L is tyrosine phosphorylated upon Reelin stimulation and recruits Crk adaptor proteins, whereas Dab1-E is not tyrosine phosphorylated, nor does it associate with Crk proteins. Knockdown of Dab1-E in the developing chick retina results in a decrease in the number of retinal progenitor cells (Gao et al. 2010). Here, we demonstrate that there are multiple phosphorylated forms of Dab1-E in the developing chick retina. In contrast to Dab1-L, Dab1-E phosphorylation exclusively involves S/T residues and is independent of Reelin. Unlike Dab1-L which is phosphorylated at S/T residues by Cdk5, Dab1-E appears to be primarily phosphorylated by Cdk2. Dab1-E S475, the counterpart of Dab1-L S491, is a major site of phosphorylation, which in turn destabilizes Dab1-E protein. We also demonstrate that Dab1-E stability is controlled by ubiquitination-mediated proteasome degradation and protein phosphatases 1 and/or 2A.

3.2 MATERIALS AND METHODS

3.2.1 DNA constructs

pEGFP-C1-Dab1-E and pEGFP-C1-Dab1-L have been previously described (Katyal and Godbout 2004; Gao et al. 2010). DNA constructs expressing GST-Dab1-E-middle (residues 140-263) and GST-Dab1-E-C-terminus (residues 441-535) were generated by cloning the corresponding PCR fragments from pEGFP-C1-Dab1-E into pGEX-4T2 at the *Bam*HI and *Eco*RI sites. Full-length Dab1-E cDNA derived from pEGFPC1-Dab1-E was subcloned into pCMV-Tag4A at the *Bam*HI and *Xho*I sites to produce the FLAG-tagged Dab1-E. pGEX-4T2-Dab1-E-S475A, pEGFP-C1-Dab1-E-S475A and other pCMV-Tag4A-Dab1-E mutants were made by quick-change site-directed mutagenesis (Stratagene). Cdk2-HA (plasmid 1884), Cdk2-HA dominant negative (plasmid 1885) and HA-Ubiquitin (plasmid 18712) constructs were obtained from Addgene (van den Heuvel and Harlow 1993; Kamitani et al. 1997). The construct expressing GST-RAP (receptor-associated protein) was a gift from Dr. Joachim Herz (University of Texas, Southwestern Medical Center).

3.2.2 Antibodies and pharmacological reagents

The rabbit anti-Dab1-E and rabbit anti-DDX1 antibodies have been described previously (Bleoo et al. 2001; Gao et al. 2010). The following antibodies were used for western blot analysis: rabbit anti-Dab1-E (1:400), rabbit anti-Dab1 (100-4101-225, Rockland, 1:5000), mouse anti-actin (A5441, Sigma, 1:200,000), rabbit anti-Cdk2 (sc-163, Santa Cruz, 1:400), mouse anti-Cdc2/Cdk1

(CC16, Calbiochem, 1:100), mouse anti-Cdc2 p34 (sc-54, Santa Cruz, 1:200), rabbit anti-Cdk4 (sc-260, Santa Cruz, 1:200), rabbit anti-Cdk4 (06-139, Millipore), rabbit anti-Cdk5 (sc-173, Santa Cruz, 1:400), rabbit anti-p35 (sc-820, Santa Cruz, 1:200), mouse anti-Cyclin A (ab39, Abcam, 1:500), rabbit anti-Cyclin B1(sc-752, Santa Cruz, 1:200), mouse anti-Cyclin D1/2 (05-362, Upstate, 1:1000), mouse anti-Cyclin E (554182, BD Bioscience, 1:500), rabbit anti-pS491 Dab1 (ab5776, Abcam, 1:1000), mouse anti-phosphotyrosine antibody (pY-100， 9411, Cell Signaling Technology, 1:1000) and rabbit anti-phosphoserine CDK substrate antibody (2324, Cell Signaling Technology, 1:1000). The following antibodies were used for immunohistochemical analysis: rabbit anti-pS491 Dab1 (ab5776, Abcam, 1: 200), rabbit anti-Cdk2 (sc-163, Santa Cruz, 1:400) and rabbit anti-Dab1-E (1:400).

MG132, okadaic acid (OA), roscovitine [2-(R)-(1-Ethyl -2-hydroxyethylamino)-6-benzylamino-9-isopropylpurine], purvalanol A [2-(1R-Isopropyl-2-hydroxyethylamino)-6-(3-chloroanilino)-9-isopropylpurine], glycogen synthase kinase 3 (GSK3) inhibitor and the serine/threonine kinase inhibitor set were obtained from Calbiochem. Cycloheximide (CHX), cyclosporine A (CsA) and *N*-ethylmaleimide (NEM) were obtained from Sigma.

3.2.3 Cell culture, drug treatment and DNA transfection

Hela and HEK293T cells were maintained in DMEM supplemented with 10% fetal calf serum, penicillin (100 U/ml) and streptomycin (100 μg/ml). Primary retinal cultures were prepared from embryonic day (ED) 5 or ED10 chick retinas

dissociated with trypsin as previously described (Katyal et al. 2007). The treatments and transfections were carried out twenty-four h after plating. For drug treatment, cells were treated with different kinase inhibitors, CHX, MG132, Reelin, or RAP, as indicated. For transfection, the DNA was introduced into cells by calcium phosphate-mediated DNA precipitation and removed after 16-18 h. Cells were lysed in RIPA buffer [50 mM Tris-HCl pH 7.5, 150 mM NaCl, 1% Triton X-100, 1% sodium deoxycholate, 0.1% SDS, 50 mM NaF, 1 mM PMSF, 1 mM Na_3VO_4 and 1X Complete protease inhibitor cocktail (Roche)] followed by immunoprecipitation or western blot analysis.

3.2.4 Purification of GST Fusion Protein

pGEX constructs encoding the GST-fused middle (140-263 aa) or C-terminus (441-535 aa) of chicken Dab1-E, and RAP, were transformed into the *E. coli* strain BL21. Expression of the fusion protein was induced with 1 mM IPTG for 4 h at 30˚C. Cells were resuspended in phosphate buffered saline (PBS) containing 1 mM phenylmethylsulfonyl fluoride and 2 mM DTT and lysed by sonication (40% output for 10 bursts). Triton X-100 was added to a final concentration of 1% to increase protein solubility. Cleared lysates were incubated with glutathione-Sepharose beads (GE Healthcare) and bound proteins were eluted in 10 mM reduced glutathione (Sigma). The eluants were concentrated using Centricon-30 (Millipore) with three buffer exchanges in PBS.

3.2.5 Western blot analysis, immunoprecipitation and phosphatase

treatment

Chick retinal tissue and cultures were lysed in RIPA buffer. For western blotting, lysates were either used fresh, or stored at -80˚C before use. For immunoprecipitation, cell lysates were precleared with protein A (for primary antibodies raised in rabbit) or protein G (for primary antibodies raised in mouse) Sepharose beads (GE Healthcare) for 1 h at 4˚C, incubated with primary antibodies or IgG control overnight at 4˚C. The immunocomplexes were then collected with protein A or protein G Sepharose beads. Immunoprecipitates or cell lysates were separated by SDS-PAGE, blotted onto nitrocellulose or PVDF membranes and immunostained with antibodies as indicated. For phosphatase treatment, Dab1 immunoprecipitates bound to protein A Sepharose beads were washed in lysis buffer three times and incubated in phosphatase buffer [50 mM Tris-HCl pH 7.5, 100 mM NaCl, 2 mM dithiothreitol (DTT), 0.1 mM EGTA, 0.01% Brij-35 and 20 μM $MnCl_2$] containing 400 U protein phosphatase (λ PPase, New England Biolabs) at 30˚C for 1 h.

3.2.6 In vitro kinase assay

ED5 chick retinas were lysed in ELB buffer (50 mM HEPES pH 7.2, 250 mM NaCl, 0.5% NP-40, 5 mM NaF, 0.5 mM DTT, 1 mM PMSF, 1 mM Na_3VO_4 and 1X Complete protease inhibitor cocktail). Endogenous Cdk1, Cdk2, Cdk4 and Cdk5 proteins were immunoprecipitated from precleared retinal lysates as described above. The immunocomplexes were washed three times in lysis buffer and twice in kinase buffer (50 mM HEPES pH 7.2, 10 mM MgCl2, 1 mM DTT).

The immunoprecipitates were incubated with 2 μg of GST-fused Dab1-E fragments in 30 μl kinase buffer supplemented with 10 μM cold ATP and 5 μCi [γ-^{32}P]-ATP at 30˚C for 30 min. Two μg histone H1 (New England Biolabs) and GST were used as positive and negative controls, respectively. To examine the effect of Cdk inhibition on Dab1-E phosphorylation, 20 μM roscovitine was added to the kinase buffer. The reaction was terminated by the addition of 30 μl 2X SDS sample buffer. Samples were resolved by SDS-PAGE and transferred to nitrocellulose membranes. Proteins were visualized by 3,4',4'',4-copper phthalocyanine tetrasulfonic acid, tetrasodium salt (CPTS) staining and [γ-^{32}P]-ATP incorporation was analysed by autoradiography.

3.2.7 Inorganic 32P (32Pi) labeling of retinal cultures

ED5 retinal cells were cultured for 24 h and labeled with 2 mCi $^{32}P_i$ (PBS13, GE healthcare) in phosphate-free medium supplemented with 10% dialyzed fetal calf serum (Invitrogen) for 1 h at 37˚C. Cells were washed in ice-cold Tris-buffered saline (TBS, pH 7.5) and lysed in RIPA buffer. Dab1 or IgG immunoprecipitates were resolved by SDS-PAGE and transferred to a PVDF membrane followed by immunostaining with anti-Dab1 antibody. ^{32}P-labeled proteins were visualized by autoradiography.

3.2.8 Ubiquitination assays

HEK293T cells were transfected with pcDNA3-Dab1-E or HA-Ubiquitin alone, or co-transfected with pcDNA3-Dab1-E or pcDNA3-Dab1-L and HA-

Ubiquitin constructs using calcium phosphate-mediated DNA precipitation. Forty-eight h after transfection, cells were treated with 10 μM MG132 for 4 h followed by cell lysis in RIPA buffer containing protease inhibitors and 10 mM NEM to inhibit deubiquitinases. To immunoprecipitate the Dab1 protein, 200 μg of precleared cell lysates were incubated with 2 μl rabbit-anti-Dab1 at 4˚C for 2 h, and the immunocomplexes were collected using 50 μl of Protein A Sepharose beads, followed by western blot analysis.

3.2.9 Immunohistochemical analysis

Chick embryos or eyes were collected at ED5 or ED7, fixed in 10% formalin and embedded in paraffin. Tissue sections (5 μm) were deparaffinized in xylene. Antigen retrieval was by microwaving in a pressure cooker in 0.01 M citrate pH 6.0 for 20 min, followed by blocking in 500 mM glycine. Sections were immunostained with primary antibodies as indicated. The signal was detected using the Dakocytomation Envision+ anti-rabbit secondary system. Tissue sections were counterstained with hematoxylin to label the nuclei.

3.2.10 Quantitative and statistical analysis

The density of protein bands from at least three independent experiments was quantified using Image J software. ANOVA (analysis of variance) and *t* test were used to compare Dab1-E protein levels.

3.3 RESULTS

3.3.1 Phosphorylation of Dab1-E serine/threonine, but not tyrosine, in the developing chick retina

Our previous studies have shown that Dab1-E, unlike Dab1-L, is not tyrosine phosphorylated in the developing chick retina (Gao et al. 2010). Western blot analysis of Dab1 immunoprecipitates from ED10 retina using anti-Dab1-E antibody reveals up to four Dab1-E bands (depending on the SDS-PAGE conditions) suggesting posttranslational modification and/or multiple isoforms of Dab1-E (Figure 3.1A, left panel). Immunostaining the same blot with anti-phosphotyrosine antibody confirmed that only Dab1-L (top band detected with anti-Dab1 antibody, as shown in the middle panel of Figure 3.1A) is tyrosine phosphorylated (Figure 3.1A, right panel).

We then carried out $^{32}P_i$ metabolic labeling and dephosphorylation assays to determine whether Dab1-E was phosphorylated on S/T residues. Since Dab1-E is predominantly expressed at early stages of retinal development, we prepared primary retinal cells from ED5 chick embryos and cultured them in $^{32}P_i$ for 1 h. Immunoprecipitation of endogenous Dab1 proteins was carried out, followed by autoradiography and western blot analysis. Autoradiography revealed a strong phosphorylated band corresponding to the slowest migrating form of Dab1-E in the Dab1 immunoprecipitates (Figure 3.1B). Additional weaker bands were also observed in the Dab1 immunoprecipitates, indicating that these bands also represent phosphorylated forms of Dab1-E.

To further assess Dab1-E phosphorylation status in retina, Dab1

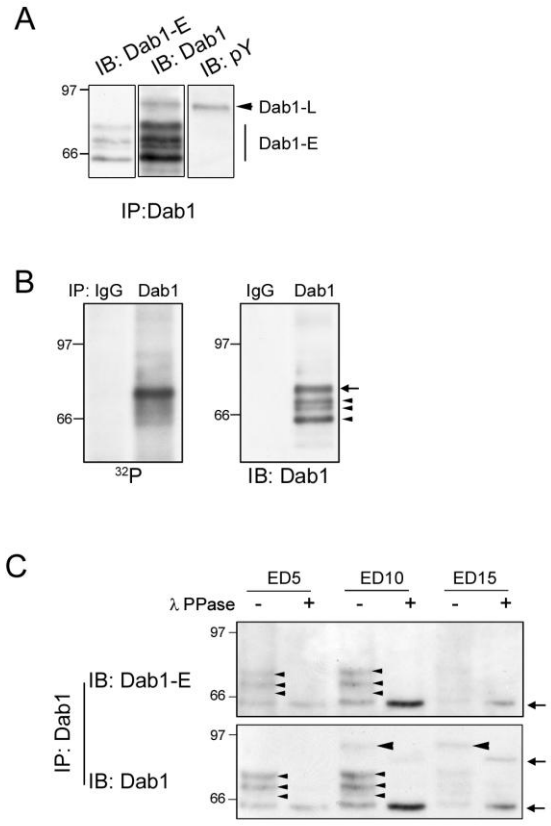

Figure 3.1 Dab1-E phosphorylation in the developing retina. Dab1 proteins were immunoprecipitated from ED10 retinal lysates using anti-Dab1 antibody and analyzed by western blotting. The blot was immunostained with anti-Dab1-E antibody (left panel), anti-Dab1 antibody (middle panel) and anti-phosphotyrosine antibody (right panel). The arrowhead indicates Dab1-L, whereas the vertical bar indicates the different forms of Dab1-E. (B) ED5 chick retinal cells were metabolically labeled with ^{32}Pi. Endogenous Dab1 proteins were immunoprecipitated with anti-Dab1 antibody. The immunoprecipitates were resolved by SDS-PAGE and transferred to a PVDF membrane. Phosphorylated Dab1 proteins were visualized by autoradiography. The membrane was immunostained with anti-Dab1 antibody. The arrow indicates the major Dab1-E band labeled with ^{32}Pi, whereas arrowheads indicate weaker bands labeled with ^{32}Pi. (C) Endogeneous Dab1 was immunoprecipitated from lysates prepared from ED5, ED10 and ED15 chick retinas. The immunoprecipitates were treated with lambda phosphatase (λ PPase) (+) or left untreated (-). Blots were immunostained with anti-Dab1-E antibody (top panel) and anti-Dab1 antibody (bottom panel). Thin arrowheads indicate phosphorylated Dab1-E and thick arrowheads indicate phosphorylated Dab1-L, whereas arrows point to dephosphorylated Dab1-E and -L.

immunoprecipitates from ED5, ED10 and ED15 chick retina were treated with λ PPase. As shown in Figure 3.1C, four Dab1-E bands are present at both ED5 and ED10. However, at ED15, the Dab1-E signal is barely detectable. In contrast, Dab1-L is not detected at ED5, but is present at ED10 and ED15 (see thick arrowheads in the bottom panel). PPase treatment results in the collapse of the Dab1-E bands into a single band, indicating multiple phosphorylated forms of Dab1-E, in agreement with the $^{32}P_i$ metabolic labeling experiments. PPase treatment also significantly alters the migration of Dab1-L (Figure 3.1C, bottom panel), consistent with previous reports indicating that Dab1 (-L) is phosphorylated (Arnaud et al. 2003a; Gao et al. 2010). These results show that Dab1-E is phosphorylated on multiple S/T residues.

3.3.2 Inhibition of Cdk, but not Reelin signaling, reduces Dab1-E serine/threonine phosphorylation

Reelin induces Dab1 (-L) tyrosine phosphorylation but has no effect on its serine phosphorylation (Howell et al. 1999b; Keshvara et al. 2001). To examine whether Reelin regulates Dab1-E S/T phosphorylation, we treated primary retinal cells with recombinant RAP at ED10, a stage when Dab1-E, Dab1-L and Reelin signaling components are all expressed. RAP is a receptor chaperone that blocks Reelin signaling by interfering with Reelin binding to its receptors VLDLR and ApoER2 (Hiesberger et al. 1999). As shown in Figure 3.2A (top panel), levels of tyrosine-phosphorylated Dab1-L were reduced in RAP-treated retinal cells; however, neither Dab1-E levels nor its phosphorylation was affected by RAP

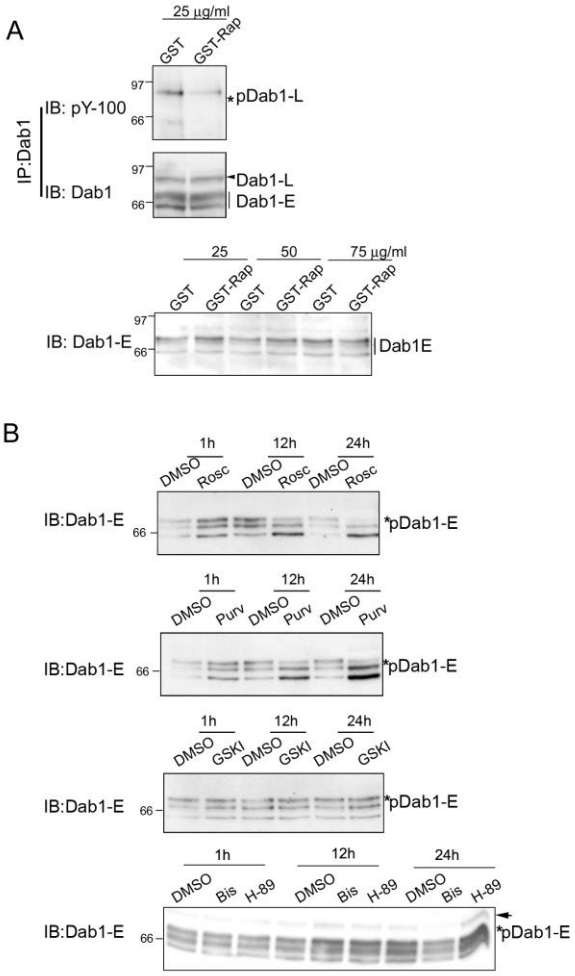

Figure 3.2 Cdk inhibition reduces Dab1-E phosphorylation. (A) Lysates were prepared from ED10 retinal cultures treated with 25 μg/ml of GST or GST-RAP for 24 h and subjected to immunoprecipitation with anti-Dab1 antibody. The immunoprecipitates were resolved by 8% SDS-PAGE and blots immunostained with anti-phosphotyrosine and anti-Dab1 antibodies (top panel). ED10 retinal cultures were treated with GST or GST-RAP for 24 h at the indicated concentrations. Western blot analysis was carried out using anti-Dab1-E antibody. (B) ED5 retinal cultures were treated with DMSO, 20 μM roscovitine (Rosc, Cdk inhibitor), 20 μM purvananol A (Purv, Cdk inhibitor), 20 μM GSKI (Gsk 3 inhibitor), 1 μM bisindolylmaleimide I (Bis, PKC inhibitor) or 1 μM H-89 (PKA inhibitor) for 1, 12 and 24 h. Cell lysates were resolved by 8% SDS-PAGE and immunoblotted using an anti-Dab1-E antibody. The arrow indicates a non-specific band labeled by the antibody.

treatment even when cells were treated with higher doses of RAP (Figure 3.2A, bottom panel). Similar results were observed in retinal cultures treated with the SFK inhibitor PP2 (data not shown). As well, Reelin treatment of ED10 primary retinal cells had no effect on Dab1-E phosphorylation (Gao et al. 2010), in support of Dab1-E S/T phosphorylation being independent of Reelin.

To identify potential kinases responsible for Dab1-E phosphorylation, we carried out bioinformatic analysis using the NetPhos, Motif Scan and Scansite software programs to predict putative kinase phosphorylation motifs in Dab1-E. Protein kinase A (PKA), protein kinase C (PKC), glycogen synthase kinase 3 (GSK3) and Cdk were all found to be strong candidates for Dab1-E phosphorylation at multiple sites. We then examined whether Dab1-E phosphorylation was affected in ED5 primary retinal cultures upon inhibition of these different kinases. Treatment of cells with the two Cdk inhibitors, roscovitine (Rosc) and purvalanol A (Purv), significantly reduced the levels of the slowest migrating Dab1-E band, presumably the most highly-phosphoryated form of Dab1-E. In contrast, solvent control (DMSO), PKA, PKC and GSK3 inhibitors had no effect on the Dab1-E banding pattern (Figure 3.2B). These results implicate Cdk in Dab1-E phosphorylation.

3.3.3 Cdk2 is involved in Dab1-E phosphorylation in the developing retina

Previous studies have shown that Cdk5 phosphorylates Dab1 (i.e. Dab1-L) in a Reelin-independent manner (Keshvara et al. 2001). Hence, Cdk5 is a strong candidate for Dab1-E phosphorylation. However, Cdk5 is mainly active in

postmitotic neurons where its activators p35 and p39 are expressed whereas Dab1-E is preferentially found in proliferating retinal progenitor cells. To determine whether Cdk5 is involved in Dab1-E phosphorylation, we carried out western blot analysis to examine the levels of Cdk5 and its activator p35 in the developing chick retina. As shown in Figure 3.3A, Cdk5 is expressed throughout retinal development from ED5 to post-hatching day 1 (P1). Importantly, p35 is primarily expressed at later stages of development (ED10- P1), thus correlating with the Dab1-L, but not Dab1-E, expression pattern. These data support a role for Cdk5 in phosphorylating Dab1-L in the retina.

We then examined the expression of other Cdks including Cdk1, Cdk2, Cdk4 and their regulatory subunits in the developing chick retina. Although cyclin D, the Cdk4 regulatory subunit, was highly expressed at early stages of retinal development, we were not able to detect Cdk4 using two anti-Cdk4 antibodies. As Cdk4 has previously been shown to be expressed in newborn rodent retina (Tong and Pollard 2001), it is likely that our two antibodies do not recognize chicken Cdk4. Neither Cdk1 nor its regulatory subunit cyclin B was detected in the chick retina (data not shown). Cdk2 and its regulatory subunit cyclin E were both detected at early stages of retinal development (Figure 3.3A). Immunohistochemical analysis of ED7 retinal tissue sections with anti-Dab1-E and anti-Cdk2 antibodies revealed that both Cdk2 and Dab1-E are expressed in proliferating retinal progenitor cells, but not in differentiated ganglion cells (Figure 3.3B). Together, these data suggest a connection between Cdk2 and Dab1-E phosphorylation.

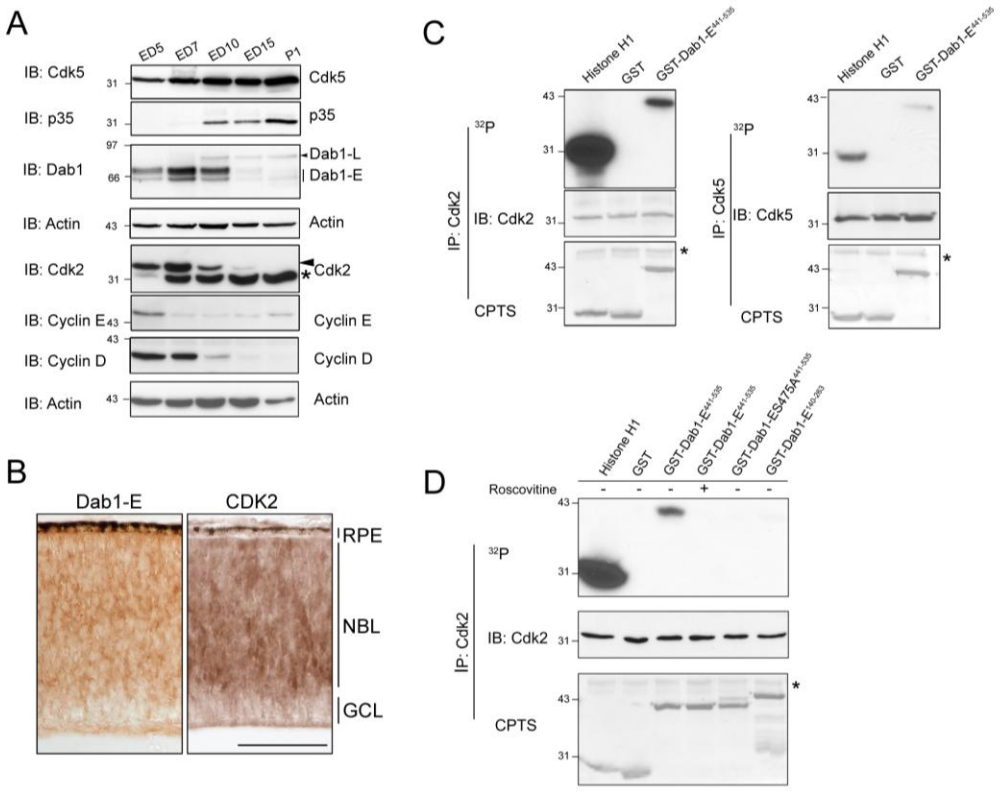

Figure 3.3 Cdk phosphorylates Dab1-E *in vitro*. (A) Expression of Cdk and cyclins in the developing retina. Retinal lysates prepared from ED5, ED7, ED10, ED15 and P1 chick embryos were resolved by SDS-PAGE and blots immunostained with anti-Cdk5, anti-p35, anti-Dab1, anti-Cyclin D1, anti-Cyclin E, anti-Cdk2 and anti-actin antibodies. The two Cdk2 bands (indicated by arrowhead and asterisk) may represent posttranslationally-modified or alternatively-spliced Cdk2 isoforms. (B) Immunohistochemical analysis of Dab1-E and Cdk2 in ED7 chick retina. Tissue sections from formalin-fixed paraffin-embedded ED7 chick retina were immunostained with anti-Dab1-E or anti-Cdk2 antibody. Abbreviations: RPE, retinal pigmented epithelium; NBL, neuroblastic layer; GCL, ganglion cell layer. Scale bar, 50 μm. (C) Endogenous Cdk2 and Cdk5 proteins were immunoprecipitated from ED5 retinal tissue lysates and incubated with histone H1, GST and GST-Dab1-E$^{441-535}$, in the presence of [γ-^{32}P] ATP. The complexes were separated in a 10% SDS-polyacrylamide gel and transferred to a nitrocellulose membrane. Protein phosphorylation was visualized by autoradiography. Histone H1, GST and GST-Dab1-E fragments were visualized by CPTS staining. Cdk2 and Cdk5 identity was verified by immunostaining the membranes with anti-Cdk2 and anti-Cdk5 antibodies. (D) The Cdk2 complex was immunoprecipitated and incubated with putative substrates as indicated in (B) in the absence/presence of 20 μM roscovitine. Autoradiography, CPTS and western blot analysis are described in (B).

Next, we assessed Cdk activity at early stages of chick retinal development. Using the well-known Cdk substrate, histone H1, we assayed the activity of Cdk2 and Cdk5 complexes immunoprecipitated from ED5 chick retina. The Cdk2 immunocomplex was much more efficient in phosphorylating histone H1 than the Cdk5 immunocomplex at this developmental stage (Figure 3.3C).

Cdks phosphorylate serines and threonines located upstream of a proline residue (S/TP) (Songyang et al. 1996). Both Dab1-E and Dab1-L contain eleven such serine and threonine residues. These serine and threonine sites are clustered in two regions, with 4 sites located in the middle of Dab1, and 6 sites in the C-terminus (Figure 3.4B). We immunoprecipitated the endogenous Cdk2 and Cdk5 complexes from ED5 chick retina and tested their ability to phosphorylate Dab1-E protein *in vitro*. The immunocomplexes were incubated with recombinant GST-fused Dab1-E middle (residues 140-263, containing 4 Cdk sites) and Dab1-E C-terminal (residues 441-535, containing 6 Cdk sites) fragments. The GST-Dab1-E C-terminal fragment, but not the Dab1-E middle fragment, was phosphorylated by both the Cdk5 and Cdk2 immunocomplexes, with the Cdk2 immunocomplex demonstrating considerably higher activity (Figures 3.3C and 3.3D, data not shown). In the presence of 20 μM roscovitine, the phosphorylation of Dab1-E C-terminus by Cdk2 was abolished, confirming that Cdk activity is required for Dab1-E phoshorylation (Figures 3.3D). Combined with the spatial expression pattern of Cdk2, these phosphorylation data indicate that Cdk2 is a good candidate for Dab1-E phosphorylation at S/T residues at early developmental stages of chick retina.

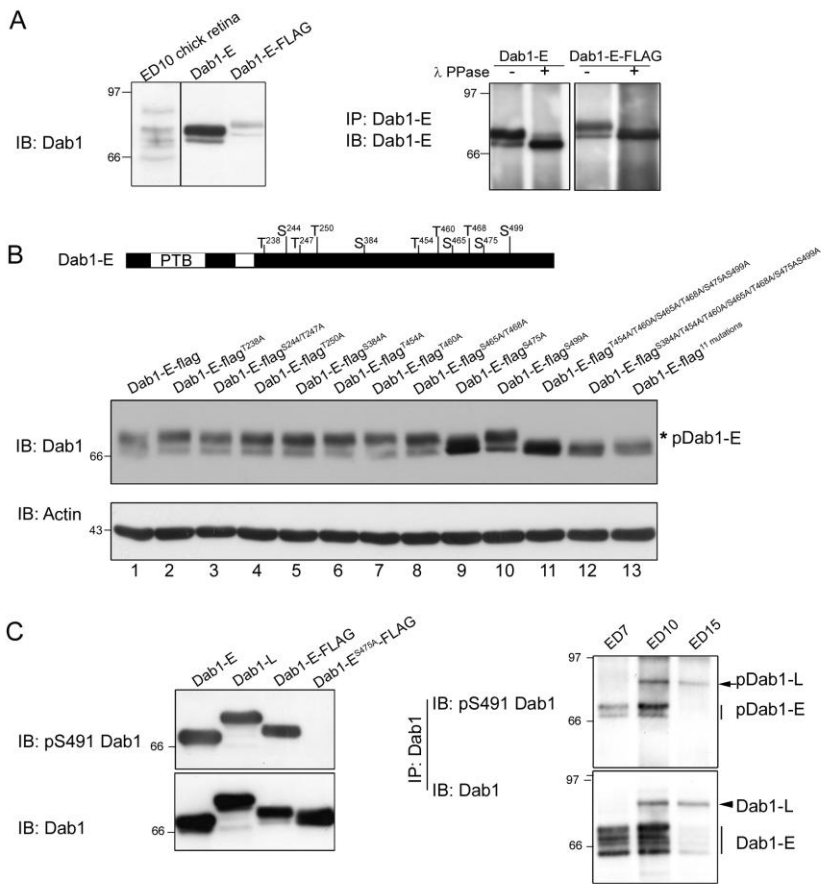

Figure 3.4 Dab1-E serine 475 phosphorylation in transfected cells and in the retina. (A) ED10 chick retinal lysates and lysates prepared from HeLa cells transfected with pcDNA3-Dab1-E and pCMV-Tag4A-Dab1-E (Dab1-E-FLAG) expression constructs were subjected to western blot analysis using anti-Dab1 antibody (left panel). Dab1-E immunoprecipitations were carried out using HeLa cells transfected with pcDNA3-Dab1-E or pCMV-Tag4A-Dab1-E expression constructs. The immunoprecipitates were treated with λ protein phosphatase (λ PPase +) or left untreated (-) before separating the proteins in an 8% SDS-polyacrylamide gel and immunoblotting with anti-Dab1-E antibody. (B) Schematic representation of putative Cdk phosphorylation sites in Dab1-E protein (top panel). Lysates prepared from HeLa cells transfected with pCMV-Tag4A-Dab1-E wild-type and mutants were subjected to western blot analysis using anti-Dab1 and anti-actin antibodies (bottom panel). The asterisk indicates phosphorylated Dab1-E. (C). Protein extracts prepared from HEK293T cells transfected with pcDNA3-Dab1-E, pcDNA3-Dab1-L, pCMV-Tag4A-Dab1-E wild-type and pCMV-Tag4A-Dab1-E^{S475A} were analysed by western blotting using the anti-S491 Dab1 phosphorylation specific antibody (pS491Dab1, left panel). Dab1 immunoprecipitates prepared from ED7, ED10 and ED15 chick retina lysates were resolved by 8% SDS-PAGE (20X20 cm), transferred to a PVDF membrane and immunostained with anti-pS491 Dab1 antibody and Dab1 antibody.

3.3.4 Serine 475 is a critical residue for Dab1-E phosphorylation both in vitro and in vivo

To identify the Cdk S/T phosphorylation sites, we substituted the 11 S/T residues with alanines in FLAG-tagged Dab1-E expression constructs. Analysis of exogenously expressed wild-type Dab1-E (with or without FLAG tag) in either retinal cultures or HeLa cells by western blotting revealed two forms of Dab1-E (Figure 3.4A). λ PPase treatment resulted in the collapse of the upper form into the lower form, indicating that exogenous Dab1-E can be phosphorylated (Figure 3.4A). Western blot analysis of FLAG-tagged Dab1-E wild-type and S/T mutants in transfected HEK293T cells indicate a similar migration pattern to that of wild-type Dab1-E for the majority of Dab1-E mutants (Figure 3.4B, lanes 1-8, 10). However, substitution of S475 with alanine (S475A mutant, lane 9) significantly reduced the levels of the slower migrating band, indicating that S475 is a critical residue for Dab1-E phosphorylation. It is noteworthy that there is still a residual upper band in the S475 mutant. This upper band disappeared completely only when all six Cdk sites in the C-terminus of Dab1-E were substituted with alanines (Figure 3.4B, lane 11), suggesting multiple sites of Dab1-E phosphorylation.

The counterpart of S475 (Dab1-E) is S491 in Dab1-L. We used anti-Dab1 pS491 antibody, which specifically recognizes phosphorylated S491, to examine Dab1-E S475 phosphorylation *in vivo*. As shown in Figure 3.4C (left panel), anti-Dab1 pS491 antibody recognizes both exogenous wild-type Dab1-E and Dab1-L, but not the Dab1-E-S475A mutant, in HEK293T transfected cells. As expected,

immunoblotting analysis of Dab1 immunoprecipitates from ED7, ED10 and ED15 chick retinal lysates using this phospho-antibody reveals S491-phosphorylation of Dab1-L at ED10 and ED15. Importantly, the two slower migrating forms of Dab1-E in ED7 and ED10 retina were both labeled by the anti-Dab1 pS491 antibody, providing direct evidence that Dab1-E is phosphorylated at S475 in this tissue (Figure 3.4C, right panel). The fact that two bands with different migration rates are recognized by the pS491 antibody suggests phosphorylation of residues other than S475 in Dab1-E.

3.3.5 Cdk2 phosphorylates Dab1-E at serine 475 in the developing retina

Our kinase assays show that Cdk2 is the most active Cdk in ED5 chick retina and that Cdk2 phosphorylates the C-terminus of Dab1-E *in vitro* (Figure 3.3C and 3.3D). To determine whether Cdk2 phosphorylates Dab1-E S475 *in vivo*, we transfected primary ED5 retinal cultures with a Cdk2 dominant negative mutant and examined the levels of Dab1-E S475 phosphorylation in these transfectants. A significant reduction in the levels of Dab1-E phosphorylated at S475 was observed in Dab1-E immunoprecipitates (Figure 3.5A), indicating that Cdk2 mediates Dab1-E phosphorylation at S475 in retinal cultures.

Next, we immunostained consecutive ED5 retinal tissue sections with anti-pS491 Dab1 and anti-Cdk2 antibodies. As shown in Figure 3.5B, phospho-S491 Dab1 antibody labeled both proliferating retinal progenitor cells and differentiated ganglion cells. In contrast, Cdk2 was detected in proliferating retinal progenitor cells known to be positive for Dab1-E, but not in the differentiated ganglion cells

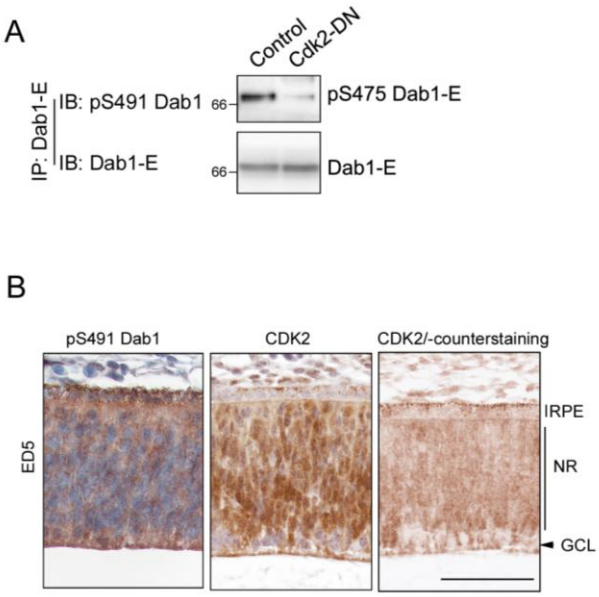

Figure 3.5 Cdk2 phosphorylates Dab1-E in the retina. (A) Dab1-E was immunoprecipitated from ED5 retinal cultures transfected with pcDNA3 and pcDNA3-HA-Cdk2 dominant negative (Cdk2-DN) expression constructs. The immunoprecipitates were analysed by western blotting using anti-pS491 Dab1 (pS475 Dab1-E) and anti-Dab1-E antibodies. (B) Immunohistochemical analysis of pS491 Dab1 and Cdk2 in ED5 chick retina. Consecutive tissue sections from formalin-fixed paraffin-embedded ED5 chick retina were immunostained with anti-pS491 Dab1 or anti-Cdk2 antibody. Sections were either counterstained with hematoxylin (left and middle panels) or not counterstained (right panel) in order to better visualize the cellular distribution of Cdk2 protein in the retina. Abbreviations: RPE, retinal pigmented epithelium; NR, neural retina; GCL, ganglion cell layer. Scale bar, 50 μm.

where Dab1-L is expressed. Thus, the cellular distribution of Cdk2 is in agreement with its proposed role in phosphorylating Dab1-E at S475 in retinal progenitor cells. Our data also indicate that a kinase other than Cdk2 (likely Cdk5) is involved in phosphorylating Dab1-L at S491 in postmitotic neurons, such as ganglion cells, as previously reported (Keshvara et al. 2001).

3.3.6 S475 phosphorylation destabilizes Dab1-E protein and promotes ubiquitination-mediated proteasome degradation

Previous studies have suggested a potential but controversial role for S491 Dab1 phosphorylation in regulating Dab1 levels, with two reports indicating increased levels of Dab1 in *Cdk5-/-* mouse brain (Keshvara et al. 2001; Ohshima et al. 2007), and two reports indicating no change in Dab1 levels in these mice (Ohshima et al. 2001; Beffert et al. 2004). In support of a role for Cdk in regulating Dab1 levels, we have observed that inhibition of Cdk in primary retinal cultures results in a significant increase in Dab1-E (Figure 3.2B). Furthermore, we have observed increased levels of Dab1-E S475A mutant protein compared to wild-type protein in transfected HeLa and HEK293T cells (compare lanes 1 and 9 in Figure 3.4B and lanes 3 and 4 in Figure 3.4C), suggesting that S475 phosphorylation may destabilize Dab1-E protein and/or enhance its turnover.

To test the effect of serine/threonine phosphorylation on Dab1-E protein stability, we treated primary ED5 retinal cultures with cycloheximide (CHX), an inhibitor of *de novo* protein synthesis. As shown in Figure 3.6A, a preferential decrease in the levels of the slower migrating form of Dab1-E relative to the two

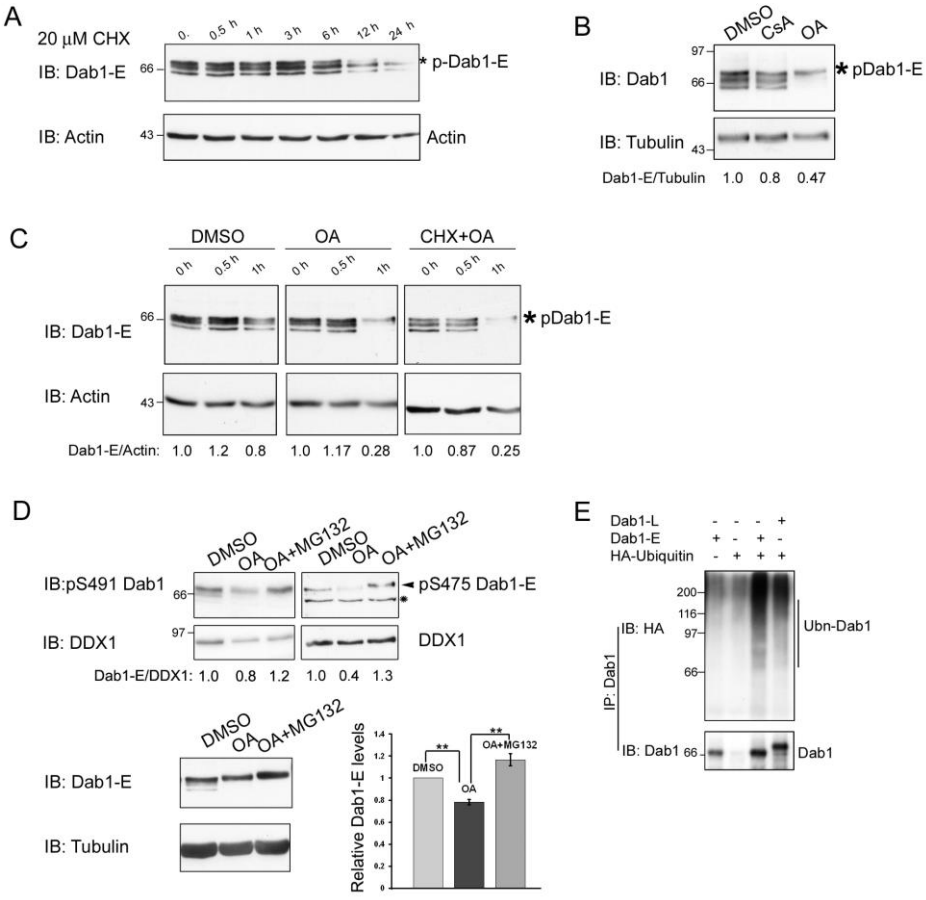

Figure 3.6 Serine 475 phosphorylation destabilizes Dab1-E and promotes ubiquitination. (A) Lysates were prepared from ED5 retinal cultures treated with 20 μM cycloheximide (CHX) for 0 to 24 h (as indicated) and subjected to western blot analysis using anti-Dab1-E and anti-actin antibodies. (B) ED5 retinal cultures were treated with DMSO, 1 μM cyclosporin A (CsA) or 250 nM okadaic acid (OA) for 1 h. Cell lysates were resolved by 8% SDS-PAGE, transferred and immunostained with anti-Dab1-E and anti-tubulin antibodies. Protein band density was quantified by Image J. Values indicate the ratio between Dab1-E and tubulin levels, with the ratio arbitrarily set at 1 for DMSO-treated samples. (C) ED5 retinal cultures were treated with DMSO, 250 nM okadaic acid (OA) or 250 nM OA in the presence of 20 μM CHX for the indicated times. Western blot analysis and quantitation were carried out as in (B), with actin used as the loading control. (D) ED5 retinal cultures were treated with DMSO, 100 nM okadaic acid (OA) or 100 nM OA in the presence of 10 μM MG132 for 4 h. Western blot analysis and quantitation were carried out as in (B), with DDX1 and tubulin serving as loading controls, respectively. The asterisk indicates a non-specific band. The histogram shows relative Dab1-E protein levels from three independent experiments. Significant differences between DMSO, OA and OA+MG132 treated cultures are indicated by double asterisks ($p<0.01$, ANOVA and *t* test). (E) HEK293T cells were transfected with pcDNA3-Dab1-E, pcDNA3-HA-Ubiquitin (HA-Ubiquitin), pcDNA3-HA-Ubiquitin and pcDNA3-Dab1-E, or pcDNA3-HA-Ubiquitin and pcDNA3-Dab1-L. Dab1 proteins were immunoprecipitated from cell lysates using anti-Dab1 antibody and immunoprecipitates analysed by western blotting using anti-HA and anti-Dab1 antibodies.

faster migrating bands was noted in the presence of CHX. These results indicate that the slower migrating form of Dab1-E, which is phosphorylated at S475 and likely at other S/T residues, is less stable than the other phosphorylated and/or nonphosphorylated forms of Dab1-E.

To further address the role of S/T phosphorylation in regulating Dab1-E protein turnover, ED5 primary retinal cultures were treated with S/T protein phosphatase inhibitors okadaic acid (OA), a protein phosphatase 2A (PP2A) and protein phosphatase 1 (PP1) inhibitor, or cyclosporine A (CsA), an inhibitor of calcineurin/protein phosphatase 2B (PP2B). If S/T phosphorylation destabilizes Dab1-E protein, one would expect that inhibition of PPase would lead to increased Dab1-E phosphorylation and decreased protein levels. As shown in Figure 3.6B, OA treatment results in loss of the faster migrating Dab1-E bands which represent the less-phosphorylated and non-phosphorylated forms of Dab1-E. Importantly, this upward migration shift was accompanied by an overall reduction in Dab1-E protein levels, in agreement with the idea that S/T phosphorylation destabilizes Dab1-E protein. In contrast, CsA treatment had no effect on the Dab1-E banding pattern and levels (Figure 3.6B), indicating that Dab1-E protein levels are highly sensitive to PP2A/PP1, but not PP2B, phosphatase activity. We also treated retinal cultures with DMSO, OA and OA in the presence of CHX to inhibit protein synthesis. As shown in Figure 3.6C, similar decreases in Dab1-E levels were observed whether cells were treated with OA alone or OA plus CHX.

Next, we examined whether the single band observed upon OA treatment

contained S475-phosphorylated Dab1-E. As shown in Fig. 6C, the single Dab1-E band observed in OA-treated cells was recognized by the pS491 antibody. Furthermore, addition of the proteasome inhibitor MG132 prevented OA-induced decrease in S475 phosphorylated-Dab1-E levels (Figure 3.6D, $P<0.01$, ANOVA and *t* test). Together, these data demonstrate that S/T phosphorylation destabilizes Dab1-E and may target it for proteasome-mediated degradation.

Proteasome-mediated protein degradation usually involves ubiquitin conjugation to the target protein. We next addressed whether Dab1-E can be ubiquitinated by co-transfecting HEK293T cells with a pcDNA3-Dab1-E expression construct and a HA-tagged ubiquitin construct. Cells co-transfected with the pcDNA3-Dab1-L and ubiquitin constructs were included as a positive control. Transfected cells were incubated with MG132 for 4 h and cell lysates immunoprecipitated with anti-Dab1 antibody and subjected to western blot analysis using an anti-HA antibody (Figure 3.6E, top panel) or anti-Dab1 antibody (Figure 3.6E, bottom panel). A ladder of polyubiquitinated Dab1 was detected in the immunoprecipitates prepared from Dab1-E or Dab1-L and ubiquitin double-transfected cells, indicating that both Dab1-E and Dab1-L serve as a substrate for the ubiquitination machinery.

3.3.7 DISCUSSION

Fine tuning of Reelin signaling and the correct positioning of neurons during development depends on precise regulation of Dab1 levels (Arnaud et al. 2003a; Bock et al. 2004; Feng et al. 2007). Reelin-induced Dab1 tyrosine phosphorylation is a key factor in regulating its levels, as tyrosine-phosphorylated Dab1 recruits SH2 domain-containing E3 ligase complexes and targets itself for rapid proteasome degradation. In contrast to the commonly studied Dab1 (Dab1-L), Dab1-E is not tyrosine phosphorylated in response to Reelin and appears to play a role in the maintenance of retinal progenitor cells rather than neuronal cell migration and positioning (Gao et al. 2010). We show that, like Dab1-L, Dab1-E activity is modulated by phosphorylation and degradation via the proteasome; however, regulation of Dab1-E activity is driven by S/T phosphorylation rather than tyrosine phosphorylation. Although S/T phosphorylation of Dab1 has previously been documented in the literature (Homayouni et al. 1999; Keshvara et al. 2002; Arnaud et al. 2003a; Ohshima et al. 2007), this is the first study demonstrating a direct role for S/T phosphorylation in the regulation of Dab1 levels.

Previous reports have alluded to serine phosphorylation playing a role in the regulation of Dab1 levels. For example, reduced S491 phosphorylation and elevated Dab1-L protein levels are observed in ectopically positioned neurons in *Cdk5*-/- mice (Keshvara et al. 2002). Furthermore, p45, a truncated form of Dab1 missing the C-terminal S/T residues (including S491), is expressed at higher levels than full-length Dab1, suggesting that the C-terminus reduces Dab1

protein stability (Herrick and Cooper 2002). However, as most of the work carried out to date on Dab1 has focused on Reelin-induced Dab1 tyrosine phosphorylation-mediated degradation, we still have little mechanistic insight into the role of S/T phosphorylation in regulating Dab1 levels. Since Dab1-E is not tyrosine-phosphorylated, our data clearly demonstrate a role for S/T phosphorylation, particularly S475, in the regulation of Dab1-E turnover. We postulate that the same proteolysis mechanism may apply to Dab1-L as this isoform is also phosphorylated at S491, the counterpart of S475. Thus, Dab1-L levels may be regulated by both Cdk5-mediated S491 phosphorylation and Reelin-induced tyrosine phosphorylation. Regulation of Dab1-L levels by both Cdk5 and Reelin would explain why increased Dab1 levels are observed in *Cdk5-/-* mice (Keshvara et al. 2002) even though Cdk inhibition has no effect on Reelin-induced Dab1 degradation (Bock et al. 2004).

A computer-based motif search has revealed one PEST motif in the central region and three PEST motifs in the C-terminal region of Dab1 (Figure 3.7). PEST motifs are hydrophilic stretches rich in proline (P), glutamate (E), aspartate (D), serine (S) and threonine (T) residues, frequently targeted by the ubiquitination-proteasome degradation pathway (Rechsteiner and Rogers 1996). These motifs are usually dormant, but phosphorylation can unmask dormant PEST signals, likely through direct recruitment of E3 ubiquitin ligases or phosphorylation-induced conformational changes, thus priming the protein for proteolysis (Rechsteiner and Rogers 1996). As S475/S491 is located in the 10-amino acid region separating PEST motifs 2 and 3 (Figure 3.7), phosphorylation

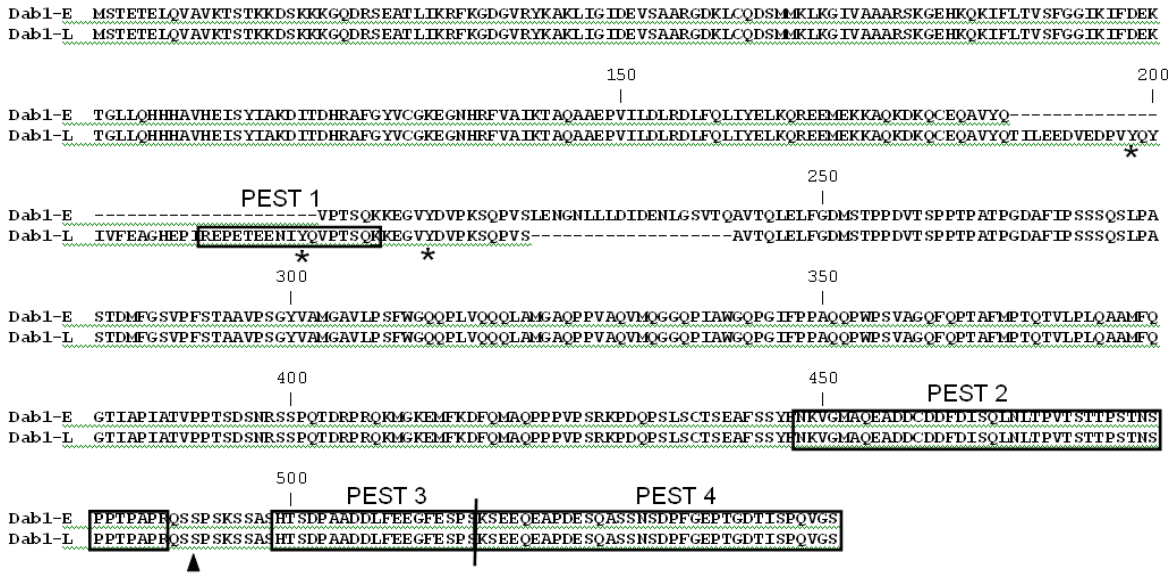

Figure 3.7. PEST motif search in Dab1-E and Dab1-L. The protein sequences of both Dab1-E (AY242122) and Dab1-L (AY242123) were scanned for potential PEST motifs using a web-based algorithm, ePESTfind (http://emboss.bioinformatics.nl/cgi-bin/emboss/epestfind). Four potential PEST motifs with a PESTfind Score >5 are highlighted in black boxes. Tyrosines that are phosphorylated upon Reelin stimulation in Dab1-L are marked with asterisks, whereas the S475/S491 residue phosphorylated by Cdk in Dab1-E/Dab1-L is indicated with a triangle. Amino acid numbering is based on the Dab1-L sequence.

of this site may activate the latent PEST signals, thus triggering ubiquitination and targeting Dab1 for degradation. Our *in vitro* data demonstrate that Dab1-E, like Dab1-L, can be polyubiquitinated, in support of both these proteins being targets for proteasome degradation. Interestingly, the Reelin-responsive site Y220 is located within PEST motif 1 and Y220 phosphorylation has been proposed to generate a recognition signal for the ubiquitin-proteasome machinery, leading to Reelin-triggered Dab1 degradation (Bock et al. 2004). Loss of Y220 and PEST motif 1 in Dab1-E suggests that Dab1-E turnover is primarily regulated through S/T phosphorylation.

Cdk2 is central to G1/S transition and S-phase progression through the cell cycle. The Cdk2-cyclin E complex has recently been shown to play an important role in regulating the cell cycle of chondroitin sulfate proteoglycan NG2+ progenitor cells, a major population of proliferating cells located in the anterior subventricular zone of the olfactory bulb (Ghiani and Gallo 2001). Loss of Cdk2 reduces self-renewal potential and promotes differentiation of NG2+ progenitor cells in adult brain (Jablonska et al. 2007). Like Cdk2-cyclin E, Dab1-E appears to play a role in the maintenance of the retinal progenitor pool since Dab1-E knock-down reduces cell proliferation and promotes ganglion cell differentiation in the retina (Gao et al. 2010). Thus, we propose that Cdk2-mediated Dab1-E phosphorylation and degradation is involved in regulating cell cycle progression. It has recently been shown that overexpression of a Dab1-E-like isoform, Dab1.7bc, causes aberrant neuronal positioning in the mouse cortex (Yano et al. 2010), in support of the idea that Dab1-E and Dab1-L levels must be

tightly regulated for normal neuronal migration.

Our results demonstrate that Cdk2-mediated Dab1-E phosphorylation at S475 is critical for the regulation of Dab1-E turnover. Other kinases may also be involved in Dab1-E phosphorylation, as Dab1-E is phosphorylated at multiple sites in the developing retina. It has previously been shown that Cdks can function as priming kinases for polo-like kinases (Plks), a family of S/T kinases that play critical roles in the regulation of the cell cycle (Elia et al. 2003a; Elia et al. 2003b; Fabbro et al. 2005). Plks have a C-terminal polo-box domain (PBD) which binds preferentially to peptides containing the consensus sequence S(pS/pT)P (Elia et al. 2003a; Elia et al. 2003b). Importantly, Cdk-mediated Dab1-E/L phosphorylation at S475/S491 (SSP) generates a PBD-binding site (SpSP). It is therefore possible that phosphorylated Dab1-E/L can recruit Plk for additional phosphorylation at S/T sites. In keeping with this idea, Plks are differentially expressed in the developing brain, with Plk1 preferentially associated with proliferating cells and Plk2 primarily found in differentiated neurons (Seeburg et al. 2008). Cdk2 and Cdk5 may thus work in conjunction with Plk1 and Plk2 to phosphorylate Dab1-E and Dab1-L, respectively.

In summary, we have found that Cdk2-mediated S/T Dab1-E phosphorylation regulates its turnover independently of Reelin signaling. A main site of S/T phosphorylation in Dab1-E is S475, the counterpart of S491 previously shown to be phosphorylated in Dab1-L. Based on the results reported here combined with data from previous studies, we propose that Dab1 protein levels are under dual regulation by Reelin-independent S/T phosphorylation and Reelin-

dependent tyrosine phosphorylation (Figure 3.8). At early developmental stages, Dab1-E levels are regulated by Cdk2-mediated S/T phosphorylation. As development proceeds, alternative splicing is activated resulting in the production of Reelin-responsive Dab1-L, whose levels are regulated by both Cdk5-mediated serine phosphorylation and Reelin-induced tyrosine phosphorylation. This dual mechanism may be critical to the control of developmental stage-specific events that are dependent on Dab1-E and Dab1-L functions.

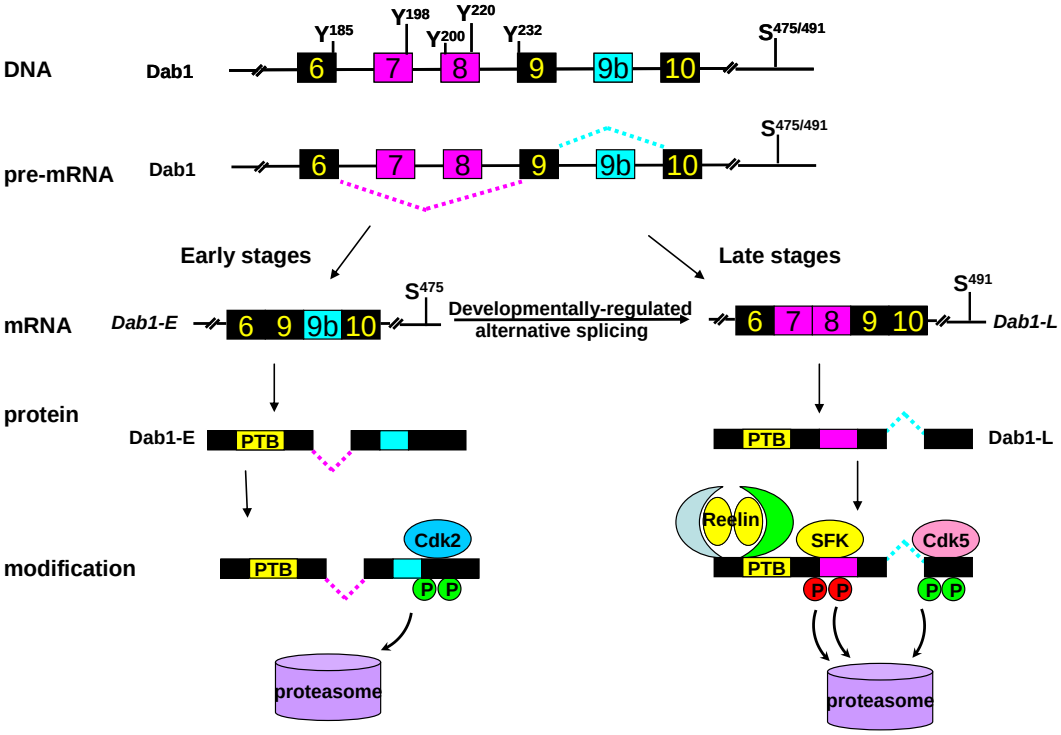

Figure 3.8 Model depicting the dual regulatory mechanism controlling Dab1-E and Dab1-L levels during development. The Dab1 gene structure (exons 6, 7, 8, 9, 9b and 10), pre-mRNA (dotted lines indicate alternative splicing), mRNA and protein are diagrammatically represented. At early developmental stages, Dab1-E is the main isoform expressed in the retina. As development progresses, alternative splicing results in a switch from Dab1-E to Dab1-L isoform. S/T phosphorylation of Dab1-E occurs independently of Reelin, whereas tyrosine phosphorylation of Dab1-L is dependent on Reelin stimulation. Dab1 levels are tightly regulated by Reelin-induced Dab1-L tyrosine phosphorylation and Cdk-mediated S/T serine phosphorylation through proteasome degradation.

3.4 ACKNOWLEDGEMENTS

We are grateful to Dr. Joachim Herz for the pGEX-RAP construct, and to Dr. Joan Turner for Cdk5, Cdk2 and p35 antibodies. We thank Shuo Chen, Darryl Glubrecht, Elizabeth Monckton and Stanley Poon for excellent technical assistance with cloning and immunohistochemical analysis. This work was supported by the Canadian Institutes of Health Research. ZG is supported by an Alberta Heritage Foundation for Medical Research studentship and a Dissertation Fellowship from the University of Alberta.

3.5 REFERENCES

Arnaud L, Ballif BA, Cooper JA. 2003a. Regulation of protein tyrosine kinase signaling by substrate degradation during brain development. *Mol Cell Biol* **23**: 9293-9302.

Arnaud L, Ballif BA, Forster E, Cooper JA. 2003b. Fyn tyrosine kinase is a critical regulator of disabled-1 during brain development. *Curr Biol* **13**: 9-17.

Ballif BA, Arnaud L, Arthur WT, Guris D, Imamoto A, Cooper JA. 2004. Activation of a Dab1/CrkL/C3G/Rap1 pathway in Reelin-stimulated neurons. *Curr Biol* **14**: 606-610.

Beffert U, Weeber EJ, Morfini G, Ko J, Brady ST, Tsai LH, Sweatt JD, Herz J. 2004. Reelin and cyclin-dependent kinase 5-dependent signals cooperate in regulating neuronal migration and synaptic transmission. *J Neurosci* **24**: 1897-1906.

Bleoo S, Sun X, Hendzel MJ, Rowe JM, Packer M, Godbout R. 2001. Association of human DEAD box protein DDX1 with a cleavage stimulation factor involved in 3'-end processing of pre-MRNA. *Mol Biol Cell* **12**: 3046-3059.

Bock HH, Herz J. 2003. Reelin activates SRC family tyrosine kinases in neurons. *Curr Biol* **13**: 18-26.

Bock HH, Jossin Y, Liu P, Forster E, May P, Goffinet AM, Herz J. 2003. Phosphatidylinositol 3-kinase interacts with the adaptor protein Dab1 in response to Reelin signaling and is required for normal cortical lamination. *J Biol Chem* **278**: 38772-38779.

Bock HH, Jossin Y, May P, Bergner O, Herz J. 2004. Apolipoprotein E receptors are required for reelin-induced proteasomal degradation of the neuronal adaptor protein Disabled-1. *J Biol Chem* **279**: 33471-33479.

Chai X, Forster E, Zhao S, Bock HH, Frotscher M. 2009. Reelin stabilizes the actin cytoskeleton of neuronal processes by inducing n-cofilin phosphorylation at serine3. *J Neurosci* **29**: 288-299.

Elia AE, Cantley LC, Yaffe MB. 2003a. Proteomic screen finds pSer/pThr-binding domain localizing Plk1 to mitotic substrates. *Science* **299**: 1228-1231.

Elia AE, Rellos P, Haire LF, Chao JW, Ivins FJ, Hoepker K, Mohammad D, Cantley LC, Smerdon SJ, Yaffe MB. 2003b. The molecular basis for phosphodependent substrate targeting and regulation of Plks by the Polo-box domain. *Cell* **115**: 83-95.

Fabbro M, Zhou BB, Takahashi M, Sarcevic B, Lal P, Graham ME, Gabrielli BG, Robinson PJ, Nigg EA, Ono Y et al. 2005. Cdk1/Erk2- and Plk1-dependent

phosphorylation of a centrosome protein, Cep55, is required for its recruitment to midbody and cytokinesis. Dev Cell 9: 477-488.

Feng L, Allen NS, Simo S, Cooper JA. 2007. Cullin 5 regulates Dab1 protein levels and neuron positioning during cortical development. Genes Dev 21: 2717-2730.

Gao Z, Monckton EA, Glubrecht DD, Logan C, Godbout R. 2010. The early isoform of disabled-1 functions independently of Reelin-mediated tyrosine phosphorylation in chick retina. Mol Cell Biol 30: 4339-4353.

Ghiani C, Gallo V. 2001. Inhibition of cyclin E-cyclin-dependent kinase 2 complex formation and activity is associated with cell cycle arrest and withdrawal in oligodendrocyte progenitor cells. J Neurosci 21: 1274-1282.

Herrick TM, Cooper JA. 2002. A hypomorphic allele of dab1 reveals regional differences in reelin-Dab1 signaling during brain development. Development 129: 787-796.

Hiesberger T, Trommsdorff M, Howell BW, Goffinet A, Mumby MC, Cooper JA, Herz J. 1999. Direct binding of Reelin to VLDL receptor and ApoE receptor 2 induces tyrosine phosphorylation of disabled-1 and modulates tau phosphorylation. Neuron 24: 481-489.

Homayouni R, Rice DS, Sheldon M, Curran T. 1999. Disabled-1 binds to the cytoplasmic domain of amyloid precursor-like protein 1. J Neurosci 19: 7507-7515.

Howell BW, Hawkes R, Soriano P, Cooper JA. 1997. Neuronal position in the developing brain is regulated by mouse disabled-1. Nature 389: 733-737.

Howell BW, Herrick TM, Cooper JA. 1999a. Reelin-induced tryosine phosphorylation of disabled 1 during neuronal positioning. Genes Dev 13: 643-648.

Howell BW, Herrick TM, Hildebrand JD, Zhang Y, Cooper JA. 2000. Dab1 tyrosine phosphorylation sites relay positional signals during mouse brain development. Curr Biol 10: 877-885.

Howell BW, Lanier LM, Frank R, Gertler FB, Cooper JA. 1999b. The disabled 1 phosphotyrosine-binding domain binds to the internalization signals of transmembrane glycoproteins and to phospholipids. Mol Cell Biol 19: 5179-5188.

Jablonska B, Aguirre A, Vandenbosch R, Belachew S, Berthet C, Kaldis P, Gallo V. 2007. Cdk2 is critical for proliferation and self-renewal of neural progenitor cells in the adult subventricular zone. *J Cell Biol* **179**: 1231-1245.

Jossin Y, Goffinet AM. 2007. Reelin signals through phosphatidylinositol 3-kinase and Akt to control cortical development and through mTor to regulate dendritic growth. *Mol Cell Biol* **27**: 7113-7124.

Kamitani T, Kito K, Nguyen HP, Yeh ET. 1997. Characterization of NEDD8, a developmentally down-regulated ubiquitin-like protein. *J Biol Chem* **272**: 28557-28562.

Katyal S, Gao Z, Monckton E, Glubrecht D, Godbout R. 2007. Hierarchical disabled-1 tyrosine phosphorylation in Src family kinase activation and neurite formation. *J Mol Biol* **368**: 349-364.

Katyal S, Godbout R. 2004. Alternative splicing modulates Disabled-1 (Dab1) function in the developing chick retina. *Embo J* **23**: 1878-1888.

Kerjan G, Gleeson JG. 2007. A missed exit: Reelin sets in motion Dab1 polyubiquitination to put the break on neuronal migration. *Genes Dev* **21**: 2850-2854.

Keshvara L, Benhayon D, Magdaleno S, Curran T. 2001. Identification of reelin-induced sites of tyrosyl phosphorylation on disabled 1. *J Biol Chem* **276**: 16008-16014.

Keshvara L, Magdaleno S, Benhayon D, Curran T. 2002. Cyclin-dependent kinase 5 phosphorylates disabled 1 independently of Reelin signaling. *J Neurosci* **22**: 4869-4877.

Ohshima T, Ogawa M, Veeranna, Hirasawa M, Longenecker G, Ishiguro K, Pant HC, Brady RO, Kulkarni AB, Mikoshiba K. 2001. Synergistic contributions of cyclin-dependant kinase 5/p35 and Reelin/Dab1 to the positioning of cortical neurons in the developing mouse brain. *Proc Natl Acad Sci U S A* **98**: 2764-2769.

Ohshima T, Suzuki H, Morimura T, Ogawa M, Mikoshiba K. 2007. Modulation of Reelin signaling by Cyclin-dependent kinase 5. *Brain Res* **1140**: 84-95.

Rechsteiner M, Rogers SW. 1996. PEST sequences and regulation by proteolysis. *Trends Biochem Sci* **21**: 267-271.

Seeburg DP, Feliu-Mojer M, Gaiottino J, Pak DT, Sheng M. 2008. Critical role of CDK5 and Polo-like kinase 2 in homeostatic synaptic plasticity during elevated activity. *Neuron* **58**: 571-583.

Songyang Z, Lu KP, Kwon YT, Tsai LH, Filhol O, Cochet C, Brickey DA, Soderling TR, Bartleson C, Graves DJ et al. 1996. A structural basis for substrate specificities of protein Ser/Thr kinases: primary sequence preference of casein kinases I and II, NIMA, phosphorylase kinase, calmodulin-dependent kinase II, CDK5, and Erk1. *Mol Cell Biol* **16**: 6486-6493.

Songyang Z, Shoelson SE, Chaudhuri M, Gish G, Pawson T, Haser WG, King F, Roberts T, Ratnofsky S, Lechleider RJ et al. 1993. SH2 domains recognize specific phosphopeptide sequences. *Cell* **72**: 767-778.

Tong W, Pollard JW. 2001. Genetic evidence for the interactions of cyclin D1 and p27(Kip1) in mice. *Mol Cell Biol* **21**: 1319-1328.

Trommsdorff M, Borg JP, Margolis B, Herz J. 1998. Interaction of cytosolic adaptor proteins with neuronal apolipoprotein E receptors and the amyloid precursor protein. *J Biol Chem* **273**: 33556-33560.

van den Heuvel S, Harlow E. 1993. Distinct roles for cyclin-dependent kinases in cell cycle control. *Science* **262**: 2050-2054.

Yano M, Hayakawa-Yano Y, Mele A, Darnell RB. 2010. Nova2 regulates neuronal migration through an RNA switch in disabled-1 signaling. *Neuron* **66**: 848-858.

CHAPTER 4: CHARACTERIZATION OF DISABLED-1 ALTERNATIVE SPLICING IN MOUSE

4.1 INTRODUCTION

The Reelin-Disabled-1 (Dab1) signaling pathway plays a key role in regulating neuronal cell positioning and synaptic plasticity during brain development (Rice and Curran 2001; Herz and Chen 2006). Binding of Reelin to its receptors, very low density lipoprotein receptors (VLDLR) and apolipoprotein E receptor 2 (ApoER2), activates Src family kinases (SFK) and induces tyrosine phosphorylation of the intracellular adaptor protein, Dab1 (Hiesberger et al. 1999; Howell et al. 1999a; Arnaud et al. 2003b; Bock and Herz 2003). Inactivation of Dab1 in mice, either by targeted disruption (*Dab1*$^{-/-}$) or spontaneous mutation (*scrambler or yotari*) leads to extensive migration defects indistinguishable from those observed in mice deficient in Reelin (*reeler*) and Reelin receptors (*Vldlr*$^{-/-}$ */Apoer2*$^{-/-}$) (D'Arcangelo et al. 1995; Howell et al. 1997b; Trommsdorff et al. 1999; Howell et al. 2000; Niu et al. 2004), demonstrating the pivotal importance of Dab1 in Reelin signaling.

Dab1 contains an N-terminal protein interaction/phosphotyrosine binding (PI/PTB) domain, which associates with the NPxY motifs located within the cytoplasmic domains of VLDLR and ApoER2 (Trommsdorff et al. 1998; Howell et al. 1999b). The PI/PTB domain is followed by a tyrosine-rich region, which contains five conserved tyrosine residues (Y185, Y198, Y200, Y220 and Y232). These residues correspond to two consensus Src family kinase (SFK) recognition sites (Y185 and Y198/Y200) and two consensus Abl family kinase recognition sites (Y220 and Y232) (Songyang et al. 1993). Three of these tyrosine sites (Y198, Y220 and Y232) have been shown to be phosphorylated in

Reelin-stimulated cortical neurons (Keshvara et al. 2001; Ballif et al. 2004). Upon phosphorylation, Dab1 recruits Src homology 2 (SH2) domain-containing proteins, such as the p85 regulatory subunit of phosphatidylinositide-3-kinase (PI3K) and cellular adaptor proteins Crk and Nckβ, leading to activation of downstream signaling and accurate neuronal positioning in the brain (Howell et al. 1997a; Ballif et al. 2004; Chen et al. 2004; Huang et al. 2004). Mice expressing Dab1 with substitutions at tyrosine residues Y185, Y198, Y200, Y220 and Y232 exhibit a phenotype similar to that seen in Reelin-deficient (*reeler*) and *Dab1*$^{-/-}$ mice, suggesting that tyrosine phosphorylation of Dab1 is essential for Reelin signaling (Howell et al. 2000). Different tyrosine sites in Dab1 appear to play distinct roles in Reelin signaling, with Y185 and Y198 functioning as primary kinase switches to activate the PI-3K/Akt pathway and regulate Dab1 protein turnover, whereas Y220 and Y232 serve as scaffold to recruit adaptors such as Nckβ and Crk family proteins (Feng et al. 2007; Feng and Cooper 2009).

The genomic organization of the *Dab1* gene is highly complex and conserved in vertebrates. The mammalian *Dab1* gene consists of 15 exons spanning over 1 Mb with a small open reading frame (1668 bp) (Bar et al. 2003). The PI/PTB domain of Dab1 is encoded by exons 3-6, whereas the Reelin responsive tyrosine phosphorylation sites (Y198, Y220 and Y232) are encoded by exons 7-9 (schematically shown in Figure 4.1A). Other than the commonly-studied Dab1 form described above, several alternatively-spliced Dab1 transcripts have been documented in mouse, human, chicken, lizard and zebrafish (Howell et al. 1997a; Bar et al. 2003; Katyal and Godbout 2004;

Costagli et al. 2006). In mouse, Dab1 isoforms resulting from alternative promoter usage and alternative exons in the coding region (Dab1^{217}, Dab1^{271} and Dab1^{555*}) have been identified (Howell et al. 1997a; Bar et al. 2003; Yano et al. 2010). Among these variants, of particular interest is Dab1^{555*} (also called Dab1.7bc), which contains two duplicated alternative exons [exons 9b (51 bp) and 9c (48 bp), 99 bp in total] inserted in-frame between exons 9 and 10. In contrast to Dab1 which is primarily expressed in neurons, Dab1^{555*} is expressed in non-neuronal cells (Bar et al. 2003; Yano et al. 2010).

In chicken, we have identified two alternatively-spliced Dab1 isoforms in the retina, chicken (ch) Dab1-E and chDab1-L, expressed in undifferentiated cells and differentiated neurons, respectively (Katyal and Godbout 2004). chDab1-L represents the well-documented Dab1, whereas chDab1-E is similar to Dab1^{555*} in that it includes an exon 9b (57 bp) homologous to the murine exons 9b and 9c. However, in contrast to Dab1^{555*}, two exons [exon 7 (39 bp) and exon 8 (66bp), 105 bp in total] are excluded from chDab1-E. These two exons encode a 35 aa region containing the Y198 and Y220 phosphorylation sites that are implicated in the relay of Reelin signaling. As a result, chDab1-E is not tyrosine phosphorylated, nor does it associate with Crk proteins (Gao et al. 2010), suggesting that it is incapable of transmitting the Reelin signal.

Despite the extensive documentation of complex alternative splicing events in *Dab1*, factors that regulate Dab1 splicing have only been identified recently. The neuron specific RNA-binding protein, neuron-oncological ventral antigen (Nova) has been shown to inhibit the inclusion of exons 9b and 9c in *Dab1* (Ule

et al. 2006; Jelen et al. 2007; Yano et al. 2010). Ablation of Nova2 in mice leads to increased expression of Dab1^{555*} and migration defects similar to that observed in *reeler* mice (Yano et al. 2010). Introducing Dab1 into the *Nova2*$^{-/-}$ mice rescues the migration defects, suggesting that Dab1 and Dab1^{555*} may have counteracting functions and that maintaining a correct balance between Dab1 and Dab1^{555*} is important for precise neuronal migration. Intriguingly, both Dab1 and Dab1^{555*} can be tyrosine-phosphorylated and recruit Crk proteins when co-transfected with c-Src into 293T cells (Yano et al. 2010), suggesting that both forms are active in Reelin signaling. Thus, how Dab1 and Dab1^{555*} function antagonistically remains an enigma. It should be noted, however, that Yano et al. have only examined the expression of exons 9b and 9c in *Nova2*$^{-/-}$ mice. Whether a murine Dab1-E isoform, with the simultaneous inclusion of exons 9b and 9c and exclusion of exons 7 and 8, is expressed in these mice remains unknown. As our previous studies suggested the inability of chDab1-E to relay the Reelin signal, the presence of a murine Dab1-E form, likely inactive in Reelin signaling, would explain the antagonistic effects between Dab1 and exons 9b/9c-containing isoforms.

To examine whether a Dab1 isoform, similar to the chDab1-E, is present in mouse, we carried out RT-PCR analysis in the developing mouse brain and retina. To our surprise, we identified 11 alternatively-spliced Dab1 variants in mouse, including Dab1, Dab1^{555*} and a form similar to the chDab1-E, revealing the complex aspects of Dab1 alterative splicing. These alternatively spliced Dab1 variants have distinct temporal expression profiles during brain development. The

predicted protein sequences of these Dab1 variants indicate that these isoforms mainly differ in the tyrosine-enriched region or in the region encoded by exons 9b and 9c. Co-transfection of expression constructs encoding different Dab1 isoforms with c-Src into 293T cells reveals that Dab1 isoforms are differentially phosphorylated on tyrosines. As different tyrosine sites in Dab1 control different downstream effects in Reelin signaling (Sanada et al. 2004; Feng and Cooper 2009), Dab1 isoforms containing different tyrosines may respond differentially to Reelin, thus regulating distinct aspects of the Reelin signaling pathway. We also show that increased expression of $Dab1^{555*}$ reduces Dab1 levels in 293T cells, suggesting inter-regulaton between these two isoforms. We propose that Dab1 alternative splicing provides a fine-tuning mechanism to modulate the activity of Reelin signaling in a temporal and spatial manner, thus precisely regulating Reelin-dependent neuronal migration and synaptic plasticity.

4.2 MATERIALS AND METHODS

4.2.1 Primers

Primers used in this study for the analysis of Dab1 alternative splicing include: i) primers flanking exons 7 and 8 of Dab1, P1, 5'-CGGCT GAACCTGTTATCCTG-3'; P2, 5'-CTTCCTTCTTTTGGCTGGTG-3'; ii) primers flanking exons 9b and 9c of Dab1, P3, 5'-TGTGCCAAAAAGTCAA CCTG-3'; P4, 5'-CAG CAGTGCCGAAAGACATA-3'; iii) primers flanking exons 6-10 of Dab1, P5, 5'-GCGAAGGACATCACAGATCA-3'; P6, 5'-CAG CAGTGCCGAAAGACATA -3'; iv) primers flanking the entire Dab1 open reading frame (ORF), P7, 5'-AGCTGGATCCACCATGTCAACTGAGACAGAAC-3';P8, 5'-AGCTCTCGAGC TAGCTACCGTCTTGTGGAC-3'. The underlined sequences are *Bam*HI and *Xho*I sites, respectively. Primers used for Nova 1 RT-PCR analysis span exons 3 and 5: forward, 5'-ACCACCGTTAATCCTGATCG-3', reverse, 5'-CGGTTTTGTTCA GGTTCTCC-3'.Primers used for Nova2 RT-PCR analysis are: forward, 5'-CTT CCTGAAGGTGCTCATCC-3', reverse, 5'-GCTCCTCCCTTACCGATGAT-3'.

4.2.2 Antibodies and plasmids

Anti-Dab1-E antiserum was generated by immunizing rabbits with KLH-conjugated peptide PLEDFDSRFAAATP (encoded by exon 9b). Anti-Dab1-L antiserum was generated by immunizing goats with KLH-conjugated peptide GHEPIRDPETEENI (encoded by exon 8). The antisera were affinity-purified using the immunizing peptides (Genscript). Rabbit anti-Dab1 antibody (Rockland), recognizing the C-terminus (440-555 aa) of Dab1, has been described previously

(Katyal et al. 2007). Rabbit anti-Dab1 B3 antibody was a gift from Dr. Jonathan Cooper (Fred Hutchison Cancer Centre). Other antibodies, including rabbit anti-GFP antibody (Abcam), mouse anti-phospho-tyrosine antibody pY 4G10 (Millipore), mouse anti-actin (Sigma), and mouse anti-TUJ1 (Covance) were obtained commercially. The pCI-c-Src plasmid was a gift from Dr. Don Fujita at the University of Calgary.

4.2.3 Mice

The strains of mice used in this study were FVB and C57BL/6. Mouse care, husbandry, and handling were performed in compliance with federal and institutional regulations and policies.

4.2.4 Reverse transcription (RT)-PCR analysis and cloning of mouse Dab1 cDNAs

Total RNAs were extracted from mouse brain and retinal tissues at different developmental stages using UltraClean Tissue RNA Isolation Kit (MO BIO Laboratories) according to the manufacturer's instructions. Five μg RNA were reverse-transcribed using oligo d(T) primer and Superscript II reverse transcriptase (Invitrogen). For detailed analysis of alternatively-spliced Dab1 isoforms, cDNAs obtained from mouse tissues at various developmental stages were PCR-amplified using the following primer sets: i) P1/P2 primers spanning exons 7 and 8 (for analysis of the deletion region), ii) P3/P4 primers spanning exons 9b and 9c (for analysis of the insertion region), and iii) P5/P6 primers

flanking exons 6 to 10 (for analysis of both the deletion and insertion region). PCR products were electrophoresed in 8% polyacrylamide gels. For sequencing, DNA fragments were cloned into pCRII-TOPO vector (Invitrogen) and sequenced using T7 and SP6 primers.

The entire coding region of Dab1 cDNA was generated by PCR amplification of embryonic day (E) 16.5 and postnatal day (P)1 retina cDNAs using P7/P8 primers. Amplified DNA fragments were cloned into pCRII-TOPO vector for sequence analysis. The inserts of interest were transferred into the expression plasmid pCIG2 (Dr. Franck Polleux, University of North Carolina) at *Eco*RI site, followed by sequence verification.

4.2.5 DNA transfections and western blot analysis

293T cells were cultured in Dulbecco's modified Eagle's medium supplemented with 10% fetal calf serum and antibiotics. Transfections were carried out with polyethylenimine (PEI) transfection reagent according to the manufacturer's protocol. Cells were lysed in RIPA buffer [50 mM Tris-HCl pH 7.5, 150 mM NaCl, 1% Triton X-100, 0.5% sodium deoxycholate, 0.1% SDS, 50 mM NaF, 1 mM PMSF, 1 mM Na_3VO_4, tyrosine phosphatase cocktail (Sigma) and 1X Complete protease inhibitor cocktail (Roche)]. Proteins were resolved by 8% SDS-PAGE and transferred to nitrocellulose or PVDF membranes, followed by immunodetection using anti-Dab1 (1:5000, Rockland), mouse anti-pY 4G10 (1:5000, Millipore), anti-Dab1-E (1:8000) and anti-Dab1-L (1:500) antibodies.

4.2.6 Culture of P19 cells

P19 embryonic carcinoma cells were cultured at a density of 10^5/ml in Petri dishes in DMEM with 7.5% bovine serum and 2.5% fetal calf serum. Neural differentiation of P19 cells was carried out by treatment of aggregated cells with all-trans-retinoic acid (RA) (Sigma R2625) as previously described (Jones-Villeneuve et al. 1983). Briefly, two days after plating (day 0), cells were treated with 0.5 μM RA. At day 2, the medium was replaced with fresh RA. At day 4, cell aggregates were harvested, trypsinized, then triturated into single cell suspension using 9 inch Pasteur pipets. Dissociated cells were replated on 100 ng/ml poly-D-lysine coated tissue culture plates or coverslips and cultured in normal medium (DMEM supplemented with 10% fetal calf serum). Two days after replating, 5 μg/ml Ara-C (Sigma C1768) was added to kill the proliferating cells. Two days later, cells were fixed in 4% paraformaldehyde for immunofluorescence analysis. Cells were harvested at different stages (as indicated) and used for either total RNA isolation using TRIzol reagent (Invitrogen) or cell lysate preparation in RIPA buffer.

4.2.7 Immunofluorescence analysis

RA-treated P19 cells (at day 8) were fixed in 4% PBS-buffered paraformaldehyde for 10 min and permeabilized in PBS-T (0.1% Triton X-100) for 5 min at room temperature. Cells were blocked in 10% donkey serum containing 1% BSA for 1 h and incubated in 1/2000 mouse anti-β III tubulin (TUJ1) antibody (Covance) at 4°C overnight, followed by incubation with Alexa-488 conjugated

secondary antibody for 2 h at room temperature. Cells were mounted using Prolong Gold mounting medium (Invitrogen) containing DAPI to stain the nuclei.

4.3 RESULTS

4.3.1 Identification of alternatively spliced Dab1 transcripts in mouse retina and brain

chDab1-E arises from mutually exclusive splicing events which involve exclusion of exons 7 and 8 and inclusion of exons 9b and 9c. To examine whether a similar Dab1 isoform is present in mouse, we carried out RT-PCR analysis of RNA prepared from E16.5 and P1 mouse retina using primers flanking exons 6-10 (P5/P6) as well as primers flanking the entire ORF of *Dab1* (P7/P8). As multiple bands were detected, we cloned the PCR fragments into pCRII-TOPO vector, followed by sequence analysis. By sequencing 35 clones (15 from E16.5 and 20 from P1 retina), we identified 11 alternatively-spliced Dab1 transcripts (schematically shown in Figure 4.1A) including the commonly studied Dab1 and Dab1^{555*} (variant 5). These transcripts are generated from either a single splicing event, such as alternative exclusion of exon 7 or 8, alternative inclusion of exons 9b and 9c, alternative usage of the 5' splice site in intron 9, or different combinations of these splicing events. Among these isoforms, variant 6, which excludes exons 7 and 8 but includes exons 9b and 9c, has the same organization as chDab1-E (referred to as murine Dab1-E from hereon in), suggesting that these alternative splicing events are conserved in vertebrates. The mRNA sequences and predicted protein sequences of different alternatively-spliced forms are aligned and shown in Figures 4.1B-D. Detailed information regarding the exons excluded (deletion) and included (insertion) in each RNA variant relative to Dab1 is listed in Table 4.1. It should be noted that

Table 4.1 Alternatively-spliced murine Dab1 isoforms

Name	Alias	Alternatively splicing events	Predicted differences in protein sequence relative to Dab1
Dab1	Dab1-L, $Dab1^{555}$		
Dab1-variant 2		Exclusion of exon 7	Deletion of 13 aa containing Y198
Dab1-variant 3		Exclusion of exon 8	Deletion of 22 aa containing Y200 and Y220
Dab1-variant 4		Exclusion of exons 7 and 8	Deletion of 35 aa containingY198, Y200 and Y220
Dab1-variant 5	$Dab1^{555*}$, Dab1.7bc	Inclusion of exons 9b and 9c	Insertion of 33 aa
Dab1-variant 6	Dab1-E	Exclusion of exons 7 and 8, inclusion of exons 9b and 9c	Deletion of 35 aa containingY198, Y200 and Y220, insertion of 33 aa
Dab1-variant 7		Exclusion of exon 8, inclusion of exons 9b and 9c	Deletion of 22 aa containing Y200 and Y220, insertion of 33 aa
Dab1-variant 8		Alternative 5'splice site of intron 9	Deletion of 2 aa (Valine and Serine)
Dab1-variant 9		Alternative 5'splice site of intron 9, exclusion of exons 7 and 8	Deletion of 2 aa (Valine and Serine), deletion of 35 aa containingY198, Y200 and Y220
Dab1-variant 10		Alternative 5'splice site of intron 9, inclusion of exons 9b and 9c	Deletion of 2 aa (Valine and Serine), insertion of 33 aa
Dab1-variant 11		Alternative 5'splice site of intron 9, exclusion of exons 7 and 8, inclusion of exons 9b and 9c	Deletion of 2 aa (Valine and Serine), deletion of 35 aa containingY198, Y200 and Y220 and insertion of 33 aa

A

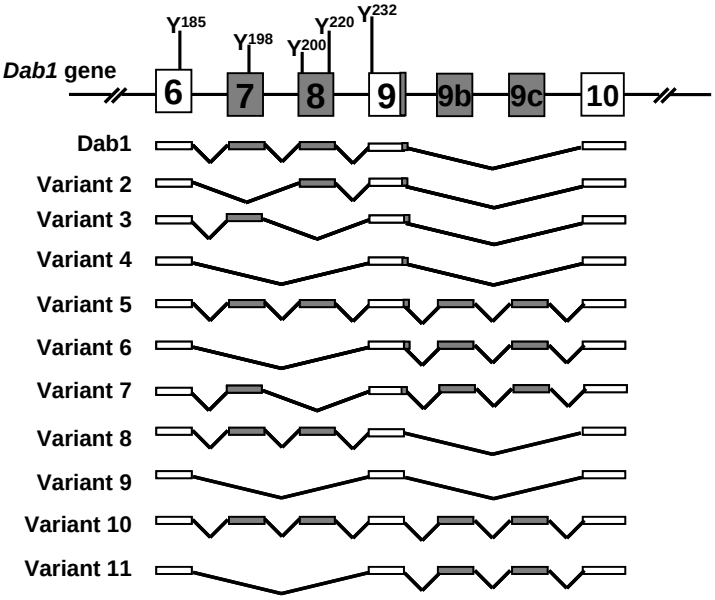
Y185
Y198
Y200
Y220
Y232
Dab1 gene
6
7
8
9
9b
9c
10
Dab1
Variant 2
Variant 3
Variant 4
Variant 5
Variant 6
Variant 7
Variant 8
Variant 9
Variant 10
Variant 11

B

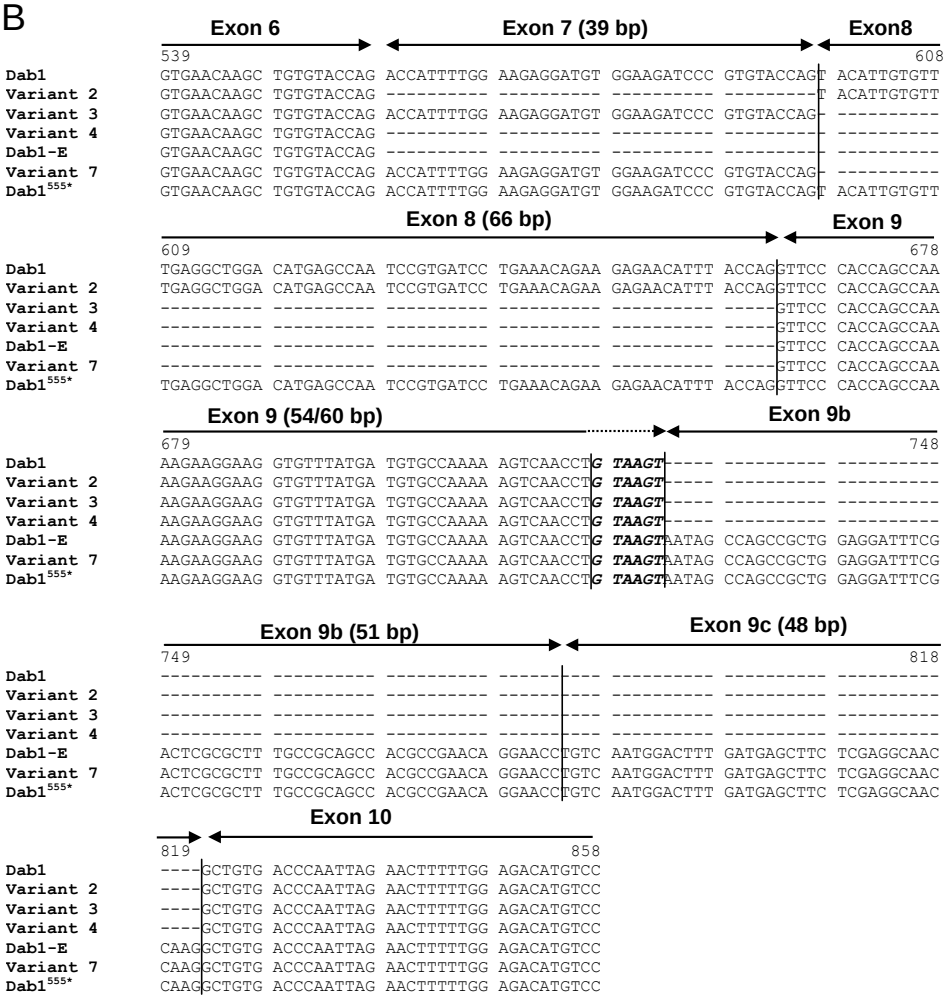
Exon 6
Exon 7 (39 bp)
Exon8
539
608
Dab1 GTGAACAAGC TGTGTACCAG ACCATTTTGG AAGAGGATGT GGAAGATCCC GTGTACCAGT ACATTGTGTT
Variant 2 GTGAACAAGC TGTGTACCAG ---------- ---------- ---------- ---------T ACATTGTGTT
Variant 3 GTGAACAAGC TGTGTACCAG ACCATTTTGG AAGAGGATGT GGAAGATCCC GTGTACCAG- ----------
Variant 4 GTGAACAAGC TGTGTACCAG ---------- ---------- ---------- ---------- ----------
Dab1-E GTGAACAAGC TGTGTACCAG ---------- ---------- ---------- ---------- ----------
Variant 7 GTGAACAAGC TGTGTACCAG ACCATTTTGG AAGAGGATGT GGAAGATCCC GTGTACCAG- ----------
Dab1555* GTGAACAAGC TGTGTACCAG ACCATTTTGG AAGAGGATGT GGAAGATCCC GTGTACCAGT ACATTGTGTT
Exon 8 (66 bp)
Exon 9
609
678
Dab1 TGAGGCTGGA CATGAGCCAA TCCGTGATCC TGAAACAGAA GAGAACATTT ACCAGGTTCC CACCAGCCAA
Variant 2 TGAGGCTGGA CATGAGCCAA TCCGTGATCC TGAAACAGAA GAGAACATTT ACCAGGTTCC CACCAGCCAA
Variant 3 ---------- ---------- ---------- ---------- ---------- -----GTTCC CACCAGCCAA
Variant 4 ---------- ---------- ---------- ---------- ---------- -----GTTCC CACCAGCCAA
Dab1-E ---------- ---------- ---------- ---------- ---------- -----GTTCC CACCAGCCAA
Variant 7 ---------- ---------- ---------- ---------- ---------- -----GTTCC CACCAGCCAA
Dab1555* TGAGGCTGGA CATGAGCCAA TCCGTGATCC TGAAACAGAA GAGAACATTT ACCAGGTTCC CACCAGCCAA
Exon 9 (54/60 bp)
Exon 9b
679
748
Dab1 AAGAAGGAAG GTGTTTATGA TGTGCCAAAA AGTCAACCTG TAAGT----- ---------- ----------
Variant 2 AAGAAGGAAG GTGTTTATGA TGTGCCAAAA AGTCAACCTG TAAGT----- ---------- ----------
Variant 3 AAGAAGGAAG GTGTTTATGA TGTGCCAAAA AGTCAACCTG TAAGT----- ---------- ----------
Variant 4 AAGAAGGAAG GTGTTTATGA TGTGCCAAAA AGTCAACCTG TAAGT----- ---------- ----------
Dab1-E AAGAAGGAAG GTGTTTATGA TGTGCCAAAA AGTCAACCTG TAAGTAATAG CCAGCCGCTG GAGGATTTCG
Variant 7 AAGAAGGAAG GTGTTTATGA TGTGCCAAAA AGTCAACCTG TAAGTAATAG CCAGCCGCTG GAGGATTTCG
Dab1555* AAGAAGGAAG GTGTTTATGA TGTGCCAAAA AGTCAACCTG TAAGTAATAG CCAGCCGCTG GAGGATTTCG
Exon 9b (51 bp)
Exon 9c (48 bp)
749
818
Dab1 ---------- ---------- ---------- ----------- ---------- ---------- ----------
Variant 2 ---------- ---------- ---------- ----------- ---------- ---------- ----------
Variant 3 ---------- ---------- ---------- ----------- ---------- ---------- ----------
Variant 4 ---------- ---------- ---------- ----------- ---------- ---------- ----------
Dab1-E ACTCGCGCTT TGCCGCAGCC ACGCCGAACA GGAACCTGTC AATGGACTTT GATGAGCTTC TCGAGGCAAC
Variant 7 ACTCGCGCTT TGCCGCAGCC ACGCCGAACA GGAACCTGTC AATGGACTTT GATGAGCTTC TCGAGGCAAC
Dab1555* ACTCGCGCTT TGCCGCAGCC ACGCCGAACA GGAACCTGTC AATGGACTTT GATGAGCTTC TCGAGGCAAC
Exon 10
819
858
Dab1 ----GCTGTG ACCCAATTAG AACTTTTTGG AGACATGTCC
Variant 2 ----GCTGTG ACCCAATTAG AACTTTTTGG AGACATGTCC
Variant 3 ----GCTGTG ACCCAATTAG AACTTTTTGG AGACATGTCC
Variant 4 ----GCTGTG ACCCAATTAG AACTTTTTGG AGACATGTCC
Dab1-E CAAGGCTGTG ACCCAATTAG AACTTTTTGG AGACATGTCC
Variant 7 CAAGGCTGTG ACCCAATTAG AACTTTTTGG AGACATGTCC
Dab1555* CAAGGCTGTG ACCCAATTAG AACTTTTTGG AGACATGTCC

C

tagGTTC*CCA* *C*CAGCCAAAA GAAGGAAGGT GTTTATGATG
TGCCAAAAAG TCAACCT***gta*** ***agtgtaagt***a catgtgcctc
tgcagcggcc caat*tcac*gc agaggctgca cctgacgggg

D

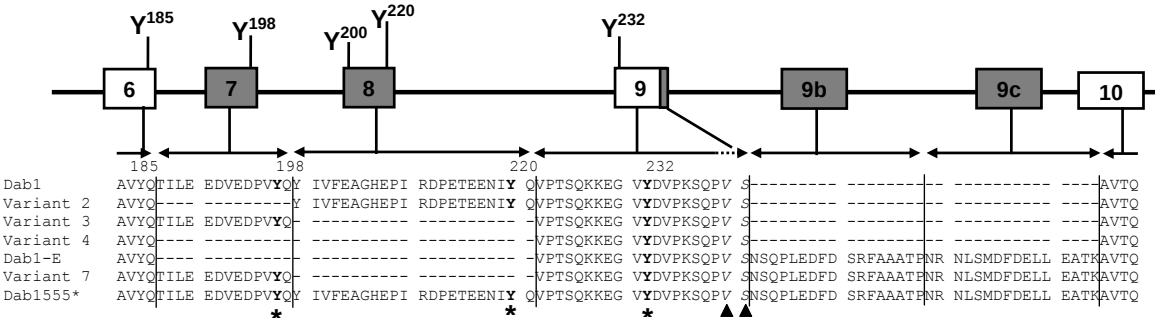

Figure 4.1 Identification of multiple alternatively-spliced Dab1 isoforms. (A) Schematic representation of Dab1 gene structure and alternatively-spliced variants. Constitutive exons are shown in white blocks, whereas alternatively-spliced exons are indicated in shaded blocks. Tyrosine residues encoded by exons 6-9 are shown. The exons and introns are not drawn to scale. **(B) mRNA sequence alignment of representative Dab1 variants.** The sequences of exons 6-10 are indicated by arrows. The italicized and bold nucleotides at the 3' end of exon 9 indicate the 5' alternative splice site. Nucleotide numbering is based on *Dab1* mRNA and starts from the ATG codon. **(C) Alternative 5' splice site in intron 9.** Two consensus 5' splice sites are located at either the 3' end of exon 9 or 5' end of intron 9 (gtaagtgtaagt, italicized). The sequences of exon 9 ares shown in uppercase letters and underlined, whereas the intronic sequence is shown in lowercase letters. Alternative usage of the splice sites leads to inclusion/exclusion of 6 bp (GTAAGT) that encode valine and serine. **(D) Alignment of predicted protein sequences of representative Dab1 isoforms.** The exon-intron structure (exons 6-10) of the mouse *Dab1* gene is depicted. Constitutive exons are shown in white blocks, whereas alternative exons are shown in shaded blocks. Amino acid sequences encoded by these exons are indicated. Tyrosine residues (Y198, Y220 and Y232) that are phosphorylated upon Reelin stimulation are in bold and indicated with asterisks. Note that exclusion of exons 7/8 changes the tyrosine phosphorylation sites in different isoforms. The two amino acids affected by the alternative 5' splice site in intron 9 are italicized and indicated with triangles. Amino acid numbering is based on Dab1 protein sequence.

none of the alternative splicing events identified in this study change the open reading frame of *Dab1*. Instead, alternative splicing results in partial deletion of residues (encoded by exons 7 and 8) in the tyrosine-enriched region, insertion of a 33 aa fragment (encoded by exons 9b and 9c), or micro-deletion of valine 240 and serine 241 (alternative 5' splice site of intron 9). All the Dab1 variants retain an intact PI/PTB domain and the C-terminus. As the alternative 5' splice site selection in intron 9 only affects two amino acids, we have focused our studies on the characterization of Dab1 variants in which exons 7/8 are excluded and/or exons 9b/9c are included. Together, these data demonstrate that Dab1 alternative splicing produces multiple forms which primarily differ in the tyrosine-rich region.

4.3.2 Differential expression of Dab1 variants in the developing mouse brain

To examine whether Dab1 variants are differentially expressed during development, we carried out RT-PCR analysis of mouse brain and retina at different developmental stages, using primers flanking the deletion region (P1/P2, spanning exons 7 and 8) and the insertion region (P3/P4, spanning exons 9b and 9c), respectively (schematically shown in Figure 4.2A). As shown in Figure 4.2B (left panel), RT-PCR analysis of the deletion region in E9.5 mouse brain generated three bands, of 252 bp, 195/207 bp and 147 bp. At later stages of development, the top band became the predominant form, with the bottom two bands barely detectable. Sequence analysis confirmed that the top band contains

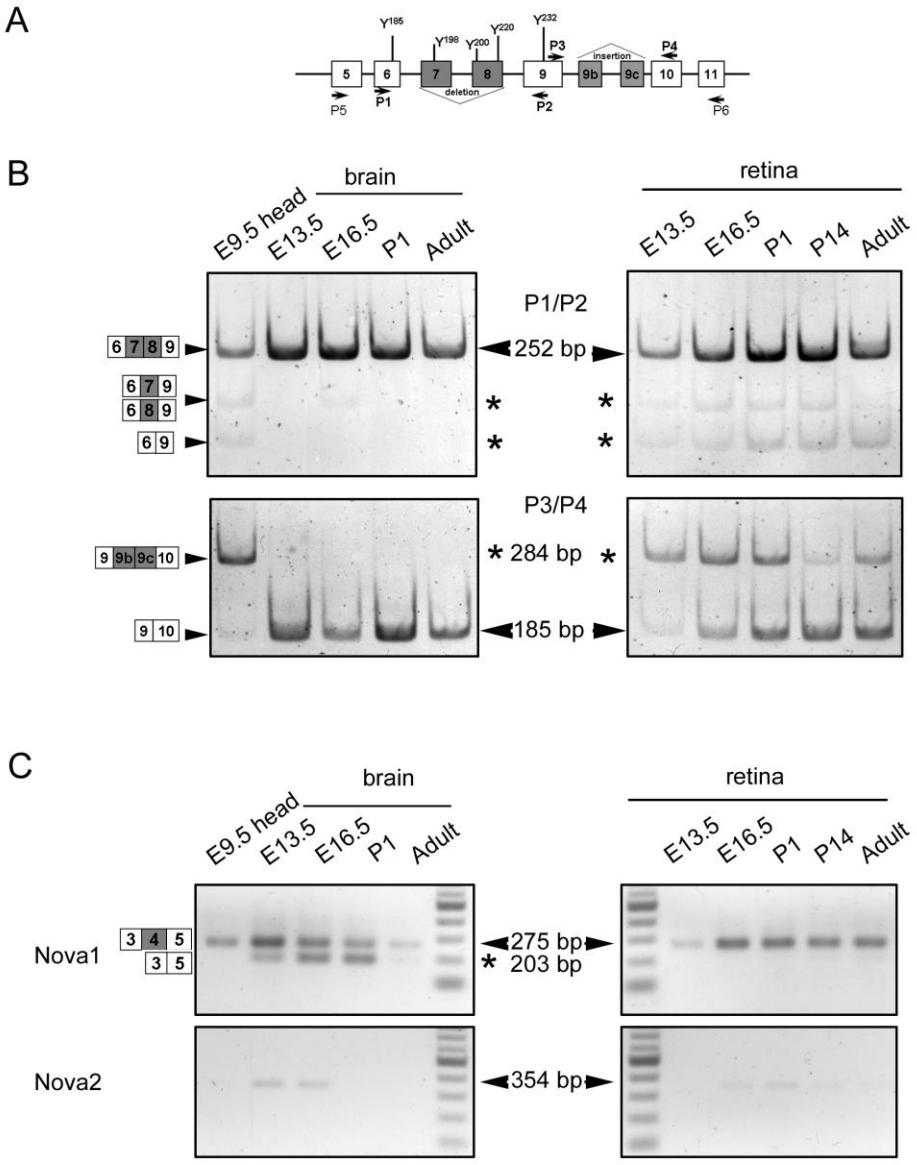

Figure 4.2 Differential expression of Dab1 and Nova during development. (A) Locations of primers used for the analysis of the deletion and insertion regions of Dab1 are indicated. (B) RT-PCR analysis of Dab1 deletion and insertion regions in the developing mouse brain and retina. cDNAs from mouse brain and retina at different developmental stages (as indicated) were amplified using primer sets P1/P2 or P3/P4. Sizes of amplified bands and included exons are shown. **(C) RT-PCR analysis of Nova1 and Nova2 in the developing mouse brain and retina.** cDNAs from mouse brain and retina at different developmental stages (as indicated) were amplified using Nova1 and Nova2 specific primers. Sizes of amplified bands are shown.

exons 7 and 8, while the bottom two bands are missing exon 7 and/or 8. In contrast, two bands, of 284 bp and 185 bp, were observed using primers P3 and P4 which flank the insertion region of Dab1 (Figure 4.2B, bottom left panel). The 284 bp band was predominant in E9.5 mouse head, yet undetectable in E13.5 and later stages of mouse brain development. Conversely, the 185 bp band was found at low abundance in E9.5 mouse head, but became the prominent band at later developmental stages (E13.5 and afterwards). The presence/absence of exons 9b and 9c in the 284 bp and 185 bp bands was verified by sequence analysis, respectively. Intriguingly, RT-PCR analysis of mouse retina reveals complex alternative splicing patterns of Dab1 that do not correspond to a clear-cut developmentally-regulated alternative splicing pattern (Figure 4.2B, right panels). These results indicate that Dab1 alternative splicing is differentially regulated in mouse brain and retina.

As the neuron specific RNA-binding proteins Nova1 and Nova2 have been shown to inhibit the inclusion of exons 9b and 9c (Ule et al. 2005; Ule et al. 2006; Yano et al. 2010), we examined the expression of Nova1 and Nova2 in the developing brain and retina by RT-PCR analysis. As shown in Figure 4.2C (left panels), Nova2 is specifically expressed in E13.5 and E16.5 mouse brain and likely mediates exclusion of exons 9b and 9c at E13.5, as shown in a recent study (Yano et al. 2010). Interestingly, the extensively studied Nova1 form, which does not include exon 4 (Dredge et al. 2005), is specifically expressed in the brain, whereas the alternatively-spliced Nova1 (which includes exon 4) is expressed in both brain and retina at all stages examined. The expression of

Nova1 correlates with the specific inclusion of Dab1 exons 7 and 8 in the brain, suggesting a possible role for Nova1 in regulating exons 7 and 8 inclusion during brain development.

4.3.3 Dab1 isoforms are differentially expressed during P19 cell differentiation

Our previous studies have shown that chDab1-E is prominently expressed in actively proliferating cells, whereas chDab1-L is found in differentiated neurons. Knockdown of chDab1-E in chick retina reduces retinal progenitor cell proliferation and promotes ganglion cell differentiation, demonstrating a correlation between the expression of specific Dab1 isoforms and cell proliferation/differentiation (Gao et al. 2010). To further investigate this correlation, we examined the expression of Dab1 isoforms during the course of P19 cell differentiation to postmitotic neurons using primers P1/P2 and P3/P4. Exponentially growing P19 cells were aggregated in the presence of 0.5 μM RA, which results in cell differentiation along the neural cell lineage (Jones-Villeneuve et al. 1983). Immunostaining of P19 cells 8 days post-RA treatment with the neuron-specific marker TUJ1 suggests that the majority of cells have successfully differentiated into neurons (Figure 4.3B). A concomitant increase in Dab1 exons 7 and 8 inclusion and exons 9b and 9c exclusion was observed during the course of P19 cell differentiation (Figure 4.3A), consistent with previous observations showing that exclusion of exons 9b and 9c parallels neuronal differentiation (Bar et al. 2003). The relative abundance of the 284 bp product (which contains exons

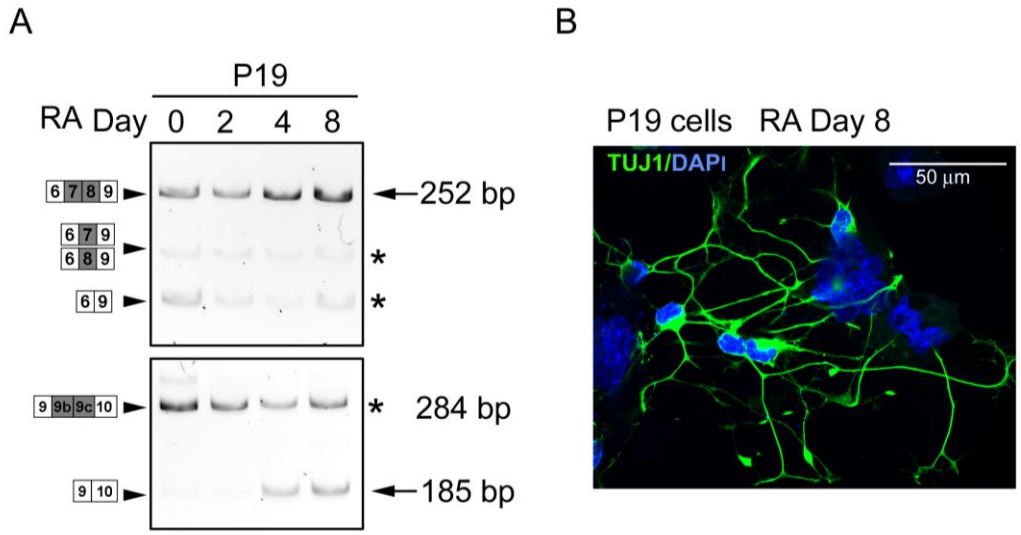

Figure 4.3 Differential expression of Dab1 isoforms during P19 cell differentiation. (A) cDNAs from P19 cells treated with 0.5 μM retinoic acid (RA) for 0, 2, 4 and 8 days were amplified using the primer sets shown in Figure 2A. Sizes of amplified bands and included exons are shown. **(B)** Immunofluorescence analysis of P19 cells at day 8 post-RA treatment using mouse anti-TUJ1 antibody which specifically labels neurons. Nuclei are labeled with DAPI. Micrographs were collected with a Zeiss LSM 710 confocal microscope equipped with a 40X lens. Scale bars, 50 μm.

9b and 9c) in RA-treated P19 cells is likely due to the presence of subpopulations of non-neuronal cells.

4.3.4 Dab1 variants are translated and differentially expressed in mouse brain

To examine the expression of Dab1 isoforms at the protein level, we generated two antibodies that specifically target the insertion and deletion regions in Dab1 isoforms. In light of the similarities between the mouse and chicken Dab1 isoforms, these antibodies are referred to as anti-(mouse) Dab1-E and anti-(mouse) Dab1-L antibodies, respectively. The anti-Dab1-E and anti-Dab1-L antibodies were generated against the regions encoded by exon 9b and exon 8, respectively (schematically shown in Figure 4.4). The specificity of these antibodies was determined by testing their ability to recognize exogenously expressed Dab1 proteins in 293T cells. Full-length Dab1 cDNAs encoding different Dab1 isoforms (Dab1, Dab1-E, Dab1^{555*}, variant 4 and variant 7) were cloned into the pCIG2 vector and introduced into 293T cells. Western blot analysis of transfected cells indicates that anti-Dab1-E antibody specifically recognizes Dab1 isoforms containing exons 9b and 9c (Dab1-E, Dab1^{555*} and Dab1 variant 7) (Figure 4.4, top panel), whereas the anti-Dab1-L antibody only recognizes Dab1 isoforms containing the exon 8 (Dab1 and Dab1^{555*}) (Figure 4.4, second panel). Notably, Dab1 variant 7, which contains exons 9b and 9c but excludes exon 8, is recognized by the anti-Dab1-E antibody, but not by the anti-Dab1-L antibody, demonstrating the isoform specificity of these antibodies. An

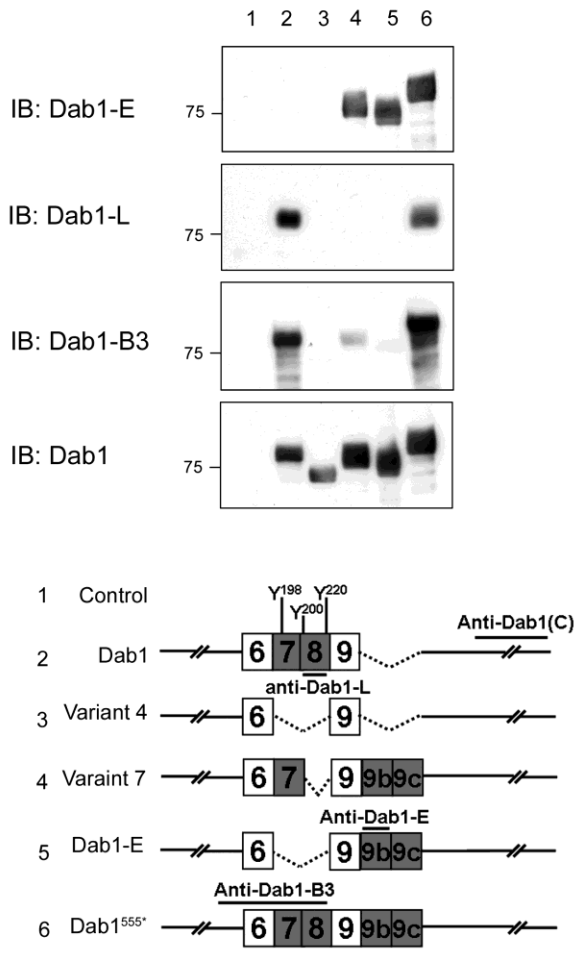

Figure 4.4 Specificity of Dab1 isoform antibodies. Western blot analysis of cell lysates prepared from 293T cells transfected with different Dab1 isoforms (schematically shown at the bottom) using anti-mouse Dab1-E (1:8000), anti-mouse Dab1-L (1:500), anti-Dab1-B3 (1:5000) and anti-Dab1 (1:10,000) antibodies. The immunogens that were used to generate these antibodies are schematically indicated.

immunoblot of the same cell lysates using Dab1 B3 antibody demonstrates that this antibody does not recognize Dab1 isoforms that exclude exons 7 and 8 (Dab1-E and variant 4) (Figure 4.4, third panel), consistent with our previous observations (Gao et al. 2010). It should be noted, however, that the B3 antibody recognizes variant 7 (which includes exon 7 but excludes exon 8), suggesting that it likely binds to an epitope located within the region encoded by exon 7. Western blot analysis using an anti-Dab1 antibody generated against the C-terminus of Dab1 recognizes all the Dab1 isoforms (Figure 4.4, bottom panel). These data indicate that our Dab1-E and Dab1-L antibodies are isoform specific.

Next, we examined the expression of endogenous Dab1 proteins in mouse brain using a panel of Dab1 antibodies. As shown in Figure 4.5, the anti-Dab1-E antibody recognizes an 80 kDa band that is specifically expressed in E12.5 mouse brain (Figure 4.5, top panel). The presence of this band is consistent with RNA variants containing exons 9b and 9c at this developmental stage. Although we cannot distinguish between the exons 9b and 9c-containing isoforms (Dab1-E, Dab1.7bc and other variants) based on western blot analysis, our data indicate that Dab1 isoforms containing exons 9b and 9c are translated and expressed at early developmental stages. Reprobing of the blot with anti-Dab1 B3 antibody revealed the presence of exon 7-containing Dab1 isoforms at E12.5, E16.5, P1 and adult mouse brain (Figure 4.5, second panel)

The anti-Dab1-L antibody recognizes an 80 kDa band that is present in E12.5, E16.5 and P1 mouse brain but absent in adult brain (Figure 4.5, third panel). Reblotting the same membrane with Dab1 C-terminal and Dab1-B3

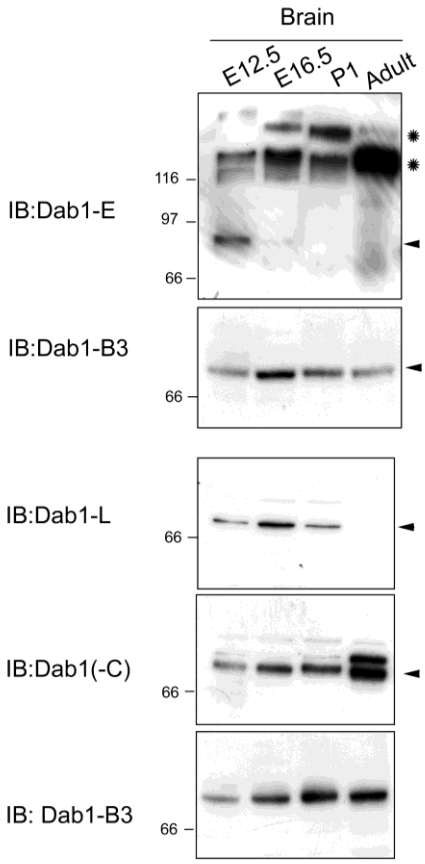

Figure 4.5 Expression of Dab1 isoforms in the developing mouse brain. Western blot analysis of brain lysates from different developmental stages (as indicated) using anti-mouse Dab1-E (1:500), anti-mouse Dab1-L (1:100), anti-Dab1-B3 (1:2000) and anti-Dab1 (1:5000) antibodies. The asterisks indicate non-specific bands recognized by the anti-mouse Dab1-E antibody.

antibodies reveals an 80 kDa band at all the stages examined. The inability of the anti-Dab1-L antibody to detect an 80 kDa band in adult mouse brain suggests that the 80 kDa Dab1 protein expressed in adult brain does not include exon 8, although it does include exon 7. Of note, anti-Dab1 (C-terminus) also recognizes a band of >80 kDa in adult brain.

Our attempts to examine the cellular distribution of Dab1 isoforms in the brain using anti-Dab1-E and anti-Dab1-L antibodies were unsuccessful as these antibodies generate a high background (anti-Dab1-L antibody) or cross-react with other proteins (anti-Dab1-E antibody).

4.3.5 Differential tyrosine phosphorylation of Dab1 isoforms

Our previous studies demonstrate that chDab1-E and chDab1-L are differentially phosphorylated (Gao et al. 2010), with chDab1-L phosphorylated on both tyrosine and serine/threonine residues, whereas chDab1-E phosphorylation is limited to serine/threonine residues (Gao and Godbout 2010). To examine whether mouse Dab1 isoforms are differentially tyrosine-phosphorylated, we transfected the expression constructs encoding different Dab1 isoforms into 293T cells along with wild-type c-Src or control vector. Low levels of Dab1 tyrosine phosphorylation were detected in cells expressing Dab1 in the absence of c-Src (Figure 4.6, lane 3). Co-transfection with c-Src resulted in robust enhancement of Dab1 tyrosine phosphorylation (Figure 4.6, lane 4). The $Dab1^{555*}$ isoform was tyrosine phosphorylated and its tyrosine phosphorylation was induced in the presence of c-Src, consistent with a recent study (Yano et al. 2010). The

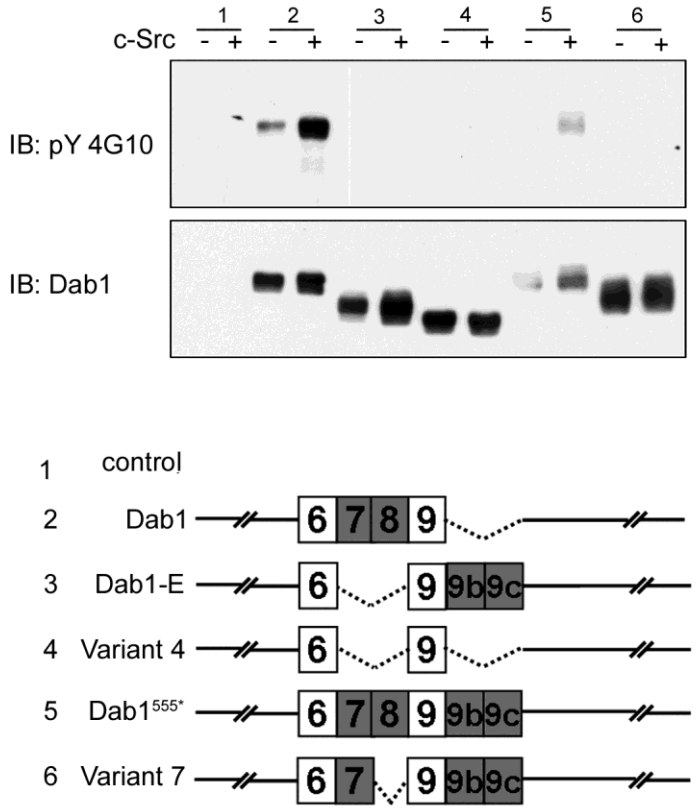

Figure 4.6 Differential tyrosine phosphorylation of Dab1 isoforms. Cell lysates were prepared from 293T cells co-transfected with 0.25 μg c-Src and 0.25 μg of Dab1 or different variants. Cell lysates were analyzed by western blotting with anti-phosphotyrosine 4G10 (top panel) and anti-Dab1 (bottom panel) antibodies.

relatively low levels of tyrosine-phosphorylated Dab1^{555*} may be due to the low levels of total Dab1^{555*} protein in these transfectants (Figure 4.6, bottom panel). Dab1-E and Dab1 variant 4, which exclude exons 7 and 8 encoded regions, are not tyrosine phosphorylated, even when co-transfected with the c-Src expression construct. Strikingly, Dab1 variant 7, which excludes only exon 8 but includes exons 7, 9b and 9c, is not tyrosine phosphorylated. This isoform contains Y185 and Y198 residues, both of which are implicated in Reelin signaling (Keshvara et al. 2001; Ballif et al. 2004; Katyal et al. 2007). However, exclusion of exon 8 converts the Y198 site (YQYI), an SFK consensus site, into an Abl consensus site (YQVP). This suggests that the surrounding residues are important for Dab1 tyrosine phosphorylation.

4.3.6 Increased ratio of Dab1 555* to Dab1 reduces Dab1 levels

Recent studies suggest that the balance between Dab1^{555*} and Dab1 is important for accurate neuronal migration in the developing mouse brain (Yano et al. 2010). To determine whether Dab1 activity may be affected by other Dab1 isoforms, we examined the tyrosine phosphorylation of Dab1 in 293T cells co-transfected with Dab1 and other variants at different ratios (1:1 and 1:2) along with c-Src. At a 1:1 ratio, there was no apparent difference in the levels of Dab1 tyrosine phosphorylation for all the co-transfectants (data not shown). However, when we doubled the concentration of the variants relative to Dab1 (variants:Dab1, 2:1), we observed a significant decrease in Dab1 tyrosine phosphorylation in cells co-transfected with Dab1^{555*} (Figure 4.7). These results

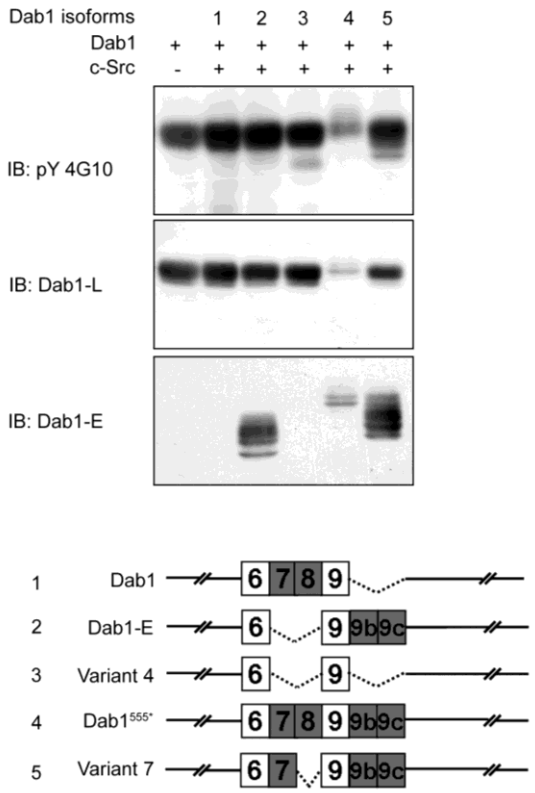

Figure 4.7 Increased expression of Dab1^{555*} reduces Dab1 levels. Cell lysates were prepared from 293T cells co-transfected with 0.5 μg of the specified Dab1 variants, 0.25 μg of Dab1 and 0.25 μg c-Src. Cell lysates were resolved on a 20X20 cm 8% SDS-polyacrylamide gel, transferred to a PVDF membrane and immunostained with anti-phosphotyrosine 4G10 (top panel), anti-mouse Dab1-L (middle panel) and anti-mouse Dab1-E (bottom panel) antibodies.

suggest a specific inhibitory effect of Dab1^{555*} on Dab1. Reblotting the membrane with anti-Dab1-E and anti-Dab1-L antibodies, revealed dramatically reduced levels of both Dab1^{555*} and Dab1, suggesting that an increased ratio of Dab1^{555*} relative to Dab1 affects the levels of both these proteins.

4.4 DISCUSSION

In this study, we have identified multiple alternatively-spliced *Dab1* variants in mouse. These *Dab1* variants have specific temporal expression profiles, with inclusion of exons 9b and 9c associated with early brain development, and exclusion of exons 9b and 9c associated with late brain development. Based on sequence prediction, all these identified transcripts encode Dab1 proteins that share the same N- and C-termini, but differ in the tyrosine-enriched region as well as a domain of unknown function. Importantly, by regulating tyrosine-coding exons (7 and 8) during development, alternative splicing controls the inclusion/exclusion of tyrosine residues critical for Dab1 activity, thus tightly regulating Dab1 function in a temporal manner. Based on our *in vitro* data, these Dab1 isoforms are differentially phosphorylated on tyrosine, and thus may respond differentially to Reelin stimulation *in vivo*. Intriguingly, we observe that increased expression of $Dab1^{555*}$ relative to Dab1 in 293T cells dramatically reduces the levels of Dab1, suggesting that $Dab1^{555*}$ may directly inhibit Dab1 function by reducing its levels. Since different tyrosine sites in Dab1 have been shown to mediate different downstream events in Reelin signaling (Sanada et al. 2004; Feng and Cooper 2009), it is likely that these alternatively-spliced Dab1 isoforms, with different tyrosine combinations, may regulate different aspects of the Reelin signal pathway. We propose that developmentally-regulated alternative splicing of *Dab1* in the brain provides a finely-tuned approach to modulate the activity of Reelin signaling and control neuronal positioning and synaptic circuitry.

The 11 alternatively-spliced Dab1 transcripts identified in this study were generated from individual splicing events such as alternative exon exclusion/inclusion (exons 7 or 8, and 9b/9c) and alternative usage of a 5' splice site in intron 9, as well as combinations of the above. If all possible combinations were used, the single *Dab1* gene could produce 16 Dab1 variants. The fact that we only detected 11 of the 16 possible combinations suggests that the remaining 5 variants may be present at low levels, not produced at the developmental stages examined, or not generated in this animal species. We did not detect either mouse Dab1^{217} and Dab1^{271} variants, both of which were previously identified by library screening (Howell et al. 1997a). It should be noted that the alternative exons included in Dab1^{217} and Dab1^{271} introduce in-frame premature termination codons, which likely trigger transcript degradation by nonsense-mediated mRNA decay (Lewis et al. 2003; Pan et al. 2006). Thus, these variants may be present at low levels. In addition, although an alternatively-spliced Dab1 transcript which excludes exons 8 and 9 was reported in zebrafish, we did not detect a similar variant in mouse (Costagli et al. 2006).

Our previous studies have demonstrated that the switch between ch*Dab1-E* and ch*Dab1-L* in chicken is mutually exclusive, i.e. the inclusion of exons 7 and 8 is accompanied by the exclusion of exon 9b and vice versa (Katyal and Godbout 2004). However, we have observed multiple murine Dab1 splice variants which either include exons 7/8 and exons 9b/9c or exclude exons 7/8 and exons 9b/9c, suggesting a higher diversity of Dab1 alternative splicing. The numerous alternative splicing patterns of Dab1 in mouse are likely a

consequence of the more complex splicing regulatory mechanisms in mammals (Blencowe 2006). Nova2 has been shown to bind YCAY clusters (Y indicates pyrimidine) upstream of exons 9b and 9c to suppress inclusion of exons 9b and 9c in *Dab1* (Yano et al. 2010); however, the splicing factors regulating exclusion of exons 7 and 8 are unknown. In this study, we show that alternative splicing of Nova1 correlates with inclusion of exons 7 and 8 in the brain. Therefore, it will be important to determine whether Nova1 regulates inclusion of exons 7 and 8 in neurons. We propose that different Nova proteins coordinately regulate alternative splicing of Dab1. For example, Nova2 may inhibit inclusion of exons 9b and 9c, whereas Nova1 may promote inclusion of exons 7 and 8.

In support of a role for Nova in regulating exons 7 and 8 inclusion, we have found a Nova binding element located downstream of exon 8 (Figure 4.8). According to Ule et al, a Nova element located downstream of the alternative exon usually enhances exon inclusion (Ule et al. 2006). Thus, the Nova element downstream of exon 8 in *Dab1* likely promotes exon 8 inclusion. However, the element that we have identified is ~3100 bp downstream of exon 8, in comparison to the ~300 bp downstream elements described by Ule et al (Ule et al. 2006). Whether such a remote element can affect exon inclusion needs to be further investigated. Other neuron-specific splicing factors, such as RNA binding proteins Feminizing gene on X (Fox) and the newly-identified neuronal serine-arginine protein (nSR) 100, may also be involved in the regulation of exons 7 and 8 inclusion in *Dab1* (Calarco et al. 2009; Lee et al. 2009; Yeo et al. 2009). Furthermore, despite the fact that no apparent difference in splicing activity was

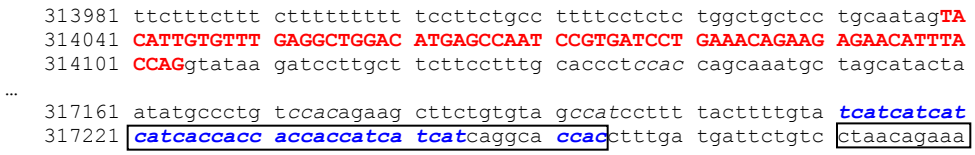

Figure 4.8 Nova binding elements located downstream of Dab1 exon 8. Sequences in exon 8 are shown in uppercase letters (red), whereas sequences in introns 7 and 8 are shown in lowercase letters. The Nova binding element (YCAY clusters, Y stands for pyrimidine) is indicated in blue and blocked (italicized). The numbers are directly derived from Genbank (Accession number: NC_000070).

observed between Nova1 and the alternatively-spliced Nova1 (which includes exon 4) in mediating the splicing of neurotransmitter receptor subunits GABA receptor $\gamma 2$ and glycine receptor $\alpha 2$ (Dredge et al. 2005), we cannot rule out the possibility that alternatively-spliced Nova1 isoforms may differentially regulate Dab1 splicing.

Recent studies have revealed that Nova2-mediated timely switch from exons 9b and 9c inclusion (Dab1^{555*}) to exclusion (Dab1) is important in regulating neuronal positioning in the brain (Yano et al. 2010). Increased expression of Dab1^{555*} in *Nova2*$^{-/-}$ mice leads to aberrant neuronal migration of late-born neurons, whereas ectopic expression of Dab1 in *Nova2*$^{-/-}$ mice rescues the migration defects, suggesting that the balance between Dab1^{555*} and Dab1 is critical for accurate neuronal positioning. By co-transfecting constructs expressing different Dab1 isoforms along with Dab1 (2:1; Dab1 variant:Dab1), we have observed reduced levels of both Dab1^{555*} and Dab1 in cells transfected with Dab1^{555*} and Dab1, suggesting that increased concentration of Dab1^{555*} relative to Dab1 may directly inhibit Dab1 function by reducing Dab1 levels.

Both transcriptional and post-transcriptional mechanisms may be involved in decreasing the levels of Dab1 and Dab1^{555*}. Previous studies have shown that tyrosine-phosphorylated Dab1 recruits SH2 domain-containing E3 ligase complexes and targets itself for degradation through the ubiquitination and proteasome pathway (Arnaud et al. 2003a; Bock et al. 2004; Feng et al. 2007). As both Dab1 and Dab1^{555*} are tyrosine-phosphorylated, it is possible that both isoforms can be ubiquitinated and undergo proteasome degradation. However,

whether increased ratio of Dab1^{555*} relative to Dab1 enhances ubiquitination and proteasome degradation needs to be determined. In addition, although we did not observe an inhibitory effect upon co-expression of Dab1-E with Dab1 in transfection assays, we cannot exclude the possibility that endogenous Dab1-E may compete with Dab1 to bind to the Reelin receptors, thus limiting the access of Dab1 to Reelin receptors. Since chDab1-E is incapable of transmitting the Reelin signal (Gao et al. 2010), we propose that murine Dab1-E is also unable to relay the Reelin signal and may play a dominant-negative role in Reelin-Dab1 signaling.

It is noteworthy that Nova2-regulated exclusion of exons 9b and 9c peaks at E14.5-E16.5 in mouse cortex (Yano et al. 2010), a critical time for the migration of late-born cortical neurons. The fact that *Nova2*$^{-/-}$ mice only have migration defects in late-born cortical neurons suggests an important role for exon 9b/9c-containing isoforms in the migration of early-born neurons. Examining the cellular distribution of these Dab1 isoforms, in particular exons 9b/9c-containing isoforms, would be important to address this question. We are currently carrying out *in situ* hybridization to examine the spatial distribution of different Dab1 isoforms in the brain. Another possibility is that different Dab1 isoforms may interact with different Reelin receptors that play divergent roles during cortical development. For example, exons 9b/9c-containing Dab1 isoforms may preferentially associate with VLDLR, which mediates a “stop signal” to prevent migrating neurons from invading into the marginal zone at early developmental stages. In contrast, exons 9b/9c-excluding Dab1 isoforms may

interact with ApoER2 which is involved in the migration of late-born neurons at late stages of development (Hack et al. 2007).

Recent studies have found that approximately 92-94% of human genes are alternatively spliced (Wang et al. 2008). Alternatively spliced variants of numerous genes, including the Reelin receptor *Apoer2*, Down syndrome cell adhesion molecule *(Dscam)*, presynaptic receptors neurexins and the axon guidance receptor *ROBO3* are involved in multiple processes during development, such as synaptic transmission, synaptogenesis, neurite self-avoidance and commissural axon midline crossing (Sugita et al. 1999; Schmucker et al. 2000; Beffert et al. 2005; Chen et al. 2008; Hattori et al. 2009). The identification of multiple Dab1 alternatively-spliced isoforms, with distinct temporal expression and differential phosphorylation patterns, reveals an elegant mechanism to fine-tune Dab1 activity and Reelin signaling. We propose that alternative splicing of Dab1 provides a tight temporal and spatial control of complex processes such as neuronal migration and synaptic plasticity during development.

4.5 REFERENCES

Arnaud L, Ballif BA, Cooper JA. 2003a. Regulation of protein tyrosine kinase signaling by substrate degradation during brain development. *Mol Cell Biol* **23**: 9293-9302.

Arnaud L, Ballif BA, Forster E, Cooper JA. 2003b. Fyn tyrosine kinase is a critical regulator of disabled-1 during brain development. *Curr Biol* **13**: 9-17.

Ballif BA, Arnaud L, Arthur WT, Guris D, Imamoto A, Cooper JA. 2004. Activation of a Dab1/CrkL/C3G/Rap1 pathway in Reelin-stimulated neurons. *Curr Biol* **14**: 606-610.

Bar I, Tissir F, Lambert de Rouvroit C, De Backer O, Goffinet AM. 2003. The gene encoding disabled-1 (DAB1), the intracellular adaptor of the Reelin pathway, reveals unusual complexity in human and mouse. *J Biol Chem* **278**: 5802-5812.

Beffert U, Weeber EJ, Durudas A, Qiu S, Masiulis I, Sweatt JD, Li WP, Adelmann G, Frotscher M, Hammer RE et al. 2005. Modulation of synaptic plasticity and memory by Reelin involves differential splicing of the lipoprotein receptor Apoer2. *Neuron* **47**: 567-579.

Blencowe BJ. 2006. Alternative splicing: new insights from global analyses. *Cell* **126**: 37-47.

Bock HH, Herz J. 2003. Reelin activates SRC family tyrosine kinases in neurons. *Curr Biol* **13**: 18-26.

Bock HH, Jossin Y, May P, Bergner O, Herz J. 2004. Apolipoprotein E receptors are required for reelin-induced proteasomal degradation of the neuronal adaptor protein Disabled-1. *J Biol Chem* **279**: 33471-33479.

Calarco JA, Superina S, O'Hanlon D, Gabut M, Raj B, Pan Q, Skalska U, Clarke L, Gelinas D, van der Kooy D et al. 2009. Regulation of vertebrate nervous system alternative splicing and development by an SR-related protein. *Cell* **138**: 898-910.

Chen K, Ochalski PG, Tran TS, Sahir N, Schubert M, Pramatarova A, Howell BW. 2004. Interaction between Dab1 and CrkII is promoted by Reelin signaling. *J Cell Sci* **117**: 4527-4536.

Chen Z, Gore BB, Long H, Ma L, Tessier-Lavigne M. 2008. Alternative splicing of the Robo3 axon guidance receptor governs the midline switch from attraction to repulsion. *Neuron* **58**: 325-332.

Costagli A, Felice B, Guffanti A, Wilson SW, Mione M. 2006. Identification of alternatively spliced dab1 isoforms in zebrafish. *Dev Genes Evol* **216**: 291-

299.

D'Arcangelo G, Miao GG, Chen SC, Soares HD, Morgan JI, Curran T. 1995. A protein related to extracellular matrix proteins deleted in the mouse mutant reeler. *Nature* **374**: 719-723.

Dredge BK, Stefani G, Engelhard CC, Darnell RB. 2005. Nova autoregulation reveals dual functions in neuronal splicing. *Embo J* **24**: 1608-1620.

Feng L, Allen NS, Simo S, Cooper JA. 2007. Cullin 5 regulates Dab1 protein levels and neuron positioning during cortical development. *Genes Dev* **21**: 2717-2730.

Feng L, Cooper JA. 2009. Dual functions of Dab1 during brain development. *Mol Cell Biol* **29**: 324-332.

Gao Z, Godbout R. 2010. Serine phosphorylation regulates disabled-1 early isoform turnover independently of Reelin. *Cell Signal*.

Gao Z, Monckton EA, Glubrecht DD, Logan C, Godbout R. 2010. The early isoform of disabled-1 functions independently of Reelin-mediated tyrosine phosphorylation in chick retina. *Mol Cell Biol* **30**: 4339-4353.

Hack I, Hellwig S, Junghans D, Brunne B, Bock HH, Zhao S, Frotscher M. 2007. Divergent roles of ApoER2 and Vldlr in the migration of cortical neurons. *Development* **134**: 3883-3891.

Hattori D, Chen Y, Matthews BJ, Salwinski L, Sabatti C, Grueber WB, Zipursky SL. 2009. Robust discrimination between self and non-self neurites requires thousands of Dscam1 isoforms. *Nature* **461**: 644-648.

Herz J, Chen Y. 2006. Reelin, lipoprotein receptors and synaptic plasticity. *Nat Rev Neurosci* **7**: 850-859.

Hiesberger T, Trommsdorff M, Howell BW, Goffinet A, Mumby MC, Cooper JA, Herz J. 1999. Direct binding of Reelin to VLDL receptor and ApoE receptor 2 induces tyrosine phosphorylation of disabled-1 and modulates tau phosphorylation. *Neuron* **24**: 481-489.

Howell BW, Gertler FB, Cooper JA. 1997a. Mouse disabled (mDab1): a Src binding protein implicated in neuronal development. *Embo J* **16**: 121-132.

Howell BW, Hawkes R, Soriano P, Cooper JA. 1997b. Neuronal position in the developing brain is regulated by mouse disabled-1. *Nature* **389**: 733-737.

Howell BW, Herrick TM, Cooper JA. 1999a. Reelin-induced tryosine phosphorylation of disabled 1 during neuronal positioning. *Genes Dev* **13**: 643-648.

Howell BW, Herrick TM, Hildebrand JD, Zhang Y, Cooper JA. 2000. Dab1 tyrosine phosphorylation sites relay positional signals during mouse brain development. *Curr Biol* **10**: 877-885.

Howell BW, Lanier LM, Frank R, Gertler FB, Cooper JA. 1999b. The disabled 1 phosphotyrosine-binding domain binds to the internalization signals of transmembrane glycoproteins and to phospholipids. *Mol Cell Biol* **19**: 5179-5188.

Huang Y, Magdaleno S, Hopkins R, Slaughter C, Curran T, Keshvara L. 2004. Tyrosine phosphorylated Disabled 1 recruits Crk family adapter proteins. *Biochem Biophys Res Commun* **318**: 204-212.

Jelen N, Ule J, Zivin M, Darnell RB. 2007. Evolution of Nova-dependent splicing regulation in the brain. *PLoS Genet* **3**: 1838-1847.

Jones-Villeneuve EM, Rudnicki MA, Harris JF, McBurney MW. 1983. Retinoic acid-induced neural differentiation of embryonal carcinoma cells. *Mol Cell Biol* **3**: 2271-2279.

Katyal S, Gao Z, Monckton E, Glubrecht D, Godbout R. 2007. Hierarchical disabled-1 tyrosine phosphorylation in Src family kinase activation and neurite formation. *J Mol Biol* **368**: 349-364.

Katyal S, Godbout R. 2004. Alternative splicing modulates Disabled-1 (Dab1) function in the developing chick retina. *Embo J* **23**: 1878-1888.

Keshvara L, Benhayon D, Magdaleno S, Curran T. 2001. Identification of reelin-induced sites of tyrosyl phosphorylation on disabled 1. *J Biol Chem* **276**: 16008-16014.

Lee JA, Tang ZZ, Black DL. 2009. An inducible change in Fox-1/A2BP1 splicing modulates the alternative splicing of downstream neuronal target exons. *Genes Dev* **23**: 2284-2293.

Lewis BP, Green RE, Brenner SE. 2003. Evidence for the widespread coupling of alternative splicing and nonsense-mediated mRNA decay in humans. *Proc Natl Acad Sci U S A* **100**: 189-192.

Niu S, Renfro A, Quattrocchi CC, Sheldon M, D'Arcangelo G. 2004. Reelin promotes hippocampal dendrite development through the VLDLR/ApoER2-Dab1 pathway. *Neuron* **41**: 71-84.

Pan Q, Saltzman AL, Kim YK, Misquitta C, Shai O, Maquat LE, Frey BJ, Blencowe BJ. 2006. Quantitative microarray profiling provides evidence against widespread coupling of alternative splicing with nonsense-mediated mRNA decay to control gene expression. *Genes Dev* **20**: 153-158.

Rice DS, Curran T. 2001. Role of the reelin signaling pathway in central nervous system development. *Annu Rev Neurosci* **24**: 1005-1039.

Sanada K, Gupta A, Tsai LH. 2004. Disabled-1-regulated adhesion of migrating neurons to radial glial fiber contributes to neuronal positioning during early corticogenesis. *Neuron* **42**: 197-211.

Schmucker D, Clemens JC, Shu H, Worby CA, Xiao J, Muda M, Dixon JE, Zipursky SL. 2000. Drosophila Dscam is an axon guidance receptor exhibiting extraordinary molecular diversity. *Cell* **101**: 671-684.

Songyang Z, Shoelson SE, Chaudhuri M, Gish G, Pawson T, Haser WG, King F, Roberts T, Ratnofsky S, Lechleider RJ et al. 1993. SH2 domains recognize specific phosphopeptide sequences. *Cell* **72**: 767-778.

Sugita S, Khvochtev M, Sudhof TC. 1999. Neurexins are functional alpha-latrotoxin receptors. *Neuron* **22**: 489-496.

Trommsdorff M, Borg JP, Margolis B, Herz J. 1998. Interaction of cytosolic adaptor proteins with neuronal apolipoprotein E receptors and the amyloid precursor protein. *J Biol Chem* **273**: 33556-33560.

Trommsdorff M, Gotthardt M, Hiesberger T, Shelton J, Stockinger W, Nimpf J, Hammer RE, Richardson JA, Herz J. 1999. Reeler/Disabled-like disruption of neuronal migration in knockout mice lacking the VLDL receptor and ApoE receptor 2. *Cell* **97**: 689-701.

Ule J, Stefani G, Mele A, Ruggiu M, Wang X, Taneri B, Gaasterland T, Blencowe BJ, Darnell RB. 2006. An RNA map predicting Nova-dependent splicing regulation. *Nature* **444**: 580-586.

Ule J, Ule A, Spencer J, Williams A, Hu JS, Cline M, Wang H, Clark T, Fraser C, Ruggiu M et al. 2005. Nova regulates brain-specific splicing to shape the synapse. *Nat Genet* **37**: 844-852.

Wang ET, Sandberg R, Luo S, Khrebtukova I, Zhang L, Mayr C, Kingsmore SF, Schroth GP, Burge CB. 2008. Alternative isoform regulation in human tissue transcriptomes. *Nature* **456**: 470-476.

Yano M, Hayakawa-Yano Y, Mele A, Darnell RB. 2010. Nova2 regulates neuronal migration through an RNA switch in disabled-1 signaling. *Neuron* **66**: 848-858.

Yeo GW, Coufal NG, Liang TY, Peng GE, Fu XD, Gage FH. 2009. An RNA code for the FOX2 splicing regulator revealed by mapping RNA-protein interactions in stem cells. *Nat Struct Mol Biol* **16**: 130-137.

CHAPTER 5: DISCUSSION AND FUTURE DIRECTIONS

5.1 DISCUSSION

5.1.1 Cortical neuronal migration and Reelin-Dab1 signaling

Neuronal migration is a dynamic process during which neurons frequently change their morphology, speed, and polarity (Hatten 1999; Nadarajah et al. 2001; Nadarajah and Parnavelas 2002). Time-lapse analysis has revealed that cortical neurons adopt two main modes of cell migration: radial glia-independent somal translocation and radial glia-guided locomotion (Nadarajah and Parnavelas 2002). Translocating cells extend long leading processes attached to the pial surface (PS) and move continuously at a relatively fast speed. In contrast, locomoting cells have shorter processes and move in a slower saltatory (jerky) manner. At early stages of development (~E10.5-12.5 in mouse), somal translocation is the prevalent mode of cell migration and underlies subplate formation and layer VI migration in the cerebral cortex. Locomotion appears to be the main mode of cell migration for late-generated neurons and underlies the "inside-out" lamination characteristic of later stages of development (~E13.5 and onwards in mouse) (Nadarajah et al. 2001; Hatanaka et al. 2004; Ayala et al. 2007). Intriguingly, locomoting neurons switch to the somal translocation mode once their leading processes reach the PS during the final phase of migration.

A large number of proteins, including Reelin, serine/threonine kinase Cdk5, the microtubule associated protein Lis1, and the actin depolymerizing protein n-cofilin, have been implicated in the regulation of neuronal migration (D'Arcangelo et al. 1995; Ohshima et al. 1999; Tsai et al. 2005; Bellenchi et al. 2007; Tsai et al. 2007). Among these regulators of migration, the Reelin signaling pathway has a

particularly well-established role in regulating neuronal migration and positioning. Reelin is expressed in Cajal-Retzius cells of the marginal zone (MZ), whereas its receptors and the intracellular adaptor Dab1 are expressed in migrating neurons and radial glia. Binding of Reelin to VLDLR and ApoER2 directs the radial migration of neurons, leading to the formation of neuronal layers in the cortex. As described in Section 1.1, mice deficient in Reelin signaling (*reeler*, *Dab1*$^{-/-}$ and *Vldlr*$^{-/-}$*Apoer2*$^{-/-}$) exhibit two types of neuronal migration defects: (i) failure of early-born neurons to split the preplate and form the subplate, and (ii) inability of late-born neurons to bypass their predecessors, causing inversion of neuronal layers in the cortical plate (Caviness 1973; Caviness 1982; Tissir and Goffinet 2003). Despite recent advances in our understanding of the molecular mechanisms of Reelin-Dab1 signaling in neuronal migration, how Reelin co-ordinates the intracellular signaling pathways and guides ordered migration of individual neurons at different migratory stages remains controversial.

Previous studies have primarily focused on the role of Reelin-Dab1 signaling in radia glia-guided migration. Reelin/Dab1 have been shown to promote detachment of neurons from radial glia and inhibit neuronal migration (Dulabon et al. 2000; Sanada et al. 2004). Recently, it has been proposed that Reelin regulates cortical lamination through a “detach and go” model. In this model, Reelin induces detachment of neurons from radial glia and stimulates translocation to the cell soma to the top of the cortical plate (Cooper 2008). For example, at early developmental stages, Reelin stimulates the translocation of layer VI cortical neurons, which allows them to bypass the subplate in a radial

glia-independent manner. In contrast, late-generated neurons initially use radial-glia dependent locomotion to move toward the cortical plate. Once their leading processes reach the Reelin-containing MZ, Reelin induces detachment from the radial glia and promotes their translocation so that they bypass their predecessors (Cooper 2008). This “detach and go” model can explain many aspects of the *Reeler* phenotype and the effects of Reelin signaling observed in *in utero* experiments as well as by time-lapse analysis of brain slice cultures (Nadarajah et al. 2001; Cooper 2008; Simo et al. 2010). It should be noted, however, that this model cannot explain why Reelin has different effects on different subpopulations of neurons at early and late developmental stages.

5.1.2 Dab1 alternative splicing regulates neuronal migration

A recent study indicates that Nova2-regulated Dab1 alternative splicing modulates neuronal migration at different developmental stages (Yano et al. 2010). The neuron-specific splicing factor Nova2 promotes a critical switch from Dab1^{555*} to Dab1 by excluding exons 9b and 9c. The exclusion of exons 9b and 9c parallels the prominent migration of late-generated neurons in the cerebral cortex, with peak activity at ~E14. Ablation of Nova2 leads to increased expression of Dab1^{555*} and decreased expression of Dab1 in *Nova2*$^{-/-}$ mice from E10.5-P1 in the cortex, the window of time during which there is extensive cortical neuronal migration. In contrast to *Dab1*$^{-/-}$ mice which show migration defects in both early- and late-born neurons, *Nova2*$^{-/-}$ mice only exhibit defects in late-born neuronal migration. This study supports a role for Dab1^{555*} and Dab1 in

the regulation of early- and late-born neuronal migration, respectively. Interestingly, the aberrant neuronal migration observed in *Nova2*$^{-/-}$ mice is very similar to that observed in *Apoer2*$^{-/-}$ mice (Hack et al. 2007), indicating a strong link between Dab1 and ApoER2 in regulating the migration of late-generated neurons.

We have identified multiple alternatively-spliced Dab1 variants in the developing mouse brain and retina. Consistent with previous studies, we have found that exclusion of exons 9b and 9c correlates with neural differentiation and neuronal migration in mouse brain. Most importantly, however, we have identified Dab1 isoforms with different combinations of tyrosines in the developing brain, as a result of exclusion/inclusion of tyrosine-coding exons 7 and 8. These isoforms are differentially tyrosine-phosphorylated when co-expressed with c-Src in 293T cells. As different tyrosine phosphorylation sites have been shown to be involved in different aspects of Reelin signaling (Sanada et al. 2004; Feng et al. 2007), we propose that alternative inclusion of exons 7, 8, 9b and 9c in Dab1, fine-tunes intracellular responses to Reelin signaling *in vivo* and tightly controls the migration of different populations of neurons at different developmental stages (Figure 5.1).

Three lines of evidence favor a role for Dab1 alternative splicing in the regulation of migration in different populations of neurons. First, our studies clearly show that chDab1-E and chDab1-L are expressed at early and late developmental stages of retinal development, respectively (Katyal and Godbout 2004). Consistent with our analysis in chick retina, murine Dab1 variants are also

expressed at different developmental stages, with exons 9b and 9c included at early developmental stages (~E10.5-14.5 in mouse), but excluded as development proceeds (Bar et al. 2003; Yano et al. 2010). Our RT-PCR analysis indicates a developmentally-correlated transition from exons 7/8 exclusion to inclusion at ~E10-12.5 in mouse brain (Figure 4.2). Together, these studies suggest that Dab1 variants excluding exons 7/8 and/or including exons 9b/9c are expressed at early developmental stages, whereas Dab1 variants including exons 7/8 and variants excluding exons 9b/9c are expressed at later developmental stages. We propose that different forms of Dab1 orchestrate the coordinated regulation of neuronal migration at different developmental stages.

Second, previous *in situ* hybridization analyses have suggested that exons 9b and 9c are expressed in proliferating progenitor cells in the ventricular zone (Bar et al. 2003), whereas Dab1 (excluding exons 9b and 9c) is primarily found in the neuronal cells of the cortical plate (Howell et al. 1997). In general agreement with this, our *in situ* hybridization and immunohistochemical analysis reveals predominant expression of chDab1-E in retinal progenitor cells, whereas chDab1-L is primarily found in differentiated retinal cells (Katyal and Godbout 2004; Gao et al. 2010). We speculate that, similar to chDab1-E, the murine counterpart of chDab1-E and other forms of Dab1 that exclude exons 7 and 8 are likely expressed in proliferating neural progenitor cells and early neuronal precursors. We further hypothesize that alternative splicing of Dab1 may be closely correlated with the laminar fates of cortical neurons, with early Dab1 isoforms expressed in early-born neurons (e.g. preplate and layer VI neurons),

and late Dab1 isoforms expressed in late-born neurons (e.g. layers V, IV, III and II neurons) (Figure 5.1). Thus, the differential cellular distribution of Dab1 isoforms may define the final positioning of cells in response to Reelin signaling.

Third, cells expressing different Dab1 isoforms may differentially respond to Reelin stimulation and activate different downstream signaling components. For example, cells expressing the murine Dab1-E isoform may not respond to Reelin stimulation, but may undergo ubiquitination-mediated proteasome degradation as revealed by our analysis of chDab1-E (Gao and Godbout 2010). On the other hand, cells expressing $Dab1^{555*}$ may recruit Crk adaptor proteins but evade ubiquitination-mediated proteasome degradation (Yano et al. 2010). Such a mechanism would allow different subpopulations of cells to respond differently to Reelin stimulation, thus tightly regulating neuronal migration in a spatio-temporal manner. Taken together, there is strong evidence for developmentally-regulated Dab1 alternative splicing playing a key role in orchestrating neuronal migration, detachment and lamination in the developing brain.

5.1.3 Coupling neurogenesis and migration by Dab1 alternative splicing

Recent studies support the idea that proper neuronal positioning is directly related to correct neurogenesis. Furthermore, proteins that regulate neuronal migration have also been found to regulate neurogenesis. For example, the microtubule associated protein Lis1, well known for its role in neuronal migration,

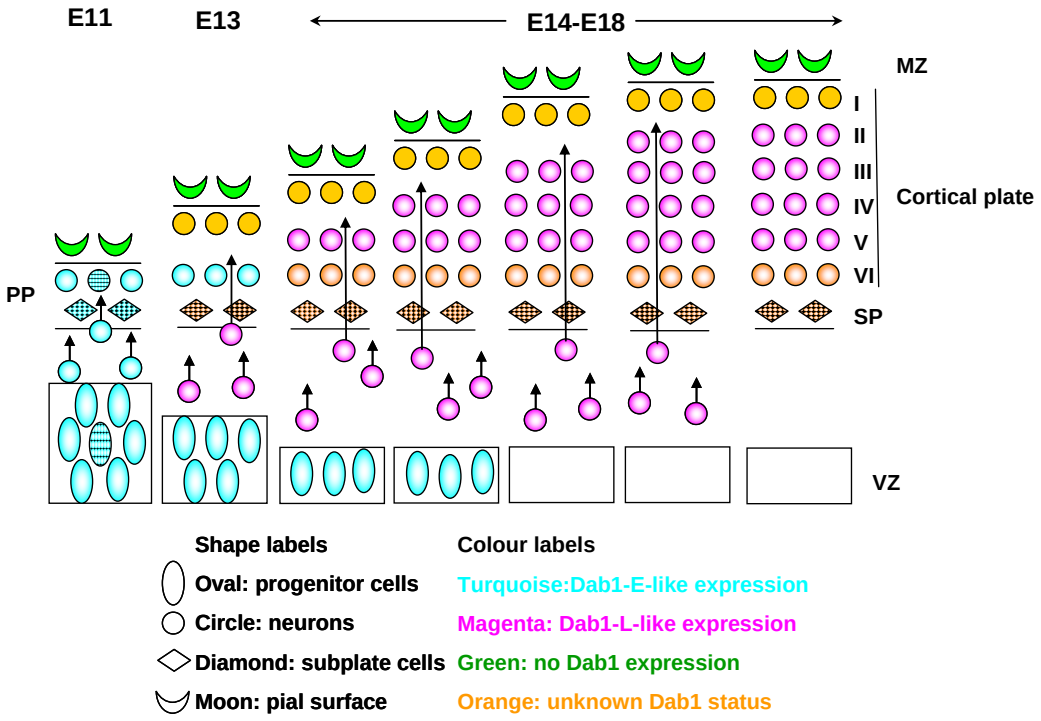

Figure 5.1 Model for alternative splicing of Dab1 in neurogenesis and cortical neuron migration. Dab1-E-like isoforms that contain exons 9b and 9c are expressed in proliferating cells (indicated with turquoise ovals) in the ventricular zone (VZ). Expression of Dab1-E like isoforms in the VZ maintains the progenitor pool and ensures proper neurogenesis. These isoforms are also transiently expressed in early-born neurons such as preplate (PP, indicated with turquoise circles and diamonds) and layer VI neurons at early migratory stages (E11-E13 in mouse). Layer VI neurons split the preplate into subplate (SP) and marginal zone (MZ). As development proceeds, alternative splicing results in the production of Dab1-L-like isoforms that contain exons 7/8 in late-born neurons (layers V, IV, III and II neurons, indicated with magenta circles). Cells that express Dab1-L-like isoforms respond to Reelin migration cues and move towards the Reelin-containing MZ, bypassing their predecessors to reach their final positions. Different subpopulations of neurons express specific Dab1 isoforms, which allow them to differentially respond to Reelin, resulting in their distribution into distinct layers. Alternative splicing of Dab1 may occur during migration so that the same population of migrating cells dynamically adjust their responsiveness to Reelin at different migratory stages, thus precisely controlling the final positioning of neurons in the cerebral cortex.

has been shown to regulate neurogenesis (Tsai et al. 2005). In addition, n-cofilin controls both neuronal migration and cell cycle progression. Loss of n-cofilin leads to impaired radial migration, premature cell cycle exit and increased neuronal differentiation in the cerebral cortex (Bellenchi et al. 2007). In agreement with a similar dual function for Dab1, we have shown that knockdown of chDab1-E in the chick retina reduces the number of retinal progenitor cells and promotes the differentiation of ganglion cells, which are early-born retinal cells. We have also found that chDab1-E is phosphorylated by Cdks that play important role in cell cycle control. At this time, we do not know whether Cdk-mediated chDab1-E phosphorylation directly regulates cell cycle progression of retinal progenitor cells.

Consistent with our studies in chick retina, Dab1 isoforms which include exons 9b and 9c are expressed in the ventricular zone in mouse cortex (Bar et al. 2003). However, in contrast to the chDab1-E/L isoforms found in chick, there are multiple forms of Dab1 in mouse, including Dab1-E, Dab1^{555*} and other variants which include exons 9b and/or 9c. It will be important to determine the identity and tyrosine-phosphorylation state of Dab1 isoforms expressed in the ventricular zone. We propose that progenitor cells in the ventricular zone express non-tyrosine phosphorylated Dab1 forms (e.g. Dab1-E), and may not respond to Reelin migration cues at early developmental stages. Instead, Dab1 isoforms expressed in proliferating cells are likely involved in maintaining the progenitor cell pool. As development proceeds, progenitor cells exit the cell cycle and generate neuronal precursors that are geared for migration. Neuronal cell

generation is likely accompanied by developmentally-regulated splicing events which result in the modulation of splice site selection at the junctions of exon/intron 7, 8, 9b and 9c. As a consequence, there is a switch from non-tyrosine-phosphorylated to tyrosine-phosphorylated Dab1 isoforms which are responsive to Reelin. Nova2 and other splicing factors may promote this timely switch which converts cells from a Reelin-irresponsive state to a Reelin responsive state, leading to correct migration and lamination in the brain.

5.1.4 Alternative splicing of Dab1 in the retina

It should be noted, however, that Dab1 alternative splicing does not show a clear-cut developmentally-regulated pattern in mouse retina. Dab1 is expressed in AII amacrine cells in mouse retina (Rice and Curran 2000; Rice et al. 2001). However, these studies were carried out using anti-Dab1-B3 antibody, which does not recognize exon 7-excluded Dab1 isoforms as demonstrated in our study (Gao et al. 2010). Thus, it is possible that Dab1 isoforms that exclude exon 7 are expressed in other cell types in the retina. As amacrine cells are highly diverse retinal cells, it is also possible that different Dab1 isoforms are expressed in different amacrine cell types.

In addition, the distinct distribution of both chDab1-L and mouse Dab1 (using the Dab1 B3 antibody for IHC analysis) in the sublaminae of the IPL, a layer that is rich in synapses, suggests a role for Dab1 in regulating retinal synaptic transmission and circuitry. Recent studies show that alternatively-spliced DSCAM isoforms direct the laminar-specific synaptic connections between RGC

and bipolar cells (Fuerst et al. 2008). As Reelin-Dab1 has been implicated in the modulation of retinal synaptic circuitry (Rice et al. 2001), it is likely that multiple alternatively-spliced Dab1 isoforms are directly involved in the laminar specification and modification of the ON-OFF synaptic pathway in the retina.

5.1.5 Dab1 splicing in disease

To date, no mutations in *Dab1* have been associated with human disease. Interestingly, naturally-occurring mutations in both *scrambler* and *yotari* mice disrupt the splicing of *Dab1*, leading to low or undetectable levels of Dab1 protein (Sheldon et al. 1997; Ware et al. 1997; Kojima et al. 2000). In *scrambler* mice, a segment (1651 bp) of an intracisternal A particle (IAP) retrotransposon sequence is inserted in the intron 4 of the *Dab1* gene (Sheldon et al. 1997; Ware et al. 1997; Bar et al. 2003) . The insertion likely activates a cryptic splice site in intron 4 which leads to aberrant splicing. As a consequence, an abnormally long *Dab1* transcript is produced (Sheldon et al. 1997; Ware et al. 1997; Bar et al. 2003). In *yotari* mice, replacement of normal *Dab1* genomic DNA from the junction of exon 5/intron 5 to exon 8 with an L1 fragment leads to exclusion of exons 5-8 from the Dab1 mRNA. No protein is produced from this altered *Dab1* transcript (Kojima et al. 2000). These results in mice indicate that mutations in human *Dab1* may also contribute to a disease state. Interestingly, the splicing factor Nova that suppresses the inclusion of Dab1 exons 9b and 9c is an autoantigen in patients with a paraneoplastic neurological syndrome called paraneoplastic opsoclonus myoclonus ataxia (POMA) (Buckanovich et al. 1993; Yang et al. 1998). POMA is

a neurological disorder accompanied by tumour formation (small cell lung cancer, ovarian cancer and neuroblastoma cells). The tumour cells express neuronal antigens that are believed to induce an antibody-mediated immune response that suppresses tumour growth, but destroys neurons (Albert and Darnell 2004). Strikingly, this neurological disorder is characterized by ataxia and tremors, which are also typical phenotypes observed in mice deficient in the Reelin pathway. It is not known whether aberrant Dab1 splicing occurs in patients with POMA and whether it contributes to the pathogenesis of the disease.

5.1.6 Regulation of chDab1-E function by serine/threonine phosphorylation

The importance of SFK-mediated Dab1 tyrosine phosphorylation in Dab1 signaling has been well-characterized (Howell et al. 2000; Feng and Cooper 2009). However, the role of Dab1 serine phosphorylation (S491) by Cdk5 remains unclear. We have shown that chDab1-E is exclusively phosphorylated on serine/threonine residues by Cdk2. As opposed to Cdk5 which is induced upon retinal differentiation, Cdk2 is expressed in proliferating retinal progenitor cells. Cdk2 mediates chDab1-E phosphorylation at S475, the counterpart of S491 (in chDab1-L), independent of Reelin. Serine phosphorylation destabilizes chDab1-E and primes this Dab1 isoform for ubiquitination and proteasome degradation. Thus, chDab1 levels appear to be regulated by both Reelin-dependent tyrosine phosphorylation and Reelin-independent serine phosphorylation.

Cdk2 is a critical regulator of cell cycle progression. The role of Cdk2-mediated chDab1-E phosphorylation in the process is unknown. In light of our prelimimary data indicating that chDab1-E phosphorylation and levels change in a cell cycle-dependent manner (data not shown), we propose that phosphorylation of chDab1-E is involved in the control of cell cycle progression in retinal progenitors. However, our attempts to directly address the role of chDab1-E in retinal cell proliferation versus differentiation by misexpressing chDab1-E and chDab1-E^{S475A} *in ovo* were not conclusive (data not shown).

Several reasons may explain the absence of a clear-cut phenotypic difference in the number of proliferating versus differentiated cells upon manipulation of Dab1-E levels in chick retinas. First, wild-type and mutant chDab1-E expression constructs were introduced into chick embryos at ~E1.5-E2, and retinas were analyzed at E5 and E7. At E5 and E7, endogenous chDab1-E is prominently expressed in the retina. In order for the misexpressed wild-type and mutant chDab1-E to induce changes in the developing retina, they would have to act in a dominant-negative manner. Second, the chDab1-E mutant expressed in the chick retina only contains a single substitution at S475. This single substitution may be insufficient to significantly affect Dab1-E function. Expression of a chDab1-E mutant with substitutions at all putative Cdk sites may be required to abolish Dab1-E function. Third, phosphorylation of serines/threonines by kinases other than Cdk may regulate chDab1-E function, which may have confounded the results of our misexpression analysis.

Furthermore, despite the fact that treatment with the PP1/PP2A

phosphatase inhibitor okadaic acid rapidly converts chDab1-E to a hyperphosphorylated state and reduces chDab1-E levels in retinal cultures, we cannot rule out the possibility that the changes in Dab1-E phosphorylation and levels may be an indirect consequence of PP1/PP2A inhibition. The role of PP1/PP2A in the dephosphorylation and function of chDab1-E could be addressed by co-immunoprecipitating, knocking-down or over-expressing PP1/PP2A in retinal cells. Finally, Cdks other than Cdk2, in particular, cyclin D-associated Cdks (Cdk4 and Cdk6), implicated in the regulation of neural precursor cell cycle control (Ferguson et al. 2000), may mediate chDab1-E phosphorylation and regulate its function *in vivo*.

5.1.7 Divergence between Reelin and Dab1 signaling

The phenotypic similarity observed in Dab1 mutants (*Dab1*$^{-/-}$*, scrambler and yotari*), *reeler* and *Vldlr/Apoer2*$^{-/-}$ mice, reveals a clear dependence of Dab1 function on Reelin and its receptors. However, our recent studies suggest that chDab1-E, expressed at early developmental stages, functions independently of the conventional Reelin signaling, indicating divergence between Reelin and Dab1 signaling. Previous studies have reported differences between *reeler* and *scrambler/Dab1*$^{-/-}$ mice; however, these differences have been largely overlooked (Goldowitz et al. 1997). It should be noted that Dab1 remains tyrosine phosphorylated, albeit at lower levels, in *reeler* mice (Howell et al. 1999), suggesting that other signal pathways/kinases may be involved in regulating its activity. In support of a role for Dab1 independent of Reelin, Simo et al. noted

that cortical neurons from *reeler* mice can migrate partially through the cortex, whereas *Disabled-1*$^{-/-}$ neurons fail to do so based on *in utero* analysis, suggesting that Dab1 regulates specific neuronal migratory properties in a Reelin-independent manner (Simo et al. 2010).

In addition, studies have shown that Reelin, but not VLDLR, ApoER2 or Dab1, is required for migration of some neurons in the brain (Cariboni et al. 2005). For example, Reelin plays a role in guiding the migration of gonadotropin-releasing hormone (GnRH) neurons, from the olfactory placode to the hypothalamic region in the basal forebrain at late embryonic stages. Reelin is expressed along the migration route. Interestingly, ApoER2 is only expressed in a small subset (5%) of GnRH neurons, whereas Dab1 is not expressed in GnRH neurons (Cariboni et al. 2005). Analysis of *reeler* mice has revealed reduced GnRH neurons in the hypothalamus; however, the number and distribution of GnRH neurons appear to be unaffected in *Vldlr*$^{-/-}$*Apoer2*$^{-/-}$ and *Disabled-1*$^{-/-}$ mice (Cariboni et al. 2005), suggesting that migration of GnRH neurons is not mediated by the conventional Reelin-Dab1 signal pathway.

A careful re-evaluation of phenotypes unrelated to neuronal migration, such as neurogenesis, dendrite development and synapse formation in *reeler* and *Disabled-1*$^{-/-}$ mice, may reveal additional differences between these mutants. Moreover, as Reelin-responsive Dab1 isoforms are primarily expressed in neurons, it will be important to examine whether phenotypic differences between *reeler* and *Disabled-1*$^{-/-}$ mice exist in non-neuronal tissues, such as liver, spleen and other organs. These analyses may reveal important roles for Reelin-

independent Dab1 isoforms during development.

5.2 FUTURE DIRECTIONS

5.2.1 Signaling-regulated Dab1 alternative splicing

We have previously shown that cultured chick retinal cells have the ability to naturally undergo transition from Dab1-E to Dab1-L (Katyal et al. 2007). In an attempt to identify potential upstream signaling events that regulate Dab1 splicing, we treated retinal cultures with inhibitors to block different signaling pathways. We have found that inhibition of γ-secretase suppresses the natural transition from Dab1-E to Dab1-L in chick retinal cultures, suggesting a potential role for γ-secretase-induced cleavage in the modulation of Dab1 alternative splicing. Interestingly, two important substrates of γ-secretase, Notch and APP, have both been shown to interact with Dab1. Further investigations will be required to determine whether Notch and/or APP signaling directly or indirectly regulate Dab1 alternative splicing. Future experiments using pharmaceutical reagents or shRNAs that specifically target Notch or APP signaling would be helpful to address this question.

5.2.2 Identification of cis-splicing elements and trans-splicing regulators in Dab1 alternative splicing

Alternative exons are often regulated by coordinated interactions between trans-regulator splicing factors and cis-acting elements in a cell/tissue-specific manner. Minigene assays are commonly used to identify specific cis-acting

elements that control usage of alternative exons (Cooper 2005). Once the cis-acting elements are defined, the minigene assay can then be used to identify potential trans-regulatory factors bound to these elements.

Our recent data have suggested correlation between Nova (both Nova1 and Nova2) and inclusion of exons 7 and 8 in Dab1 during development. A putative Nova binding element is located downstream of exon 8. To examine whether Nova regulates inclusion of Dab1 exons 7 and 8, we can knockdown the expression of both Nova1 and Nova2 and determine whether inclusion of Dab1 exons 7 and 8 is affected. This experiment would be carried out in P19 teratocarcinoma cell line, as Nova is expressed in P19 cells induced to differentiate along the neuronal cell lineage (Shinozaki et al. 1999). We could also carry out minigene analysis to identify the elements required for Dab1 exons 7/8 inclusion/exclusion. To carry out this analysis, we will generate a PCR fragment encompassing 500 bp upstream of exon 7 to 3100 bp downstream of exon 8 (the putative Nova binding element is located 3100 bp downstream of exon 8). This DNA fragment will be inserted into a minigene reporter plasmid (pRHC-Glo) which contains two exons from the globin gene and essential splicing elements adjacent to these two exons (Cooper 2005). This construct will be transfected into P19 cells. RNA will be isolated from transfected cells and analyzed by RT-PCR using primers that span the alternative exons 7 and 8. If we find that the inserted fragment is required for inclusion of exons 7 and 8, we will narrow down the region by generating mutants with truncations or deletions in the intronic region. Should we: (i) find that Nova depletion leads to reduced Dab1

exon 7/8 inclusion and (ii) identify elements within or adjacent to the putative Nova elements that are required for exon 7/8 inclusion, we will mutate the elements and carry out transfection and RT-PCR analysis as described above. Should we find no correlation between Nova knockdown and Dab1 splicing, we will search for consensus binding sites for neuron-specific splicing factors such as Fox and poly-pyrimidine tract binding protein. Once consensus binding sites are identified, we will assess whether altering the levels of appropriate splicing factors can affect Dab1 exon inclusion.

5.2.3 Structural analysis of exons 9b and 9c encoded region

The identification of multiple alternatively-spliced Dab1 variants in mouse reveals a high diversity of Dab1 splicing events. Of particular interest, alternatively splicing events described to date appear to specifically target two regions of Dab1: the tyrosine-enriched region found in exons 7 and 8, and a region encoded by exons 9b and 9c with unknown function. Given the importance of tyrosine phosphorylation sites in Dab1 function, changes in tyrosine residues resulting from alternative splicing may be critical for the tightly-regulated activity of Dab1. Although the 33 aa encoded by exons 9b and 9c have no homology to any known protein motifs, Yano et al. have suggested that in-frame insertion of this 33 aa region has an inhibitory effect on Dab1 function (Yano et al. 2010). Our c-Src/Dab1 mutant co-transfection experiments in 293T cells also support a role for the 33 aa region in reducing Dab1 activity. Whether insertion of 33 aa in Dab1 causes conformational changes that disrupt its

function is currently unknown. Crystallography analysis may help to unravel the role of the 33 aa insertion region in Dab1.

5.2.4 Functional characterization of Dab1 isoforms in vivo

An ideal and effective way to study the function of alternatively-spliced Dab1 isoforms during development would be to generate transgenic mice in a *Dab1*$^{-/-}$ background (*Dab1*$^{-/-}$ mice are available from Jackson Laboratory). Comparing phenotypes in mice that express different Dab1 isoforms in a Dab1 null background would help to establish a physiological role for individual Dab1 isoforms during neurodevelopment. Time-lapse microscopy analysis could be used to track the migratory behaviour of cortical neurons in brain slice cultures derived from wild-type, mutant and transgenic mice expressing different Dab1 isoforms. Specific aspects of migration could be studied, such as speed, polarity, morphology.

Given the complex procedures related to transgenic mice generation, a relatively simple and quick way to address the role of Dab1 isoforms would be by *in utero* electroporation of constructs that express different Dab1 isoforms into *Dab1*$^{-/-}$ or wild-type mice. By electroporating wild-type Dab1, Dab1 degradation-resistant mutant and Dab1^{555*} expression constructs into wild-type, *Dab1*$^{-/-}$ or Dab1 knockdown mouse cortex, Yano et al. (2010) and Simo et al. (2010) have successfully characterized the function of Dab1^{555*} and Dab1 mutants in the developing cortex (Simo et al. 2010; Yano et al. 2010)Again, time-lapse microscopy analysis could be used to track the migratory property of

electroporated cells and determine how different aspects of migration are affected by different Dab1 isoforms.

5.2.5 Role of Dab1 alternative splicing in P19 cell proliferation and differentiation

We have found that Dab1 is alternatively-spliced during the course of P19 cell differentiation along the neural cell lineage, with increased exclusion of exons 9b and 9c and inclusion of exons 7 and 8 as cells differentiate. Reelin-Dab1 signaling has been shown to regulate cell differentiation by promoting dendritogenesis and neurite outgrowth (Niu et al. 2004; Katyal et al. 2007). Our studies have demonstrated a role for chDab1-E in regulating the proliferation of progenitor cells in the developing chick retina. Whether Dab1 splicing produces Dab1 isoforms that are specifically involved in cell proliferation and differentiation is not known. This question can be addressed using the P19 terotocarcinoma cell line.

In the first series of experiments, P19 cells will be induced to undergo neural cell differentiation in the presence of low concentrations of RA as described in Chapter 4. Constructs designed to ubiquitously express early Dab1 isoforms such as those that include exons 9b and 9c but exclude exons 7/8 will be introduced into RA-treated P19 cells in an attempt to reverse the normal splicing transition pattern. Percentages of P19 cells that have differentiated into the neuronal and glia cell lineages will be assessed and quantified by staining with neuronal and glial-specific markers. Should altered Dab1 levels change P19

cell differentiation, knockdown experiments that specifically target Dab1 exons 9b and 9c or exons 7 and 8 will be carried out in P19 cells to confirm the observations.

Next, we will examine the role of Nova-mediated Dab1 splicing in P19 cell proliferation and differentiation using lentiviral Nova shRNAs and scrambled shRNAs. Alterations in Dab1 splicing patterns will be determined by RT-PCR analysis, and cell proliferation and differentiation of P19 cells assessed by BrdU incorporation and approaches described above. Should Nova-knockdown alter the relative percentage of cell proliferation versus cell differentiation, we will examine whether expression of late Dab1 isoforms (those that exclude exons 9b and 9c but include exons 7 and 8) can rescue the phenotype. These experiments will tell us whether Dab1 alternative splicing couples cell proliferation and differentiation in P19 cells.

5.3 SIGNIFICANCE

Our analysis of alternatively-spliced chDab1 isoforms in the developing chick retina has revealed under-appreciated aspects of Reelin signaling by demonstrating a role for chDab1-E that is independent of Reelin-induced tyrosine phosphorylation. ChDab1-E phosphorylation by Cdk presents a strong link between the early isoform of chDab1 and the regulation of cell cycle progression and neurogenesis. Our observation that knockdown of Dab1-E in the developing chick retina affects cell proliferation and differentiation provides strong support for a novel role for Dab1 in neurogenesis. The high diversity of Dab1 alternative splicing in mouse suggests the need for a finely-tuned mechanism for the

modulation of both Reelin-independent and Reelin-dependent signaling events in the developing CNS. Together, our studies shed light into the complexity of Dab1 functions in the developing CNS and point to new avenues of research to better understand the complex processes of neurogenesis, neuronal migration and synaptic circuitry.

5.4 REFERENCES

Albert ML, Darnell RB. 2004. Paraneoplastic neurological degenerations: keys to tumour immunity. *Nat Rev Cancer* **4**: 36-44.

Ayala R, Shu T, Tsai LH. 2007. Trekking across the brain: the journey of neuronal migration. *Cell* **128**: 29-43.

Bar I, Tissir F, Lambert de Rouvroit C, De Backer O, Goffinet AM. 2003. The gene encoding disabled-1 (DAB1), the intracellular adaptor of the Reelin pathway, reveals unusual complexity in human and mouse. *J Biol Chem* **278**: 5802-5812.

Bellenchi GC, Gurniak CB, Perlas E, Middei S, Ammassari-Teule M, Witke W. 2007. N-cofilin is associated with neuronal migration disorders and cell cycle control in the cerebral cortex. *Genes Dev* **21**: 2347-2357.

Buckanovich RJ, Posner JB, Darnell RB. 1993. Nova, the paraneoplastic Ri antigen, is homologous to an RNA-binding protein and is specifically expressed in the developing motor system. *Neuron* **11**: 657-672.

Cariboni A, Rakic S, Liapi A, Maggi R, Goffinet A, Parnavelas JG. 2005. Reelin provides an inhibitory signal in the migration of gonadotropin-releasing hormone neurons. *Development* **132**: 4709-4718.

Caviness VS, Jr. 1973. Time of neuron origin in the hippocampus and dentate gyrus of normal and reeler mutant mice: an autoradiographic analysis. *J Comp Neurol* **151**: 113-120.

Caviness, V. S., Jr. 1982. Neocortical histogenesis in normal and reeler mice: a developmental study based upon [3H]thymidine autoradiography. *Brain Res* **256**: 293-302.

Cooper JA. 2008. A mechanism for inside-out lamination in the neocortex. *Trends Neurosci* **31**: 113-119.

Cooper TA. 2005. Use of minigene systems to dissect alternative splicing elements. *Methods* **37**: 331-340.

D'Arcangelo G, Miao GG, Chen SC, Soares HD, Morgan JI, Curran T. 1995. A protein related to extracellular matrix proteins deleted in the mouse mutant reeler. *Nature* **374**: 719-723.

Dulabon L, Olson EC, Taglienti MG, Eisenhuth S, McGrath B, Walsh CA, Kreidberg JA, Anton ES. 2000. Reelin binds alpha3beta1 integrin and inhibits neuronal migration. *Neuron* **27**: 33-44.

Feng L, Allen NS, Simo S, Cooper JA. 2007. Cullin 5 regulates Dab1 protein

levels and neuron positioning during cortical development. *Genes Dev* **21**: 2717-2730.

Feng L, Cooper JA. 2009. Dual functions of Dab1 during brain development. *Mol Cell Biol* **29**: 324-332.

Ferguson KL, Callaghan SM, O'Hare MJ, Park DS, Slack RS. 2000. The Rb-CDK4/6 signaling pathway is critical in neural precursor cell cycle regulation. *J Biol Chem* **275**: 33593-33600.

Fuerst PG, Koizumi A, Masland RH, Burgess RW. 2008. Neurite arborization and mosaic spacing in the mouse retina require DSCAM. *Nature* **451**: 470-474.

Gao Z, Godbout R. 2010. Serine phosphorylation regulates disabled-1 early isoform turnover independently of Reelin. *Cell Signal*.

Gao Z, Monckton EA, Glubrecht DD, Logan C, Godbout R. 2010. The early isoform of disabled-1 functions independently of Reelin-mediated tyrosine phosphorylation in chick retina. *Mol Cell Biol* **30**: 4339-4353.

Goldowitz D, Cushing RC, Laywell E, D'Arcangelo G, Sheldon M, Sweet HO, Davisson M, Steindler D, Curran T. 1997. Cerebellar disorganization characteristic of reeler in scrambler mutant mice despite presence of reelin. *J Neurosci* **17**: 8767-8777.

Hack I, Hellwig S, Junghans D, Brunne B, Bock HH, Zhao S, Frotscher M. 2007. Divergent roles of ApoER2 and Vldlr in the migration of cortical neurons. *Development* **134**: 3883-3891.

Hatanaka Y, Hisanaga S, Heizmann CW, Murakami F. 2004. Distinct migratory behavior of early- and late-born neurons derived from the cortical ventricular zone. *J Comp Neurol* **479**: 1-14.

Hatten ME. 1999. Central nervous system neuronal migration. *Annu Rev Neurosci* **22**: 511-539.

Howell BW, Hawkes R, Soriano P, Cooper JA. 1997. Neuronal position in the developing brain is regulated by mouse disabled-1. *Nature* **389**: 733-737.

Howell BW, Herrick TM, Cooper JA. 1999. Reelin-induced tryosine phosphorylation of disabled 1 during neuronal positioning. *Genes Dev* **13**: 643-648.

Howell BW, Herrick TM, Hildebrand JD, Zhang Y, Cooper JA. 2000. Dab1 tyrosine phosphorylation sites relay positional signals during mouse brain development. *Curr Biol* **10**: 877-885.

Katyal S, Gao Z, Monckton E, Glubrecht D, Godbout R. 2007. Hierarchical

disabled-1 tyrosine phosphorylation in Src family kinase activation and neurite formation. *J Mol Biol* **368**: 349-364.

Katyal S, Godbout R. 2004. Alternative splicing modulates Disabled-1 (Dab1) function in the developing chick retina. *Embo J* **23**: 1878-1888.

Kojima T, Nakajima K, Mikoshiba K. 2000. The disabled 1 gene is disrupted by a replacement with L1 fragment in yotari mice. *Brain Res Mol Brain Res* **75**: 121-127.

Nadarajah B, Brunstrom JE, Grutzendler J, Wong RO, Pearlman AL. 2001. Two modes of radial migration in early development of the cerebral cortex. *Nat Neurosci* **4**: 143-150.

Nadarajah B, Parnavelas JG. 2002. Modes of neuronal migration in the developing cerebral cortex. *Nat Rev Neurosci* **3**: 423-432.

Niu S, Renfro A, Quattrocchi CC, Sheldon M, D'Arcangelo G. 2004. Reelin promotes hippocampal dendrite development through the VLDLR/ApoER2-Dab1 pathway. *Neuron* **41**: 71-84.

Ohshima T, Gilmore EC, Longenecker G, Jacobowitz DM, Brady RO, Herrup K, Kulkarni AB. 1999. Migration defects of cdk5(-/-) neurons in the developing cerebellum is cell autonomous. *J Neurosci* **19**: 6017-6026.

Rice DS, Curran T. 2000. Disabled-1 is expressed in type AII amacrine cells in the mouse retina. *J Comp Neurol* **424**: 327-338.

Rice DS, Nusinowitz S, Azimi AM, Martinez A, Soriano E, Curran T. 2001. The reelin pathway modulates the structure and function of retinal synaptic circuitry. *Neuron* **31**: 929-941.

Sanada K, Gupta A, Tsai LH. 2004. Disabled-1-regulated adhesion of migrating neurons to radial glial fiber contributes to neuronal positioning during early corticogenesis. *Neuron* **42**: 197-211.

Sheldon M, Rice DS, D'Arcangelo G, Yoneshima H, Nakajima K, Mikoshiba K, Howell BW, Cooper JA, Goldowitz D, Curran T. 1997. Scrambler and yotari disrupt the disabled gene and produce a reeler-like phenotype in mice. *Nature* **389**: 730-733.

Shinozaki A, Arahata K, Tsukahara T. 1999. Changes in pre-mRNA splicing factors during neural differentiation in P19 embryonal carcinoma cells. *Int J Biochem Cell Biol* **31**: 1279-1287.

Simo S, Jossin Y, Cooper JA. 2010. Cullin 5 regulates cortical layering by modulating the speed and duration of Dab1-dependent neuronal migration. *J Neurosci* **30**: 5668-5676.

Tissir F, Goffinet AM. 2003. Reelin and brain development. *Nat Rev Neurosci* **4**: 496-505.

Tsai JW, Bremner KH, Vallee RB. 2007. Dual subcellular roles for LIS1 and dynein in radial neuronal migration in live brain tissue. *Nat Neurosci* **10**: 970-979.

Tsai JW, Chen Y, Kriegstein AR, Vallee RB. 2005. LIS1 RNA interference blocks neural stem cell division, morphogenesis, and motility at multiple stages. *J Cell Biol* **170**: 935-945.

Ware ML, Fox JW, Gonzalez JL, Davis NM, Lambert de Rouvroit C, Russo CJ, Chua SC, Jr., Goffinet AM, Walsh CA. 1997. Aberrant splicing of a mouse disabled homolog, mdab1, in the scrambler mouse. *Neuron* **19**: 239-249.

Yang YY, Yin GL, Darnell RB. 1998. The neuronal RNA-binding protein Nova-2 is implicated as the autoantigen targeted in POMA patients with dementia. *Proc Natl Acad Sci U S A* **95**: 13254-13259.

Yano M, Hayakawa-Yano Y, Mele A, Darnell RB. 2010. Nova2 regulates neuronal migration through an RNA switch in disabled-1 signaling. *Neuron* **66**: 848-858.